The American Mineralogist

Journal of the Mineralogical Society of America

VOL. 45 JANUARY–FEBRUARY, 1960 Nos. 1 and 2

Contents

Crystal structure of perrierite.................Glauco Gottardi 1
Effect of ion substitution on cell dimensions of clinopyroxenes....G. M. Brown 15
Weeksite, a new uranium silicate.....W. F. Outerbridge, M. H. Staatz, R. Meyrowitz and A. M. Pommer 39
Blue asbestos from Northern Rhodesia.....A. R. Drysdall and A. R. Newton 53
X-ray diffraction study of orientation in the Chattanooga shale.................E. N. Silverman and T. F. Bates 60
Chemical analyses of rocks with the petrographic microscope.................Gerald M. Friedman 69
Paulingite, a new zeolite, in association with erionite and filiform pyrite.................W. B. Kamb and W. C. Oke 79
Doverite, a possible new yttrium fluocarbonate.................W. L. Smith, Jerome Stone, D. R. Ross and H. Levine 92
Autunite from Mt. Spokane, Washington.................G. W. Leo 99
Metamorphism of Lower Paleozoic rocks of the Taconic range in Vermont.................E-an Zen 129
Studies of manganese oxide minerals. III. Psilomelane......Michael Fleischer 176
Reedmergnerite, $NaBSi_3O_8$, the boron analogue of albite.................C. Milton, E. C. T. Chao and J. M. Axelrod 188
X-ray study of alteration in the uranium mineral wyartite......Joan R. Clark 200
Crystal chemistry of dahllite.................Duncan McConnell 209
Notes and News: Very high pressure-high temperature research apparatus and the synthesis of diamond...A. A. Giardini, J. E. Tydings and S. B. Levin 217
  Identity of calcium rinkite and götzenite.................Th. G. Sahama 221
  Plastic universal stage for student use.....R. H. Clark and W. J. Clarke 224
  Vermicular gibbsite in the Pensauken of New Jersey...William Lodding 228
  Low temperature phase transformation of colemanite.................A. Perloff and S. Block 229
  X-ray crystallography and crystal chemistry of gowerite.................C. L. Christ and J. R. Clark 230

(*Continued on Cover 2*)

UNIVERSITY OF ILLINOIS
LIBRARY
APR 1 1960
CHICAGO

EDITOR: LEWIS S. RAMSDELL

BOARD OF ASSOCIATE EDITORS:

D. JEROME FISHER
GEORGE W. BRINDLEY
RICHARD H. JAHNS
GEORGE T. FAUST (1958–60)
ADOLF PABST (1959–61)
EDWARD W. ROEDDER (1960–62)

Published bi-monthly by the Society

(*Contents continued*)

Todorokite and pyrolusite from Vermlands Taberg, Sweden .... **Pontus Ljunggren 235**
***X*-ray fluorescence method for determination of montmorillonite in kaolin clays** .... **D. N. Hinckley and T. F. Bates 239**
Cell constants of artificial siderite .... **W. E. Sharp 241**
Book Reviews **246**
New Mineral Names **252**

Mineralogical Society of America

Associated with the Geological Society of America

President: **Joseph Murdoch,** University of California at Los Angeles, Los Angeles 24, California.
Past-President: **Ralph E. Grim,** University of Illinois, Urbana, Illinois.
Vice-President: **E. F. Osborn,** Pennsylvania State University, University Park, Pennsylvania.
Secretary: **George Switzer,** U. S. National Museum, Washington 25, D. C.
Treasurer: **Marjorie Hooker,** U. S. Geological Survey, Washington 25, D. C.
Editor: **Lewis S. Ramsdell,** University of Michigan, Ann Arbor, Michigan.
Councillors:
(1958–60) **Richard H. Jahns,** California Institute of Technology, Pasadena, California.
(1958–60) **Charles Milton,** U. S. Geological Survey, Washington 25, D. C.
(1959–61) **Wilfrid R. Foster,** Ohio State University, Columbus 10, Ohio.
(1959–61) **Edward W. Nuffield,** University of Toronto, Toronto 5, Ontario, Canada.
(1960–62) **Julian R. Goldsmith,** University of Chicago, Chicago 37, Illinois.
(1960–62) **Horace Winchell,** Yale University, New Haven, Connecticut.
Advertising Manager: **Martin Ehrmann,** 1135 S. Beverly Drive, Los Angeles 35, California.

The enlarged issues of this journal for 1960 are made possible by a grant from the Penrose Fund of the Geological Society of America.

The American Mineralogist—Journal of the Mineralogical Society of America

The journal, containing articles on mineralogy, crystallography, and allied sciences, is issued every two months. Contributions are invited.

The general conduct of the journal is in the hands of the editor, Lewis S. Ramsdell, Department of Mineralogy, University of Michigan, to whom all manuscripts should be submitted.

Authors are requested to submit two copies of each manuscript, typewritten on standard size paper, 8½ by 11 inches. Photographs submitted for cuts should be glossy prints. Tables, figures and cuts should be planned for the page size of the American Mineralogist, approximately 4 by 7 inches. If possible, tracings and large tables should be photographed and submitted as glossy prints.

Authors are entitled to 50 free reprints, without covers, of each article published.

Sent to all members and fellows of the Mineralogical Society of America, Membership dues $4.00 annually, fellowship dues $5.00 annually, which includes receipt of the American Mineralogist and GeoTimes, which is published by the American Geological Institute. Subscriptions for libraries, colleges, institutions, companies and similar organizations $6.00 annually ($10.00, beginning January, 1961).

Entered as second class matter at the post office at Menasha, Wis., under Act of March 3, 1879. Acceptance for mailing at the special rate of postage provided for in section 1103, Act of Oct. 3, 1917, paragraph 4 section 429 P. L. & R. authorized March 13, 1922.

Notice of change of address, orders, and remittances should be sent to Marjorie Hooker, c/o U. S. Geological Survey, Washington 25, D. C.

Printed by the George Banta Company, Inc., Menasha, Wisconsin
Printed in the United States of America

TEM-PRES RESEARCH INC.
STATE COLLEGE, PENNSYLVANIA

RESEARCH CONSULTING
INSTRUMENTATION

X-RAY DIFFRACTION

The invention of the x-ray diffractometer helped make x-ray techniques among the more popular tools available to the mineralogist. However, high temperature x-ray studies were generally classified more as art than science because each furnace which was designed seemed to obtain results only for the original designer. Our units are used in laboratories throughout the country for precise studies in air or controlled atmosphere to 1400°C. Furthermore, since our unit fits all the popular diffractometers, you do not have to decide which diffractometer you will use for your high temperature work. Finally, the unit comes completely equipped with a highly sensitive temperature controller—all at less than the cost required if you built it yourself.

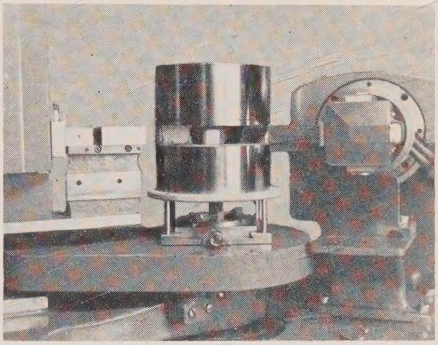

TAILOR-MADE MINERALS

With all our research equipment and personnel, Tem-Pres Research is especially qualified to synthesize controlled purity minerals of such quality that Mother Nature would be jealous. For a modest sum, we can make clays, tridymite, high albite or anything else you might need for your collection or research. If you want a raise and can impress your boss by naming a new mineral after him, write us the composition and properties desired. Not only will we make it, but we'll also tell you where to look for it. While we can't guarantee your finding it, we'll help you write the paper if you do!

HYDROTHERMAL RESEARCH

Our hydrothermal unit, the HR-1B, is among the best buys which we offer. In fact, we often wonder why we sell the equipment for such a low price. However, we enjoy thinking that each unit we sell to a university means that Tem-Pres eventually will have more experienced people applying for jobs in their research group and that each unit sold to an industrial laboratory means more jobs for geochemists. In the meantime, for less than the cost of a decent field trip, you can duplicate Mother Nature (to 1000°C and 60,000 psi) all the year round, while sitting in a soft office chair within hearing distance of a gurgling coffee pot.

NOTE: *The coffee pot and soft office chair are optional equipment not normally supplied nor essential for proper operation of our hydrothermal unit.*

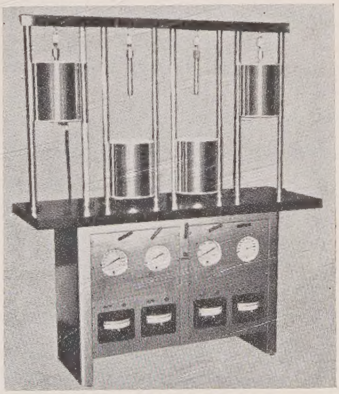

Besides doing research and designing equipment, we also carry complete stocks of replacement parts for hydrothermal equipment and noble metal foil and tubing.

Inquiries on any of the above or on any high temperature, high pressure equipment, materials or research are invited.

TEM-PRES RESEARCH, Inc.
146 N. Atherton Street
State College, Pennsylvania

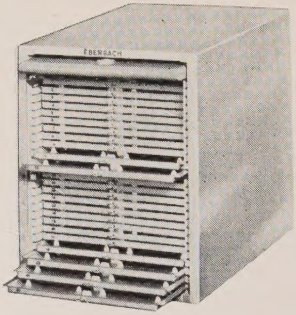

Eberbach

PETROGRAPHIC SLIDE FILING CABINETS

These cabinets provide an expandable filing system. They may be stacked beside or on top of each other as the collection increases. The cabinet holds 750 slides, each of the 25 aluminum trays holding thirty 45 by 26 mm. slides. The door disappears, as shown, into the top of the cabinet which measures 10″ high, 8½″ wide by 12″ deep. The cabinets are sturdily constructed of seasoned hardwood which is carefully filled and lacquered to retain the attractive light oak hue. The cabinet carries catalog number 4040 and sells for $55.00.

Eberbach
CORPORATION
P. O. Box 1024 Ann Arbor, Michigan

MINERAL SPECIMENS

Large variety of crystals, crystal groups, rare minerals, and ore minerals for collectors, universities and museums.

Mineral Catalog 25¢, or sent free when requested on official letterhead.

Filer's are interested in buying or exchanging for good quality minerals, especially from foreign countries. Correspondence is invited.

FILER'S
P. O. Box 372, Redlands, California

Our Specialty is

SELECTED MINERAL SPECIMENS

FROM WORLD-WIDE LOCALITIES FOR COLLECTORS AND MUSEUMS

we also carry a complete line of
MINERALIGHTS, DETECTRON GEIGER COUNTERS, ESTWING PROSPECTOR PICKS, MINERALOGICAL BOOKS, ETC.

Send for free current bulletin

SCHORTMANN'S MINERALS
6 McKinley Avenue Easthampton, Massachusetts

For Mineralogists:

Index of Refraction Liquids

Range: 1.35 to 2.11 index; available in sets of limited range, or in sets with various intervals, or in any selection. Note that liquids 2.01 to 2.11 are now available.

Write for Price List Nd-AM

Allen Reference Sets for Microscopical Studies in Mineralogy and Petrology

Six sets of Authentic materials for use as standards for refractive index, for standard materials mounted in balsam to be compared with unknowns, and for demonstration of typical optical characteristics under microscopical study.

Write for descriptive material A-AM

Text: Practical Refractometry by Means of the Microscope

By ROY M. ALLEN, D.SC.

Describes the technique of the immersion method of microscopy, with particular reference to the identification of minerals. Written primarily for elementary instruction, but this text will be very useful also to advanced workers. Price $1.00. Copy will be sent on approval.

Heavy Liquids

Formulated especially for determination of specific gravity of minerals, but special formulations are being made to order for various procedures. If you have any special problem in this field of separation of minerals or other materials by differences in specific gravity, please write us about your problem. Or, just write for leaflet HL-AM.

Gems, Testing For Identity and For Defects

The CARGILLE-ALLEN GEM TESTING SET is the title of our new book describing the properties of gems and also the equipment for certain identification of gems by a new simple procedure. Price $1.00; this amount applicable to purchase price of any of the items listed in the book.

R. P. Cargille Laboratories, Inc.
117 Liberty St., New York 6, N.Y.

MINERAL SPECIMENS *For Sale or Exchange*
MICROSCOPES BOOKS · GEOLOGICAL SUPPLIES

Catalog on request

SCOTT J. WILLIAMS
Mineralogist

440 N. SCOTTSDALE ROAD · SCOTTSDALE, ARIZONA, U.S.A.

The Lapidary Journal

SUBSCRIBE NOW

THE ORIGINAL GEM MAGAZINE

for gem cutters, gem collectors
and jewelry craftsmen

A non-technical craft publication, not a gemological or mineralogical magazine. Most quoted publication in its field. Bimonthly. Now in its 14th year.

RATES: $3.00 in U.S., North and South America
$3.50 in other foreign countries

Address: P.O. Box 518G, Del Mar, California

ADVANCED COLLECTORS

and Museums buy from us regularly. Choice mineral specimens and crystals. New items offered in each monthly list. Write for current copy.

Plummer's Minerals, 4720 Point Loma Ave., San Diego 7, Calif.

d. m. organist

petrographic
laboratory

BOX 176, NEWARK, DELAWARE

THIN SECTIONS OF

ROCKS, MINERALS, ORES, CERAMICS
PREPARED ROCK SECTIONS FOR
STUDENT USE
PHOTOMICROGRAPHS
PETROGRAPHIC ANALYSIS

SOUTHERN GEM MINING COMPANY

Leading Importers of Fine Gem Materials

VERY SPECIAL—SOUTH AFRICAN DIAMONDS:

1. (a) RARE RED, GOLDEN, BRILLIANT YELLOW, GREEN AND BLUE DIAMONDS. Stones averaging about 5 points, $15.00 per stone. (b) BLACK DIAMONDS, about 10 points each, $20.00 per stone; stones of approximately 25 points each, $50.00 per stone. (c) GREEN or BLUE DIAMONDS, approximately 25 points each, $75.00 per stone. (d) GOLDEN DIAMONDS, about 15 points each, $45.00 per stone. (e) RED DIAMONDS, approximately 10 points each, $30.00 per stone. (All stones are round, brilliant cuts of excellent quality.) (f) SMALL ROUGH DIAMOND SPECIMENS in several colors $2.50 each.

2. MEXICAN MATERIALS: (a) RUTILATED QUARTZ, deep pink and reddish colors, with good crystal faces. Suitable for spheres, cabs or for specimens. Some pieces contain 2 or 3 colors. This is very interesting and spectacular material in short supply. $7.00 per lb. or $3.75 per ½ lb. (b) PSILOMELANE 75¢ per lb. (c) RARE BOTRYOIDAL and TUBE AGATE SPECIMENS $2.00 per lb. (d) No. 1 grade BEST LAGUNA BANDED AGATE NODULES, $4.00 per lb. (e) mixed small and medium LAGUNA and CORYMITO NODULES $1.25 per lb. (f) DEEP BLUE AGATE for tumbling or cabs $1.25 per lb. (g) VERY COLORFUL IACE AGATE $1.00 per lb. (h) BIRD OF PARADISE AGATE $1.50 per lb. (i) BIRD OF PARADISE AGATE with COLORFUL MOSS AGATE 80¢ per lb. (j) Unusual TOURMALINE SPECIMEN GROUPS with black velvety sheen, $4.00 to $8.00 each according to size. (k) AMETHYST, Uruguay, deep purple color, faceting grade, 60¢ per gram. (l) MEXICAN FIRE OPAL WITHOUT MATRIX, best select, medium pieces of high value, $25.00 per ½ oz; small pieces $7.50 per ½ oz. (m) MEXICAN FIRE OPAL IN MATRIX, specimens from $1.00 to $5.00.

3. INDIAN MATERIALS: (a) high grade BANDED CARNELIAN $1.50 for ½ lb. (b) AVENTURINE, $1.00 for ½ lb. (c) BLOODSTONE: $1.50 for ½ lb. (d) SUNSTONE or MOONSTONE in all available colors, 80¢ per oz. (e) GREEN MOSS AGATE 85¢ for ½ lb. (f) BRILLIANT RED GARNETS, mine run, medium sizes, 90¢ per oz. (g) PYROPE (red) GARNET for faceting 25¢ per gram. (h) STAR RUBY ROUGH, superior grade, 35¢ per carat.

4. BRAZILIAN FACETING MATERIALS: (a) Top grade GREEN TOURMALINE, $1.35 per gram. (b) AMETHYST (Rose of France), terminated pieces averaging about 12 grams each, good medium color with unusual overtones of red, 30¢ per gram. (c) Excellent MEDIUM GREEN SPODUMENE: pieces from 15 carats up, 25¢ per carat. (d) LIGHT GREEN SPODUMENE, large pieces, 15¢ per carat. (e) CACOXENITE in AMETHYSTINE QUARTZ, $2.50 for ½ lb. (f) CHRYSOPRASE $4.00 for ½ lb. (g) GOLDEN RUTILATED QUARTZ for faceting, cabs or specimens, $2.50 for ½ lb. (h) ANDALUSITE $1.20 per carat. (i) SMOKY QUARTZ, $1.00 for ¼ lb. (j) DEEP PURPLE RUTILATED AMETHYST 55¢ per gram.

5. COLOMBIAN EMERALD ROUGH: (a) For cutting fine cabochons or for specimens $1.00 per carat in pieces over 4 carats. (b) Faceting grade, excellent color with a minimum of natural inclusions $40.00 per carat (no small pieces). (c) Faceting grade, good color but inferior in grade to (b) $15.00 per carat. (d) Faceting grade, excellent color, smaller pieces but with more internal inclusions than the above described grades $5.00 per carat.

6. CABOCHON ROUGH: (a) CAT'S-EYE TOURMALINE, 80¢ per ounce. (b) IMPERIAL GOLDEN TOPAZ, 90¢ per ounce. (c) BLUE TOPAZ 80¢ per ounce. (d) GOLDEN CITRINE or RED CITRINE 80¢ per ounce. (e) AQUAMARINE 80¢ per ounce. (f) IOLITE or ENSTATITE $1.00 per ounce. (g) LAPIS LAZULI, Afghanistan, commercial grade, $1.00 per ounce; select material $1.50 per ounce. (h) RHODOCHROSITE, Patagonia, $2.00 for ½ lb.

7. SOUTH AFRICAN TIGEREYE: GOLDEN $1.00 per lb. (b) CHERRY RED $1.50 per lb. (c) STRIPED, $2.50 per lb.

8. MISCELLANEOUS: (a) GENUINE BANDED AGATE MARBLES, 16 to 20 mm. size, 85¢ each. (b) BALTIC AMBER CABOCHONS WITH INSECT INCLUSIONS, $8.00 to $20.00, according to quality. (c) RARE BRILLIANT RED SIAM ZIRCON, best faceting grade, 4 to 8 carats, 46¢ per carat; BROWNISH and GOLDEN colors, 19¢ per carat. (d) URUGUAYAN DEEP PURPLE AMETHYST GEODE SECTIONS $2.50 to $8.00, according to size. (e) SHATTUCKITE $2.50 for ½ lb. (f) OLIVE GREEN JADE $2.00 for ½ lb. (g) High grade GOLDSTONE BAROQUES, GOLDEN or BLUE Colors, 50¢ per ½ oz. (Finest baroque assortments available.) (h) EMERALD CABOCHONS $2.00 per carat. (i) AUSTRALIAN OPAL—JELLY OPAL $7.00 to $60.00 per ounce; COOBER PEDY OPAL $2.50 to $45.00 per ounce. (Largest and best stock available.) (j) LARGE RUBY CORUNDUM CRYSTALS IN GREEN CHROME DIOPSIDE, Africa, 50¢ to 75¢ each. (k) Finely carved SCARABS and many other CARVINGS such as animals, buddhas, fish, etc. in carnelian, lapis lazuli, goldstone, amethyst, tigereye, rose quartz and other interesting gem materials, $1.00 to $1.50 each, according to size and quality.

9. POLISHING COMPOUNDS: per lb:—(a) Chrome Oxide $2.00. (b) Levigated Alumina 40¢. (c) Jewelers' Red Rouge Polishing Powder 40¢. (d) Air Float Tripoli 40¢. (e) A-1 Fine Buffing Powder 75¢ per ½ lb. (f) Cerium Oxide $1.50. (g) Tin Oxide $1.00.

Minimum order $5.00 plus 10% Federal Excise Tax on taxable items, and postage. Remittance must accompany order. Any materials may be returned in the same condition as received within the usual ten-day period for immediate refund. Wholesale price list No. 13 and supplements thereto are available to dealers. For a great many years we have maintained in our display rooms the finest exhibits of rare gems and minerals in the country. Visitors are welcome. Open 11:00 A.M. to 6:00 P.M.

5241 Montoya Road   Phone JUniper 4-0086   El Paso, Texas

THE GEOLOGICAL SOCIETY OF AMERICA
ANNOUNCES NEW MEMOIRS

Memoir 77 RELATION OF ORE DEPOSITION TO DOMING IN THE NORTH AMERIC
CORDILLERA. By Edward Wisser. Approximately 140 pages, 34 figu
Expected date of issue: January 25, 1960

A study of deformation on local and regional scales, and its relation to formation of ore deposits; a structural classification of ore deposits

Prices:	To Nonmembers of GSA on orders received after January 25	$4.00	☐
	To Nonmembers of GSA on orders received before January 25	3.50	☐
	To Fellows, Members, and Correspondents of GSA, any time	2.50	☐

Memoir 78 MOLLUSCAN FAUNAS OF THE FLAGSTAFF FORMATION. By Aurele
La Rocque. Approximately 150 pages, 2 figures, 4 photographic plate
Expected date of issue: February 1, 1960

A study of nonmarine mollusks of the western interior. The author uses the record of the animal life in the strata to interpret the changing envi ment and to determine the history of lakes from inception to extinction.

Prices:	To Nonmembers of GSA on orders received after February 1	$4.50	☐
	To Nonmembers of GSA on orders received before February 1	3.75	☐
	To Fellows, Members, and Correspondents of GSA, any time	3.00	☐

Memoir 79 ROCK DEFORMATION. David Griggs and John Handin, Editors. Appro
mately 430 pages, 40 photographic plates, more than 150 figures.
Expected date of issue: February 25, 1960

Contains 13 papers presented at a Symposium on Rock Deformation, held at the Institute of Geophysics at UCLA, by theoretical and experimental leaders in the field. Gives recent results of active workers in experimental rock deformation and includes new theoretical contributio

Prices:	To Nonmembers of GSA on orders received after February 25	$12.00	☐
	To Nonmembers of GSA on orders received before February 25	10.00	☐
	To Fellows, Members, and Correspondents of GSA, any time	7.50	☐

Secretary's Note:

Especially to dispel reported erroneous assumptions that publications of GSA are not available to nonmembers, the Society turns for the first time to this form of advertising in announcing new volumes. Note List Prices above and special discounts on prepublication orders. For prices on other volumes in stock see price lists on current Bulletin covers.

Fellows and Members of GSA: No individual announcement cards will be distributed. For immediate use return this sheet; for future purchases see price lists on current Bulletin covers.

To those who have placed Standing Orders with the Society: This list is for your information only; the publications will be shipped to you automatically as issued.

Please check the appropriate boxes, make checks payable to The Geological Society of America and mail promptly, with remittance, to The Geological Society of America, 419 West 117 Street, New York 27, N. Y.

FGSA MGSA Other
Name.............................. ☐ ☐ ☐
Please check
Mailing Address..............................

....

.... Amount enclosed $______

THE AMERICAN MINERALOGIST
JOURNAL OF THE MINERALOGICAL SOCIETY OF AMERICA

Vol. 45 JANUARY–FEBRUARY, 1960 Nos. 1 and 2

THE CRYSTAL STRUCTURE OF PERRIERITE

GLAUCO GOTTARDI, *Istituto di Mineralogia dell'Università di Pisa, Italy*

ABSTRACT

The crystal structure of perrierite (space group $C2/m$) has been determined by x-rays. The following chemical formula has been attributed to the mineral:

$$(\mathrm{Ce, La, Y, Th, Ca, Na})_4(\mathrm{Fe}^{2+}, \mathrm{Ca})(\mathrm{Ti, Fe}^{3+}, \mathrm{Fe}^{2+}, \mathrm{Mg})_2\mathrm{Ti}_2[\mathrm{O}_4|(\mathrm{Si, Al})_2\mathrm{O}_7]_2$$

The unit cell contains two formula units.

Perrierite is a sorosilicate, with a high number of O-atoms not bonded to silicon. In its structure there are two types of Ti-O octahedral chains along the b-axis; the chains are connected in order to give a sheet parallel to (001). Each Ce atom is surrounded by 10 oxygens; each Fe^{2+} by 6 oxygens. Interatomic distances are of the expected magnitude.

INTRODUCTION

Perrierite, a titanosilicate of rare earth and iron, was found as a new mineral in the shore sands at Nettuno, Roma, Italy, by Bonatti and Gottardi (1950), who gave the morphological crystallography and a chemical analysis. Later the same authors (1954) published the x-ray crystallography of the mineral and a new chemical analysis made on a purer sample, and pointed out that perrierite was a mineral distinct from chevkinite; the crystallographic similarity of the two minerals and epidote was illustrated. The relation between perrierite, chevkinite, and epidote was fully described on the basis of new data on chevkinite [Jaffe, Evans and Chapman (1956)] by Bonatti (1959). The chemical formulas of both chevkinite and perrierite were not known until now: a solution of the problem is offered by the knowledge of the structure and is presented in this paper.

X-RAY CRYSTALLOGRAPHY

The unit cell of perrierite, as determined by Bonatti and Gottardi (1954), has the following dimensions:

$a = 13.59\ kX = 13.61$ Å
$b = 5.61\ kX = 5.62$ Å
$c = 11.61\ kX = 11.63$ Å
$\beta = 113°28'$
Space group $C/2m$

The *a* axis of the unit cell corresponds to the *c* axis of the morphological interpretation. Such a change is advisable to obtain the conventional orientation of the centered monoclinic cell; moreover the original morphological interpretation emphasizes the similarities with epidote.

As to the number of atoms per unit cell, this is uncertain, but it is very probable that there are eight Ce atoms (more exactly rare earth-atoms).

For purposes of structure determination, Buerger precession photographs around [010] were taken with Zr-filtered Mo-radiation as follows: two equators, one with a precession angle $\mu = 25°$ (exposure 18 hours), the other with $\mu = 30°$ (exposure 50 hours); first layer with $\mu = 30°$ (20 hours), second layer with $\mu = 20°$ (20 hours). Intensities were measured by direct photometry of the negatives, since the Kodak Crystalex films used have a linear increase of density with the intensity of incident beam. Long exposures were needed in view of the small crystal size (about 100μ in length, 40μ in diameter). No absorption correction was applied. Intensities were put into an absolute scale only after having solved the structure; at the same time a temperature factor was calculated by comparison of F_o and F_c, and a value $B = 0.65$ Å^2 was adopted.

From these films the following constants were calculated:

$$a = 13.61 \pm 0.02 \text{ A}$$
$$c = 11.67 \pm 0.01 \text{ A}$$
$$\beta = 113°30'$$

Space group *C* 2/*m* was found to be correct.

DETERMINATION OF THE STRUCTURE

In solving the structure of perrierite the following facts have been kept in mind:

(1) Perrierite, like epidote, has a very short period along [010], $b = 5.62$ Å, a length which corresponds to twice the diameter of an oxygen anion: as in the space group *C* 2/*m* there are mirror planes normal to [010] at distance $b/2$, oxygen anions can only have four values of the *y*-coordinate: 0, $\frac{1}{4}$, $\frac{1}{2}$, $\frac{3}{4}$. This limitation is practically valid for the other ions also.

(2) In view of the morphological similarities of perrierite and epidote, it is very probable that the chains of Al-O octahedra stretched along the *b* axis [found by Ito (1950) in the structure of epidote] are to be found also in the structure of perrierite as Ti-O chains.

(3) In the unit cell of perrierite there are eight Ce atoms, which are much heavier than the other atoms: this fact presents both advantages and disadvantages. The advantages are to be found in the interpretation of the Patterson synthesis (since the Ce-influenced maxima must be very easy to find) and in giving the signs to the F values. The disadvantages are present when interpreting Fourier syntheses, since the Ce maxima must be much stronger than the others, and especially much stronger in comparison with O maxima, whose localization may be very difficult.

On the basis of these facts, one can readily deduce the features of the (010) Patterson projection of perrierite. First, given a crystal belonging to space group $C\ 2/m$, its (010) projection has translations $a/2$, c, and a symmetry corresponding to plane group $p2$. In a (010) Fourier projection of perrierite one must see only four Ce maxima, and of these four maxima only two are independent. Let F_1 and F_2 represent the two independent Fourier maxima, and $F_{1'}$ and $F_{2'}$ those dependent upon the first two. Then in the Patterson projection one must find the following maxima:

$P_{11'}$ joining the Fourier maxima $F_1F_{1'}$
$P_{22'}$ joining the Fourier maxima $F_2F_{2'}$
$P_{12+1'2'}$ joining the Fourier maxima F_1F_2 and $F_{1'}F_{2'}$
$P_{12'+1'2}$ joining the Fourier maxima $F_1F_{2'}$ and $F_{1'}F_2$

Therefore in the Patterson projection the Ce atoms produce four independent peaks, two of which are twice as intense as the other two. Let us suppose, in order to simplify matters, that a Patterson peak were to have a value equal to the Z-number product of the interacting atoms; then a peak Ce-Ce is as great as $Z_{Ce}^2 = 3364$. In our Patterson projection one must find two independent maxima equal to 3364 and two equal to 6728.

As stated above, we have considered as probable the presence of Ti-O octahedra in chains running from the origin of the unit cell along the *b*-axis. Then in the (010) Fourier projection we have two superimposed Ti atoms at the origin. In the Patterson projection Ti-Ce maxima are not negligible in comparison with Ce-Ce maxima, although the atomic number of titanium is only 22: a Ti-Ce peak is equal to $Z_{Ti} \cdot Z_{Ce} = 1276$, but this value must be doubled for the superimposition of two Ti atoms in the projection and redoubled for the titanium being at the origin. Thus in Patterson projection a Ti-Ce peak may be as great as 5104. Let us observe that, since Ti atoms are placed at the origin, the Patterson Ti-Ce peaks are coincident with the Fourier Ce peaks.

Summarizing, if the hypotheses are correct, one must find in the Patterson (010) projection of perrierite: two independent peaks whose height is proportional to 6728, two independent peaks whose height is proportional to 5104, two independent peaks whose height is proportional to 3364. In this sense one must say "proportional to" rather than "equal to," because in calculating the synthesis only relative $|F|^2$ values were used.

The calculated Patterson synthesis is seen in Fig. 1. The projection is consistent with the predicted results. Since the positions of the Ce and Ti atoms in the Fourier projection are known, one has a sure method for

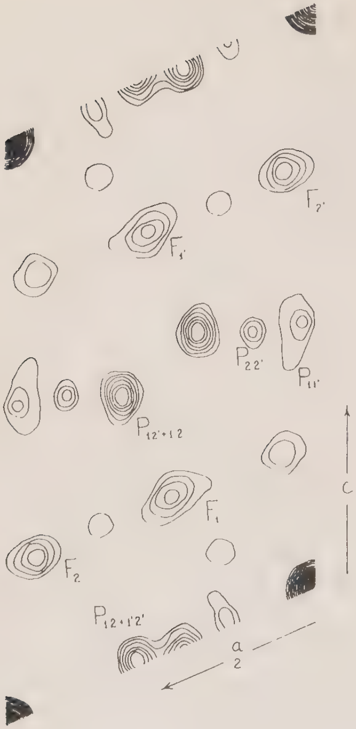

Fig. 1. Patterson (010) projection of perrierite. Contours at arbitrary intervals.

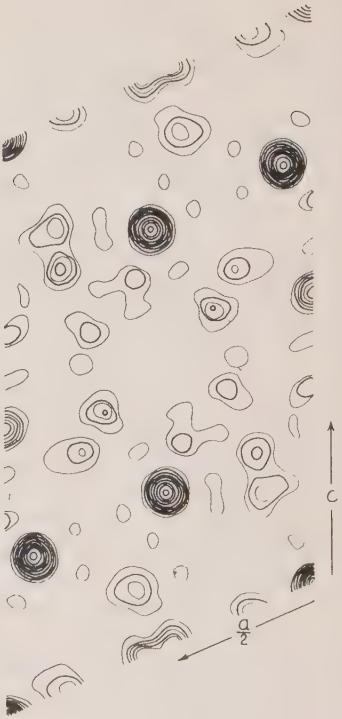

Fig. 2. Fourier (010) projection of perrierite. Heavy contours at 20 e. Å^{-2} intervals, light contours at intermediate values, zero lines being omitted.

giving the signs to the F values. On this basis four Fourier syntheses were successively calculated, introducing more and more structure factors, as the positions of the different atoms were found. After the fourth synthesis, the positions of the O atoms not superimposed in projection $(O_6O_7O_8)$ were not yet certain, since their maxima in the projection were no greater than many parasite maxima. It is necessary to point out that until the fourth synthesis, only F values with $\sin\theta < 0{,}422$ were used, these being the only ones present in the (010) equator photograph with the precession angle $\mu = 25°$. After the fourth synthesis, an equator photograph was taken with a greater precession angle ($\mu = 30°$). This introduced about forty new structure factors with $0{,}422 < \sin\theta < 0{,}500$. The fifth Fourier synthesis is represented in Fig. 2. In this projection parasite maxima are still present, especially around Ce peaks, but not so strong as in previous syntheses; in any case all peaks corresponding to atoms are distinguishable and stronger than parasite maxima.

The interpretation of this projection is as follows: the four major peaks are due to Ce atoms; and the peak at the origin is due to two superimposed Ti atoms. There are three other relevant maxima, obviously due to heavy atoms, of which two are interdependent and one independent. Finally there are 18 weaker maxima, of which 12 are twice as intense as the other 6: from the first 12, 8 were attributed to two superimposed oxygens, and 4 to silicon; the remaining 6 were attributed to single oxygens.

One can exclude the possibility that the above-mentioned three relevant maxima represent superimposed atoms, as these maxima are half as intense as the origin peak, and also because we know that these positions are occupied only by Ti and Fe atoms, i.e. by atoms as heavy as those at the origin. Hence the complete unit cell contains the following atoms:

$$Ce_8Me_2Me_4'Ti_4Si_8O_{44}$$

or as oxides

$$2[(Ce_2O_3)_2(Me^{2+}O)(Me_2{}^{3+}O_3)(TiO_2)_2(SiO_2)_4]$$

From the known chemical composition of perrierite [Bonatti and Gottardi (1954)] it is possible to write the exact formula as:

$$[(Ce, La, Y, Th, Ca, Na)_2O_3]_2 \cdot (Fe^{2+}, Ca)O \cdot (Ti, Fe^{3+}, Fe^{2+}, Mg)_2O_3 \cdot (TiO_2)_2 \cdot [(Si, Al)O_2]_4,$$

In the following, a simplified formula will be used:

$$(Ce_2O_3)_2 \cdot FeO \cdot Me_2{}^{3+}O_3 \cdot (TiO_2)_2 \cdot (SiO_2)_4$$

This will be discussed in detail later on.

Regarding the interpretation of Fourier synthesis, there is yet an uncertainty, since it is not known whether there are Ti atoms or Me^{3+} atoms at the origin. But the problem is unsolvable with perrierite, because it has a chemical composition such that the Me^{3+} is represented almost entirely by Ti.

The above interpretation of the Fourier synthesis is seen in Fig. 3, in which one can read the height of each atom from the (010) plane as a fraction of the *b* length. The determination of the *y* parameters is obvious, as previously mentioned. For most cations the choice is even more limited, as only values such as 0 and $\frac{1}{2}$ are permitted by symmetry. The choice is uncertain only for Fe^{++} ($x=0$, $z=\frac{1}{2}$) and for Me^{3+} ($x=0$, 230, $z=0$), for which either the parameter $y=0$ or $y=\frac{1}{2}$ is possible. To avoid these uncertainties comparisons were made of F_o and F_c values with indices *h*1*l*. Parameters so selected are given in Table 1.

F_o and F_c values are listed in Tables 2, 3 and 4. One observes that, of the values of the first and second layers, those corresponding to the "blind zone" are missing (the blind zone is always present in non-

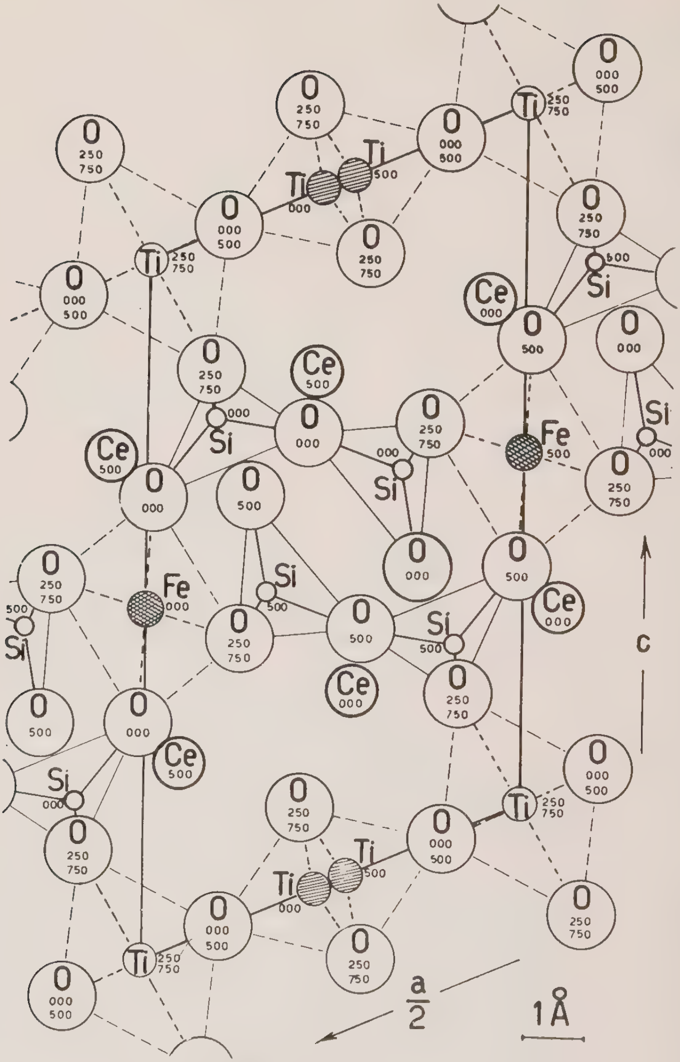

Fig. 3. The structure of perrierite projected on (010). The numbers give the *y*-parameters as permillage of the *b*-length. Coordination tetrahedra and octahedra are indicated.

equator photographs taken with the Buerger camera). This is no disadvantage, as these structure factors are of use only in a simple comparison of F_o and F_c.

As said previously, calculated structure factors have been corrected by a temperature factor with $B = 0,65$ Å².

TABLE 1. ATOMIC PARAMETERS OF PERRIERITE

Atom	Number of atoms in unit cell	Position	x/a	y/b	z/c
Si_1	4	i	0.4085	0.000	0.734
Si_2	4	i	0.1615	0.000	0.546
Ti	4	g	0.000	0.250	0.000
Me^{+++}	4	i	0.270	0.000	0.000
Fe^{++}	2	d	0.000	0.500	0.500
Ce_1	4	i	0.238	0.000	0.266
Ce_2	4	i	0.047	0.000	0.742
O_1	8	j	0.085	0.250	0.194
O_2	8	j	0.291	0.250	0.123
O_3	8	j	0.3745	0.250	0.400
O_4	4	i	0.103	0.000	0.997
O_5	4	i	0.397	0.000	0.003
O_6	4	i	0.492	0.000	0.660
O_7	4	i	0.286	0.000	0.657
O_8	4	i	0.1385	0.000	0.399

Reliability indexes of the structure are given in Table 5. The agreement between the observed and the calculated structure factors is satisfactory, bearing in mind the difficulty of getting strong reflections.

DESCRIPTION OF THE STRUCTURE

Perrierite is a sorosilicate because of the presence of Si_2O_7 groups in its structure. Its cationic charges are also balanced by oxygen ions not bounded to Si, there being 4 of these for each Si_2O_7 group.

But the more obvious structural groups in perrierite are the Ti-O chains parallel to the *b*-axis: every two octahedra have an edge in common (hence two vertices, that is, two oxygen ions). Actually there are two series of octahedral chains parallel to the *b*-axis, which together form a layer. The first series of chains starts at the origin of the lattice, as was apparent before beginning the solution of the structure. The other series is rotated 90° with respect to the first and is formed by oyxgen with one cation which it is necessary to denote by Me^{+++}, even though, in the perrierite samples examined, about 75% of the lattice position is taken up by Ti^{4+} itself, while the rest is taken by Fe^{3+} and Mg^{2+}. The lattice position of Me^{+++} is such that the various cations of the chain form a zigzag structure parallel to *b*. This arrangement is obviously due to the strong repulsion between the near cations Me^{3+} and Ce^{3+}. The resulting distortion in the Me^{3+} octahedron is very great, but probably is compensated by a similar pattern of the O_4 and O_5 oxygens, which should not

TABLE 2. F_o AND F_c VALUES FOR $h0l$ REFLECTIONS

h	k	l	F_o	F_c
0	0	2	146	−161
0	0	3	177	+209
0	0	4	335	+421
0	0	5	67	+36
0	0	6	110	−110
0	0	7	240	+235
0	0	8	276	+318
0	0	9	43	−55
0	0	10	39	−42
0	0	11	181	+206
0	0	12	166	+168
0	0	13	111	−100
0	0	14	0	−20
0	0	15	193	+197
2	0	0	0	+6
2	0	1	0	−62
2	0	2	32	−7
2	0	3	0	+25
2	0	4	87	+59
2	0	5	146	+107
2	0	6	0	−25
2	0	7	126	−112
2	0	8	0	+26
2	0	9	75	+51
2	0	10	39	+22
2	0	11	87	−59
2	0	12	79	+56
2	0	13	0	+36
2	0	14	0	−1
−2	0	2	32	+66
−2	0	3	87	−89
−2	0	4	118	+104
−2	0	5	59	−20
−2	0	6	103	+109
−2	0	7	55	−35
−2	0	8	0	+11
−2	0	9	71	−62
−2	0	10	39	+4
−2	0	11	32	+50
−2	0	12	110	+82
−2	0	13	0	−11
−2	0	14	39	−28
−2	0	15	0	+2
4	0	0	225	+256
4	0	1	193	+198
4	0	2	181	−185
4	0	3	39	−64
4	0	4	272	+313
4	0	5	47	+22
4	0	6	0	−7
4	0	7	39	−32
4	0	8	225	+235
4	0	9	87	+45
4	0	10	0	−76
4	0	11	0	+11
4	0	12	114	+149
4	0	13	0	+3
−4	0	1	0	−25
−4	0	2	0	−20
−4	0	3	244	+251
−4	0	4	154	+178
−4	0	5	256	−276
−4	0	6	0	+26
−4	0	7	237	+243
−4	0	8	154	+134
−4	0	9	143	−126
−4	0	10	0	+20
−4	0	11	197	+216
−4	0	12	87	+76
−4	0	13	158	−159
−4	0	14	79	+91
−4	0	15	67	+100
6	0	0	185	−158
6	0	1	0	+43
6	0	2	264	+242
6	0	3	146	−149
6	0	4	103	−118
6	0	5	67	+82
6	0	6	130	+85
6	0	7	162	−155
6	0	8	47	−53
6	0	9	177	+138
6	0	10	39	+30
6	0	11	130	−119
6	0	12	16	−14
−6	0	1	178	−178
−6	0	2	173	+187
−6	0	3	0	−5
−6	0	4	181	−187
−6	0	5	79	−63
−6	0	6	201	+208
−6	0	7	0	−10
−6	0	8	118	−76
−6	0	9	0	+32
−6	0	10	28	+63
−6	0	11	75	−71
−6	0	12	47	−58
−6	0	13	39	+64
−6	0	14	32	+71
−6	0	15	0	−32
8	0	0	79	+119
8	0	1	158	+207
8	0	2	63	+41
8	0	3	79	−78
8	0	4	39	+83
8	0	5	142	+192
8	0	6	0	+3
8	0	7	0	−13
8	0	8	47	+100
8	0	9	51	+58
8	0	10	0	−8
−8	0	1	193	−205
−8	0	2	193	+172
−8	0	3	280	+330
−8	0	4	39	+65
−8	0	5	177	−142
−8	0	6	162	+152
−8	0	7	181	+166
−8	0	8	0	+30
−8	0	9	138	−119
−8	0	10	233	+240
−8	0	11	138	+145
−8	0	12	47	−52
−8	0	13	0	−37
−8	0	14	158	+168
−8	0	15	95	+102
10	0	0	87	−88
10	0	1	0	+42
10	0	2	248	+216
10	0	3	0	+17
10	0	4	154	−122
10	0	5	0	+8
10	0	6	193	+211
10	0	7	0	−50
10	0	8	0	−50
10	0	9	0	+54
−10	0	1	87	+92
−10	0	2	185	+163
−10	0	3	0	−44
−10	0	4	91	−82
−10	0	5	142	+125
−10	0	6	197	+193
−10	0	7	51	−71
−10	0	8	0	−47
−10	0	9	146	+167
−10	0	10	142	+129
−10	0	11	122	−121
−10	0	12	0	+13
−10	0	13	32	+61
−10	0	14	138	+102
−10	0	15	20	−52
12	0	0	32	+45
12	0	1	0	+29
12	0	2	32	+51
12	0	3	0	−18
12	0	4	55	+80
12	0	5	0	+18
12	0	6	35	+59
12	0	7	0	−8
−12	0	1	0	−18
−12	0	2	67	+79
−12	0	3	0	+18
−12	0	4	87	+68
−12	0	5	0	−5
−12	0	6	110	+110
−12	0	7	0	+47
−12	0	8	95	−70
−12	0	9	0	+16
−12	0	10	95	+92
−12	0	11	39	+73
−12	0	12	0	−38
−12	0	13	0	+6
−12	0	14	122	+112
14	0	0	0	−19
14	0	1	146	−154
14	0	2	87	+126
14	0	3	162	+125
14	0	4	75	−106
14	0	5	59	−58
−14	0	1	217	+193
−14	0	2	79	+106
−14	0	3	209	−181
−14	0	4	0	−19
−14	0	5	209	+167
−14	0	6	55	+86
−14	0	7	221	−201
−14	0	8	110	+84
−14	0	9	193	+165
−14	0	10	0	+3
−14	0	11	154	−141
−14	0	12	83	+80
−14	0	13	142	+128
−14	0	14	95	−77
16	0	0	0	+18
16	0	1	47	−27
16	0	2	0	+17
−16	0	1	0	+6
−16	0	2	0	−6
−16	0	3	0	+10
−16	0	4	0	+1
−16	0	5	0	+22
−16	0	6	0	+29
−16	0	7	0	+ 6
−16	0	8	0	+18
−16	0	9	0	−27
−16	0	10	0	+45
−16	0	11	51	−54
−16	0	12	24	+40
−18	0	3	87	−68
−18	0	4	110	+110
−18	0	5	118	+115
−18	0	6	32	−52
−18	0	7	32	−52
−18	0	8	146	+125
−18	0	9	150	+150
−18	0	10	79	−58

TABLE 3. F_o AND F_c VALUES FOR $h1l$ REFLECTIONS

h	k	l	F_o	F_c
1	1	3	116	+107
1	1	4	32	+46
1	1	5	0	−42
1	1	6	148	−136
1	1	7	136	+148
1	1	8	0	−35
1	1	9	0	−26
1	1	10	0	−35
1	1	11	0	+56
−1	1	3	124	−98
−1	1	4	200	+150
−1	1	5	100	+71
−1	1	6	240	−200
−1	1	7	0	−19
−1	1	8	192	+153
−1	1	9	0	−17
−1	1	10	188	−157
−1	1	11	52	+55
−1	1	12	64	+66
3	1	0	0	−6
3	1	1	398	+420
3	1	2	116	−141
3	1	3	184	−223
3	1	4	144	+134
3	1	5	240	+267
3	1	6	184	−171
3	1	7	164	−123
3	1	8	201	+171
3	1	9	164	+133
3	1	10	144	−150
−3	1	2	96	−97
−3	1	3	410	+398
−3	1	4	32	−29
−3	1	5	240	−246
−3	1	6	60	+74
−3	1	7	248	+248
−3	1	8	44	−71
−3	1	9	164	−152
−3	1	10	100	+103
−3	1	11	164	+144
−3	1	12	92	−87
5	1	0	0	+5
5	1	1	40	−31
5	1	2	140	−128
5	1	3	44	−42
5	1	4	0	+58
5	1	5	0	−48
5	1	6	48	−67
5	1	7	0	+5
5	1	8	0	−3
5	1	9	0	−24
−5	1	1	0	−29
−5	1	2	180	−139
−5	1	3	0	+8
−5	1	4	52	+53
−5	1	5	0	−32
−5	1	6	224	−231
−5	1	7	152	+138
−5	1	8	0	+10
−5	1	9	56	−83
−5	1	10	132	−117
−5	1	11	136	+104
−5	1	12	0	+3
7	1	0	44	−60
7	1	1	272	+246
7	1	2	124	+84
7	1	3	128	−128
7	1	4	0	−56
7	1	5	196	+189
7	1	6	0	−7
7	1	7	64	−93
7	1	8	0	+2
−7	1	1	176	−183
−7	1	2	224	+195
−7	1	3	220	+222
−7	1	4	132	−138
−7	1	5	38	−91
−7	1	6	188	+186
−7	1	7	160	+162
−7	1	8	140	−156
−7	1	9	0	−32
−7	1	10	156	+163
−7	1	11	108	+101
−7	1	12	144	−153
9	1	0	168	−148
9	1	1	56	−41
9	1	2	0	−39
9	1	3	48	+48
9	1	4	148	−116
9	1	5	0	−39
9	1	6	0	+8
−9	1	1	72	+86
−9	1	2	0	−57
−9	1	3	40	−71
−9	1	4	52	−71
−9	1	5	0	+24
−9	1	6	52	−61
−9	1	7	0	−48
−9	1	8	0	−16
−9	1	9	0	−36
−9	1	10	0	−27
−9	1	11	0	−31
−9	1	12	0	−34
11	1	0	180	−187
11	1	1	60	−125
11	1	2	208	+182
11	1	3	0	−58
11	1	4	64	−93
−11	1	1	0	+13
−11	1	2	208	+229
−11	1	3	0	+57
−11	1	4	180	−233
−11	1	5	80	+107
−11	1	6	160	+208
−11	1	7	0	+14
−11	1	8	160	−194
−11	1	9	104	+146
−11	1	10	140	+165
13	1	0	0	−36
13	1	1	112	−105
13	1	2	0	−23
−13	1	1	0	+51
−13	1	2	0	−31
−13	1	3	88	−124
−13	1	4	0	+22
−13	1	5	0	+42
−13	1	6	0	−76
−13	1	7	0	−62
−13	1	8	0	−30
−13	1	9	0	+39

be exactly superimposed along *b*. But with the experimental data available, it is impossible to demonstrate such a zigzag pattern for these oxygens, for their Z value is too small in comparison with that of the other ions. The two series of chains, that of Ti^{4+} and that of Me^{3+}, form a layer parallel to (001) through the origin. The Si_2O_7 groups, which include all 6 oxygens coordinated by Fe^{++}, are arranged midway between two layers of octahedra.

The Ce^{+++} ions in coordination 10 lie between these layers of octahedra and the Si_2O_7 groups. Of the 10 oxygens which surround Ce, 6 are located at the vertices of a hexagon with a cation at the center, 3 above the hexagon, and one below.

TABLE 4. F_o AND F_c VALUES FOR $h2l$ REFLECTIONS

h	k	l	F_o	F_c	h	k	l	F_o	F_c	h	k	l	F_o	F_c
0	2	6	213	-172	-6	2	6	48	+36	-10	2	8	67	-104
0	2	7	124	+118	-6	2	7	137	-106	-10	2	9	0	-32
0	2	8	223	+206	-6	2	8	242	-253	-10	2	10	0	+51
0	2	9	105	-114	-6	2	9	0	-6	-10	2	11	102	-127
0	2	10	169	-162	-6	2	10	0	+50	-10	2	12	0	-20
0	2	11	143	+153	-6	2	11	73	-102	12	2	0	0	-2
0	2	12	140	+129	-6	2	12	0	+23	12	2	1	54	-32
2	2	5	83	-101	8	2	0	0	+30	12	2	2	0	+23
2	2	6	70	-73	8	2	1	159	+158	12	2	3	0	+58
2	2	7	83	-88	8	2	2	0	-47	-12	2	1	0	-100
2	2	8	0	-43	8	2	3	146	-141	-12	2	2	0	+38
2	2	9	0	-12	8	2	4	0	+48	-12	2	3	0	-27
2	2	10	54	-68	8	2	5	0	+77	-12	2	4	0	-62
2	2	11	182	-139	8	2	6	0	-76	-12	2	5	48	-94
-2	2	7	217	-173	8	2	7	146	-36	-12	2	6	0	-2
-2	2	8	54	+48	-8	2	1	207	-193	-12	2	7	0	+23
-2	2	9	76	-83	-8	2	2	0	+17	-12	2	8	0	-64
-2	2	10	70	-51	-8	2	3	92	-95	-12	2	9	0	-44
-2	2	11	127	--84	-8	2	4	60	-46	-12	2	10	0	+32
-2	2	12	0	-38	-8	2	5	229	-242	14	2	0	0	-103
4	2	4	134	+143	-8	2	6	175	+181	14	2	1	178	-178
4	2	5	0	-3	-8	2	7	124	+120	-14	2	1	0	+69
4	2	6	83	-108	-8	2	8	76	-60	-14	2	2	0	+46
4	2	7	115	-113	-8	2	9	185	-196	-14	2	3	188	-230
4	2	8	134	+124	-8	2	10	111	+108	-14	2	4	0	-18
4	2	9	0	-44	-8	2	11	73	-116	-14	2	5	105	+119
4	2	10	80	-80	-8	2	12	80	-116	-14	2	6	0	-3
-4	2	7	153	+127	10	2	0	175	-198	-14	2	7	172	-244
-4	2	8	0	+32	10	2	1	134	-121	-14	2	8	0	-2
-4	2	9	229	-221	10	2	2	162	+171	-14	2	9	96	+117
-4	2	10	0	-18	10	2	3	0	-38					
-4	2	11	89	+93	10	2	4	92	-136					
-4	2	12	0	+12	10	2	5	0	-30					
6	2	2	86	+42	10	2	6	111	+125					
6	2	3	255	-205	-10	2	1	60	+47					
6	2	4	191	-241	-10	2	2	102	-98					
6	2	5	76	+60	-10	2	3	0	-43					
6	2	6	108	+79	-10	2	4	169	-178					
6	2	7	210	-230	-10	2	5	0	-4					
6	2	8	108	-108	-10	2	6	130	+125					
6	2	9	0	+55	-10	2	7	150	-163					

TABLE 5. RELIABILITY INDEXES

	Number of reflections	Reliability indexes	
		including all reflections	including only observed reflections
(010) equator	218	0.244	0.165
(010) first layer	130	0.282	0.171
(010) second layer	112	0.332	0.156
All reflections	460	0.276	0.159

TABLE 6. INTERATOMIC DISTANCES IN PERRIERITE

Atom	Neighbour	Distance (Å)*	Atom	Neighbour	Distance (Å)*
Si_1	O_1 (2)	1.62	Ce_1	O_1 (2)	2.37
	O_6	1.67		O_2 (2)	2.48
	O_7	1.53		O_3 (2)	2.36
				O_4	2.93
Si_2	O_3 (2)	1.68		O_7 (2)	3.02
	O_7	1.67		O_8	2.44
	O_8	1.61			
			Ce_2	O_1 (2)	2.60
Ti	O_1 (2)	2.08		O_2 (2)	2.55
	O_4 (2)	1.99		O_3 (2)	2.70
	O_5 (2)	1.99		O_4	2.76
				O_6 (2)	2.96
Me^{+++}	O_2 (4)	1.95		O_8	2.40
	O_4	2.21			
	O_5	1.72			
Fe^{++}	O_3 (4)	2.15			
	O_6 (2)	1.91			

* The interionic distance error in the oxygen parameters is ±0.05 Å, while that for the cation parameters is decidedly smaller.

Table 6 gives the interatomic distances between the various cations and the anions coordinated by them. There is a remarkable regularity, particularly in consideration of the difficulty in determining the position of light atoms, such as Si and O, close to heavy atoms, such as Ce.

Table 7 illustrates the balance between the oxygen anion charges and the cations surrounding them. Pauling's rule is normally fulfilled.

Finally it should be pointed out that the existence of the layer of octahedra parallel to (001), which morphologically is the plane (100), manifests itself in an outstanding manner: the (001) plane is not only always well developed in crystals, but it is frequently also a twin-plane. Thus it is evident that nucleation occurs precisely on that layer of octahedra, whose two faces are perfectly equivalent.

THE CHEMICAL FORMULA

In the preceding section the chemical formula of perrierite has been deduced from its crystal structure. By using (Si_2O_7) groups, we can write the formula as follows:

$$C_4^{[8]3+}Me^{[6]2+}Me_2^{[6]3+}Me_2^{[6]4+}\left[O_4 \,\middle|\, A_2^{[4]4+}O_7\right]_2$$

TABLE 7. BALANCE BETWEEN OXYGEN CHARGES AND SURROUNDING CATIONS

Anion	Balancing cations	Ratio of: charges of cation to coordination number	Total charges surrounding anion
O_1	Ti	4/6	2.27
	Si	4/4	
	Ce	3/10	
	Ce	3/10	
O_2	Me^{+++}	3/6	1.60
	Me^{+++}	3/6	
	Ce	3/10	
	Ce	3/10	
O_3	Si	4/4	1.93
	Fe	2/6	
	Ce	3/10	
	Ce	3/10	
O_4	Ti	4/6	2.43
	Ti	4/6	
	Me^{+++}	3/6	
	Ce	3/10	
	Ce	3/10	
O_5	Ti	4/6	1.83
	Ti	4/6	
	Me^{+++}	3/6	
O_6	Si	4/4	1.93
	Fe	2/6	
	Ce	3/10	
	Ce	3/10	
O_7	Si	4/4	2.60
	Si	4/4	
	Ce	3/10	
	Ce	3/10	
O_8	Si	4/4	1.60
	Ce	3/10	
	Ce	3/10	

where

C^{3+} = rare earths, Th^{4+}, Ca^{2+}, Na^{+}
Me^{2+} = Fe^{2+}, Ca^{2+}
Me^{3+} = Ti^{4+}, Fe^{3+}, Mg^{2+}, Fe^{2+}
Me^{4+} = Ti^{4+}
A^{4+} = Si^{4+}, Al^{3+}

The isomorphic substitutions here listed have been found in perrierite from Nettuno, but obviously other substitutions are possible according to crystallochemical laws.

The exact formula, which is calculated from the chemical analysis of perrierite from Nettuno, is as follows:

$$(Ce_{2,31}La_{0,50}Y_{0,16}Th_{0,19}Ca_{0,53}Na_{0,31})(Fe^{2+}_{0,63}Ca_{0,34})$$
$$(Ti_{1,48}Fe^{3+}_{0,19}Mg_{0,24}Fe^{2+}_{0,05})Ti_2[O_4|(Si_{1,92}Al_{0,08})O_7]_2$$

A second occurrence of perrierite is known: the mineral of Kobe-Mura, Japan, studied by Takubo and Nishimura (1953) and named chevkinite, although it was demonstrated by Bonatti (1959) to be perrierite. From the chemical composition [analysis (2)] of the Kobe-Mura perrierite one can calculate the formula:

$$(Ce_{1,34}La_{1,31}Y_{0,36}Th_{0,03}Ca_{0,97})(Fe^{2+}_{0,99}Mn_{0,07})$$
$$(Ti_{0,75}Fe^{3+}_{0,19}Al_{1,03}Mg_{0,06}Mn_{0,04})Ti_2[O_4|(Si_{1,86}Al_{0,18})O_7]_2$$

This formula does not seem applicable to the analyses of chevkinite; moreover chevkinite has a unit cell volume 7% greater than that of perrierite, and this leads one to suspect that there are more O atoms in the chevkinite unit cell than in the perrierite unit cell.

On the basis of this formula and of the unit cell dimensions, the theoretical specific gravity has been calculated, the result being $G = 4.77$; the experimental value [Bonatti and Gottardi (1954)] is $G = 4.45$. The theoretical value normally is greater than the experimental one; in this case the difference is large, but explainable considering that the measurement was made on a sample of very small crystals. The sample used for the determination of specific gravity was then destroyed during the chemical analysis. It did not seem useful to purify a new sample in order to make a new measurement of specific gravity, which would not contribute anything new to the information already secured.

ACKNOWLEDGMENTS

This research was supported by the Consiglio Nazionale delle Ricerche, Roma.

I thank Dr. Luciano Guerri of the Centro Studi Calcolatrici Elettroniche of the Pisa University for his calculation of Patterson and

Fourier series; my wife Laura and Dr. Giuseppe Carrai for their assistance in structure factor calculations; Prof. Stefano Bonatti for his critical reading of the manuscript.

REFERENCES

BONATTI S. (1959), Chevkinite, perrierite and epidotes, *Am. Mineral.*, **44,** 115–137.

BONATTI S. AND GOTTARDI G. (1950), Perrierite, nuovo minerale ritrovato nella sabbia di Nettuno (Roma), *R.C. Acad. Lincei* [8], **9,** 361–368.

BONATTI S. AND GOTTARDI G. (1954), Nuovi dati sulla perrierite, *R.C. Soc. Miner. ital.*, **10,** 208–225.

ITO, T. (1950), *X-ray studies on polyporphism*, Tokyo, 50–69.

JAFFE, H. W., EVANS H. T., JR. AND CHAPMAN, R. W. (1956): Occurrence and age of chevkinite from the devil's slide fayalite-quartz syenite near Stark, New Hampshire, *Am. Mineral.*, **41,** 474–487.

TAKUBO J. AND NISHIMURA S. (1953), On tscheffkinite from Kobe-Mura, Kyoto Prefecture, Japan, *Mem. Coll. Sci. Kyoto* B, **20,** 323–328.

Manuscript received Feb. 16, 1959.

THE AMERICAN MINERALOGIST, VOL. 45, JANUARY–FEBRUARY, 1960

THE EFFECT OF ION SUBSTITUTION ON THE UNIT CELL DIMENSIONS OF THE COMMON CLINOPYROXENES

G. M. Brown, *Department of Geology and Mineralogy, University Museum, Oxford, England.*

Abstract

The unit-cell dimensions of eleven analyzed augites and ferroaugites from the Skaergaard intrusion are presented. The variation of the unit-cell dimensions b and $a \sin \beta$ is examined in relation to ion substitution, for the twenty-three analyzed common clinopyroxenes for which data are now available. For the three major substitution series, $Mg^{2+}:Fe^{2+}$, $Ca^{2+}:Fe^{2+}$ and $Ca^{2+}:Mg^{2+}$, the relationship between these two unit-cell dimensions and the ion substitution is regular, and linear equations are given for each series. The slope of the graph relating b-dimension to $Mg^{2+}:Fe^{2+}$ substitution is identical to that for the orthorhombic pyroxenes. The three series are combined in a triangular diagram relating unit-cell dimensions to $Ca^{2+}:Mg^{2+}:Fe^{2+}$ ratio, for the common clinopyroxene trapezium. The amount of substitution of Al^{3+} in octahedral coordination, and its effect on the b-cell dimension, is reconsidered.

Introduction

The fundamental pyroxene structure was determined in the case of diopside by Warren and Bragg (1929), while Warren and Biscoe (1931) later showed that hedenbergite and augite possessed a similar structure. The first attempt to study the changes in unit cell dimensions with ionic substitution in a group of pyroxenes (after a more general study by Ramberg and De Vore, 1951) was that of Hess (1952), who related the variation in a, b and c dimensions of the orthorhombic pyroxenes to substitution of Fe^{2+} for Mg^{2+}, and Al^{3+} for Mg^{2+} and Si^{4+}.

A beginning was made on the monoclinic pyroxenes by Kuno and Hess (1953) by determining the unit-cell dimensions of clinoenstatite, two pigeonites and three calcium-rich clinopyroxenes. A gradual change in unit cell dimensions throughout the main clinopyroxene trapezium (diopside—clinoenstatite—ferrosilite—hedenbergite) was tentatively suggested, and the degree of change was illustrated by sections across the field from diopside to hedenbergite, and from diopside to pigeonite. Kuno (1955) selected the diopside-pigeonite series for further detailed study, introducing four measured pyroxenes from the augite field which, together with the diopside and pigeonite used by Kuno and Hess, constituted a series of six pyroxenes showing the effect on unit-cell dimensions of the substitution of Fe^{2+} for Ca^{2+} (Mg^{2+} almost constant).

The effect of substitution of Fe^{2+} for Mg^{2+} was, so far, only illustrated in a general way by the three specimens studied by Kuno and Hess (1953, Fig. 5) which came from unrelated metamorphic rocks. The writer decided, therefore, to examine a series of chemically analyzed clinopyroxenes from the Skaergaard intrusion, which showed continuous replacement of Mg^{2+} by Fe^{2+}, becoming almost complete, during the fractionation of a single body of basic magma, with Ca^{2+} varying only slightly between 35 and 45 atomic per cent, and with the minor cations showing hardly any variation. The greater part of this series has been described elsewhere in connection with their chemistry, optics and crystallization history (Brown, 1957), their specific magnetic susceptibility (Chevallier and Mathieu, 1958), and the magnetic moment of their contained ferrous ion (Chevallier and Martin, 1959).

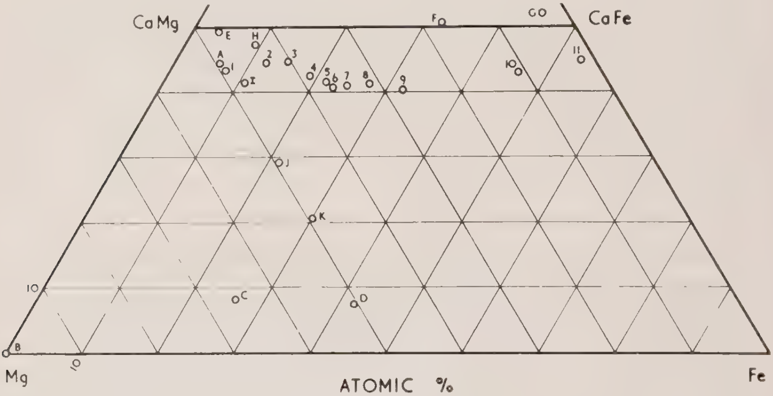

FIG. 1. The plotted points refer to chemically analyzed clinopyroxenes for which data on unit-cell dimensions are at present available. Points 1 to 11 refer to newly-measured Skaergaard specimens (corrected for exsolution), while points A to K refer to specimens described in previous literature. See Table 2 for further details.

Eleven measurements of unit-cell dimensions have been made of the Skaergaard pyroxenes, while at the same time one was made of a diopsidic pyroxene from Rhum (Brown, 1956, table 4). When the data for these twelve are considered in relation to the six of Kuno and Hess and the four of Kuno (with certain corrections made, see p. 17) several points of general significance emerge, quite apart from the effect of $Mg^{2+}:Fe^{2+}$ substitution. With data now available for twenty-two clinopyroxenes, it is possible to consider $Ca^{2+}:Fe^{2+}$ substitution (in relation to the problem of the character of the *b*-dimension change), $Ca^{2+}:Mg^{2+}$ substitution, and the effect of Al^{3+} in six-fold coordination. The information afforded by a knowledge of the three major substitutions, $Mg^{2+}:Fe^{2+}$, $Ca^{2+}:Fe^{2+}$, and $Ca^{2+}:Mg^{2+}$, make it possible to estimate, with some accuracy, the variation of cell-dimensions within the triangular diagram $Ca^{2+}:Mg^{2+}:Fe^{2+}$. It will be apparent, however, that as a check more information is required for certain parts of even the common clinopyroxene field. This is also true of the ferrosilite region, although in view of the instability of these minerals at magmatic temperatures (Sahama and Torgeson, 1949), and the fact that if they crystallized stably at lower temperatures (e.g. metamorphic rocks) they will have subsequently inverted to the orthorhombic form, such information may not be forthcoming.

The twelve new measurements of the unit-cell dimensions were made on the same instrument used for the other ten by Kuno and Hess (the North American Philips X-ray diffractometer at Princeton University). This advantage simplified the author's work a great deal, for it was possible to relate and index the diffraction peaks by direct reference to the charts obtained by these two investigators.

Ionic-Ratio Determinations

The commoner clinopyroxenes of igneous rocks vary chiefly in the relative proportions of the cations Ca^{2+}, Mg^{2+}, and Fe^{2+}. The effect of this variation on the unit-cell dimensions largely eclipses the effect of variation in the minor cations, apart from aluminum. Hence it is not practicable to discuss the effect in this series of the minor cations although ultimately it will be necessary for the effects of Ti, Na and Fe''' to be determined in those pyroxenes enriched in these elements. In the present study, particular attention has been paid to the manner in which the effects of Ca^{2+}, Mg^{2+}, Fe^{2+} and Al^{3+} can be estimated with fair accuracy.

In order to do this, with the commoner augites, two slight modifications to the methods of determination of ionic ratios used by Kuno and Hess (1953) and Kuno (1955) have been made. These concern the effect of exsolution on composition, and the meaning of the "Fe" co-ordinate in the Ca:Mg:Fe diagrams.

The Skaergaard clinopyroxenes have formed from a slowly-cooled body of magma, and many of those investigated show, as a result, evidence of having exsolved lamellae of calcium-poor pyroxene at subsolidus temperatures (Brown, 1957). These lamellae are subordinate to the host mineral, and are not believed (although evidence is desirable) to greatly affect the position of the reflection peaks of the host augite. If this is so, then the cell-dimensions determined are those of the host augite, while the chemical composition obtained from analysis is that of the host plus exsolved lamellae. So far, this problem has not affected the work of Kuno and Hess, who examined clinopyroxenes which were mostly from either volcanic or metamorphic rocks, and thus free from exsolved pyroxene. However, there is the risk that the determinative diagrams presented in their paper will be applied directly to the commoner clinopyroxenes of plutonic rocks, which invariably contain exsolved pyroxene, with resultant errors. The Skaergaard suite of pyroxenes has therefore been corrected for exsolution to illustrate the need for this step and in this way can be used in conjunction with those from the other environments. The amount and identity of the exsolution (usually *ca.* 20% pigeonite) was determined, in each case, by optical and modal measurement, and the composition of the exsolved material assumed, in each case, to be that of the co-existing calcium-poor pyroxene analyzed from the same, or an adjacent, rock. The errors inherent in such estimates are obvious, but fortunately slight errors do not affect the most important and dependable parameter for determinative diagrams, the *b*-cell dimension, which is little-affected by calcium-content (p. 29). The uncorrected analyses which are so far unpublished are given in Table 1. The rest of the uncorrected analyses, together with the composition of the exsolved phases used in the recalculations, and a description of the exsolution phenomena, are given in a previous paper (Brown, 1957). Once these corrections are made, the value of the initial, accurate chemical analysis is reduced. Sub-solidus exsolution, in fact, reduces the accuracy of a correlation between chemical composition and optical properties or unit-cell dimensions. A solution to this problem would seem

TABLE 1. CHEMICAL ANALYSES OF THREE OF THE SKAERGAARD CLINOPYROXENES

(*not previously published*)

Wt. per cent	3	10	11	Atomic No. on basis of 6 oxygen atoms		3		10		11	
SiO_2	50.82	48.18	46.90		Si^{4+}	1.908		1.941		1.928	
Al_2O_3	2.40	1.06	2.20	Z	Ti^{4+}	—	1.999	0.008	2.000	—	1.996
Fe_2O_3	1.88	1.46	1.66		Al^{3+}	0.091		0.051		0.068	
FeO	10.75	26.08	29.10		Ti^{4+}	0.025		0.013		0.002	
MnO	0.19	0.53	0.67		Al^{3+}	0.015		—		0.038	
MgO	14.36	3.52	0.58		Fe^{3+}	0.054		0.044		0.052	
CaO	18.12	18.90	18.87		Cr^{3+}	0.002		—		—	
Na_2O	0.39	0.23	0.32	WXY	Fe^{2+}	0.336	2.001	0.879	2.001	0.999	2.009
K_2O	0.03	0.04	0.04		Mn^{2+}	0.007		0.019		0.022	
TiO_2	0.96	0.70	0.10		Mg^{2+}	0.803		0.211		0.037	
Cr_2O_3	0.06	n.d.	n.d.		Ca^{2+}	0.729		0.816		0.832	
					Na^{1+}	0.029		0.017		0.025	
					K^{1+}	0.001		0.002		0.002	
Total	99.96	100.70	100.44								

3. Augite from lower olivine gabbro, E.G.4389, Skaergaard intrusion, Anal. P. E. Brown.
10. Ferroaugite from ferrogabbro, E.G.4318, Skaergaard intrusion. Anal. E. A. Vincent.
11. Ferrohedenbergite from transgressive granophyre sill, E.G.4489, Skaergaard intrusion. Anal. E. A. Vincent.

to be either homogenization by re-heating before making the physical measurements, or determination of the chemical composition of the host separately from that of the exsolved lamellae by, say, *x*-ray emission microspectroscopy.

The three major variables, in the common clinopyroxenes, are the divalent cations of Ca, Mg and Fe, and variation in cell-dimensions can be fairly-well related to these elements, and to some extent predicted from our knowledge of their ionic radii. The same cannot be said of minor cations such as Fe^{3+} and Mn^{2+}, although they have been grouped together with Fe^{2+} in the previous works by Kuno and Hess, obscuring the effect of any single cation replacement. This grouping would be alright if Fe^{3+} and Mn^{2+} were almost identical to Fe^{2+} in ionic radius and structural site. While this may be the case for Mn^{2+}, it is not so for Fe^{3+}. The grouping together of Fe^{2+}, Fe^{3+} and Mn^{2+}, as single variable, is useful when contrasting the compositions of pyroxenes, particularly on a "molecular" basis, and was probably introduced for this purpose (Hess, 1949, p. 626). However, it is proposed here that the grouping be discontinued, together with the plotting of pyroxene compositions on a molecular Wo-En-Fs diagram, which introduces the same error, for Fs usually includes $Fe^{2+}+Fe^{3+}+Mn^{2+}$. It is nowadays usual to consider variation in isomorphous mineral groups in terms of ionic substitution, and the changes in optical properties (e.g. Hori, 1954 and 1956, and Ahrens 1958), as well as cell-dimensions, can be related to such substitution. The number of ionic substitutions involved in a group like the clinopyroxenes is such that it would be advantageous to isolate, ultimately, the effect of each variable cation on the mineral's physical properties; the grouping of cations under symbol headings (e.g. $Fe=Fe^{2+}+Fe^{3+}+Mn^{2+}$, or $Mg=Mg^{2+}+Ni^{2+}$, or $Ca=Ca^{2+}+Sr^{2+}$) is therefore a disadvantage for this purpose.

The pyroxenes under discussion have been examined for the effect of only the three major cations, Ca^{2+}, Mg^{2+} and Fe^{2+} (and to a lesser extent, Al^{3+}). The analyses of clinopyroxenes measured for cell-dimensions by Kuno and Hess have been recalculated to obtain the $Ca^{2+}:Mg^{2+}:Fe^{2+}$ percentage ratio in each case (Table 2). In one case (specimen G) this results in $Ca:Mg+Fe^{2+}$ exceeding 0.5. This is due to the large amount of Mn^{2+} ($MnO=3.7\%$) substituting in octahedral co-ordination; only its inclusion with Fe^{2+} (or Mg^{2+}) in the ratio calculation will reduce the Ca% to the likely figure of 50% or less.

UNIT-CELL DIMENSION MEASUREMENTS OF SKAERGAARD PYROXENES

The pyroxene samples were powdered and mixed with acetone, and examined as a smear mount on a glass microscope slide. All measure-

TABLE 2. UNIT-CELL DIMENSIONS AND MAJOR VARIABLE CATION CONTENTS OF THE COMMONER CLINOPYROXENES

Specimen No.	Ca^{2+}	Mg^{2+}	Fe^{2+}	Al^{iv}	Al^{vi}	a Å	b Å	c Å	β	$a \sin \beta$ Å	Cell Volume Å^3	Reference
1	43.4	49.1	7.5	0.099	0.040	9.746	8.910	5.268	73° 53′	9.363	439.6	Brown, 1957, No. 1
2	44.3	43.2	12.5	0.099	0.032	9.751	8.926	5.260	73° 57′	9.371	439.9	Brown, 1957, No. 3
3	44.6	40.3	15.1	0.096	0.015	9.753	8.928	5.259	73° 56′	9.373	440.0	Table 1, No. 3
4	42.3	38.7	19.0	0.084	0.018	9.754	8.940	5.270	73° 59′	9.375	441.7	Brown, 1957, No. 5
5	41.6	37.0	21.4	0.077	0.011	9.751	8.945	5.267	74° 02′	9.376	441.6	Brown, 1957, No. 6
6	40.5	36.5	23.0	0.086	0.019	9.753	8.944	5.267	74° 03′	9.378	441.7	Brown, 1957, No. 7
7	40.9	34.5	24.6	0.091	0.010	9.757	8.948	5.251	74° 06′	9.383	441.0	Brown, 1957, No. 8
8	41.0	31.4	27.6	0.058	—	9.758	8.954	5.255	74° 07′	9.385	441.5	Brown, 1957, No. 9
9	40.2	27.6	32.2	0.063	—	9.763	8.965	5.272	74° 13′	9.395	444.8	Brown, 1957, No. 10
10	42.8	11.1	46.1	0.051	—	(9.802)	9.004	(5.252)	(74° 45′)	9.457	(447.2)	Table 1, No. 10
11	44.5	2.0	53.5	0.068	0.038	—	9.024	—	—	9.486	—	Table 1, No. 11
A	44.3	49.6	6.1	0.094	0.051	9.734	8.907	5.246	73° 51′	9.350	436.9	Brown, 1956, table 4
B	—	100.0	—	—	—	9.618	8.828	5.186	71° 38½′	9.128	417.9	Kuno and Hess, 1953 No. 1
C	8.0	65.7	26.3	0.018	—	9.692	8.917	5.239	71° 27′	9.185	429.3	Kuno and Hess, 1953 No. 2
D	7.3	50.5	42.2	0.033	—	9.712	8.959	5.251	71° 27′	9.208	433.2	Kuno and Hess, 1953 No. 3
E	49.2	47.2	3.6	0.012	0.005	9.750	8.930	5.249	74° 10′	9.380	439.7	Kuno and Hess, 1953 No. 4
F	50.5	17.5	32.0	0.027	0.022	9.804	8.980	5.259	74° 46′	9.460	446.7	Kuno and Hess, 1953 No. 5
G	52.4	3.6	44.0	0.015	—	9.854	9.024	5.263	75° 40′	9.548	453.4	Kuno and Hess, 1953 No. 6
H	47.2	43.2	9.6	0.149	0.065	9.742	8.901	5.268	73° 55′	9.361	438.9	Kuno, 1955, No. 1
I	41.4	47.8	10.8	0.089	0.005	9.744	8.909	5.260	73° 28′	9.341	437.7	Kuno, 1955, No. 5
J	29.0	49.5	21.5	0.094	0.019	9.722	8.925	5.242	72° 57′	9.295	434.9	Kuno, 1955, No. 6
K	20.5	49.4	30.1	0.028	—	9.716	8.944	5.242	72° 20′	9.258	434.1	Kuno, 1955, No. 9

NOTES: (1) Specimens 1–11 are newly measured Skaergaard clinopyroxenes. Analyses corrected for exsolution in specimens 2-9 inclusive.
(2) Specimens A–K are measured clinopyroxenes in the literature, all apparently free from exsolution.
(3) Divalent cations expressed as a percentage of $Ca^{2+}+Mg^{2+}+Fe^{2+}$; in previous literature they have been expressed as a percentage of Ca+Mg+Fe (where $Fe=Fe^{2+}$ $Fe^{3+}+Mn^{2+}$).
(4) Aluminium expressed as number of atoms in 4-fold and 6-fold co-ordination on the

ments were made with a North American Philips X-ray diffractometer using copper radiation at 35 kv and 15 ma.

A reconnaissance traverse was run on each sample at a scan speed of $\frac{1}{2}°$ 2θ per minute, the chart speed being such that 1° 2θ is represented by $\frac{1}{2}$ inch of chart paper. A range of 2θ from 93° to 28° was chosen, in order to locate the best peaks for measurement, and to assess their quality. As the measurements were done on the diffractometer at Princeton University, used earlier by Hess and Kuno (1953, 1955) for all the preceding studies of this type, on clinopyroxenes, the peaks were located and indexed by reference to the original, carefully indexed charts with the help of Professor Hess. The selected peaks were then examined individually at a slower scan speed of $\frac{1}{4}°$ 2θ per minute, so that 1° 2θ is represented by 1 inch of chart paper. Each peak was run six times, and the center could be established within $\pm 0.01°$.

The unit cell dimensions *a*, *b* and *c*, and β, were determined using the 2θ angles for the reflections from the following planes, in decreasing order of 2θ: $\{750\}$, $\{062\}$, $\{53\bar{1}\}$, $\{060\}$, $\{350\}$, $\{600\}$, $\{531\}$, $\{150\}$, $\{510\}$, $\{041\}$, $\{330\}$, $\{31\bar{1}\}$, $\{311\}$, $\{310\}$. An external standard of silicon powder mounted on a glass slide was used. For each run, the standard was introduced and reflection peaks obtained, from which a correction graph was constructed. Values for *d* were obtained using the value $\lambda\mathrm{CuK}\alpha_1 = 1.54050$ Å.

The four most ferriferous pyroxenes (Nos. 8–11) were measured by Hess, Coleman and co-workers after the writer had returned to Oxford, and they reported (written communication 1/2/57) that the peaks became progressively poorer with increasing Fe content. The writer found that, with the magnesian members, only the peaks $\{750\}$ and $\{062\}$ were, at times, unusable, whereas Hess et al. found that with the ferriferous members only $\{531\}$, $\{53\bar{1}\}$ and $\{150\}$ were good peaks, $\{510\}$ fair, while $\{311\}$, $\{31\bar{1}\}$, $\{060\}$ and $\{600\}$ were poor but usable. As a check, the three good peaks were measured with iron radiation ($\lambda\mathrm{FeK}\alpha_1 = 1.93597$ Å), and although the peaks were more ragged than with copper radiation, the 2θ values were larger and therefore allowed more accuracy. Hess (written communication 23/2/57) reported that with specimen numbers 10 and 11, the background was high, the peaks poor, and overlap of some peaks caused complications in $\{531\}$ and $\{53\bar{1}\}$. Thus the results for *a* sin β and *b* are consistent and believed dependable for the iron-rich members, whereas values for *c*, β and *a* are open to some doubt in specimens 10 and 11.

THE EFFECT OF ION SUBSTITUTION ON CELL-DIMENSIONS

The space group of diopside was determined as C_{2h}^6-$C2/c$ by Warren and Bragg (1929) while Warren and Biscoe (1931) showed that hedenbergite and augite possessed a similar structure. Since then, the clinopyroxenes have all been considered to have the diopside structure until Ito (1950) suggested, and Morimoto (1956) and Bown and Gay (1957) demonstrated, that monoclinic pyroxenes of the pigeonite group possessed a space-group C_{2h}^5-$P2_1/c$. The likelihood of a solid-solubility gap between augite and pigeonite had earlier been demonstrated by Hess's (1941) description of the natural associations of clinopyroxenes, and their sub-solidus exsolution textures. Kuno (1955, p. 89) has shown that, except in rapid cooling, the pyroxenes of lavas fall into two groups, one with Ca^{2+} higher than 25%, and the other lower than 15%. Boyd and Schairer (1957, p. 33) find that, in the synthetic system $MgSiO_3$-$CaMgSi_2O_6$, the solvus intersects the solidus over a composition interval of about 15% (wt). They conclude that "homogeneous pyroxenes cannot exist stably in the composition interval between En40 (Di60) and En55 (Di45)," an interval corresponding to between Ca 30% and Ca 22% in the Ca:Mg:Fe diagram used by Kuno, and lying on the Ca-Mg join rather than within the Fe bearing field. Kuno's discovery (1955) of subcalcic augites, however, suggests that supercooling may bridge the miscibility gap between stable pyroxene phases.

Despite this structural break, the cell-dimensions of augites and pigeonites are very similar (Kuno and Hess, 1953), and it is difficult at the moment to detect such a break, from any abrupt change in character of the cell-dimension curves across the pyroxene field. For the purposes of this account, therefore, the clinopyroxenes are considered as a single structural group.

In view of our knowledge of the diopside structure, some prediction can be made as to the particular cell-dimensions affected by certain cations, while a consideration of the relevant ionic radii indicates the probable magnitude of these effects. For example, the *c*-dimension is unlikely to be affected by changes other than Al^{3+} for Si^{4+} in the tetrahedra of the chains aligned in this direction, whereas Ca^{2+}-Mg^{2+}-Fe^{2+} substitutions are likely to have their major effect on the *a*- and *b*-dimensions, and the angle β. In 6-fold coordination the ionic radii are $Ca^{2+} = 0.99$ Å, $Mg^{2+} = 0.66$ Å, $Fe^{2+} = 0.74$ Å (Ahrens, 1952), whereas the radius of Ca^{2+} in 8-fold coordination will be about 1.02 Å. Hence the change from augite to pigeonite should result in a marked decrease in *a* and *b*, whereas the change from diopside to hedenbergite ought to produce an increase (less marked) in *a* and *b*. Kuno and Hess (1953, fig. 5) have already shown that the latter increase does take place, Hess having earlier (1952) discussed it in more detail for orthopyroxenes, but the results of both Kuno and Hess (1953, Fig. 4) and Kuno (1955, Fig. 4) showed, somewhat unexpectedly, that the substitution of the large

Ca^{2+} by the much smaller Fe^{2+} ion resulted in an *increase* in the b-dimension (though a marked decrease in a). An attempt to analyze the cause of this has been made, by considering separately the effects on the b cell-dimension of the replacement of Ca^{2+} by Fe^{2+} and of Ca^{2+} by Mg^{2+}.

The substitution of Fe^{2+} for Mg^{2+} is fairly straightforward, and has the effect on b to be expected from the crystal chemistry. It is shown to be more regular than previously suggested, and this is therefore considered in some detail as an important diagnostic property for clinopyroxenes, as for orthopyroxenes.

The effect of Al^{3+} substitution in the octahedral position is considered separately from the effect of total Al^{3+} substitution in both tetrahedral and octahedral positions, and is shown to be unimportant in the common clinopyroxenes, only having a measurable effect on the b-dimension of one pyroxene so far determined.

In considering the cell-dimensions likely to be most critical in studying the major cation substitutions, attention has been focussed on two: the b-dimension and the value of $a \sin \beta$. The latter usefully combines the size of a and β and in this form indicates the spacing between (100) planes. The third dimension of the cell volume, c, is not yet believed dependable for diagnostic purposes, and the effect upon it of ionic subsitution cannot be demonstrated.

(a) *Substitution of* Fe^{2+} *for* Mg^{2+}

As the common clinopyroxenes contain calcium as the third major divalent cation, $Mg^{2+}:Fe^{2+}$ substitution can only be examined by taking groups which lie on lines parallel to the base-line of the pyroxene trapezium, such as the pigeonite series or the diopside-hedenbergite series. However, detailed studies with full chemical analyses are rare in these compared with the commoner augite-ferroaugite series. So far, Kuno and Hess (1953, Fig. 5) have shown the general effect of $Mg^{2+}:Fe^{2+}$ replacement by plotting three members of the diopside-hedenbergite series, indicating that iron enrichment results in an increase in a, b and β, and has little effect on c. The increase is not linear, in the case considered, for any of the cell-dimensions. For the pigeonite series, figures for only two members have so far been published (Kuno and Hess, 1953, Table 1 and Kuno, 1955, Table 6); there is an additional figure by Morimoto (1956, p. 751) but this pigeonite has unfortunately not been chemically analyzed. With only two points available for the pigeonite series, and three for the diopside-hedenbergite series, the effect of substitution of Fe^{2+} for Mg^{2+} could not be evaluated with precision.

The eleven augites and ferroaugites measured from the Skaergaard intrusion all contain between 40 and 45% Ca (corrected for exsolution).

Taken together with the three diopside-hedenbergites studied by Kuno and Hess, a salite and an augite studied by Kuno (1955, Table 6, Nos. 1 and 5) and an augite studied by Brown (1956, Table 4), there are available chemical analyses and unit-cell dimensions of seventeen calcium-rich clinopyroxenes containing between 40% and 50% Ca. In addition there is the first member of the series to be measured, the diopside of Warren and Bragg (1929, p. 169). If the effect of $Mg^{2+}:Fe^{2+}$ replacement can be shown graphically for these eighteen clinopyroxenes, they then form a series comparable with the orthopyroxenes examined in this way by Hess (1952) and Kuno (1954), and a means exists for comparing ionic substitution in the orthorhombic and monoclinic pyroxenes.

The results cannot be plotted merely as an approximation to a series along the line, say, Ca 44%, because variation in calcium content from this mean figure will influence the iron percentage, desirable as the abcissa. As $Ca^{2+}/Ca^{2+}+Mg^{2+}+Fe^{2+}$ in the present samples averages 44%, however, the $Ca^{2+}:Mg^{2+}:Fe^{2+}$ ratios have been recalculated so that Ca = 44 in each case. In a graph showing changes in unit-cell dimensions with Fe^{2+} content, constructed for clinopyroxenes containing 44% Ca, those pyroxenes containing appreciably more or less than 44% Ca will be displaced from the ideal graph by an amount depending on the effect of Ca on the cell-dimension plotted. Fortunately, in the case of the *b*-dimension, which is of greatest significance in $Mg^{2+}:Fe^{2+}$ replacement, calcium has little effect (Fig. 5), and is negligible in the range ±5% Ca. In the $a \sin \beta$ graphs (Figs. 3 and 4), the effect is more marked and when changes in this dimension with $Mg^{2}:Fe^{2+}$ substitution were graphed (not shown), the series had to be divided into a 'high-calcium' (50%) and a 'low-calcium' (40%) group.

The *b*-dimension (Fig. 2) increases regularly, as Fe^{2+} substitutes for Mg^{2+} in the clinopyroxene structure. The increase is linear and can be expressed by the following equation:

$$b = 8.890\ \text{Å} + 0.00256(\text{Fe})\ \text{Å}^* \qquad (1)$$

where

$$\text{Fe} = 56\text{Fe}^{2+}/\text{Mg}^{2+} + \text{Fe}^{2+}$$

The most striking property of this equation is that the increment is the same as that obtained by Hess for the orthopyroxenes (1952, p. 176) in which

$$b = 8.805\ \text{Å} + 0.00255\ (100 - \text{mg})\ \text{Å}$$

---

* For the reasons stated by Yoder and Sahama (1957, p. 485), in such equations the independent variable should often be the spacing or cell-dimension, in which case this equation becomes:

$$\text{Fe} = \frac{b}{.00256} - 3473$$

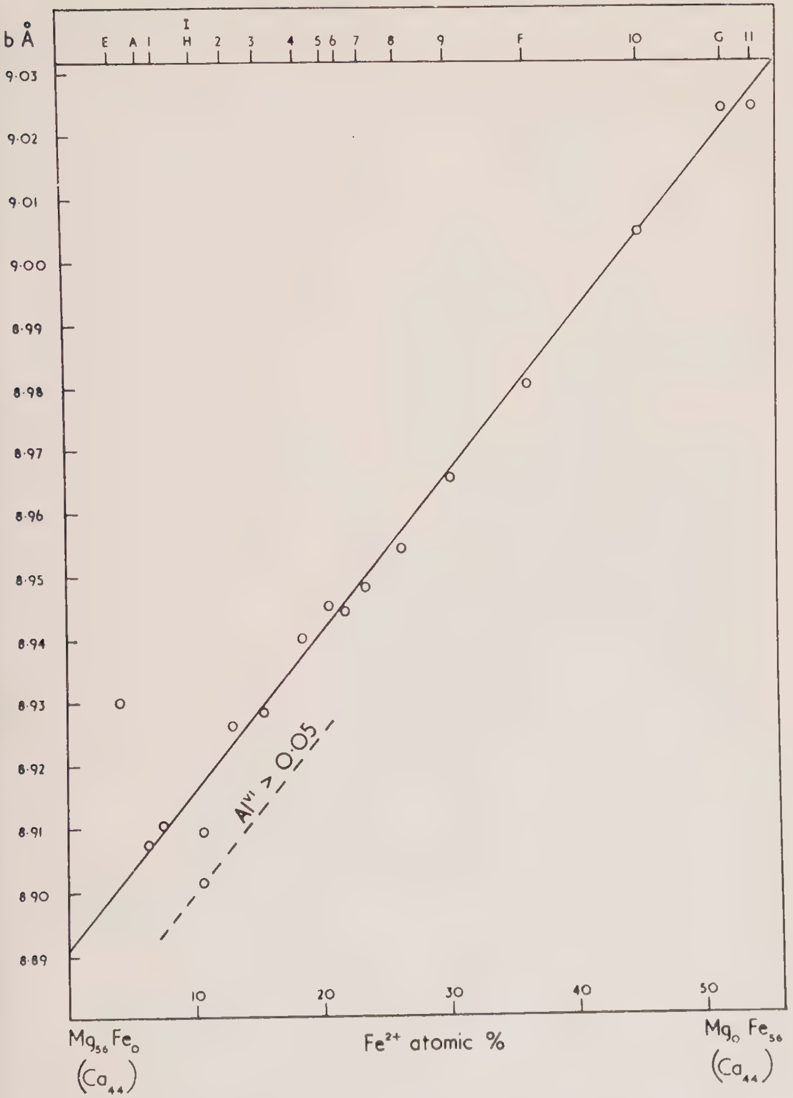

FIG. 2. Variation in the *b*-dimension of the clinopyroxene unit-cell, with $Mg^{2+}:Fe^{2+}$ substitution. The specimen numbers refer to those on Fig. 1 and in Table 2.

In the two equations, the factors (Fe) and (100-mg) mean the same thing, that is they represent the steadily increasing percentage of iron at the expense of magnesium, while the figures 8.890 Å and 8.805 Å represent the *b*-dimension of the magnesian end-members of the two series. The significant figure is the factor of 0.00256, which corresponds to the slope of the line. The identical nature of the increase in both monoclinic and orthorhombic pyroxenes emphasizes their similarity of structure, and the fact that in each series the iron and magnesium atoms are stacked along the *b*-axis.

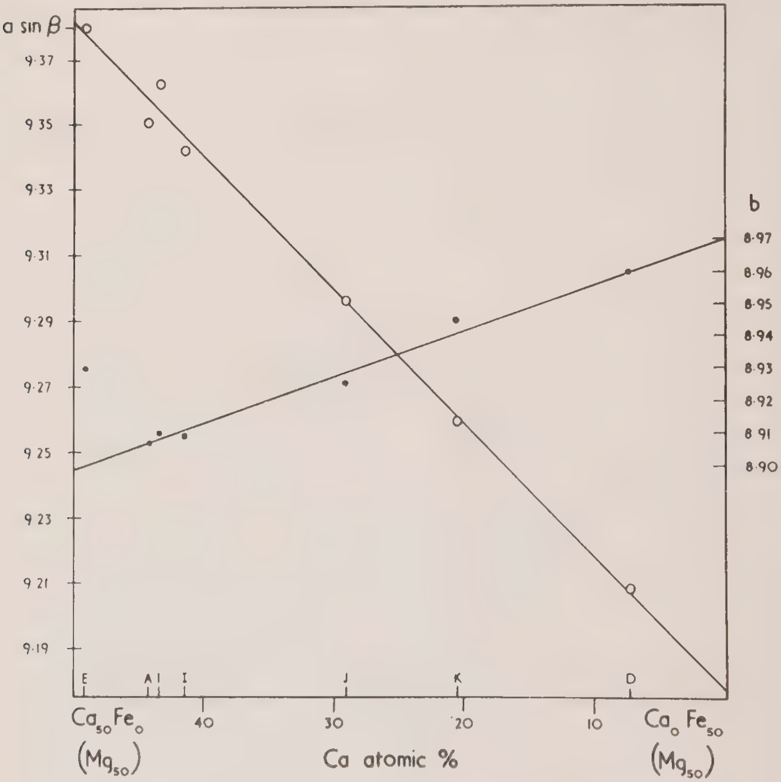

FIG. 3. Variation in *b* (dots) and *a* sin *β* (circles) with $Ca^{2+}:Fe^{2+}$ substitution.

The regular identical increase in *b* for $Mg^{2+}:Fe^{2+}$ substitution in both groups of pyroxenes makes it possible to estimate the *b*-dimensions of hedenbergite and ferrosilite, knowing those of diopside and clinoenstatite respectively, and the intermediate members of each series. Before doing this, however, a cross-check was made by establishing the nature of the changes in *b* from diopside to clinoenstatite and from hedenbergite to ferrosilite (see later), so that given a dependable figure for diopside, the values for the other three end-members could be estimated from more than one variable. Using Warren and Bragg's figure for almost pure diopside (1929, p. 169) of $b = 8.89$ Å, pure hedenbergite ought to have

$b=9.018$ Å $(8.89+50\times0.00256)$. However, as the main purpose of the present paper is to present curves and a determinative diagram for common clinopyroxenes, with average amounts of minor constituents, the values for the diopside corner of the trapezium are taken by extrapolation from the two linear series ($Mg^{2}:Fe^{2+}$ and $Ca^{2+}:Fe^{2+}$) intersecting

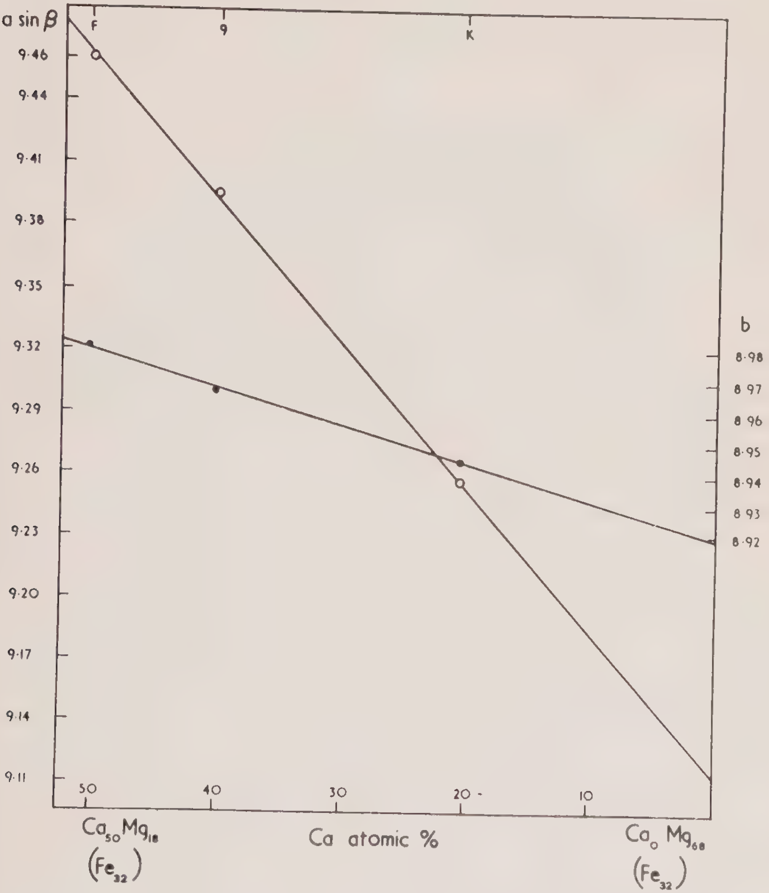

FIG. 4. Variation b (dots) and $a \sin \beta$ (circles) with $Ca^{2+}:Mg^{2+}$ substitution.

at this corner (Fig. 2 being corrected so as to be appropriate for Ca 50, rather than Ca 44). Thus diopside has $b=8.90$ Å (p. 29) and similarly hedenbergite has $b=9.028$ Å, the latter being checked against the $Ca^{2+}:Mg^{2+}$ substitution series (p. 31).

The linear relationship discussed above is shown by fifteen of the pyroxenes (Fig. 2) within a band indicating a probable accuracy of ±0.003 Å (equivalent, from the above equation, to ±1% Fe). Two pyroxenes fall outside this band, the one falling below having an abnormally high Al^{3+} content (specimen H, Table 2). The pyroxene falling above the band, a skarn diopside (specimen E, Table 2) is comparable with many falling on the line in containing low amounts of Al^{3+}, Fe^{3+}, Ti^{4+} and Na^{+}. No satisfactory explanation can, at the moment, be offered for the anomalous *b*-dimension of this specimen.

The *a* sin *β* dimension is too much affected by calcium-content to be profitably illustrated on a $Mg^{2+}:Fe^{2+}$ substitution diagram. The effect of such substitution on *a* sin *β* can be seen, however, in Fig. 5, constructed from the other two substitution series involving calcium. The relationship is probably linear, as shown, and can be checked by taking groups with approximately equal calcium-content (e.g. specimens E and F, or I, 4 and 10, Table 2), although these are too rare and closely-spaced to be of much value.

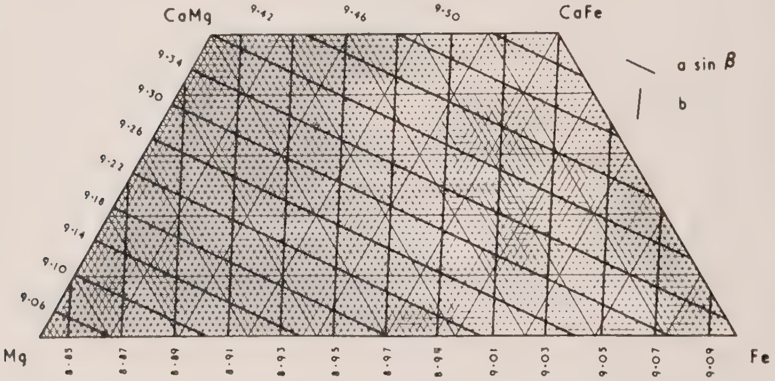

Fig. 5. Variation in *b* and *a* sin *β* throughout the common clinopyroxene trapezium. The lines are constructed on the basis of the results illustrated in Figs. 2, 3 and 4, and are only tentative in those parts of the field for which no data are available.

The changes in *c*-dimension (Table 2) are not shown graphically as the plotted points show no pattern, possibly due to the difficulty of determining *c*. The *c*-dimensions of the Skaergaard series are consistently higher than the others, particularly in those members containing exsolved pigeonite ||001, and it is tentatively suggested that expansion along *c* may be related to this exsolution.

(b) *Substitution of Fe^{2+} for Ca^{2+}*

This type of substitution is demonstrated by examining a series of clinopyroxenes which lie on, or close to, a line parallel to the CaFe-Fe side of the trapezium. A similar series has already been examined by Kuno (1955), the graphical representation of changes in cell-dimensions from diopside to pigeonite (loc. cit. Fig. 4) being a refinement of those shown by Kuno and Hess (1953, Fig. 4). The latter did not give β measurements, and therefore a and c values, for the series.

The reasons for re-considering this substitution are two-fold. Firstly, the curves of both Kuno and Hess, and Kuno, show the surprising result that the replacement of the large Ca^{2+} ion by the much smaller Fe^{2+} ion results in an *increase* in the b-dimension, though they did not comment upon this phenomenon. Secondly, the effect of Al^{3+} on the b-dimension was stressed, by constructing separate curves for pyroxenes high in Al^{3+}. The graphs for b, in each paper, are curved. As the present writer believes that the greater part of the Al^{3+} in these pyroxenes is in four-fold co-ordination, with little effect on the b-dimension, the graphs of Hess and Kuno have been re-drawn with this in mind. Anticipating that the change in b might prove to be linear, it was hoped that an examination of the regular change with $Ca^{2+}:Fe^{2+}$ substitution, compared with that for $Mg^{2+}:Fe^{2+}$ and $Ca^{2+}:Mg^{2+}$ substitution, would help to solve the problem of why b should increase with Fe^{2+} substitution for Ca^{2+}.

Two pyroxenes of the new series are introduced (from Skaergaard and Rhum) which, taken together with the three calcium-poor pyroxenes of Kuno and Hess, form a series (Fig. 1) on the line $Mg = 50\%$ ($\pm 1\%$). Two of the calcium-rich specimens previously plotted by Kuno (H and I, Table 2) are also included and, although they contain 43% and 48% Mg respectively, they clearly form part of the regular series. The St. Lawrence County diopside (E, Table 2) cannot be used, because of the high value for b (mentioned earlier (p. 28)).

The variation of b with $Ca^{2+}:Fe^{2+}$ substitution (Fig. 3) is clearly linear, and there is no doubt that this cell-dimension *increases* as iron substitutes for calcium. The change can be expressed by the equation:

$$b = 8.90 + 0.0014\,(50 - \mathrm{Ca})\ \mathrm{A} \qquad (2)$$

where

$$\mathrm{Ca} = \frac{100 \cdot Ca^{2+}}{Ca^{2+} + 50 + Fe^{2+}}$$

The points fall in a zone defining a probable accuracy of ±0.003 Å. Extrapolation backwards indicates a figure for diopside of 8.90 Å (±0.003 Å). If the value of 8.90 were replaced in this equation by the value for b of hedenbergite, then the equation would probably represent the changes in the hedenbergite-ferrosilite series (the same can be said of equation (3)). The total replacement of Ca^{2+} by Fe^{2+}, with Mg constant, results in an increase in b of 0.07 Å, so that in the calcium-free clinoenstatite-ferrosilite series the clinopyroxene with a composition $Mg_{50}Fe_{50}$ should have a *b*-dimension of 8.97 Å.

The cause for the regular increase in *b*, as iron substitutes for calcium, remains to be considered. The Fe^{2+} ions cannot be directly substituting in the Ca^{2+} sites of the structure, or this would result in a decrease in *b;* nor can it be suggested that they are substituting without a shrinkage, for this would not explain the actual expansion observed. However, in passing from $Ca_{50}Mg_{50}$ to $Fe_{50}Mg_{50}$, the $Fe^{2+}:Mg^{2+}$ ratio increases. As will be shown in the next section in passing from $Ca_{50}Mg_{50}$ to Mg_{100}, *b* decreases by a small amount, but in passing from Mg_{100} to $Fe_{50}Mg_{50}$ *b* increases by about twice that amount. Thus the difference between this loss and gain must be made up in the passage from $Ca_{50}Mg_{50}$ to $Fe_{50}Mg_{50}$. In other words, the change in *b* is really governed by the change in the $Fe^{2+}:Mg^{2+}$ ratio, which increases in $Ca^{2+}:Fe^{2+}$ substitution because Mg^2 remains constant (the decrease in Ca^{2+} is reflected in the decrease in $a \sin \beta$).

This means that the substitution discussed in this section is not a simple one, as the substitution of Fe^{2+} for Mg^{2+} discussed earlier, where expansion of both $a \sin \beta$ and *b* took place. Here there has been a change in shape of the unit-cell with a decrease in $a \sin \beta$ and expansion along *b*. This change of structure would require more mobility of the ions than is necessary for the $Mg^{2+}:Fe^{2+}$ substitution. It is of interest, in this connection, to note that the series considered in this section includes a high-temperature assemblage of sub-calcic augites and pigeonite. The ionic mobility required for this type of structural change would be confined to the higher temperature range of crystallization, and the presence of a miscibility gap at lower temperatures (p. 22) understandable. This is in direct contrast to the augite and orthopyroxene series, in which the simple substitution of Fe^{2+} for Mg^{2+} results in complete isomorphous series at lower temperatures, given chemical fractionation under equilibrium conditions.

The $a \sin \beta$-dimension decreases regularly with substitution of Fe^{2+} for for Ca^{2+} (Fig. 3) and can be expressed by the linear equation:

$$a \sin \beta = 9.38 - 0.0040\ (50 - \mathrm{Ca})\ \text{Å} \tag{3}$$

where

$$\mathrm{Ca} = \frac{100 \cdot Ca^{2+}}{Ca^{2+} + 50 + Fe^{2+}}.$$

The change in $a \sin \beta$ is marked, and indicates the importance of this dimension as a diagnostic parameter for the estimation of calcium-content in the clinopyroxenes. The change with total replacement of Ca^{2+}

by Fe^{2+} is 0.20 Å, so that $Mg_{50}Fe_{50}$ in the clinoenstatite-ferrosilite series would have $a \sin \beta = 9.18$ Å.

(c) *Substitution of Mg^{2+} for Ca^{2+}*

This substitution series falls on a line parallel to the CaMg-Mg side of the trapezium. There are not as many data available for this as for the other two series considered, but they suffice for the present purpose of establishing the general effect of this substitution compared with the other two. There are three clinopyroxenes which form a series parallel to the line $Fe = 31 \pm 1\%$ (specimens F, 9 and K, Table 2 and fig. 1), and a less useful series of three parallel to the line $Fe = 44 \pm 2\%$ (specimens G, 10 and D, Table 2 and fig. 1). Both series were used to determine the most probable slope of the graphs for in the case of both b and $a \sin \beta$ the two series fall on almost parallel straight lines, separated by an amount determined by their difference in iron content. In view of their similarity, only the graphs for the less ferriferous series have been reproduced (Fig. 4), as they serve to illustrate the points under consideration; the validity of the graphs and equations can be checked, if desired, by plotting the other series (Table 2).

The b-dimension decreases regularly with the substitution of Mg^{2+} for Ca^{2+}, in direct contrast with the increase shown by the substitution of Fe^{2+} for Ca^{2+}. The relationship is linear, and can be expressed by the equation:

$$b = 8.98 - 0.0012\,(50 - \mathrm{Ca})\ \text{Å} \qquad (4)$$

where

$$\mathrm{Ca} = \frac{100 \cdot Ca^{2+}}{Ca^{2+} + Mg^{2+} + 31}$$

This equation would be of more general application (as would equation (5)) if the figure of 8.98 were replaced by the b dimension of either diopside (for the diopside-clinoenstatite series) or hedenbergite.

The total replacement of Ca^{2+} by Mg^{2+} results in a decrease in b of 0.06 Å, which is rather less than the increase of 0.07 Å for total replacement of Ca^{2+} by Fe^{2+} (equation (2)). Assuming a figure of $b = 9.028$ Å for hedenbergite, then the clinopyroxene $Mg_{50}Fe_{50}$ of the clinoenstatite-ferrosilite series would have $b = 8.968$ Å. From the $Ca^{2+}:Fe^{2+}$ substitution series, this latter clinopyroxene was expected to have $b = 8.970$ Å (p. 30). The fact that these two figures are almost identical is the best possible evidence for accepting the values obtained for the three substitution series.

The $a \sin \beta$ dimension decreases regularly, and most markedly, with the substitution of Mg^{2+} for Ca^{2+} (Fig. 4). The change is again linear, and can be expressed by the equation:

$$a \sin \beta = 9.46 - 0.0070\ (50 - \mathrm{Ca})\ \mathrm{A} \tag{5}$$

where

$$\mathrm{Ca} = \frac{100 \cdot \mathrm{Ca}^{2+}}{\mathrm{Ca}^{2+} + \mathrm{Mg}^{2+} + 31}$$

The total replacement of Ca^{2+} by Mg^{2+} would result in a decrease in $a \sin \beta$ of 0.35 Å. An independent figure for hedenbergite is not available, as the $Mg^{2+}:Fe^{2+}$ substitution series examined was not suitable for determining the linear variation in $a \sin \beta$. However, taking the figure for $Mg_{50}Fe_{50}$ of $a \sin \beta = 9.18$ Å obtained from the $Ca^{2+}:Fe^{2+}$ series (p. 31), hedenbergite ought to have $a \sin \beta = 9.53$ Å (the figure obtained by Kuno and Hess, 1953, Table 1, for a specimen close to hedenbergite, was $a \sin \beta = 9.55$ Å).

(d) *The effect of* Al^{3+}

For orthopyroxenes, Hess (1952) was able to demonstrate that a high Al_2O_3 content (in excess of $3\frac{1}{2}\%$) in two specimens produced a marked effect on the cell-dimensions, while the absence of Al_2O_3 from a pure enstatite produced a similar, but opposite effect. The substitution of the smaller Al^{3+} for Mg^{2+} or Fe^{2+} in the octahedral positions resulted in a decrease in b, while the substitution of small amounts of the larger Al^{3+} for Si^{4+} in the tetrahedral position resulted in a slight increase in c. Kuno (1954, Fig. 2) showed a similar effect of Al^{iv} on c, but the curve for b corresponding to a high Al^{vi} content is more appropriate for his specimens (Nos. 11 and 13) containing hardly any Al^{vi}.

For clinopyroxenes, Kuno and Hess indicated (1953, fig. 4) that for three of the specimens plotted (I, J and K of Table 2) a high Al^{3+} content decreased b, compared with the other two specimens (D and E of Table 2). Kuno (1955, fig. 4) also indicated this effect, as shown by three specimens (H, I and J of Table 2), noting also that the high Al^{3+} of two of them resulted in an increase in the c-dimension.

The effect of Al^{3+} on the b-dimension of the clinopyroxenes has been reconsidered in the present study, and although it is believed to be as significant, in theory, as suggested by the previous investigators, only one specimen among the twenty-two so far measured appears to contain enough Al^{3+} in six-fold coordination for its effect to be observed. Hess (1952, p. 177) showed why entry of Al^{3+} in six-fold coordination, and not four-fold coordination, would shorten the b-dimension of orthopyroxenes, but in later work on the clinopyroxenes both Kuno and Hess considered only the effect of *total* Al^{3+} on the b-dimension. In the three specimens shown to contain much more than 0.05 Al^{3+} atoms to 6 oxygen atoms, as revealed by the chemical analyses, the greater part of this aluminium appears to be substituting for Si^{4+} in the tetrahedral position (Kuno, 1955, Table 1, nos. 1, 5 and 6). Of the eleven Skaergaard clinopyroxenes, none contains more than 0.05 Al^{3+} atoms to six oxygens, in six-fold coordination (judging from the recalculation of the analyses, Table 2), although some contain as much as 0.139 total Al^{3+} atoms. Thus, the only clinopyroxene which contains a little more than average aluminium in the octahedral position is the salite from a eucrite block in Taga volcano (Kuno, Table 1, no. 1), which contains 0.065 Al^{3+} atoms to six oxygens, as compared with 0.040 in the most extreme example from the Skaergaard series.

The plot of *b*-dimensions in Figs. 2, 3 and 4 shows that the majority of the specimens form a linear series. One which falls well off the line is the salite mentioned above (specimen H of Fig. 2), which indicates that although much variation in Al^{3+} content below 0.05 is tolerated without change in *b*, once this critical amount is exceeded a reduction in *b* is observed. The diopside from St. Lawrence County also falls well off the line. The reason for this specimen's high *b* value is not understood; it cannot be attributed to its low Al^{3+} content, as many Skaergaard examples appear to contain none at all in six-fold coordination.

The effect of Al^{3+} on *c* has not been considered in this account, in view of the unreliability of the new *c*-values, but in view of the high proportion of Al^{3+} appearing to substitute for Si^{4+} in the more calcic clinopyroxenes (cf. Wilkinson, 1957, p. 128, and Table 3) it is likely that the "abnormal" curves for *c* will be those for low Al^{3+}, rather than for high Al^{3+} content.

The Determination of Ca:Mg:Fe Ratio from the Unit-Cell Dimensions

The commoner clinopyroxenes, such as those considered in this paper, contain only minor amounts of elements such as Fe^{3+}, Na^{+} and Ti^{4+}, and the estimation of their composition from physical properties is based on correlation of these properties with the Ca^{2+}:Mg^{2+}:Fe^{2+} ratio of the mineral. The present study of the three major substitution series makes it possible to estimate the variation of the unit-cell dimensions, *b* and $a \sin \beta$, with complete substitution of the three major variable cations. This is simplified by the linear variation in these two cell-dimensions (within the present limits of accuracy) with ionic substitution.

A preliminary diagram relating the cell-dimensions of clinopyroxenes to composition has been given by Kuno and Hess (1953, Fig. 6), outlining a general pattern for the variation which is confirmed by the present study. The present diagram (Fig. 5), however, differs from that of Kuno and Hess in several features which are largely refinements based on the extra data now available. The cell-dimensions chosen for the graph are b and $a \sin \beta$, rather than b and a. Both β and c were recorded as points, rather than curves, by Kuno and Hess; the plotting of $a \sin \beta$ usefully combines the changes in a and β, while the changes in c are too slight and irregular to be of much value at present. The second change in the new diagram is that, whereas the a and b lines of Kuno and Hess were curved, irregularly spaced and non-parallel, the present set are straight, evenly-spaced and parallel. Finally, the values for b and $a \sin \beta$ of the end-members of the trapezium CaMg-Mg-Fe-CaFe are slightly different in the present diagram.

The isodimensional lines for b were constructed as follows. Firstly, the values for hedenbergite, clinoenstatite and ferrosilite were obtained, accepting the value of $b = 8.900$ Å for diopside. From the $Mg^{2+}:Fe^{2+}$ substitution series (p. 27), hedenbergite would have $b = 8.900 + 0.128 = 9.028$ Å. From the $Ca^{2+}:Fe^{2+}$ substitution series (p. 29) ferrosilite would have $b = 9.028 + 0.07 = 9.098$ Å, while $Mg_{50}Fe_{50}$ would have $b = 8.900 + 0.07 = 8.970$ Å. From the $Ca^{2+}:Mg^{2+}$ substitution series (p. 31) clinoenstatite would have $b = 8.900 - 0.06 = 8.84$ Å, while $Mg_{50}Fe_{50}$ would have $b = 9.028 - 0.06 = 8.968$ Å. From the $Mg^{2+}:Fe^{2+}$ substitution series, ferrosilite would have $b = 8.84 + 0.256 = 9.096$ Å.

Given the values for the four corners of the trapezium, and the linear equations for $Mg^{2+}:Fe^{2+}$ substitution, the diopside-hedenbergite and clinoenstatite-ferrosilite series can be sub-divided into equal units and joined by the isodimensional lines shown in Fig. 5. As the incremental change of b with $Mg^{2+}:Fe^{2+}$ substitution (and constant Ca^{2+}) appears to be the same throughout, regardless of actual calcium content, the lines cannot be curved and irregularly spaced but must be straight, parallel, and equidistant. The slant towards the Mg side of the field is a reflection of the slight difference in total change of b in the $Ca^{2+}:Fe^{2+}$ series ($+0.07$) compared with the $Ca^{2+}:Mg^{2+}$ series (-0.06). If these were identical (0.065), then the b lines would run vertically down the field.

The isodimensional lines for $a \sin \beta$ were constructed in a somewhat similar way. Accepting a figure for diopside of $a \sin \beta = 9.38$ Å (Fig. 3), then from the $Ca^{2+}:Fe^{2+}$ substitution series $Mg_{50}Fe_{50}$ would have $a \sin \beta = 9.38 - 0.20 = 9.18$ Å. From the $Ca^{2+}:Mg^{2+}$ substitution series, $Ca_{50}Fe_{50}$ would have $a \sin \beta = 9.18 + 0.35 = 9.53$ Å, while Mg_{100} would have $a \sin \beta = 9.38 - 0.35 = 9.03$ Å. From the $Ca^{2+}:Fe^{2+}$ series ferrosilite would have $a \sin \beta = 9.53 - 0.20 = 9.33$ Å. In view of the lack of a linear equation for the $Mg^{2+}:Fe^{2+}$ series, cross-checks are not applicable in this case, and given more data the $a \sin \beta$ curves might ultimately be refined. Nevertheless, the linear relationships for the other two substitution series make it possible to construct the isodimensional lines with little difficulty. Thus the CaMg-Mg and CaFe-Fe sides of the trapezium can be divided into equal sections according to the linear equations, and straight, parallel, equidistant lines drawn. Again, it is not possible to meet the requirements of these two equations by drawing curved and irregularly-spaced lines.

The values obtained in Fig. 5 pose a problem in connection with the cell dimensions of clinoenstatite. From the diagram, it would appear to have $b=8.84$ Å, $a \sin \beta=9.03$ Å. Kuno and Hess (1953) obtained values for synthetic clinoenstatite, of $b=8.83$ Å, $a \sin \beta=9.13$ Å (Specimen B, Table 2), while Atlas (1952) obtained values of $b=8.86$ Å, $a \sin \beta=9.11$ Å. By the method used in this paper, of examining ion substitution series and extrapolating, it is difficult to arrive at a figure for $a \sin \beta$ approaching 9.13 Å. On the other hand, naturally-occurring clinopyroxenes have been used for the present study, and the values obtained for the clinoenstatite-ferrosilite series relate to somewhat hypothetical minerals, conveniently regarded as end-members of the natural series which, for direct comparison, would have had to crystallize under natural magmatic or metamorphic conditions and contain similar amounts of the minor cations.

Conclusions

There are now sufficient data, from the x-ray measurements of twenty-three analyzed clinopyroxenes, to estimate with some accuracy the effect on the unit-cell dimensions b and $a \sin \beta$ of substitution of Fe^{2+} for Mg^{2+}, Fe^{2+} for Ca^{2+}, and Mg^{2+} for Ca^{2+}, and to be more sure of the effect of Al^{3+} substitution in the octahedral lattice-sites of the structure. This stage is a necessary preliminary to any further studies on the effect of other cations such as Fe^{3+}, Ti^{4+}, Na^+ or Li^+.

The substitution of Fe^{2+} for Mg^{2+} results in a regular increase in b, and an increase which is probably regular in $a \sin \beta$ and unit-cell volume. The increase in b is linear, and the increment for each atom substituted (as expressed by the linear equation) is identical with that for the orthopyroxenes. This regularity may account for the fact that Mg^{2+}:Fe^{2+} substitution is dominant and continuous in both series during crystal fractionation. The regularity is at variance with Ramberg and De Vore's (1951) findings, but in view of Sahama and Torgeson's (1949) thermochemical studies, it is believed that complete solid solution exists in the orthopyroxene series.

The substitution of Fe^{2+} for Ca^{2+} results in a regular increase in b and decrease in $a \sin \beta$, both changes being expressible in linear equations. The linear relationship suggests complete solid solution throughout the series, which may be explicable on the grounds that the specimens corsidered include sub-calcic augites which may have crystallized metastably owing to quick-cooling from a high temperature. The increase in b is difficult to explain by simple substitution of the smaller Fe^{2+} for Ca^{2+} and may indicate greater ionic mobility in this higher-temperature series. The structural change attendant upon an increase in b and decrease in $a \sin \beta$ may not be possible with stable crystallization at lower temperatures and would help to explain the miscibility gap in this compositional range, in plutonic rocks. The absence of a break in the linear series examined is of interest in view of the slight differences which exist between the structure of augite and pigeonite (see p. 22).

The substitution of Mg^{2+} for Ca^{2+} results in a regular decrease in b, $a \sin \beta$ and unit-cell volume, the latter decrease being of a high order.

The incorporation of Al^{3+} in octahedral sites results in a slight decrease in b. However, this effect is only shown by one of the 23 clinopyroxenes so far measured, the rest containing so little Al^{3+} in this position that it has no measurable effect on the b or $a \sin \beta$ unit-cell dimensions. The distinction made between Al^{3+} in six-fold coordination and total Al^{3+} is the chief reason why the graphs shown here are linear and differ from the curves shown by previous investigators.

The effects on unit-cell dimensions of the three major ionic substitutions in the commoner clinopyroxenes can be combined in the pyroxene part of the $CaSiO_3$-$MgSiO_3$-$FeSiO_3$ triangular diagram (Fig. 5), and the diagram used to estimate composition from measured values for b and $a \sin \beta$. In this connection, the remarks made earlier (p. 17) on the effect of sub-solidus exsolution and the minor cations should be borne in mind.

The results incorporated in Fig. 5 might ultimately be used to elucidate some of the problems associated with the role of the clinopyroxenes in petrogenesis, when more is known about the stability of certain structures at different temperatures. The implication would be that in a particular magma certain pyroxene structures would form at particular temperatures, and with cooling the magma would become progressively depleted in the particular cation assemblage which could fit easily into these structures. Thus the trend of compositional change followed by the Skaergaard pyroxenes (Brown, 1957, Fig. 2) is initially one which shows no change in $a \sin \beta$. If, at a lower temperature, the $a \sin \beta$ dimension can expand, then the structure can incorporate more calcium and the direction of the trend will change (Muir, 1951, Fig. 1). This type of change has often been attributed to factors such as a decrease in the aluminium content of the magma so that less feldspar crystallizes and the clinopyroxene *must* take the surplus calcium into its structure. This implies that the magma chemistry influences structural changes in the minerals, whereas it is suggested here that the physical conditions might influence the structural changes which, in turn, affect the magma chemistry.

ACKNOWLEDGMENTS

The unit-cell measurements were made at the Department of Geology, Princeton University, and the writer takes this opportunity of thanking the staff for their generous help on many occasions. Particular thanks are extended to Prof. H. H. Hess for the opportunity of working in the Department, and for much help and encouragement, to Prof. L. C. Coleman for useful advice, and to them and Robert Hargraves and Finley Campbell for measuring the cell-dimensions of specimens 8, 9, 10 and 11. The grant of a Fellowship from the Commonwealth Fund of New York is gratefully acknowledged.

Ten of the chemical analyses were made in the Department of Geology, Oxford University, by Dr. E. A. Vincent, to whom thanks are expressed for contributing the results of his skilful and accurate semi-micro analyses, which form an important part of this study. Thanks are also due to Dr. P. E. Brown for the analysis of specimen no. 3, and to Mr. N. E. Butcher for separating specimen no. 11.

The author is deeply indebted to Prof. L. R. Wager, Oxford University, for making this study possible, and for making available the unique series of ferriferous rocks from the Skaergaard intrusion for pyroxene investigation. The material was collected during the East Greenland Geological Expedition, 1953, led by Prof. L. R. Wager and Prof. W. A. Deer, of which the author was a member. The leaders thank the Royal Society and the Percy Sladen trustees for generous financial assistance.

REFERENCES

AHRENS, L. H. (1952), The use of ionization potentials. Part 1. Ionic radii of the elements. *Geoch. Cosm. Acta*, **2,** 155–169.

——— (1958), Variation of refractive index with ionization potential in some isostructural crystals: *Min. Mag.*, **31,** 929–936.

ATLAS, L. (1952), The polymorphism of $MgSiO_3$ and solid state equilibria in the system $MgSiO_3$-$CaMgSi_2O_6$. *J. Geol.*, **60,** 125–147.

BOWN, M. G. AND GAY, P. (1957), Observations on pigeonite. *Acta Cryst.*, **10,** 440.

BOYD, F. R. AND SCHAIRER, J. F. (1957), System $MgSiO_3$-$CaMgSi_2O_6$. Program 1957 Ann. Meetings, G.S.A., p. 33.

BROWN, G. M. (1956), The layered ultrabasic rocks of Rhum, Inner Hebrides. *Phil. Trans. Roy. Soc.*, ser. B, **240,** 1–53.

——— (1957), Pyroxenes from the early and middle stages of fractionation of the Skaergaard intrusion, East Greenland. *Min. Mag.*, **31,** 511–43.

CHEVALLIER, R. AND MATHIEU, S. (1958), Susceptibilité magnétique spécifique de pyroxènes monocliniques. *Bull. de la Soc. Chim. de France,* **5,** 726–729.

——— and Martin, R. (1959), Le moment magnétique de l'ion ferreux dans une série de pyroxènes monocliniques. *Bull. de la Soc. Chim. de France*, **9**, 9–10.

Hess, H. H. (1941), Pyroxenes of common mafic magmas. *Am. Mineral.*, **26**, 515–535; 573–594.

——— (1949), Chemical composition and optical properties of common clinopyroxenes. *Am. Mineral.*, **34**, 621–666.

——— (1952), Orthopyroxenes of the Bushveld type, ion substitutions and changes in unit cell dimensions. *Am. J. Sci.*, *Bowen vol.*, 173–187.

Hori, F. (1954), Effects of constituent cations on the optical properties of the clinopyroxenes. *Sci. papers*, *College Gen. Educ.*, *Univ. Tokyo*, **4**, 71–83.

——— (1956), Effects of constituent cations on the refractive indices of orthopyroxenes. *Mineral. Jour.*, 1, no. 6, 359–371.

Ito, T. (1950), X-ray studies on polymorphism. Maruzen Co., Tokyo.

Kuno, H. (1954), Study of orthopyroxenes from volcanic rocks. *Am. Mineral.*, **39**, 30–46.

——— (1955), Ion substitution in the diopside-ferropigeonite series of clinopyroxenes. *Am. Mineral.*, **40**, 70–93.

——— and Hess, H. H. (1953), Unit cell dimensions of clinoenstatite and pigeonite in relation to other common clinopyroxenes. *Am. J. Sci.*, **251**, 741–752.

Morimoto, N. (1956), The existence of monoclinic pyroxenes with the space group $C_{2h}^{5}-P_{2}1/c$. *Proc. Japan Acad.*, **32**, 750–752.

Muir, I. D. (1951), The clinopyroxenes of the Skaergaard intrusion, eastern Greenland. *Min. Mag.*, **29**, 690–714.

Ramberg, H. and De Vore, G. (1951), The distribution of Fe^{++} and Mg^{++} in coexisting olivines and pyroxenes. *J. Geol.*, **59**, 193–210.

Sahama, Th. G. and Torgeson, D. R. (1949), Thermochemical study of the olivines and orthopyroxenes. *Rept. of investigations*, *U. S. Dept. of Interior*, *Bureau of Mines*, R.I. **4408**, 1–24.

Warren, B. E. and Biscoe, J. (1931), The crystal structure of the monoclinic pyroxenes. *Z. Krist.*, **80**, 391–401.

Warren, B. E. and Bragg, W. L. (1929) The structure of diopside, $CaMg(SiO_3)_2$. *Z. Krist.*, **69**, 168–193.

Wilkinson, J. F. G. (1957), The clinopyroxenes of a differentiated teschenite sill near Gunnedah, New South Wales. *Geol. Mag.*, **94**, 123–134.

Yoder, H. S. and Sahama, Th. G. (1957), Olivine *x*-ray determinative curve. *Am. Mineral.* **42**, 475–491.

Manuscript received April 15, 1959.

THE AMERICAN MINERALOGIST, VOL. 45, JANUARY-FEBRUARY, 1960

WEEKSITE, A NEW URANIUM SILICATE FROM THE THOMAS RANGE, JUAB COUNTY, UTAH[1]

W. F. Outerbridge, M. H. Staatz, R. Meyrowitz, and A. M. Pommer, *U. S. Geological Survey; Washington, D. C., Denver, Colorado, Washington, D. C., and Washington D. C.*

Abstract

Weeksite, $K_2(UO_2)_2(Si_2O_5)_3 \cdot 4H_2O$, is a new uranyl silicate mineral named for Dr. Alice D. Weeks. It is a soft yellow non-fluorescent mineral with a waxy to silky luster, and it crystallizes chiefly in radiating fibrous clusters. In the Thomas Range, where it was first found, it occurs in opal veinlets in rhyolite and as replacements of pebbles in a tuffaceous conglomerate. Weeksite also has been identified from eight other localities in Pennsylvania, Wyoming, California, New Mexico, Mexico, Arizona, and Texas.

Weeksite is biaxial negative $2V=$about 60°; dispersion $r>v$, strong; $\alpha=1.596$, $\beta=1.603$, $\gamma=1.606$; $X=b$, colorless, $Y=c$, pale yellow green, $Z=a$, yellow green. The measured specific gravity is about 4.1.

A chemical analysis of material from the Thomas Range showed: K_2O 5.5, Na_2O 0.7, BaO 1.4, CaO 1.1, UO_3 51.5, SiO_2 33.6, H_2O 6.6, Al_2O_3 0.6, CO_2 0.3; total 101.3%. A synthetic Na analogue of weeksite showed Na_2O 7.2, UO_3 52.0, SiO_2 33.9, H_2O (in part from wood) 8.1, C (from wood) 0.3; total 101.5%.

Weeksite is orthorhombic, pseudotetragonal; the space group is $Pnnb-D^6_{2h}$;

$$a = 14.26 \pm 0.02 \text{ A},\ b = 35.88 \pm 0.10 \text{ Å},\ c = 14.20 \pm 0.02 \text{ A};\ a:b:c = .3974:1:.3958.$$

Cell contents 16 $[K_2(UO_2)_2(Si_2O_5)_3 \cdot 4H_2O]$. The nine strongest lines of the x-ray powder pattern of weeksite are: 7.11 (10), 5.57 (9), 8.98 (8), 3.55 (7), 3.30 (7), 2.91 (6), 3.20 (5), 2.37 (5), 2.28 (5); and those of the synthetic Na analogue are: 7.11 (10), 5.57 (9), 9.03 (8), 3.56 (7), 3.30 (7), 2.94 (6), 3.19 (5), 2.37 (5), 2.28 (5).

Introduction and Acknowledgments

Weeksite, a potassium uranyl silicate mineral, closely resembles uranophane in physical appearance. It was first noted as an unknown and perhaps new mineral in 1950, when a uranium mineral from the east side of the Thomas Range in western Utah gave an unidentified x-ray powder pattern. Since that time x-ray powder patterns have indicated its presence in nine other localities in Arizona, California, Mexico, New Mexico, Pennsylvania, Texas, Utah, and Wyoming.

Weeksite, in its known occurrences, is rare, very fine grained, and intimately intermixed with other minerals. For these reasons, it was not until 1955 that enough of the material was collected for a complete chemical analysis. This material came from the east side of the Thomas Range. Although it was originally hoped to make a more thorough study of weeksite, correlating the chemical composition of this mineral with its physical and optical properties from a number of localities, the minute quantities of this mineral found at most localities made such a comparative study impossible.

---

[1] Publication authorized by the Director, U. S. Geological Survey.

The optical properties and chemical composition of specimens of weeksite from different localities are somewhat variable. Indices of refraction of weeksite vary among specimens from different localities, as well as between these specimens and a synthetic sodium analogue. Some variation in the alkali metal content is indicated by semiquantitative spectrographic analyses of weeksite from various localities. *X*-ray powder patterns of this mineral from the various localities indicate that the specimens are structurally the same. We have synthesized this mineral and its sodium analogue, and both synthetic minerals gave the same *x*-ray pattern. Thus, the chemical composition and optical properties of this mineral vary somewhat from one locality to the next. In order to have strictly comparable data, the optical properties, chemical composition, and *x*-ray diffraction data all were made on weeksite from the east side of the Thomas Range. These are compared with those of synthesized weeksite and its sodium analogue.

This new mineral is named for Dr. Alice D. Weeks of the U. S. Geological Survey, who has studied and described many new uranium and vanadium minerals. Her report with Mary E. Thompson entitled, "Identification and Occurrence of Uranium and Vanadium Minerals from the Colorado Plateaus," (1954) is a major contribution and provides mineralogists and geologists with reliable data for the recognition of these minerals.

We gratefully acknowledge the assistance of many of our colleagues in the U. S. Geological Survey. These include Samuel Rubenstein and George Ashby, who studied samples of weeksite from Easton, Pennsylvania; Joan Clark and Daphne Ross for *x*-ray studies; Malcolm Ross for electron diffraction studies; Frank Cuttitta for preliminary work on the chemical analysis; and J. C. Chandler for his work in synthesis of the mineral. Thanks are also due Eugene B. Gross of the U. S. Atomic Energy Commission for information on specimens from the Good Will claim, Utah, and from near San Carlos, Mexico; to Russell Honea of the University of Colorado for data on the mineral from the Mammoth mine, Texas; to T. C. McBurney for a specimen and data on the mineral from the Coso Mountains, California; and to Clifford Frondel of Harvard University for advice and encouragement.

This investigation is part of the project of mineralogical investigations conducted by the U. S. Geological Survey on behalf of the Division of Raw Materials of the U. S. Atomic Energy Commission.

OCCURRENCE

Weeksite has been identified from ten widely separated localities.

The type specimen of weeksite comes from the Autunite No. 8 claim, which is in the W $\frac{1}{2}$ sec. 10, T. 13 S., R. 11 W., on the east side of the Thomas Range, in central Juab County, Utah. This claim was originally located in July 1950 by W. W. Sorenson, C. S. Boyle, G. E. Wilson, and C. F. Wilson. The oldest rock in the vicinity of the Autunite No. 8 claim is a porphyritic rhyolite containing numerous phenocrysts of sanidine and quartz, some of plagioclase, and a few of biotite in a brown aphanitic groundmass. This rhyolite is overlain irregularly by a black glass welded tuff consisting of elongate pieces of pumice and crystals of plagioclase and biotite in a black to brown glass matrix. These two volcanic rocks are of probable Miocene age and, following their emplacement, were eroded to a mature topography. A white vitric tuff of probable Pliocene age was deposited on this surface. This tuff contains numerous volcanic rock fragments, mainly pumice, and some tiny crystal fragments of sanidine and quartz in a dense, white ash matrix.

The weeksite occurs in numerous veinlets, from one thirty-second to one-quarter of an inch thick, which fill a series of closely spaced fractures in the porphyritic rhyolite. These fractures have a steep dip and a general north to northwest trend, although a few trend northeast. The area in which these veinlets are exposed is about 100 feet long and has a maximum width of 25 feet. As weeksite is scattered along these veinlets, and as the veinlets are quite thin, the amount of uranium present is small. An 8.0-foot horizontal channel sample across the center of the deposit contained only 0.026 per cent uranium.

The veins are made up chiefly of bluish-white, white, or pale yellowish-green opal, which fluoresces a bright yellowish green and in places is botryoidal. The only uranium mineral observed is weeksite, which occurs in finely fibrous yellow rosettes. These rosettes are 0.2 to 1 mm. across and are found both encrusted and intergrown with the opal (Fig. 1). In a few places weeksite occurs on fracture surfaces free of opal. Other vein minerals are calcite and fluorite. The calcite is common only in parts of some veins and occurs in clear crystals as much as a quarter of an inch across. The fluorite is less common than weeksite and occurs mostly as small colorless to white crystals easily confused with the opal or calcite.

Weeksite has also been found on the Good Will claim in the NW $\frac{1}{4}$ sec. 36, T. 12 S., R. 12 W., on the west side of the main part of the Thomas Range. This property is 4.5 miles northwest of the Autunite No. 8 claim and was originally located in April 1954 by Bernard L. and Joseph Christensen. The geologic history of this area is briefly the following: 1) an ash fall formed a quartz-sanidine crystal tuff in Middle Miocene time, 2) a wide valley was formed in the tuff, 3) a lake formed in this valley into which in rapid succession were deposited a well-sorted crystal tuff, a tuffaceous sandstone, and a tuffaceous limestone conglomerate,

4) the lake dried up and an ash fall formed a white vitric tuff, 5) the region was tilted gently to the west, and a north-trending fault developed along the east side of the district, and 6) uranium mineralization occurred. Uranium minerals are found in two types of occurrences on the Good Will property: disseminated in the tuffaceous sandstone and as replacement in limestone cobbles in the conglomerate which overlies the sandstone. The only occurrences of economic significance are those in the tuffaceous sandstone. Beta-uranophane, the chief ore mineral, fills numerous pore spaces in the sandstone. The only other uranium mineral noted in this rock was schroeckingerite, which occurred in a few veinlets in one pit.

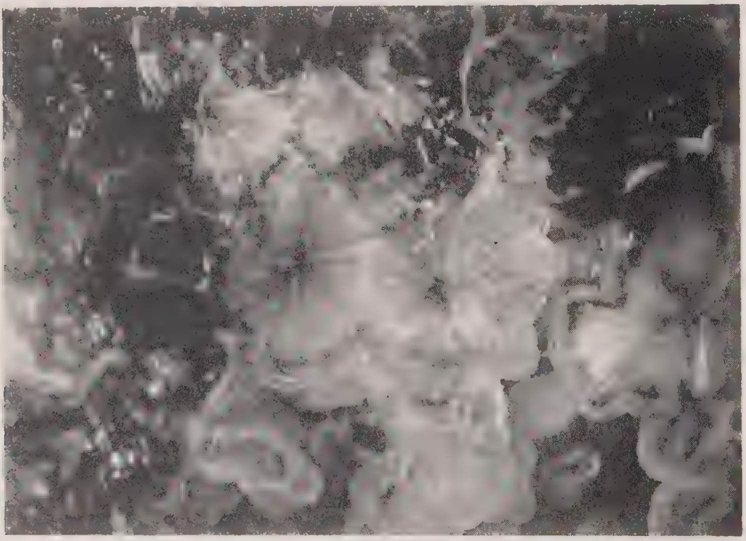

FIG. 1. Rosettes of weeksite enclosed by thin botryoidal bands of opal. East side of Thomas Range. ×38.

Weeksite occurs in the conglomerate, where it irregularly replaces parts of limestone pebbles or cobbles. In pebbles over an inch in diameter weeksite is confined to an irregular outer layer as much as one-quarter of an inch thick, but in smaller pebbles it may also replace part of the center. The pebbles containing weeksite are erratically scattered throughout the conglomerate. Weeksite occurs in extremely fine grains and is the only mineral replacing the limestone pebbles. No weeksite has been found in the uranium deposits in the underlying tuffaceous sandstone, and neither beta-uranophane nor schroeckingerite has been found in the conglomerate.

The uranium mineralization that formed the weeksite at the Autunite

No. 8 and the Good Will claims is believed to have taken place during the last stages of vulcanism (Pliocene) in the Thomas Range. It was during this period after the consolidation of most of the volcanic rocks that uraniferous fluorspar deposits were formed in the western part of the Thomas Range (Staatz and Osterwald, 1956, p. 132).

Weeksite has also been found in eight other localities: 1) from just above the Haiwee Reservoir in the Coso Mountains, California, where we identified it as a coating along fractures in granite associated with uranophane and an unknown yellow uranium mineral on a sample submitted by T. C. McBurney in 1955. This is the same locality from which the new mineral haiweeite was described by McBurney and Murdoch (1959); 2) from the Jackpile mine, Laguna, New Mexico, where it occurs in a sandstone-type deposit; 3) from the Silver Cliff mine, near Lusk, Wyoming, where it occurs in calcareous sandstone with uranophane (A. D. Weeks, 1958, oral communication); 4) from the Williams quarry, Easton, Pennsylvania (Samuel Rubenstein, 1955, written communication), where it is found in fractures in the Precambrian Franklin limestone associated with thorian uraninite, thorogummite, uranophane, carnotite, and boltwoodite (Montgomery, 1957, p. 812–813); 5) from the Red Rock district, Lassen County, California, where it is found in fractures in rhyolite (D. R. Ross, 1958, oral communication); 6) from the dump of an abandoned mercury mine, Chihuahua State, Mexico, 4½ miles southwest of Lajitas, Texas, where it is associated with carnotite (E. B. Gross, 1955, written communication); 7) from the Mammoth mine near Presidio, Texas, where it lines cavities in a welded tuff (Russell Honea, 1958, oral communication); and 8) from the Red Knob claims, Muggins Mountains, Yuma County, Arizona, where it is associated with opal, carnotite, vanadinite, gypsum, calcite, and azurite (W. I. Finch and M. E. Thompson, 1957, oral communication).

Physical and Optical Properties

Weeksite at the Autunite No. 8 claim occurs as small spherulites of yellow radiating crystals. The crystals have a waxy to silky luster and structurally resemble wavellite (Fig. 1). Uranophane and haiweeite have the same habit and appearance, and it is virtually impossible to tell them apart megascopically.

Weeksite is soft. It crushed somewhat more easily than gypsum when a sample was ground for x-ray examination. An approximate specific gravity of 4.1 was obtained by centrifuging grains of the mineral in warm concentrated Clerici solution. The specific gravity as calculated from the formula weight and the unit cell size is 4.02 for $16[K_2(UO_2)_2(Si_2O_5)_3 \cdot 4H_2O$ per cell.

The optical properties of weeksite and of uranophane are given in

Table 1. Weeksite is orthorhombic. The small acicular crystals are elongated parallel to the *c* axis and show two good prismatic cleavages. Some crystals are more bladed than acicular and are flattened on the (010) plane. Specimens of this mineral from an abandoned mercury mine in Mexico occur in flat plates. Like uranophane, weeksite is not fluorescent in either long or short wave ultraviolet light. The mean index of refraction of the synthetic sodium analogue is 1.58. The indices of refraction of weeksite are close to those of haiweeite, johannite and meta-autunite. Johannite differs from weeksite, however, in being biaxial positive instead of biaxial negative, light green instead of yellow, and a copper uranyl sulfate instead of a potassium uranyl silicate. Meta-autunite differs from weeksite in being generally crystallized in scaly aggregates instead of in fibrous rosettes, fluorescent instead of nonfluorescent, and a calcium uranyl phosphate instead of a potassium uranyl silicate. Haiweeite differs from weeksite in that it is fluorescent, crystallizes in the monoclinic system, and has a similar but distinctly different *x*-ray pattern. This pattern was a recurrent unknown under investigation in the laboratories of the U. S. Geological Survey.

TABLE 1. A COMPARISON OF THE OPTICAL PROPERTIES OF WEEKSITE AND URANOPHANE

Orientation	Index of refraction	Pleochroism	Remarks
Weeksite[1]			
$X=b$	1.596 ± .003	colorless	biaxial (−)
$Y=c$	1.603 ± .002	pale yellow-green	2 V = 50–60° (observed)
$Z=a$	1.606 ± .003	yellow-green	2 V = 66° (calculated) $r>v$, strong
Uranophane[2]			
$X\wedge a=2.8°$	1.642–1.645	colorless	biaxial negative
$Y\wedge c=10°$	1.665–1.667	pale canary yellow	2 V = 32°
$Z=b$	1.667–1.672	canary yellow	$r<v$, marked to extreme

[1] Autunite No. 8 claim on the east side of the Thomas Range, Utah.

[2] Data from Larsen, E. S., Jr., Hess, F. L., and Schaller, W. T., 1926.

CHEMICAL COMPOSITION

About 100 mg. of weeksite from the east side of the Thomas Range was purified for analysis. The mineral first was concentrated by crushing the rhyolite containing the uraniferous opal veinlets and making a heavy liquid separation of the powder. That portion of the mineral mixture which sank in bromoform was further purified by scrubbing in an ultrasonic generator and by passing it through a Frantz Isodynamic Separator. The nonmagnetic portion from the separator contained predominantly weeksite and some opal and rutile. The impurities were picked out by hand under the binocular microscope. The sample is estimated to have been entirely free of impurities.

The methods employed in the chemical analysis were guided by qualitative spectrographic analyses of the samples (Table 2). Approximately 100 mg. of the naturally occurring mineral and 35 mg. of the synthetic Na analogue of the mineral were available for chemical analysis (Table 3). There was not enough of the synthetic K compound for chemical analysis. One fraction of the sample was used for the CO_2 or C and total H_2O determinations; a second fraction of the sample for the H_2O^-, SiO_2 insoluble in (1+1) HNO_3, SiO_2 soluble in (1+1) HNO_3, UO_3, BaO, Al_2O_3, and Fe_2O_3 determinations; and a third fraction of the sample for the K_2O, Na_2O, and CaO determinations. Micro- and semimicroprocedures were used throughout.

Table 2. Spectrographic Analysis of Weeksite from Autunite No. 8 Claim and the Synthetic Na Analogue

Sample	Over 10%	1 to 5%	0.5 to 1%	0.1 to 0.5%	0.05 to 0.1%
MHS-1-50[1]	U Si	—	Al	Ba Ca	Na
MHS-1-50[2]	—	K (3%)	Na (0.7%)	—	—
G-143[1] (synthetic)	U Si	—	—	Na B Al	—

[1] Based on a 1 mg. portion of the sample using method of Stich (1953); values given are rough approximations. Analyst: Katherine V. Hazel, U. S. Geological Survey.

[2] Semiquantitative analysis for alkalies of a 10 mg. portion of the ignited residue remaining after the CO_2 and H_2O had been determined. Method of Waring and Annell (1953) was used. Analyst: Helen W. Worthing, U. S. Geological Survey. Figures are reported to the nearest number in the series 7, 3, 1.5, 0.7, 0.3, 0.15, and 0.07, in per cent. These numbers represent midpoints of group data on a geometric scale. Comparisons of this type of semiquantitative results with data obtained by quantitative methods, either chemical or spectrographic, show that the assigned group includes the quantitative value about 60 per cent of the time.

The first fraction of the sample was decomposed by ignition at 900° C. in a stream of oxygen. CO_2 or C and total water were determined by use of a modified microcombustion train of the type used for the determination of carbon and hydrogen in organic compounds.

The second fraction of the sample was dried to constant weight at $110° \pm 5°$ C. and then boiled with (1+1) HNO_3 until the insoluble material was completely white. Filter paper was used for the separation of the residue, which, after washing with dilute nitric acid, was ignited to constant weight at 850° C. Qualitative spectrographic analysis of the ignited residue showed that silicon was the only major constituent present. The soluble silica was determined gravimetrically by dehydration in a HNO_3 solution. Aliquots of the filtrate from the soluble silica determination were used for the UO_3, BaO, Al_2O_3, and Fe_2O_3 determinations. UO_3 was determined spectrophotometrically by the ammonium thiocyanate procedure in an acetone-water medium. Barium was separated and determined as the sulfate. Aluminum was determined spectrophotometrically using aluminon. To avoid the interference due to uranium in the aluminon procedure, aluminum was separated from the uranium by use of the ion-exchange resin Dowex 1X10 in a 9 molar HCl medium. Iron was determined spectrophotometrically by the o-phenanthroline procedure.

TABLE 3. CHEMICAL ANALYSES OF NATURAL WEEKSITE AND ITS SYNTHETIC Na ANALOGUE, AND HAIWEEITE

	1 MHS-1-50	2 G-143	3	4	5
SiO_2 insoluble in 1+1 HNO_3	33.0	32.0	32.79	33.77	33.1
SiO_2 soluble in 1+1 HNO_3	0.6	1.9			
Al_2O_3	0.6				
UO_3	51.5	52.0	52.09	53.66	52.8
CaO	1.1				5.4
Na_2O	0.7	7.2		5.82	
K_2O	5.5		8.56		
BaO	1.4				
C		0.3 (wood)			
CO_2	0.3				
H_2O (total)	6.6	8.1 (some from wood)	6.56	6.75	8.7
H_2O+[a]	5.5	6.2			
H_2O-	1.1	1.9			
Fe_2O_3	<0.1				
Total	101.3	101.5	100.00	100.00	100.0

1. Weeksite from the Autunite No. 8 claim on the east side of the Thomas Range. Robert Meyrowitz, analyst.
2. Synthetic sodium analogue of weeksite. Robert Meyrowitz, analyst.
3. $K_2(UO_2)_2(Si_2O_5)_3 \cdot 4H_2O$.
4. $Na_2(UO)_2(Si_2O_5)_3 \cdot 4H_2O$.
5. Haiweeite, McBurney and Murdoch, 1959.

[a] Calculated by difference between total H_2O and H_2O^-.

In the third fraction of the sample, potassium, sodium, and calcium were determined by flame photometry using aliquots of the filtrate resulting from the removal of the (1+1) HNO_3 insoluble material. The filtrate was compared to standard solutions containing approximately the same concentrations of uranium, potassium, sodium, and calcium as were present in the solution of the sample.

Weeksite is one of those silicates which, when treated with acid, yield a hard skeleton of silica. Murata (1943 and 1946) described this feature for certain common silicates and notes that it is limited to some silicate structures, including SiO_3 chains, SiO_4 double chains, Si_2O_5 sheets with but minor substitution of ferric iron for silicon, and three dimensional frameworks having an aluminum content less than the ratio of two aluminum atoms to three silicon atoms.

The formula calculated from the chemical analyses (Table 3) is $K_2(UO_2)_2(Si_2O_5)_3 \cdot 4H_2O$, but Na, Ca, and Ba and probably other metals can also substitute for K. The newly described mineral haiweeite is the calcium analogue of weeksite, having the formula $Ca(UO_2)_2(Si_2O_5)_3 \cdot 5H_2O$ (McBurney and Murdoch, 1959). In the synthetic sodium analogue (Table 3) sodium has completely substituted for potassium in the mineral, yet its *x*-ray powder pattern is identical to that of the synthetic weeksite. Weeksite is the only uranyl silicate known besides boltwoodite (Frondel and Ito, 1956) that contains an alkali as an essential cation.

Weeksite and the sodium analogue of weeksite were prepared synthetically by Pommer by heating alkaline uranate solutions in sealed pyrex tubes at 150° C. for at least three days. The calculated pressure inside the tubes was approximately 70 lbs./in.^{2}. The conditions of synthesis are summarized in Table 4. It should be noted that the solutions did not contain silica; the glass of the tube, somewhat attacked by alkaline solutions at the temperature of the experiment, was relied upon as a source of silica. The Na analogue of weeksite first appeared as a solid phase during an attempt to reduce a uranium-vanadium solution with wood at a high pH to form a mixture of uraninite and montroseite. The wood failed to act as reducing agent, probably because the pH was too high. More of the compound was prepared by this method in order to test its reproducibility and to furnish a supply of the material for further study. After the chemical composition of weeksite became known, weeksite was synthesized successfully without the addition of vanadium. The use of wood was continued, however, because in other mineral synthesis experiments (Pommer, 1958, unpublished laboratory data) wood appeared to act as a buffer in some solutions and promoted the formation of phases which otherwise did not precipitate. Finally a synthesis of the Na analogue without wood was successful. Part of the work then was repeated to form the K phase. Several of the solutions contained sodium carbonate or potassium carbonate as a buffer. The conditions of formation of boltwoodite and weeksite are similar and boltwoodite co-precipitated in several runs. The components of all the runs were identified by *x*-ray diffraction.

Table 4. Synthesis of Weeksite and Related Compounds

Simple number	pH	Molarity of uranium (added as uranyl nitrate)	Molarity of vanadium (added as vanadyl sulfate)	pH adjusted with	Buffered with carbonate	Wood added	Compound formed[1]
G-33	10.0	0.025	0.05	NaOH	no	yes	a
G-52	10.0	0.025	0.05	NaOH	no	yes	a
G-53	10.0	0.025	0.05	NaOH	no	yes	b
G-55	10.0	0.025	0.05	NaOH	no	yes	c
G-143	11.2	0.05		NaOH	yes	yes	c
G-160	11.2	0.05		NaOH	yes	yes	d
G-163	11.2	0.05		NaOH	yes	yes	e
G-166	11.2	0.05		NaOH	no	no	c
G-167	11.2	0.05		KOH	yes	yes	f
G-170	11.2	0.05		KOH	yes	yes	g
G-174	11.2	0.05		KOH	no	no	g
G-179	11.2	0.05		KOH	yes	yes	f
G-182	11.2	0.05		KOH	yes	yes	g
G-184	11.2	0.05		KOH	yes	yes	g
G-187	11.2	0.05		KOH	no	no	g
G-188	11.2	0.05		KOH	no	no	g

a. Sodium analogue of weeksite but with slightly larger spacing of some lines.

b. Sodium analogue of weeksite mixed with boltwoodite $K_2(UO_2)_2(SiO_3)_2(OH)_2 \cdot 5H_2O$).

c. Sodium analogue of weeksite.

d. Sodium analogue of weeksite plus some other unidentified compound represented by three diffraction lines.

e. Sodium analogue of weeksite, plus some other unidentified compound represented by two weak lines.

f. Boltwoodite the dominant compound with lesser amounts of weeksite.

g. Weeksite.

[1] Compound identified by *x*-ray study by Daphne R. Ross.

X-Ray Diffraction Data

The *x*-ray diffraction powder pattern of weeksite was one of the recurrent unknown patterns in the *x*-ray laboratories of the Geological Survey from 1950 until the recent detailed study. The pattern resembles the patterns of the uranophane group in a general way, but not in detail, and is similar to, but distinctly different from, that of haiweeite. No significant differences could be observed between the powder patterns of natural

TABLE 5. *X*-RAY POWDER DATA FOR NATURAL AND SYNTHETIC WEEKSITE, $K_2(UO_2)_2(Si_2O_5)_3 \cdot 4H_2O$, AND FOR THE SYNTHETIC Na ANALOGUE, COMPARED WITH HAIWEEITE

Weeksite: orthorhombic, $a = 14.26 \pm 0.02$, $b = 35.88 \pm 0.10$, $c = 14.20 \pm 0.02$ Å; space group, $Pnnb - D_{2h}^6$

Calculated		Measured[1]					
		Weeksite			Synthetic Na Analogue	Haiweeite	
		Natural		Synthetic			
hkl	d_{hkl}	I	d_{hkl}	d_{hkl}	d_{hkl}	I	d_{hkl}
040	8.97	8	8.98	8.67	9.03	10	9.14
(β, 200, 002		1	7.87)			2	8.05
200	7.13	10	7.11	7.08	7.11		
002	7.10					4	7.05
(β, 240, 042		1	6.17)				
240	5.58	9	5.57	5.57	5.57	2	5.53
042	5.56					1	5.06
222	4.84	3	4.83	4.84	4.85	½	4.90
071	4.82						
260	4.58						
062, 171	4.57	4	4.58	4.57	4.60	6	4.56
301	4.51						
080, 103	4.49	3	4.48				
322	3.86					6	4.42
262, 223	3.85	4	3.84	3.84	3.84	2	3.82
091	3.84						
280	3.80	½	3.79				
082	3.79						
400	3.57	7	3.55	3.54	3.56	4	3.54
004	3.55						
282, 303	3.35	4b	3.34				
313	3.34						
044, 440, 362	3.30	7	3.30	3.29	3.30	3	3.30
263	3.29						
144	3.22						
2.10.0	3.21	5	3.20	3.19	3.19	5	3.19
0.10.2, 402, 441	3.20						
204, 0.11.1	3.18						
422, 343	3.14						
224, 2.10.1, 372	3.13	1	3.13			5	3.106
1.10.2, 273, 292	3.12						

---

[1] Camera diameter, 114.6 mm; radiation, Cu/Ni, λ CuKα = 1.5418 Å. Film cut-off, $d \geq 13.0$ Å; b = broad.

TABLE 5 (*continued*)

Calculated		Measured[1]					
		Weeksite			Synthetic Na Analogue	Haiweeite	
		Natural		Synthetic			
hkl	d_{hkl}	I	d_{hkl}	d_{hkl}	d_{hkl}	I	d_{hkl}
432	3.08						
234	3.07	1	3.06				
460	3.06						
093, 064	3.05						
442	3.00						
244, 0.12.0, 391, 461	2.99	4	2.99	2.99	2.99		
164, 193	2.98						
2.10.2, 363	2.92						
452	2.91	6	2.91	2.91	2.94	3	2.905
2.11.1, 1.11.2, 254	2.90						
373, 3.10.1, 392	2.81	3	2.80	2.79	2.81	1	2.81
293, 1.10.3	2.80						
0.11.3, 383	2.69	½	2.69			2	2.62
3.11.2	2.52	3	2.51	2.51	2.51	½	2.51
2.11.3, 404, 414	2.51						
		4	2.41	2.41	2.44		
		5	2.37	2.37	2.37	2	2.39
		5	2.28	2.28	2.28	2	2.28
		4	2.24	2.24	2.24		
		3	2.20	2.20	2.20	1	2.21
		½	2.17				
		4	2.13	2.13	2.14		
		4	2.11	2.10	2.10	1	2.11
		4	1.994				
		3	1.973	1.977	1.973	1	1.979
		3	1.922	1.921	1.916	1	1.923
		4	1.905				
		4	1.899	1.897	1.901	1	1.898
		1	1.872				
		½	1.854			½	1.854
		2b	1.831			1	1.829
		3	1.791				
		4	1.778			1	1.781
		½	1.763				
		3b	1.741				
		1	1.726			1	1.732
		4	1.689			1	1.686
		plus additional lines, all with $I \leq 3$					

weeksite, synthetic weeksite, and the synthesized Na analogue, in spite of the wide difference between the ionic radii of Na and K. Nor were there any differences in the spacing or in the width of the lines between roughly and gently ground specimens of the same sample. Powder patterns of samples ground in acetone did not differ from the pattern of a sample ground only in air.

X-ray diffraction studies by Joan R. Clark and George Ashby lead to the following results: orthorhombic, pseudocell of dimensions $a=7.131 \pm 0.010$, $b=17.94 \pm 0.05$, $c=7.10 \pm 0.010$ Å. In the pseudocell volume of 908.4 Å^3 are contained two $[K_2(UO_2)_2(Si_2O_5)_2 \cdot 4H_2O]$. Later examination of better single crystals by precession *x*-ray techniques shows that the possible space groups for the pseudocell are: $A2mm-C_{2v}{}^{11}$, $Amm2-C_{2v}{}^{14}$, or $Ammm-D_{2h}{}^{19}$ (if centrosymmetric); $A222-D^6{}_2$ (if noncentrosymmetric). Observation of faint reflections shows that the true cell has dimensions $a=14.26 \pm 0.02$, $b=35.88 \pm 0.10$, $c=14.20 \pm 0.02$ Å, so that the true volume is eight times the volume of the pseudocell and therefore contains 16 formula units of weeksite. The space group of the true cell is $Pnnb-D_{2h}{}^6$.

Calculated interplanar spacings based on the true cell and space group are given in Table 5, together with observed *d*-spacings for natural and synthetic weeksite, the synthetic Na analogue, and haiweeite.

REFERENCES

FRONDEL, CLIFFORD, AND ITO, JUN (1956), Boltwoodite, a new uranium silicate: *Science*, **124**, no. 3228, 931.

LARSEN, E. S., JR., HESS, F. L., AND SCHALLER, W. T. (1926), Uranium minerals from Lusk, Wyoming: *Am. Mineral.*, **11**, 155–164.

MCBURNEY, T. C., AND MURDOCH, J. (1959), Haiweeite, a new uranium mineral from California: *Am. Mineral.*, **44**, 839–843.

MONTGOMERY, ARTHUR (1957), Three occurrences of high-thorian uraninite near Easton, Pennsylvania: *Am. Mineral.*, **42**, 804–820.

MURATA, K. J. (1943), Internal structure of silicate minerals that gelatinize with acid: *Am. Mineral.*, **28**, 545–562.

——— (1946), The significance of internal structure in gelatinizing silicate minerals; *in* Contributions to Geochemistry, 1942–1945: *U. S. Geol. Survey Bull.* **950**, 25–33.

STAATZ, M. H., AND OSTERWALD, F. W. (1956), Uranium in the fluorspar deposits of the Thomas Range, Utah, *in* Contributions to the Geology of Uranium and Thorium by the U. S. Geological Survey and Atomic Energy Commission for the United Nations International Conference on Peaceful Uses of Atomic Energy, Geneva, Switzerland 1955: *U. S. Geol. Survey Prof. Paper* **300**, 131–136.

STICH, J. N. (1953), Spectrographic identification of mineral grains: *U. S. Geol. Survey Circ.* **234**.

WARING, C. L., AND ANNELL, C. S. (1953), Semiquantitative spectrographic method for analysis of minerals, rocks and ores: *Anal. Chemistry*, **25**, 1174–1179.

(*over*)

Note added in proof

Since this paper was prepared, Russell Honea (1959) has applied the unit cell parameters determined for weeksite by Joan Clarke by x-ray diffraction to material he calls gastunite. Honea's material is undoubtedly identical with weeksite. More recent study of the type gastunite, which was not available to Honea at the time his paper was published, shows that gastunite and haiweeite are probably the same material.

REFERENCES

HABERLANDT, HERBERT AND SCHIENER, ALFRED (1951) Die Mineral- und Elementvergesellschaftung des Zentralgneisgebietes von Badgastein (Hohe Tauren): *Tschermaks Mitt.*, **2**, 307–313.

HONEA, RUSSELL M. (1959) New data on gastunite, an alkali uranyl silicate: *Am. Mineral.* **44**,1047–1056.

Manuscript received April 23, 1959.

THE AMERICAN MINERALOGIST, VOL. 45, JANUARY–FEBRUARY, 1960

BLUE ASBESTOS FROM LUSAKA, NORTHERN RHODESIA, AND ITS BEARING ON THE GENESIS AND CLASSIFICATION OF THIS TYPE OF ASBESTOS*

A. R. DRYSDALL AND A. R. NEWTON,
Northern Rhodesia Geological Survey

ABSTRACT

An occurrence of blue asbestos near Lusaka was investigated and proved to consist of an anastomosing stockwork of predominantly slip-fiber veins in a semi-calcareous host rock. The host rock is probably lenticular and occurs in a strongly deformed dolomite formation. Chemical analysis of the asbestos shows that it is magnesioriebeckite according to the classification of Miyashiro (1957); the geological evidence strongly suggests that it is of metasomatic origin. A similar occurrence has been described from Bolivia (Ahlfeld 1943), and both are in strong contrast to the normal South African and Australian occurrences, where the asbestos is of riebeckite composition and probably of purely metamorphic origin. The name crocidolite has been widely used to describe blue asbestos, but as it applies only to fibrous varieties of riebeckite and magnesioriebeckite, it should not be applied as a mineral name.

INTRODUCTION

Blue asbestos was discovered four and a half miles south-west of Lusaka during the excavation of several shallow pits. The occurrence was investigated by trenching and augering as there were no surface outcrops. The water-table lies within a few inches of the surface and consequently the whole exposure including the asbestos had a very weathered appearance.

FIELD RELATIONS

The predominant rock-type of the area is a creamy, dolomitic limestone striking east-west and dipping vertically. One hundred yards from the asbestos occurrence, thin-bedded dolomite is seen to be tightly folded, and some of the more competent bands display boudinage structure. The strike of the axial planes of the folds is 70° east of north and the pitch steeply westwards. This single exposure displays the only indications of structure in the immediate vicinity.

The host rock of the asbestos appears to be a lenticular body enclosed in Lusaka Dolomite, as it is not traceable along strike for more than approximately 100 yards. Within this lenticle, the asbestos occurs as an anastomosing complex of veins forming an irregular stockwork. There is no tendency for these veins to be parallel to each other or to the bedding, as in South African and Australian occurrences. The seams average half dicate that the samples are not completely unweathered. It would appear that the ferrous iron content has been to a large extent oxidized, probably by circulating ground-water. According to the classification of Miyashiro (1957), the South African, Australian and American examples are of riebeckite composition, whereas the Bolivian and Lusaka examples fall within the magnesioriebeckite field. The name crocidolite has been applied to all the varieties of blue asbestos as a term descriptive of habit, distinguishing the fibrous varieties of riebeckite and magnesioriebeckite. It is therefore not a true mineral name.

---

* Occasional Paper No. 26, Northern Rhodesia Geological Survey.

The Lusaka asbestos is a pale, powder-blue, fluffy variety, soft and silky to the touch. At the deepest part of the excavations, the fiber is deeper blue in color and harsher in texture. Red iron-staining occurs in places. In thin section, it is seen as bundles of fibers, usually orientated sub-parallel to the vein. Pleochroism is from blue-gray parallel to the length of the fibers, to pale-violet perpendicular thereto. The fibers are length-fast and since they are probably elongated parallel to *c*, it is likely that $X = c$. The asbestos fibers penetrate albite porphyroblasts.

Genesis and Comparison with Other Occurrences

From the foregoing description, it is evident that the fiber occurs in a metasomatized and metamorphosed semicalcareous horizon within the Lusaka Dolomite. It is probable that any competent horizon within this dolomite will display boudinage structures as a result of intense folding. Thus, from the exposures available, the host-rock of the asbestos could be regarded as a vertically orientated lens and might well be one of a series of such lenses aligned along an east-west strike.

The origin of South African crocidolite is discussed by Peacock (1928), Hall (1930) and Du Toit (1945), and the remarkably similar Australian examples by Finucane (1939) and Miles (1942). At all the localities, the crocidolite is present as cross-fiber veins parallel to the bedding of thin-bedded ironstone associated with dolomite. The South African crocidolite is of remarkably similar composition to the ironstone, the former being richer only in Na and Mg. The fiber is believed to have formed from constituents already present in the ironstone during a prolonged period of metamorphism caused by burial at depth. Both Peacock (1928) and Hall (1930) favor the possibility that the soda was originally uniformly distributed throughout the ironstone, and was subsequently concentrated in certain bands. Du Toit (1945) has suggested that the MgO has behaved in a similar manner. There is no evidence in any of the South African or Australian occurrences to suggest that a basic magma is in any way essential for the formation of crocidolite. "Crocidolization is conceived as a mild, static, non-additive metamorphic process, resulting in the chemical union, along soda-rich bedding planes of the necessary constituents *in situ*" (Peacock 1928, p. 283).

The Lusaka occurrence differs from the characteristic South African and Australian examples in several respects and the above hypothesis cannot be directly applied. The veins of fiber form an irregular stockwork—thus, their distribution cannot be controlled by pre-existing soda-rich horizons; rather, the soda would appear to have been introduced metasomatically, the veins marking the paths of migrating soda-rich solutions. The nearby dolomite may have been the source of any MgO required for the formation of the fiber but the presence of the talc veinlets could indicate that MgO was also introduced. The occurrence of abundant albite porphyroblasts in the host rock and the dolomite is strong evidence supporting the hypothesis of soda metasomatism, and the presence of large amounts of tourmaline (up to 50% of the rock) proves that some metasomatic process was operative. From the evidence of thin sections, it would appear that tourmaline was the first metasomatic mineral to form and was followed by albite and magnesioriebeckite. The last two minerals are probably genetically associated, but the significance of the tourmaline, monazite and apatite, representing phases of boron and phosphate metasomatism, remains an enigma.

It is interesting to note that recent experiments have shown that both tourmaline (Frondel and Collette 1957) and monazite (Anthony 1957) can be synthesized at comparatively low temperatures and high water vapor pressures, and that tourmaline fails to form in the presence of alkali-rich minerals including glaucophane. This evidence supports the hypothesis that the boron metasomatism preceded the formation of albite and magnesioriebeckite. Again, there is no evidence that basic magma is essential for the formation of blue asbestos, although the source of the introduced material is a matter for speculation. The presence of tourmaline, apatite, and monazite could be taken as an indication that a magma of acid rather than basic affinities was involved, but this assumes that all the metasomatic processes were genetically associated. Another striking difference is that the Lusaka example consists predominantly of slip-fiber, whereas the South African and Australian deposits are characterized by well developed cross-fiber structure. Hall (1930) suggests that slip-fiber occurs where differential movement has taken place, but as there is no evidence of shearing in the Lusaka exposures, it can only be assumed that the conditions under which the fiber formed were different from those which operated elsewhere. That is, metasomatic instead of a metamorphic environment in some way inhibited an exclusive development of cross-fiber.

Of all the deposits of blue asbestos, the only other example which dicate that the samples are not completely unweathered. It would appear that the ferrous iron content has been to a large extent oxidized, probably by circulating ground-water. According to the classification of Miyashiro (1957), the South African, Australian and American examples are of riebeckite composition, whereas the Bolivian and Lusaka examples fall within the magnesioriebeckite field. The name crocidolite has been applied to all the varieties of blue asbestos as a term descriptive of habit, distinguishing the fibrous varieties of riebeckite and magnesioriebeckite. It is therefore not a true mineral name.

The Lusaka asbestos is a pale, powder-blue, fluffy variety, soft and silky to the touch. At the deepest part of the excavations, the fiber is deeper blue in color and harsher in texture. Red iron-staining occurs in places. In thin section, it is seen as bundles of fibers, usually orientated sub-parallel to the vein. Pleochroism is from blue-gray parallel to the length of the fibers, to pale-violet perpendicular thereto. The fibers are length-fast and since they are probably elongated parallel to c, it is likely that $X=c$. The asbestos fibers penetrate albite porphyroblasts.

Genesis and Comparison with Other Occurrences

From the foregoing description, it is evident that the fiber occurs in a metasomatized and metamorphosed semicalcareous horizon within the Lusaka Dolomite. It is probable that any competent horizon within this dolomite will display boudinage structures as a result of intense folding. Thus, from the exposures available, the host-rock of the asbestos could be regarded as a vertically orientated lens and might well be one of a series of such lenses aligned along an east-west strike.

The origin of South African crocidolite is discussed by Peacock (1928), Hall (1930) and Du Toit (1945), and the remarkably similar Australian examples by Finucane (1939) and Miles (1942). At all the localities, the crocidolite is present as cross-fiber veins parallel to the bedding of thin-bedded ironstone associated with dolomite. The South African crocidolite is of remarkably similar composition to the ironstone, the former being richer only in Na and Mg. The fiber is believed to have formed from constituents already present in the ironstone during a prolonged period of metamorphism caused by burial at depth. Both Peacock (1928) and Hall (1930) favor the possibility that the soda was originally uniformly distributed throughout the ironstone, and was subsequently concentrated in certain bands. Du Toit (1945) has suggested that the MgO has behaved in a similar manner. There is no evidence in any of the South African or Australian occurrences to suggest that a basic magma is in any way essential for the formation of crocidolite. "Crocidolization is conceived as a mild, static, non-additive metamorphic process, resulting in the chemical union, along soda-rich bedding planes of the necessary constituents *in situ*" (Peacock 1928, p. 283).

The Lusaka occurrence differs from the characteristic South African and Australian examples in several respects and the above hypothesis cannot be directly applied. The veins of fiber form an irregular stockwork—thus, their distribution cannot be controlled by pre-existing soda-rich horizons; rather, the soda would appear to have been introduced metasomatically, the veins marking the paths of migrating soda-rich solutions. The nearby dolomite may have been the source of any MgO required for the formation of the fiber but the presence of the talc veinlets could indicate that MgO was also introduced. The occurrence of abundant albite porphyroblasts in the host rock and the dolomite is strong evidence supporting the hypothesis of soda metasomatism, and the presence of large amounts of tourmaline (up to 50% of the rock) proves that some metasomatic process was operative. From the evidence of thin sections, it would appear that tourmaline was the first metasomatic mineral to form and was followed by albite and magnesioriebeckite. The last two minerals are probably genetically associated, but the significance of the tourmaline, monazite and apatite, representing phases of boron and phosphate metasomatism, remains an enigma.

It is interesting to note that recent experiments have shown that both tourmaline (Frondel and Collette 1957) and monazite (Anthony 1957) can be synthesized at comparatively low temperatures and high water vapor pressures, and that tourmaline fails to form in the presence of alkali-rich minerals including glaucophane. This evidence supports the hypothesis that the boron metasomatism preceded the formation of albite and magnesioriebeckite. Again, there is no evidence that basic magma is essential for the formation of blue asbestos, although the source of the introduced material is a matter for speculation. The presence of tourmaline, apatite, and monazite could be taken as an indication that a magma of acid rather than basic affinities was involved, but this assumes that all the metasomatic processes were genetically associated. Another striking difference is that the Lusaka example consists predominantly of slip-fiber, whereas the South African and Australian deposits are characterized by well developed cross-fiber structure. Hall (1930) suggests that slip-fiber occurs where differential movement has taken place, but as there is no evidence of shearing in the Lusaka exposures, it can only be assumed that the conditions under which the fiber formed were different from those which operated elsewhere. That is, metasomatic instead of a metamorphic environment in some way inhibited an exclusive development of cross-fiber.

Of all the deposits of blue asbestos, the only other example which

TABLE II. COMPARISON BETWEEN METAMORPHIC AND METASOMATIC BLUE ASBESTOS

	Metamorphic type	*Metasomatic type*
Typical occurrences	S. Africa and Australia	Bolivia and N. Rhodesia
Form of deposit	Veins parallel to bedding	Stockwork
Typical composition	Riebeckite	Magnesioriebeckite
Predominant fiber	Cross-fiber	Slip-fiber
Tensile strength	Medium to high	Low
Color	Blue	Pale-blue
Associated minerals	—	Metasomatic minerals—e.g., talc and tourmaline
Country-rock	Ironstone and dolomite	Variable

bears any marked resemblance to that of Lusaka occurs in Bolivia. This occurrence, described in detail by Ahlfeld (1943) and summarized by Ahlfeld and Reyes (1955), is more extensive than that of Lusaka but shows the following points of similarity:

1. The asbestos occurs as a stockwork of veins following irregular fracture planes and bedding planes.
2. It is predominantly slip-fiber.
3. It is of magnesioriebeckite composition and pale-blue in color.
4. It has a low tensile strength.
   (Frankel (1953) has suggested that both the color and the tensile strength of blue asbestos vary with the ferrous iron content, which is low in both the Lusaka and Bolivian occurrences.)
5. Associated minerals include quartz, talc and pyrite, and a nearby horizon of dolomite contains various borosilicates including tourmaline and danburite.
6. The fiber is believed to have formed during a period of dynamometamorphism associated with the metasomatic introduction of Ca, Mg, Fe, and Na.

The main difference between the two areas is in regard to host rocks, those of Bolivia being slate and sandstone, and those at Lusaka being semicalcareous; since the asbestos seems to be of metasomatic origin this is of no great significance. Otherwise, these two deposits are similar in all major respects, and contrast strongly with the South African and Australian type of occurrence, as shown in Table II.

REFERENCES

AHLFELD, F. (1943), Los yacimientos de crocidolita en las Yungas de Cochabamba. *Notas Mus. La Plata*, **8**, 355–71.

AHFELD, F. Y REYES, J. M. (1955), *Los especies minerales de Bolivia*. Bolivia.

ANTHONY, J. W. (1957), Hydrothermal synthesis of monazite. *Am. Mineral*. **42**, 904.

DU TOIT, A. L. (1945), The origin of the amphibole asbestos deposits of South Africa. *Trans. Geol. Soc. S. Afr*. **48**, 161–206.

Finucane, K. J. (1939), The blue asbestos deposits of the Hamersley Ranges, Western Australia. *Rep. Aer. Surv. N. Aust. W. Aust.* **49**.

Frankel, J. J. (1953), South African asbestos fibers. *Mining Mag., Lond.* **49,** 73–83, 142–9.

Frondel, C. and Collette, R. L. (1957), Synthesis of tourmaline by reaction of mineral grains with NaCl-H_3BO_3 solution, and its implications in rock metamorphism. *Am. Mineral.* **42,** 754–8.

Hall, A. L. (1930), Asbestos in the Union of South Africa. *Mem. Geol. Surv. S. Afr.* **12**.

Miles, K. R. (1942), The blue asbestos bearing banded iron formations of the Hamersley Ranges, Western Australia. *Bull. Geol. Surv. W. Aust.* **100** Part **1**, 5–37.

Miyashiro, A. (1957), The chemistry, optics and genesis of the alkali-amphiboles. *J. Fac. Sci. Tokyo Univ. (II)* **11,** 57–83.

Peacock, M. A. (1928), The nature and origin of the amphibole asbestos, South Africa. *Am. Mineral.* **13,** 241–85.

Sinclair, W. E. (1955), *Asbestos*. London.

Manuscript received April 16, 1959.

THE AMERICAN MINERALOGIST, VOL. 45, JANUARY-FEBRUARY, 1960

X-RAY DIFFRACTION STUDY OF ORIENTATION IN THE CHATTANOOGA SHALE*

E. N. SILVERMAN AND THOMAS F. BATES,† *The Pennsylvania State University, University Park, Pa.*

ABSTRACT

An *x*-ray diffraction technique has been used to obtain a quantitative measure of the degree of orientation of the (001) planes of 10 Å illite and mica flakes in fifty-eight samples from a drill core taken from the Chattanooga shale. Thin sections cut perpendicular to the bedding are placed on the *x*-ray spectrometer in such a position that, upon rotation of the section in its own plane, the geiger counter records all diffraction from mica flakes with (001) perpendicular to the plane of the section. Analysis of the resulting curve, using the Chi-square statistic divided by the area under the curve, gives an "orientation index" for each specimen which is reproducible and independent of the amount of 10 Å material present.

An evaluation of the data with respect to the uranium content of the samples shows that there is no significant correlation between the concentration of the element and this particular measure of the texture of the rock. This supports other evidence which indicates that the uranium was precipitated during deposition of the sediment and that the distribution of uranium has not been affected by movement of solutions during or followng compaction.

The technique is applicable to the study of lattice orientation of any sufficiently fine-grained mineral in natural or synthetic substances.

INTRODUCTION

The problem of obtaining precise quantitative measurements of the textural characteristics of various materials is an important one which has been studied by many workers using many different techniques. For the study of preferred orientation in fine-grained crystalline substances, *x*-ray diffraction methods have proved most satisfactory and the application of *x*-ray spectrometer techniques has greatly simplified the procedures involved (Klug and Alexander, 1954, p. 580). The present paper describes the application of one of these *x*-ray spectrometer techniques to the problem of precisely measuring the degree of orientation of the (001) plane of the 10 Å micaceous minerals in fifty-eight samples of Chattanooga shale. The orientation values are then evaluated statistically in relation to the uranium content of the samples to determine whether the distribution and concentration of this element is significantly related to this particular measure of texture. Since it was established, as part of the study, that the preferred orientation of the (001) plane of the micas is parallel to the micro and megascopic laminations referred to as bedding, conclusions can be drawn in terms of megascopic as well as microscopic aspects of the rock.

---

* Contribution No. 58-4, Mineral Industries Experiment Station, College of Mineral Industries, The Pennsylvania State University, University Park, Pennsylvania.

† Technologist, U. S. Steel Corp., Applied Research Laboratory, Monroeville, Pennsylvania and Professor of Mineralogy, College of Mineral Industries, The Pennsylvania State University, University Park, Pennsylvania.

TECHNIQUES

Since the *x*-ray diffraction technique used for the measurement of degree of orientation may easily be applied to any fine-grained material, certain details of the procedure are included herein. For a more extensive discussion of instrumentation, *x*-ray optics, and pole figure diagrams, reference should be made to Decker, Asp and Harker (1948) and Schulz (1949).

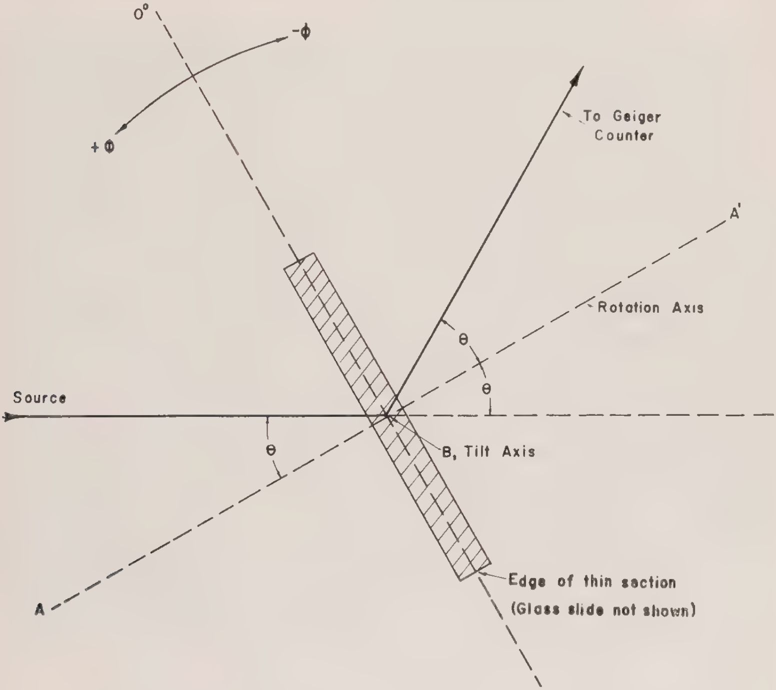

FIG. 1. Relationship of rotation and tilt axes to sample and source.

A thin section of the sample is mounted on the spectrometer so that the angle θ between the incident beam and the perpendicular to the plane of the section is equal to the Bragg angle for diffraction from the particular set of planes of atoms to be studied (4.37°θ for the (001) planes of mica and illite using Ni filtered Cu$K\alpha$ radiation). The geiger counter is set at the 2θ angle for the same set of planes (see Fig. 1). An appropriate sample holder permits rotation of the thin section in its own plane about axis AA′ and also rotation (herein referred to as "tilt") about the spectrometer axis (B) which passes through the center of the thin section. As pointed out in the references noted, most of the three dimensional orientation pattern of any given set of lattice planes can be measured by rotation of the thin section about axis AA′ at each of a series of tilt positions (in this case from $\phi = +25°$ to $-25°$).

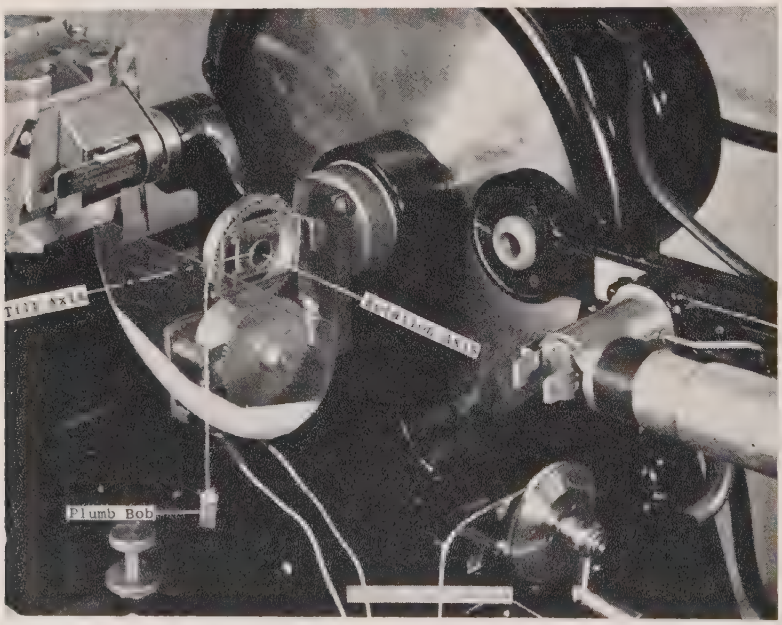

FIG. 2. Arrangement of sample and sample holder on x-ray spectrometer.

The present study was carried out on a North American Philips high angle recording spectrometer fitted with a 0.5 divergence slit and a .006° scatter slit. The arrangement of the sample holder and sample is pictured in Fig. 2. Rotation of the sample is produced by the one RPH motor seen below the sample holder. The sample holder assemblage, consisting of holder, motor, protractor and plumb bob is attached to a $\frac{5}{8}''$ diameter shaft which replaced the shaft of the ordinary sample holder on the goniometer axis. The rotating holder is so positioned that the tilt axis passing through the center of the thin section coincides with the goniometer axis. Positioning of the sample at a particular tilt angle is accomplished by manual rotation of the entire specimen holder assemblage before clamping the $\frac{5}{8}''$ shaft in position. The angle of tilt is measured by the position of the plumb line on the protractor.

The thin section can be seen mounted on the near side of the sample holder. The rock slices are cut with a diamond saw and mounted for grinding on standard microscope slides using Biggs R-313 bonding agent.* This cement permits removal of the completed 20μ thin section from the microscope slide by soaking in water. The section is then transferred to another slide with a hole in the center large enough so that no glass will be in the path of the diffracted x-ray beam.

Since the object of the research described here was to compare samples on the basis of the perfection of orientation of the mica particles having the (001) pole in a plane containing the normal to the bedding plane of the rock (as megascopically determined), no attempt was made to measure and plot the entire "pole figure." However, in order to determine whether or not there was a significant difference between the slope of the megascopically defined bedding plane and the slope of the surface containing the greatest number of (001) mica planes, a preliminary experiment was run on each of four Chattanooga shale samples using two thin sections cut perpendicular to each other and to the bedding. Each section was investigated by changing the tilt angle ϕ by increments of one degree from zero to plus and minus 25° and rotating the thin section about AA′ in each of the resulting 51 tilt positions.

The variation in the intensity of the (001) mica reflection demonstrated that although the preferred orientation of the mica flakes is in the bedding plane of the sample, a departure of a few degrees in any direction from the plane of the bedding did not result in a significant decrease in peak intensity. On the basis of this experiment it was assumed that in cutting the thin sections of other samples the measurement of the 90° angle between the megascopically-defined bedding plane and the direction of cut was not highly critical, particularly since the samples were to be compared on the basis of the degree rather than the direction of the preferred orientation.

ANALYSIS OF PATTERNS

Figure 3 shows resulting tracings from two samples: (A) in which the 10 Å mica has a high degree of preferred orientation in the plane examined; and (B) in which a larger amount of mica has less preferred orientation.

As is the case in any x-ray diffraction pattern, the intensity at any point is equal to the background intensity plus that due to the 10 Å mica. The background intensity was measured, under the same transmission conditions used for all other work, by traversing the 10 Å reflection from higher to lower values of 2θ (in the same manner as that used for the usual "reflection" pattern), measuring the background on each side of the (001) peak, and interpolating for the background intensity beneath the peak. A line representing this background is then drawn (as b and b′ in Fig. 3); the area between the lines (a and b; and a′ and b′) represents the radiation due to the (001) reflection from the 10 Å mica flakes brought into diffracting position as the thin section is rotated 180° in its own plane.

---

* C. H. Biggs Company, 2233 Barry Avenue, Los Angeles, California.

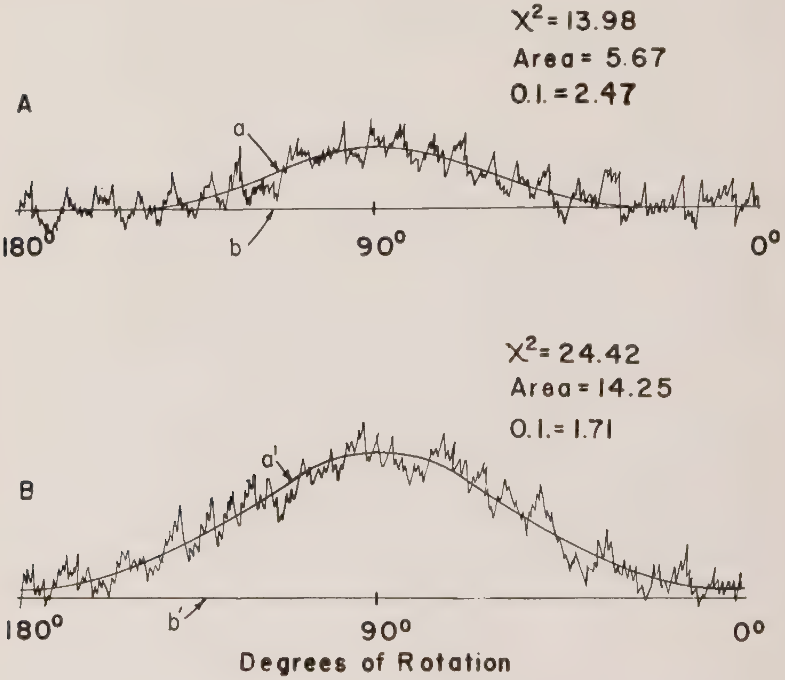

FIG. 3. Representative orientation curves.

To obtain a quantitative measure of the degree of orientation from the curves, the Chi-square statistic (χ^2) was used (Snedecor, 1946, p. 16). Chi-square is commonly employed to test goodness of fit of an observed to a theoretical distribution by comparing the two distributions, class by class. In the present case each diffraction pattern of the type shown in Fig. 3 is converted into a histogram containing 30 classes and the intensity of the curve above background is measured at the midpoint of each class. These values are summed and divided by 30 to find the expected value, and the absolute difference between each observed value and the expected value is squared. χ^2 is found by dividing the sum of the squared difference by the expected value.

Since it can be shown that the χ^2 value is dependent upon the area under the curve as well as the shape of the curve and since the area in turn is dependent upon the quantity of mica in the proper positions to diffract, a correction must be applied if the final value is to relate directly to degree of orientation of the mica independent of the amount present. Theoretical calculations having shown that the diffracted intensity from the 10 Å mica should vary linearly with the quantity of this material present, it was determined that the proper correction could be made by dividing the χ^2 value by the area between the curve and the background line. The resultant value is referred to as the orientation index: O.I. $=\chi^2/\text{Area}$. In the example illustrated in Fig. 3, for A and B, respectively, the χ^2 values are 13.98 and 24.42, the areas are 5.67 and 14.25, and the resulting orientation indices are 2.47 and 1.71. This indicates that curve A represents a better degree of orientation than is represented by curve B. The fact that the samples differ in amount of mica, as shown by the differences in areas under the curve, does not alter the conclusion that the smaller amount of mica in A has a higher degree of preferred orientation than does the larger amount in B.

STUDY OF THE SHALE

The samples of Chattanooga shale studied were selected from a drill core designated as YB-19 and taken by the U. S. Bureau of Mines from the Youngs Bend area of central Tennessee.

The Chattanooga shale in this area has been divided into five stratigraphic units by the United States Geological Survey (Table I).

An important consideration in determining the number of samples needed was the fact that the data would be used in an analysis of variance designed to test for differences between stratigraphic units. Since in analysis of variance it is desirable to have at least two degrees of freedom

TABLE I. CHATTANOOGA SHALE CORE YB-19

Stratigraphic Unit	Thickness	No. of Samples Studied
Top Black	4.46′	10
Upper Gray	2.13′	3
Middle Black	7.66′	15
Middle Gray	9.11′	20
Lower Black	6.25′	10

associated with a source of variation, at least three samples were needed from each stratigraphic unit. Consequently, sixty samples were taken from the thirty-foot core, in order to insure that the random selection would yield at least three samples from the thinnest lithologic unit, namely the 2.13′ thick Upper Gray member.

Sample numbers were determined by taking those numbers in a random number table that fell within the range of the core footage until 60 samples had been obtained. Thus, the possibility of operator bias with respect to choice of samples was eliminated. In practice, 58 of the 60 samples taken from the core were investigated, two being too small. The number of samples taken from each unit is shown in Table I.

An uncovered thin section cut perpendicular to the bedding (as determined by a contact goniometer) was prepared from each sample. The orientation index together with the fluorimetrically-determined uranium content of each sample is given in Table II.

The data have been statistically analyzed in order to provide answers to each of the following questions:

1) Are the orientation indices normally distributed?
2) Are the stratigraphic units significantly different on the basis of the orientation index?
3) Is there a significant correlation between orientation index and uranium content?

Distribution of orientation indices

To provide an answer to the first question the orientation indices, with a mean of 2.117 and a standard deviation of 0.65, were arranged in a frequency distribution. This distribution was tested for goodness of fit to a normal distribution with the same mean and standard deviation and yielded a χ^2 value of 8.625. The probability of obtaining such a value by chance alone indicates that the observed distribution is not significantly different from a normal distribution.

Lithologic variation

The variances of the orientation indices of the five lithologic units were shown to be homogeneous following a method outlined by Bartlett (Snedecor, 1945, p. 250). It was also shown, by employing a completely randomized analysis of variance, that there are no significant differences between the mean orientation indices of the stratigraphic units.

Correlation of orientation index and uranium content

A quantitative evaluation of the degree of association between the two variables was made by employing the correlation coefficient (r) statistic. The calculated correlation coefficient is 0.143, a value not sig-

TABLE II. ORIENTATION INDICES AND URANIUM CONTENT OF 58 SAMPLES OF CORE YB-19

Sample No.	O.I.	%U	Sample No.	O.I.	%U
152.1	1.645	.0091	167.2	1.747	.0005
152.4	2.317	.0076	167.8	2.769	.0021
152.7	2.003	.0115	168.0	3.392	.0016
153.1	2.295	.0108	168.5	1.667	.0010
153.8	3.421	.0086	169.0	2.495	.0009
154.0	1.615	.0073	169.5	2.342	.0010
154.5	2.071	.0087	170.1	2.336	.0000
155.1	1.686	.0089	170.5	1.445	.0002
155.7	2.872	.0097	171.1	2.101	.0007
156.4	2.182	.0044	171.3	2.729	.0001
157.3	1.549	.0036	171.9	2.296	.0006
158.1	2.011	.0022	172.1	2.307	.0010
158.5	0.600	.0023	172.8	1.878	.0007
159.0	2.466	.0040	173.4	2.533	.0008
159.2	2.688	.0055	173.9	1.717	.0003
159.5	1.283	.0056	174.2	1.651	.0007
159.9	1.413	.0057	174.5	1.507	.0009
160.2	1.714	.0037	174.8	1.395	.0002
161.5	2.075	.0051	175.2	1.833	.0014
162.1	1.399	.0071	175.8	1.921	.0012
162.6	1.550	.0068	176.1	2.408	.0020
163.2	2.882	.0047	176.7	3.188	.0019
164.1	2.006	.0071	177.0	2.572	.0038
164.4	2.104	.0063	177.3	2.084	.0032
165.0	2.468	.0070	177.7	2.699	.0055
165.3	3.224	.0071	179.0	2.687	.0046
166.0	1.993	.0057	179.9	2.089	.0027
166.2	3.603	.0039	180.7	2.137	.0017
166.8	1.755	.0014	181.5	0.015	.0005

nificant at the conventional 5% level. This indicates little or no association between uranium content and the degree of orientation of illite and mica in these samples of the Chattanooga shale.

SUMMARY AND CONCLUSIONS

Fifty-eight samples of the Chattanooga shale were studied by an x-ray diffraction technique designed to measure the degree of orientation of the (001) planes of the 10 Å micaceous minerals from thin sections cut perpendicular to the bedding. An orientation index was calculated for each sample by dividing the Chi-square statistic (used to evaluate the shape of the curve) by the area between the curve and background (to remove the effect of amount of mica present).

Statistical evaluation of the orientation indices showed that they are normally distributed and that there are no significant differences between the mean orientation indices of the five stratigraphic units represented in the drill core studied.

The correlation of this particular measure of the texture of the rock with the amount of uranium in the samples is not significant. These data agree with the results of other studies of uranium distribution in this rock which indicate that, except at weathered surfaces, there is no evidence of uranium concentration along bedding planes or microscopic laminations. Such evidence supports the hypothesis that the uranium was emplaced during deposition of the shale and that the distribution of the element has not been affected by solution movement during or after compaction.

The technique used to measure degree of orientation of the mica in these shale samples can be applied to the study of thin sections of any rock in which the mineral to be evaluated is of sufficiently fine grain size to permit representative sampling by the *x*-ray beam. Micaceous minerals are particularly well suited because the (001) lattice plane is directly and simply related to external morphology and thereby to processes which affect the orientation of the particles.

ACKNOWLEDGMENTS

The authors wish to thank Dr. G. W. Brindley for his advice regarding details of the *x*-ray procedure and Dr. J. C. Griffiths for assistance in the statistical evaluation of the data. Fluorimetric determinations of the uranium content of the samples were made by Mr. Robert O'Neil.

This research is part of a study of the mineralogy and petrography of uraniferous shales and lignites supported by the Division of Research of the United States Atomic Energy Commission.

REFERENCES

DECKER, B. F., ASP, E. T. AND HARKER, D. (1948), Preferred orientation using a geiger counter x-ray diffraction goniometer, *J. Appl. Phys.* **19,** 388–392.

KLUG, H. P. AND ALEXANDER, L. E. (1954), *X*-ray diffraction procedures, Wiley, New York.

SCHULZ, L. G. (1949), Determination of preferred orientation in flat transmission samples using a geiger counter *x*-ray spectrometer, *J. Appl. Phys.* **20,** 1033–1036.

SNEDECOR, GEORGE W. (1946), Statistical methods. The Iowa State College Press, Ames, Iowa.

Manuscript received April 9, 1959.

THE AMERICAN MINERALOGIST, VOL. 45, JANUARY–FEBRUARY, 1960

CHEMICAL ANALYSES OF ROCKS WITH THE PETROGRAPHIC MICROSCOPE

GERALD M. FRIEDMAN, *Pan American Petroleum Corp., Research Center, Tulsa, Oklahoma*

ABSTRACT

The chemical composition of the granite (G-1) was calculated from quantitative mineralogical (modal) analyses of petrographic thin-sections. The percentages of the major constituents, SiO_2, Al_2O_3, Fe_2O_3, FeO, MgO, CaO, Na_2O and K_2O were computed. These calculations were compared with the results of wet chemical analyses made by 30 chemists in 25 analytical laboratories. Each constituent calculated from the thin-section analysis of the rock standard lies within the range reported by the chemists. The arithmetic mean of the percentage of each constituent determined by the chemical analyses agrees closely with the analysis calculated from the mode.

A norite sample was also analyzed by petrographic and chemical procedures. Agreement between the two techniques for this sample was close.

This study indicates that for rocks in which the composition of the individual minerals has been obtained by optical measurements, the major constituents can be determined with the petrographic microscope by modal analyses, and the results may be considered reliable.

INTRODUCTION

Chemical analyses of rocks have been reported in the geological literature for nearly one hundred years. They are expensive and time-consuming to make, yet are essential for many types of investigation.

Calculation of the chemical composition from the mineral distribution (mode), as determined under the petrographic microscope, is not commonly reported in present-day geological literature. Delesse suggested as long ago as 1886 that the chemical composition can be determined from a modal analysis of the rock. Glagolev (1933) introduced the point-counting procedure, recently renovated by Chayes (1949), and advocated the calculation of the chemical composition of rocks from the results of modal studies. Whitten (1953) calculated the chemical composition of granite and quartzite from their modes and considered this method (p. 337) "a technique for roughly evaluating the chemical variability within a suite of rocks." Balasanyan (1957), using the techniques of Kuznetsov (1947) and Niggli (1936), determined the mode of the rock and expressed the chemical composition in terms of moles of the major minerals present. Balasanyan reported that instead of expensive, time-consuming chemical analyses, precise modal analyses can be used to give results comparable to detailed wet chemical analyses. However, this type of approach does not permit comparison of the rock under investigation with the wealth of chemical analyses available in the literature. Wahlstrom (1950, p. 237) refers to the calculation of chemical composition from the mode but notes "it cannot be assumed that the computed chemical composition of the rock is very accurate."

A recent survey by Fairbairn and others (1951) investigated the precision and accuracy in chemical and modal analyses of rocks. Two rocks, a granite designated G-1 and a diabase designated W-1, were analyzed by conventional chemical procedures in 25 reputable analytical laboratories throughout the world. These same rocks were subjected to modal analyses at the Geophysical Laboratory (Chayes 1951) and at the Massachusetts Institute of Technology (Chayes 1952). Comparisons were made between the actual mineral distribution (mode) of these rocks and the computed mineral distribution (norm), and attempts were made to explain the discrepancy between the two. The chemical composition of these rocks was not calculated from the modal analyses, and therefore no comparison was made between the results of standard chemical procedure and the chemical composition derived from thin-section petrography. A comparison would be interesting to see how the accuracy of an analysis computed from data obtained with a petrographic microscope compares with the chemical determinations. Modal analyses do not require expensive equipment normally unavailable in the petrographic laboratory, and one thin-section analysis can be made in less than an hour.

If agreement between the two techniques can be demonstrated to be close, the petrologist can extend the petrographic method of chemical analysis to many research problems. The purpose of this note is to compare the results of the two methods of analysis for one of the two rocks* and to apply the two techniques to an "unknown" rock sample. On the basis of these comparisons it can be decided whether calculation of the chemistry of the rocks from examination with the petrographic microscope can be considered reliable and adequate for petrological investigations.

The work of Fairbairn, et al. (op. cit.), revealed serious discrepancies in many of the chemical analyses made on the two rocks. The wide range of results for individual oxides reported by the chemists came as a surprise and shock to many petrologists. However Fairbairn notes (p. 69) that . . . "the likelihood of occurrences of many of these discrepancies is of course commonplace to chemists and causes no surprise if the conditions of analysis are appreciated." He continues (p. 70), "ranges reported in the granite and diabase standards are greater than the compositional limits for related but distinctly different rock types," whereas (p. 5) "precision obtained by modal analyses proved superior to that shown by norms calculated from the individual chemical analyses."

---

* The rock studied is the granite G-1. Since the optics and composition of the feldspar and pyroxene in the diabase W-1 are not available from the literature, calculation of the chemical composition from mineralogical data cannot be made satisfactorily for this rock.

PROCEDURE

Comparisons between the chemically and optically determined composition of a granite and a norite were made. The chemical composition of the granite G-1 was calculated from modal analysis made by Chayes (1951, p. 61) and represents the mean of measurements on sixteen thin sections. The results were then compared with the wet chemical analyses presented by Schlecht and Stevens (1951) (Table 1).

TABLE 1. CHEMICAL COMPOSITION OF GRANITE G-1 AS DETERMINED BY ROUTINE CHEMICAL AND PETROGRAPHIC PROCEDURES

	I	II	III	IV	V
	Range of Chemical Analyses Reported by 30 Chemists*	Arithmetic Mean of Rock Analyses†	Chemical Analysis from Mode for Comparison with I and II‡	Arithmetic Mean of Rock Analyses Recalculated to 100%	Chemical Analysis From Mode§
SiO_2	71.0–72.7%	72.2%	71.1%	72.9%	71.7%
Al_2O_3	13.2–16.0	14.4	14.7	14.6	14 9
MgO	0.2– 0.8	0.4	0.5	0.4	0.5
FeO	0.8– 1.4	1.0	1.3	1.0	1.3
Fe_2O_3	0.3– 1.7	0.9	1.0	0.9	1.0
CaO	1.2– 1.9	1.4	1.5	1.4	1.5
Na_2O	2.6– 4.0	3.3	2.8	3.3	2.8
K_2O	3.9– 6.9	5.5	6.3	5.5	6.4
		99.1%	99.2%	100.0%	100.1%

* Dennen, Ahrens, and Fairbairn, 1951, p. 33–34, Figs. 1 and 2. (TiO_2, MnO, P_2O_5, and H_2O omitted; not recalculated to 100 per cent.)

† Dennen, Ahrens, and Fairbairn, 1951, p. 37, Table 14. (TiO_2, MnO, P_2O_5, and H_2O omitted; not recalculated to 100 per cent.)

‡ As TiO_2, MnO, P_2O_5, and H_2O have been omitted from the chemical analyses listed in Columns I and II, the chemical analysis calculated from the mode (Column V) has been recomputed for direct comparison with Columns I and II.

§ Calculation by the writer from modal analyses of Chayes (1951, p. 61).

A specimen of norite from the Caribou Lake intrusion, Canada (Friedman, 1957) was analyzed in thin section by the writer. The chemical composition of the rock was computed from the mode, and the results were compared with chemical analyses of the same rock made by the Rock Analysis Laboratory of the University of Minnesota. The results are compared in Table 2.

Analysis by petrographic procedure involves three steps: 1. Identification of the minerals present and assigning each a formula based on optical data; 2. A determination of the relative abundance of each mineral using counting techniques; 3. Computation of the weight per cent chemical composition. The first two steps are routine and are discussed elsewhere (Tröger 1952, Chayes 1949).

The third step of calculating the chemical composition from the modal analysis involves the conversion of the mode to weight per cent. The weight per cent of the minerals present in the granite, except for potassium feldspar and plagioclase, was taken from Dennen, Ahrens, and Fairbairn (1951, p. 42). Specific gravity data given by Tröger (1952) were used to convert the modal values of the feldspars to weight per cent. In the norite sample the specific gravities of plagioclase, pyroxene, and biotite present were determined from tables of Tröger (1952). The specific gravities of quartz and magnetite were taken from Dana and Ford (1932). The specific gravity of the garnet in norite was determined for the writer by D. K. Smith.

TABLE 2. CHEMICAL COMPOSITION OF NORITE AS DETERMINED BY ROUTINE CHEMICAL AND PETROGRAPHIC PROCEDURES

	Chemical Composition Determined by Chemical Analysis*	Chemical Composition Calculated from Mode
SiO_2	51.8%	52.7%
Al_2O_3	19.8%	18.4%
Fe_2O_3	1.1%	1.1%
FeO	6.2%	6.6%
MgO+CaO†	18.3%	18.6%
[MgO]	[8.9%]	[10.6%]
[CaO]	[9.4%]	[8.0%]
Na_2O	2.5%	2.5%
K_2O	0.3%	0.1%
Total	100.0%	100.0%
	Analyst Doris Thaemlitz	Gerald M. Friedman

* Recalculated to 100 per cent, omitting H_2O, CO_2, TiO_2, P_2O_5, MnO, S, and Cl.

† A probable error in the identification of some pyroxene grains brought about a small discrepancy between chemical and petrographic analyses for CaO and MgO. The sums of CaO and MgO for the two techniques agree as shown in this table.

For the granite calculation the potassium feldspar was considered a pure orthoclase or microcline without Na_2O substitution. For plagioclase a value of An_{23} has been obtained from physical parameters (Chayes

1952, p. 213). The theoretical composition given by Dana and Ford (1932) was used for muscovite and magnetite. The gamma index of biotite ($\gamma = 1.637 \pm 0.005$) was experimentally determined and the biotite composition was approximated with the aid of a table by Winchell and Winchell (1951, p. 374).

Chayes (1951, p. 60–61) distinguishes between opaque and non-opaque accessory minerals. The non-opaque accessories have not been identified, but in some calculations (cf. Dennen, Ahrens, and Fairbairn, 1951, p. 42) both types of accessories have been lumped as magnetite, a procedure which has been adopted in the present study.

For the norite the composition of plagioclase, pyroxene, and garnet were determined from optical parameters with the aid of tables (Crump and Ketner 1953, p. 31; Hess, 1952, p. 180, Fig. 2; Walker and Poldervaart, 1949, p. 631; Tröger, 1952, p. 12). The detailed petrography and mineralogy of this rock are described elsewhere (Friedman, 1957, p. 1544–1545). For biotite an average chemical composition given by Wahlstrom (1950, p. 238) was used. The exact composition of amphiboles cannot be obtained from optical parameters, and an average composition given by Wahlstrom (1950, p. 238) was used.

Results and Discussion

Column I in Table 1 presents the range of values for the oxides determined in the granite G-1 by the chemists (Dennen, Ahrens, and Fairbairn, p. 33–34). Columns II and IV show the arithmetic mean of these analyses (Dennen, Ahrens, and Fairbairn, p. 37), and Columns III and V the chemical composition computed from the modal analysis of Chayes (1951). The calculations for arriving at the chemical composition from the mode are given in the Appendix.

TiO_2, MnO, H_2O, and P_2O_5 which have been determined chemically for the granite have not been obtained by calculation from the mode.

The most outstanding observation from this comparison is that each constituent computed from the mode for the granite lies within the range reported from chemical analyses. Moreover, comparison of Columns IV and V of Table 1 shows good agreements between the arithmetic mean of the chemical analyses and the calculated composition from the mode. Schlecht and Stevens (1951, p. 7) point out that assignment of "correct" values for the composition of the rock is not justified on the basis of chemical analyses. Therefore in the absence of knowledge of the "true" composition of this rock, no precise appraisal can be made of the error involved in determining the chemical composition from modal studies. However the discrepancy between chemical and petrographic procedures appears to be small enough to justify wider application of the petrographic technique to petrological and geochemical studies of rocks.

The granite G-1 contains minerals which are easily identified and for which modal analyses are relatively simple to make. To test the usefulness of the petrographic method further, a norite sample was selected in which reaction rims, cataclastic deformation, and replacement by secondary minerals make modal studies more difficult. This rock has been described in detail elsewhere (Friedman, 1957, p. 1540-1541). For the mode of the norite and the composition and specific gravity of the norite minerals refer to the appendix. Table 2 shows that the discrepancy between the results of chemical and petrographic procedures is remarkably small for six of the eight constituents. The only disparity is for CaO and MgO. However, the sum of CaO and MgO agrees closely for the two analyses. The error in these two constituents is probably a result of misidentifying some clinopyroxene grains as orthopyroxene. Even so, the discrepancy between the two analyses for CaO and MgO is not serious if the wide range of results for MgO and CaO in the diabase W-1, as reported by the chemists, is considered. Considering the complexity of the rock, agreement between the two techniques is considered highly satisfactory. Analysis of the norite sample shows that the chemical composition of mineralogically and texturally complex rocks can be determined satisfactorily with the petrographic microscope.

This study indicates that for rocks in which the composition of the individual minerals can be obtained by optical measurements, the major constituents can be determined with the petrographic microscope and the results can be considered reliable for most purposes. Petrologists should therefore make more chemical analyses with the aid of the microscope. Glasses, shales, and fine-grained rocks are not amenable to determination of chemical composition by the microscopic technique.

The major uncertainty of calculations of the kind presented in this paper is the assignment of a specific chemical composition to complex minerals, such as amphiboles, for which satisfactory correlations between optical properties and chemical composition are not available. This may be serious if these minerals make up a major part of the rock.

CONCLUSIONS

From this study it is concluded that

1. Each constituent computed from the mode for the granite G-1 lies within the range reported by the chemists. The arithmetic means of the chemical analyses agree closely with the analyses calculated from the mode.

2. Analysis of the norite sample shows that the chemical composition of mineralogically and texturally complex rocks can be determined satisfactorily with the petrographic microscope.

3. This study indicates that for rocks in which the composition of the

individual minerals can be obtained by optical measurements, the major constituents can be determined with the petrographic microscope, and the results can be considered reliable for most purposes.

4. Petrologists should make more chemical analyses with the petrographic microscope.

APPENDIX

I. Calculation of Chemical Composition of Granite, G-1, from Mode

Mineral	Mode (Chayes, 1951 p. 61)	Weight % (Dennen, Ahrens, and Fairbairn p. 42)	Sp.G	Weight %	Weight % recalculated to 100%, or grams in 100 g. of rock
Quartz	27.5%	28.0%		28.0%	27.9%
Potassium Feldspar	35.4	65.9	2.57	34.5	34.4
Plagioclase An_{23}	31.4		2.63	31.4	31.2
Muscovite	1.3	1.4		1.4	1.4
Biotite	3.2	3.6		3.6	3.6
Magnetite	1.2	1.5		1.5	1.5
		100.4%		100.4%	100.0%

Quartz SiO_2 27.9 g. SiO_2 in 100 g. of rock.

Potassium feldspar $KAlSi_3O_8$ 34.4 g. in 100 g. of rock.

	Mol. wt.	%	
$\frac{1}{2}K_2O$	47.1	16.9×34.4 g. =	5.8 g. K_2O
$\frac{1}{2}Al_2O_3$	51.0	18.3×34.4 g. =	6.3 g. Al_2O_3
$3\ SiO_2$	180.3	64.8×34.4 g. =	22.3 g. SiO_2
	278.4	100.0	34.4 g.

Plagioclase $Ab_{77}An_{23}$ 31.2 g. in 100 g. of rock.

$NaAlSi_3O_8$	Mol. wt.	$CaAl_2Si_2O_8$	Mol. wt.	Ab.
$\frac{1}{2}Na_2O$	31.0	CaO	56.1	0.77×262.3 = 202.0
$\frac{1}{2}Al_2O_3$	51.0	Al_2O_3	102.0	An.
$3\ SiO_2$	180.3	$2\ SiO_2$	120.2	0.23×278.3 = 64.0
	262.3		278.3	Mol. wt. $Ab_{77}An_{33}$ = 266.0

$$\left(\frac{0.77\times 31.0}{266.0}\right)\times 100 = 9.0\% = 2.8\text{ g. }Na_2O$$

$$\left(\frac{0.23\times 56.1}{266.0}\right)\times 100 = 4.9\% = 1.5\text{ g. CaO}$$

$$\left(\frac{0.77\times(51.0)+0.23(102.0)}{266.0}\right)\ 100 = 23.6\% = 7.4\text{ g. }Al_2O_3$$

$$\left(\frac{0.77(180.3)+0.23(120.0)}{266.0}\right)\ 100 = \underline{62.6\%} = \underline{19.5\text{ g. }SiO_2}$$

$$100.1\% \qquad 31.2\text{ g.}$$

Muscovite 1.4 g. in 100 g. of rock.

	Composition by Dana and Ford (1932)	Composition H_2O-free basis	
SiO_2	45.2%	47.3%×1.4 g.	=0.7 g. SiO_2
Al_2O_3	38.5	40.3	=0.6 g. Al_2O_3
K_2O	11.8	12.4	=0.2 g. K_2O
H_2O	4.5		
	100.0	100.0	1.5 g.

Biotite 3.6 g. in 100 g. of rock.

25% Phlogopite	$K_2Mg_6(OH)_4Si_6Al_2O_{20}$
25% Eastonite	$K_2Mg_5Al(OH)_4Si_5Al_3O_{20}$
25% Siderophyllite	$K_2Fe_5Al(OH)_4Si_5Al_3O_{20}$
25% Annite	$K_2Fe_6(OH)_4Si_6Al_2O_{20}$

Phlogopite	Eastonite	Siderophyllite	Annite
$K_2O = 94.2$	$K_2O = 94.2$	$K_2O = 94.20$	$K_2O = 94.2$
$6MgO = 242.0$	$5MgO = 201.6$	$5FeO = 359.25$	$6FeO = 431.1$
$Al_2O_3 = 102.0$	$2Al_2O_3 = 203.9$	$2Al_2O_3 = 203.92$	$Al_2O_3 = 102.0$
$6SiO_2 = 360.5$	$5SiO_2 = 300.5$	$5SiO_2 = 300.45$	$6SiO_2 = 360.2$
$2H_2O = 36.0$	$2H_2O = 36.0$	$2H_2O = 36.00$	$2H_2O = 36.0$
834.7	836.2	993.82	1023.8

$$0.25(834.7)+0.25(836.2)+0.25(993.8)+0.25(1023.8)=922.1=\text{M.W. of biotite}$$

$$\frac{94.2}{922.1}\times 100 = 10.21\%\ K_2O$$

$$\frac{0.25(242.0)+0.25(201.6)}{922.1}\times 100 = 12.03\%\ MgO$$

$$\frac{0.25(359.25)+0.25(431.1)}{922.1}\times 100 = 21.43\%\ FeO$$

$$\frac{0.25(102.0)+0.25(203.9)+0.25(203.9)+0.25(102.0)}{922.1}\times 100 = 16.59\%\ Al_2O_3$$

$$\frac{0.25(360.5)+0.25(300.5)+0.25(300.5)+0.25(360.5)}{922.1}\times 100 = 35.84\%\ SiO_2$$

$$\frac{36.0}{922.1}\times 100 = \frac{3.90\%}{100.0\%}\ H_2O$$

Recalculated on H_2O-free basis		
K_2O	10.6%×3.6 g.	=0.382 g. K_2O
MgO	12.5	=0.450 g. MgO
FeO	22.3	=0.803 g. FeO
Al_2O_3	17.3	=0.623 g. Al_2O_3
SiO_2	37.3	=1.343 g. SiO_2
	100.0	3.601 g.

Magnetite 1.5 g. in 100 g. of rock.

	Mol. wt.	
FeO	71.8	$\frac{71.8}{231.4}\times 100=31.0\%=0.5$ g.
Fe_2O_3	159.5	$\frac{159.6}{231.4}\times 100=69.0\%=1.0$ g.
	231.4	1.5 g.

Chemical Analysis (Petrographic Method)

SiO_2	71.7%
Al_2O_3	14.9
Fe_2O_3	1.0
FeO	1.3
MgO	0.5
CaO	1.5
Na_2O	2.8
K_2O	6.4
	100.1%

II. Mode of Norite, and Specific Gravity of Minerals in Norite

Mineral	*Mode*	*Sp.G.*
Plagioclase	63.2%	2.70
An_{62}		
Clinopyroxene	1.0	3.34
En_{47} Fs_{13} Wo_{40}		
Orthopyroxene	28.7	3.39
Of_{23}		
Hornblende	4.8	3.20
Biotite	1.1	3.00
Garnet	1.0	3.84
Andradite 21%		
Pyrope 47%		
Almandine 32%		
Magnetite	0.1	5.20
Quartz	0.1	2.65
	100.0%	

References

Balasanyan, S. I., 1957, (Optical determinations of petrochemical constructions): Izvest. Akad. Nauk Armyan S. S. R., Ser. Geol. i Geograf. Nauk, v. 10, No. 5–6, p. 59–74. *Chem. Abstracts* **52**, 11675i.

Chayes, Felix, 1949, A simple point counter for thin-section analysis: *Am. Mineral.*, **34**, 1–11.

Chayes, Felix, 1951, "Modal Analyses of the Granite and Diabase Test Rocks" in Fairbairn, H. W., and others, A Cooperative Investigation of Precision and Accuracy in Chemical, Spectrochemical and Modal Analysis of Silicate Rocks: *U. S. Geol. Survey Bull.* **980,** 59–68.

Chayes, Felix, 1952, "The Finer-Grained Calcalkaline Granites of New England": *Jour. Geol.*, **60,** 207–254.

Crump, R. M., and Ketner, K. B., 1953, Feldspar Optics in Emmons, R. C., Editor, Selected petrogenetic relationships of plagioclase: *Geol. Soc. Am. Mem.* **52,** 23–40.

Dana, E. S., and Ford, W. E., 1932, A textbook of mineralogy: 4th Edition John Wiley and Sons, New York, 851 p.

Delesse, M. A., 1886, Procédé mécanique pour déterminer la composition des roches: 3rd Ed., Paris. (Reference given by Glagolev 1933).

Dennen, W. H., Ahrens, L. H., and Fairbairn, H. W., 1951, "Spectrochemical Analysis of major constituent elements in minerals and rocks" in Fairbairn, H. W., and others, A Cooperative Investigation of Precision and Accuracy in Chemical, Spectrochemical and Modal Analysis of Silicate Rocks: *U. S. Geol. Survey Bull.* 980, p. 25–52.

Fairbairn, H. W., and others, 1951, A Cooperative Investigation of Precision and Accuracy in Chemical, Spectrochemical, and Modal Analyses of Silicate Rocks: *U. S. Geol. Survey Bull.* 980, 71p.

Friedman, G. M., 1957, Structure and Petrology of the Caribou Lake Intrusive Body, Ontario, Canada: *Geol. Soc. America Bull.*, **68,** 1531–1564.

Glagolev, A. A., 1933, (On geometrical methods of quantitative mineralogical analysis of rocks): Trudy Inst. Prikladnoi Mineralogii, No. 59; transl. by J. B. Sykes, Atomic Energy Research Establishment Lib. Trans. No. 567, 1955.

Hess, H. H., 1952, Orthopyroxenes of the Bushveld type, ion substitutions and changes in unit cell dimensions: *Am. Jour. Sci.*, Bowen Volume, p. 173–187.

Kuznetsov, E. A., (1947), (Calculation and graphic methods for the chemism of eruptive rocks): Vestnik Moskov Univ., No. 3, p. 37–47. *Chem. Abstracts* **44,** 83i.

Niggli, P. (1936), (Molecular norms for rock (composition) calculation): *Schweiz. mineral. petrog. Mitt.*, **16,** 295–317. *Chem. Abstracts* **31,** 1327h.

Schlecht, W. G., and Stevens, R. E., 1951, "Results of chemical analysis of samples of granite and diabase": in Fairbairn, H. W., and others, A Cooperative Investigation of Precision and Accuracy in Chemical, Spectrochemical and Modal Analysis of Silicate Rocks: *U. S. Geol. Survey Bull.* **980,** 7–24.

Tröger, W. E., 1952, Tabellen zur optischen Bestimmung der gesteinsbildenden Minerale: E. Schweitzerbartsche Verlagsbuchhandlung, 147p.

Wahlstrom, E. E., 1950, Igneous minerals and rocks: John Wiley and Sons, New York, 367 p.

Walker, Frederick, and Poldervaart, Arie, 1949, Karoo dolerites of the Union of South Africa: *Geol. Soc. America Bull.*, **60,** 591–706.

Whitten, E. H. T., 1953, Modal and Chemical Analyses in Regional Studies: *Geol. Magazine*, **90,** 337–344.

Winchell, A. N., and Winchell, Horace, 1951, Elements of optical mineralogy; part II, Descriptions of minerals: John Wiley and Sons, New York, 551 p.

Manuscript received April 20, 1959.

THE AMERICAN MINERALOGIST, VOL. 45, JANUARY–FEBRUARY, 1960

PAULINGITE, A NEW ZEOLITE, IN ASSOCIATION WITH ERIONITE AND FILIFORM PYRITE

W. Barclay Kamb and William C. Oke, *California Institute of Technology, Pasadena, California*

Abstract

A new zeolite, for which the name paulingite is proposed, has been found in vesicles in basalt from the Columbia River near Wenatchee, Washington. Paulingite is cubic, and occurs as perfect, transparent rhombic dodecahedra. The very large cubic cell has $a_0=35.10 \pm .02$ Å, and the space group is probably O_h^9-Im3m. Ca and K are the chief cations, but Ba and Na are also present. The atomic ratio of Si to Al is roughly 3. In association with the paulingite is the rare zeolite erionite. It occurs as relatively large acicular hexagonal prisms, and also as tufts of very fine fibers. The hexagonal unit cell has dimensions $a=13.27 \pm .02$ Å, $c=15.05 \pm .02$ Å, and the space group is either D_{6h}^4, C_{6v}^4, or D_{3h}^4. Erionite is a member of the chabazite group of zeolites. Also in association with the paulingite and erionite is pyrite of remarkable filiform habit.

Introduction

In the course of deepening the channel of the Columbia River at Rock Island Dam, Washington, boulders of vesicular basalt containing a suite of hydrothermal minerals were dredged up. Samples of the basalt were sent to us by Walter Muffly, of Wenatchee, Washington. The minerals, which are found as well-formed crystals attached to the walls of the vesicles, include heulandite, phillipsite, calcite, and pyrite. Some of the pyrite displays a remarkable filiform habit, and is described in detail below. In association with these minerals occur two species that are not readily identifiable. The first occurs as fine, white, acicular crystals superficially resembling natrolite but distinguished from it by the hexagonal appearance of crystals large enough to be seen in cross section under the binocular microscope. The second is present as clear, perfect rhomic dodecahedra, and was thought at first to be analcite in an unusual habit. The occurrence and association of the two minerals, as well as their appearance, suggest that they are zeolites.

Optical examination fails to distinguish the isometric mineral decisively from analcite or faujasite. The acicular mineral is distinguished from natrolite by lower birefringence. *X*-ray powder diffraction patterns of the minerals suggest that they are distinct from the isometric and acicular zeolites for which powder data are available or for which we have obtained powder patterns: analcite, natrolite, thompsonite, and mordenite.

Examination of single crystals of the acicular mineral by *x*-ray diffraction indicates that it is the zeolite erionite, for which characterizing data have recently been obtained by Gard (Barret *et al.*, 1959) and by

Deffeyes (1959). Because erionite had, previous to the work of Deffeyes (1959), been known from only one locality in the world, we shall present the data obtained in our study of the mineral.

X-ray examination of single crystals of the cubic mineral shows decisively that it is a new species, and semi-quantitative chemical tests confirm its assignment as a zeolite. We propose the name *paulingite* for it.

OCCURRENCE

The rock in which the zeolites occur is a microporphyritic basalt containing abundant 0.05 to 0.4 mm. augite phenocrysts and abundant lath-like 0.1 to 0.5 mm. labradorite (An_{53}, assumed to be the high temperature form) phenocrysts having very ragged, forked ends. A few larger, less ragged phenocrysts of labradorite up to 1.0 mm. in length are present, usually showing a slight concentric compositional zonation. The groundmass, which makes up about 30 per cent of the volume of the rock (mesostasis), is a weakly devitrified glass displaying variolitic structure, and containing numerous well-formed dendritic aggregates of magnetite (?) cubes 0.005 to 0.01 mm. in size. In addition to the groundmass, a significant portion of the space interstitial to the phenocrysts, some 15 per cent of the volume of the rock, is filled with colloform layers of goethite (possibly with some lepidocrocite) which wrap around the phenocrysts and, less commonly, around the groundmass to a depth of .02 to .03 mm., filling the smaller interstices but leaving voids at the centers of the larger ones, which are gradational in size with unmistakable vesicles 0.5 mm. and greater in diameter. The goethite coating consists usually of two distinct layers, each .01 mm. thick, and the goethite contains magnetite dendrites (in many cases small cruciform aggregates), indistinguishable from the dendrites of the groundmass. Some of the voids enclosed by the goethite layers are empty, while others are filled or partially filled with zeolitic spherulites.

As dredged from the bottom of the channel, the zeolite-bearing basalt forms large rounded boulders that appear to have been transported some distance, to judge from the roundness and smoothness of their surfaces. A large volume of boulders, all basalt, was dredged from the bottom, but most of the boulders are non-vesicular and unrounded, in contrast to the rounded vesicular boulders that contain the zeolites. Within the rounded vesicular boulders, only a small fraction of the vesicles contain the hydrothermal minerals. Several persons have searched portions of the Columbia River channel above the point where the minerals were discovered, but to date the original provenance of the material has not been found. The presence of erionite brings to mind the vicinity of the original locality of this mineral at Durkee, Oregon, as a possible source, but the drainage patterns rule out this possibility.

The zeolites are evidently the latest crystallization products in the rock, since they overlie the goethite coating. The coating itself displays seemingly contradictory features: on the one hand, the uniformity of the coating as an interstice-filling, and the apparent absence of a source for the iron (as would be exhibited in altered relicts) in the bulk of the rock, suggest a late-stage origin for the coating, as though it were deposited from solutions derived elsewhere; whereas the content of magnetite dendrites indistinguishable from the magnetite in the glassy groundmass suggests a close relation with the crystallization of the bulk of the rock. With these uncertainties of interpretation, even less can be inferred about the detailed conditions of genesis of the zeolites, and we shall not, therefore, pursue further this interesting aspect of the occurrence.

PAULINGITE

Paulingite occurs as perfect clear rhombic dodecahedra 0.1 to 1.0 mm. in diameter. Because of their attachment to the vesicle walls, the crystals are roughly hemispherical in shape, and exhibit usually only five or six of the dodecahedral planes. As seen in place on the vesicle walls, the crystals appear dark brown to black, but in fact they are clear and colorless, the apparent dark color being due to their clarity and secure attachment to the dark vesicle walls. The dodecahedral faces are smooth and planar, and display a bright vitreous luster. A few faint growth striations, parallel to the edges of the faces, are visible. The crystals appear to have no cleavage, and fragments seen under the binocular microscope remarkably resemble small chips of ice. No crystal forms other than the rhombic dodecahedron are present, even as narrow truncations or facets. The hardness is about 5. Figure 1 shows a typical paulingite crystal in place on a vesicle wall.

Under the petrographic microscope the crystals are seen to contain a scattering of minute bubble-like inclusions. These inclusions are prominent when the index of refraction of the mineral is nearly matched to that of the immersion liquid, but they evidently do not detract from the macroscopic clarity of the crystals. Paulingite is quite isotropic throughout, and only extremely rarely can faint, isolated, fuzzy, very weakly birefringent twinning (?) lamellae be found. This distinguishes paulingite from analcite, though not from faujasite.

The index of refraction, measured at 23° C. in sodium vapor light, by the immersion method, is $n_D^{23°c.} = 1.473 \pm .001$. The immersion liquids (Cargille) were not calibrated, but were taken from previously unopened and sealed bottles purchased in September, 1957.

Single crystal x-ray diffraction study, using zero and upper level Weissenberg and precession photographs, provides the following data. Paulingite is cubic, and the cubic cell has edge length $a_0 = 35.10 \pm .02$ Å.

A precise determination of this value was obtained from a rotation photograph using copper Kα radiation, nickel-filtered, with the film in self-calibrating (Straumanis-type) arrangement. The crystal used was rotated about a cubic axis, and the reflections were indexed with the help of a zero-layer Weissenberg photograph. Reflections of the type hkl for $l=0$ to $l=12$ have been examined with equi-inclination Weissenberg photographs, and only reflections having $h+k+l$ even are observed, indicating a body-centered lattice. No other systematic extinctions are present. The Laue group is O_h, and the diffraction symbol is $m3m-I\cdot\cdot\cdot$. The possible space groups are therefore O^5-$I432$, $T_d{}^3$-$I43m$, and $O_h{}^9-Im3m$. A prominent feature of the diffraction patterns for all observed values of l is the relative abundance of weak reflections as compared with reflections of intermediate intensity, suggesting a centrosymmetric structure. The space group is therefore probably $O_h{}^9-Im3m$.

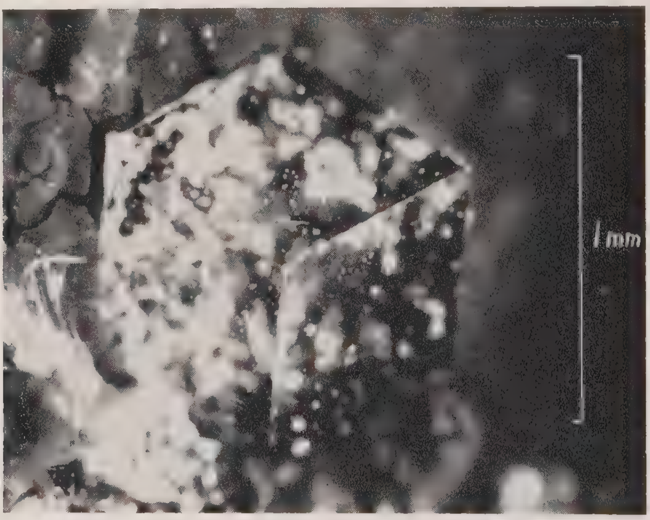

FIG. 1. Crystal of paulingite, in place on vesicle wall. The dodecahedron is viewed in the direction [111]. The bright spots are caused by light reflected at the under side of the crystal.

In Fig. 2 is shown, full size, a portion of an oscillation photograph, obtained with unfiltered copper radiation, of a paulingite crystal rotating about an a axis, and in Fig. 3 is shown part of the zero level Weissenberg photograph (also full size) of the same crystal, obtained with CuKα radiation.

The size of the paulingite unit cell is remarkable. In fact, the paulingite cell is, to our knowledge, the largest known unit cell of an inorganic

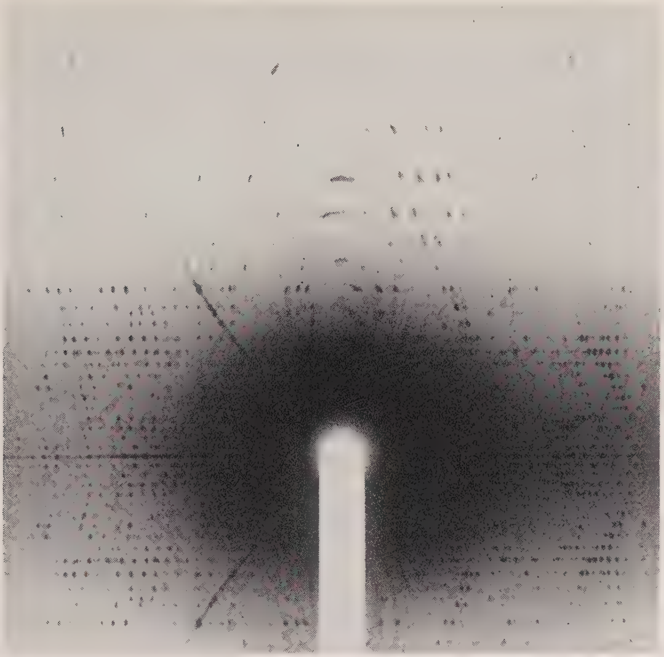

Fig. 2. 20° oscillation photograph of paulingite, reproduced at full scale. Oscillation axis [100]. Unfiltered copper radiation. Camera diameter 57.3 mm.

Fig. 3. Equatorial Weissenberg photograph of the ($hk0$) plane of paulingite, obtained with nickel-filtered copper radiation. Full scale; camera diameter 57.3 mm.

compound, exceeding in size the cells of the most complex intermetallic compounds, sulfosalts, and metallic sulfides, and surpassed only by the unit cells of crystallized proteins.

Because of the large observed size of the paulingite unit cell, we have examined the diffraction data carefully for any indication that the large cell might be accounted for by multiple twinning of a cell of smaller size and lower symmetry, or by syntaxic intergrowth of cells of different sizes. Such phenomena have been found to explain diffraction patterns of some apparently large cubic lattices (Donnay *et al.*, 1958*a* and 1958*b*). However, the absence of any systematic extinctions other than those due to the body-centering translation preclude any such interpretation of the paulingite data, and the optical isotropy in addition makes unlikely the possibility of multiple twinning of individuals of lower symmetry.

Because of the very small amount of paulingite available, a complete wet gravimetric chemical analysis is not possible. But in any case a complete chemical analysis would not be of much help in characterizing such a structurally complex substance, or in establishing its identity from other minerals. We have, however, obtained semi-quantitative information on the composition. A batch of crystals (total weight about 15 mg.) was picked by hand from the vesicle walls, and hand sorted under the binocular microscope into two lots—(1) fragments bearing a visible incrustation of goethite derived from the vesicle walls, and (2) fragments appearing perfectly clean. The fragments of lot 1 were crushed gently in a diamond mortar, and resorted into lots 1 and 2, which then weighed respectively 2.9 mg. and 10.1 mg. The water content was determined by heating the samples to a dull red heat, which was sufficient to cause fusion, in platinum crucibles, and measuring the weight loss. The two dry samples were then analyzed semi-quantitatively by emission spectroscopy. The analyses were performed by Elisabeth Godijn in the spectrographic laboratory of the Division of the Geological Sciences, California Institute of Technology. Weights of the samples available for spectrographic analysis were 0.9 mg. (lot 1) and 7.7 mg. (lot 2).

The results of the analyses are given in Table 1. The small amount of material in lot 1 allows only a qualitative interpretation of this analysis. The agreement between the two analyses is of the order expectable from the spectrographic method, except for the marked discrepancy in CaO content. The Fe_2O_3 in lot 1 is doubtless due to the goethite impurity, and presumably the MgO is to be ascribed to the same source, although its high value casts doubt on the (optical) identification of the impurity as goethite. Here we restrict our consideration to the analysis of the larger, cleaner sample (lot 2).

The indicated composition is evidently that of a zeolite. The magnesium reported doubtless derives from the goethite (?) incrustation, a small amount of which must have been present in lot 2, because a few small fragments in the sample became black upon heating. The Al/Si ratio of 0.15 given by the analysis conflicts with the cation composition in lot 2, which requires an Al/Si ratio of 0.47. Either the analysis is internally inconsistent, or else anions must be present outside the tectosilicate framework. Halogens are not detectable in the spectral range used for the analysis, but without further evidence it seems more likely that the discrepancy reflects the inherent inaccuracies of the spectrographic method.

TABLE 1. SEMI-QUANTITATIVE ANALYSES OF PAULINGITE

	Lot 1 (dirty) (0.9 mg.)	Lot 2 (clean) (7.7 mg.)
H_2O+: % of total (hydrated) wt.:	24	22
Oxides: % of dry wt.:		
SiO_2	40	67
Al_2O_3	6	9
CaO	1	7
BaO	2	2
SrO	—	—
Na_2O	*	1
K_2O	*	10
MgO	2	0.01
Fe_2O_3	0.5	—
Atoms (based on Si+Al=12):		
Si	11.0	10.4
Al	1.0	1.6
Ca	0.3	1.2
Ba	0.2	0.1
K	*	2.0
Na	*	0.4
H_2O	?	14.3

Dashes indicate that the element was not detected.

* Not observable in wavelength region employed.

We have not measured the density of paulingite, but to get an idea of the contents of the unit cell we may use the following very rough method, based on the index of refraction. From the equation of Lorentz and Lorentz

$$V_m \frac{n^2 - 1}{n^2 + 2} = \sum_i N_i \lambda_i$$

where V_m is the volume of one mole of the substance, and where there are N_i atoms or atomic groups of atomic refractivity λ_i ($i=1, 2, \cdots$) in one molecule, we calculate the refractivity λ_x for the tetrahedral groups $Si_{1-x}Al_xO_2$ in the framework of various tectosilicates, by making use of the ionic refractivities for Na^+, Ca^{++}, K^+, Ba^{++}, and Cl^- given by Wasastjerna (1923). The results, in Table 2, show a progressive increase in refractivity from about 7.4 for SiO_2 to about 8.0 for $Si_{1/2}Al_{1/2}O_2$. The method may be applied to zeolites by assuming in addition the value 3.74 for the molecular refractivity of H_2O, intermediate between the values 3.71 for liquid water and 3.77 for ice. The results scatter more widely, but remain on the average in agreement with those for the anhydrous tectosilicates.

TABLE 2. MOLECULAR REFRACTIVITIES λ_x FOR THE $Si_{1-x}Al_xO_2$ TETRAHEDRAL GROUPS IN THE FRAMEWORKS OF VARIOUS TECTOSILICATES

Mineral	x	λ_x	Mineral	x	λ_x
Quartz	0	7.25	Celsian	$\frac{1}{2}$	8.05
Tridymite	0	7.5	Sodalite	$\frac{1}{2}$	7.9
Cristobalite	0	7.4	Gmelinite	$\frac{1}{3}$	7.7
Orthoclase	$\frac{1}{4}$	7.6	Chabazite	$\frac{1}{3}$	8.1
Albite	$\frac{1}{4}$	7.6	Levynite	$\frac{1}{3}$	7.5
Leucite	$\frac{1}{3}$	7.8	Analcite	$\frac{1}{3}$	7.8
Nepheline	$\frac{1}{2}$	8.1	Faujasite	$\frac{1}{3}$	7.8±0.2
Artif. $NaAlSiO_4$	$\frac{1}{2}$	8.1	Natrolite	$\frac{2}{5}$	7.9
Kaliophilite	$\frac{1}{2}$	8.0	NaA (artif.)	$\frac{1}{2}$	7.9
Anorthite	$\frac{1}{2}$	7.9			

For a zeolite framework with $x=\frac{1}{4}$, which is of the order indicated by the analyses for paulingite, we may take $\lambda_{1/4}=7.7$. Adjusting the total number of cations in Table 1 (lot 2) to fit $x=\frac{1}{4}$, we may then calculate the cell content of paulingite from its index of refraction and cell size. We find approximately 580 silicon plus aluminum atoms (plus the corresponding 1160 framework oxygen atoms), 690 water molecules, 40 calcium atoms, 65 potassium atoms, 15 sodium atoms, and 3 barium atoms. Of course, if the cations are in fixed positions in the structure, the number of barium atoms in the cell must be either 2, or 6, 8, etc., but the above numbers must be considered only the roughest approximation.

Table 3 gives x-ray powder diffraction data for paulingite.

Paulingite is named in honor of Linus Carl Pauling, Professor of Chemistry in the California Institute of Technology, in recognition of his outstanding contributions to the understanding of the complex structures of silicate minerals and other compounds.

TABLE 3. *X*-RAY POWDER DIFFRACTION DATA FOR PAULINGITE[1]

d	*I*[2]	*hkl*[3]
12.37	1	220
9.45	1	321
8.29	10	411, 330
7.86	1	420
7.14	2	422
6.88	10	510, 431
6.21	4	440
5.86	5	600, 442
5.70	5	611, 532
5.42	3	541
4.96	5	710, 550, 543
4.78	9	721, 633, 552
4.68	3	642
4.385	4	800
4.25	4	820, 644
4.08	4	831, 750, 743
3.875	4	910, 833
3.694	2	930, 851, 754
3.582	8	844
3.440	1	10·2·0, 862
3.346	8	10·3·1, 952, 765
3.261	9	10·4·0, 864
3.176	2	11·1·0, 954, 873
3.129	7	11·2·1, 10·5·1, 963
3.078	9	11·3·0, 970
2.983	8d	
2.851	2d	
2.789	2	
2.725	6	
2.615	7	
2.574	1	
2.520	2	
2.484	1	
2.448	1	
2.046[4]	3	
2.010	3	
1.774	6	
1.290[5]	3	
1.286	1	
1.253	1	
1.181	2	
1.168	1	
1.068	2d	
1.030	2	
1.017	1	
0.979	2	

[1] Data from self-calibrated (Straumanis-type) photograph obtained with manganese-filtered iron radiation.

[2] Intensities are visual estimates, not based on an intensity calibration scale; they are therefore sequential only, from 1 = "very weak" to 10 = "very strong." The suffix *d* indicates a diffuse line, resulting from near superposition of two or more reflections.

[3] Indices assigned on the basis of $a_0 = 35.10$ Å and $\lambda_{\text{FeK}\alpha 1} = 1.936$ Å. Indexing not carried out beyond $d = 3.0$ Å.

[4] Six very weak lines in the range $2.448 > d > 2.046$ were not measured.

[5] Twenty one weak lines in the range $2.010 > d > 1.290$ were not measured.

ERIONITE

Erionite forms fine transparent acicular crystals, isolated and in radiating clusters, and white to brownish tufted masses of very fine fibers. The yellowish and brownish tufts are colored by a "limonite" stain; the individual crystals are clear and colorless. The crystals are up to 2 mm. in length, and occur in diameters ranging from a fraction of a micron up to 0.2 mm. Most of the crystals are very fine: in the tufted masses, the majority of the fibers are too narrow to be resolved clearly in width under normal high power (×400) magnification, and the largest crystals are about 3μ in width. The larger crystals, up to 0.2 mm. in diameter, are rare, and occur mostly as isolated individuals growing out from the vesicle walls. These large crystals appear to be hexagonal prisms, and the hexagonal character is confirmed on the optical goniometer, although the prism faces give very diffuse signals, probably because of the presence of numerous growth striations and vicinal faces parallel to the prism axis. The crystals show parallel extinction, length slow, and are doubtless uniaxial positive. The ordinary index ω is $1.474 \pm .001$, measured by the immersion method in sodium vapor light at 24° C. The optical properties of the fine crystals from the tufted masses and of the coarser acicular crystals are identical, confirming that they are the same material. The birefringence is very low, and was measured with a Berek compensator upon a well-shaped hexagonal crystal 0.06 mm. in diameter. The result is $\epsilon - \omega = 0.0014 \pm .0002$. The hardness and density cannot readily be determined.

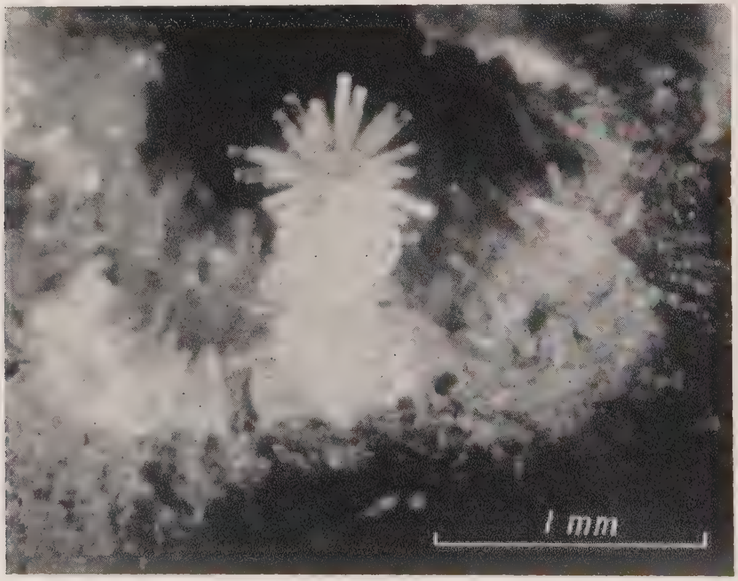

Fig. 4. Relatively large hexagonal prisms of erionite, forming a radiating cluster and lining the walls of a vesicle. The scale is indicated by the 1 mm. bar.

A cluster of the larger erionite crystals is shown in Fig. 4.

Single-crystal x-ray diffraction patterns were obtained from acicular crystals about 0.1 mm. in diameter, rotating about the needle axis. Zero and upper layer Weissenberg photographs show strict hexagonal symmetry. The length of the hexagonal *a* axis, measured by the method described above for the paulingite *a* axis, is 13.27 ± .02 Å. The *c* axis was measured from rotation photographs about [0001], and from $hh\cdot l$ and $h0\cdot l$ precession photographs for which the film-to-crystal distance *F* was simultaneously calibrated by means of the *a* axial length on the photographs. The result is $c = 15.05 \pm .02$ Å. The precession photographs show $hh\cdot l$ present only for $l = 2m$, indicating a *c* glide plane. The Laue group is D_{6h}, and the diffraction symbol is $6/mmm - P\cdot\cdot c$. The possible space groups are therefore $C_{6v}{}^4 - P6_3mc$, $D_{3h}{}^4 - P\bar{6}2c$, and $D_{6h}{}^4 - P6_3/mmc$.

The above single-crystal *x*-ray data are in good agreement with electron diffraction data obtained for erionite by J. A. Gard (given in Barrer et al., 1959), and with *x*-ray powder diffraction data obtained by K. Deffeyes (1959):

Source	*a*	*c*	*Diffraction Symbol*
Deffeyes	13.20	15.07	$6/mmm\ P\cdot\cdot c$
Gard	13.26	15.12	—
Kamb and Oke	13.27	15.05	$6/mmm\ P\cdot\cdot c$

The optical data given above agree reasonably with those obtained by Deffeyes.

The unit cell dimensions show that erionite is a member of the chabazite group of zeolites (the "würfel" zeolites), which embraces four members, whose space groups and cell dimensions (hexagonal cell) are:

chabazite	$R3m$ (nearly)	*a* 13.78	*c* 14.97	$Z=6$
gmelinite	$P6_3/mmc$	*a* 13.72	*c* 9.95	$Z=4$
levynite	(rhombohedral)	*a* 13.31	*c* 22.44	$Z=9$
erionite	$P6_3/mmc$	*a* 13.27	*c* 15.05	$Z=6$

The data for chabazite, gmelinite, and levynite are from Strunz (1956, 1958). The gmelinite space group is inferred from the ideal structure of Dent and Smith (1958).

The ideal "molecule" of the chabazite-group zeolites is $(Ca,Na_2)Al_2Si_4O_{12}\cdot 6H_2O$. The number of oxygen atoms in the erionite cell, determined by Deffeyes (1959) from the density and the original chemical analysis by Eakle (1898) agrees with this formula and with the structural relations inferred, although the number of water molecules appears to be about 4.5 rather than 6, and the mineral contains less aluminum than suggested by the formula.

Recently Dent and Smith (1958) have proposed a structural scheme for chabazite and gmelinite, according to which gmelinite is built by a stacking of double hexagonal rings of SiO_4 and AlO_4 tetrahedra in a

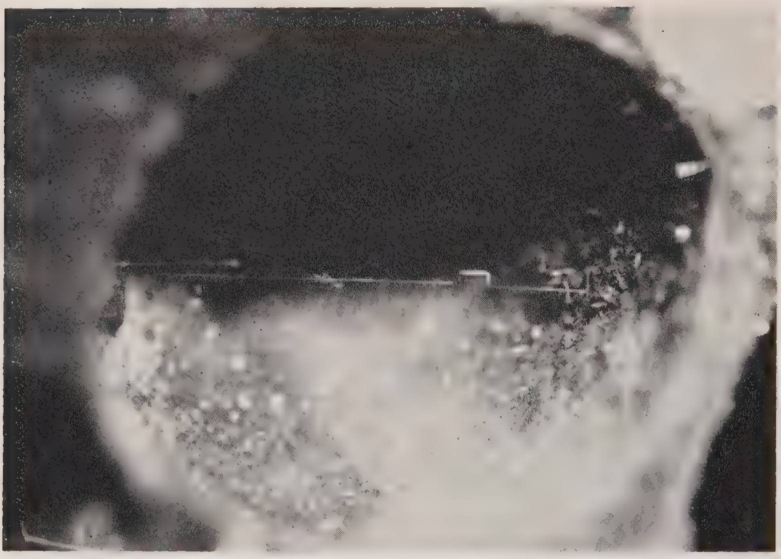

FIG. 5. Filiform crystals of pyrite growing from a pyrite cube in a vesicle. Note the right angle bends. The length of the long fiber is 6 mm.

hexagonally closest packed array, while in chabazite the same units are stacked in a sequence corresponding to cubic closest packing, thus resulting in a rhombohedral cell. It is interesting to note that erionite and levynite appear to be related in a manner analogous to the relation of gmelinite to chabazite, to judge by the ratio of c axial lengths, and the space group relations, to the extent that they are known. The kinship of erionite and levynite is further suggested by the a axial lengths, which contrast with the longer a axes of gmelinite and chabazite.

FILIFORM PYRITE

The minerals described above came to our attention because Walter Muffly asked if we could identify the fine "brass wires" in some of the vesicles. Microchemical study of the "wires" suggested that they are pyrite, and x-ray single crystal and powder diffraction study confirms this identification. The filiform crystals of pyrite are about 0.05 mm. in diameter, and vary from 1 to 4 mm. in length. Most of the crystals are square in cross section, but a few are flattened ribbons. Some crystals are simple straight needles, but most consist of several straight portions joined by right-angle bends. One crystal was noted with thirteen such bends, and some of the crystals form bizarre shapes.

The orientation of the pyrite wires has been determined by means of an *x*-ray rotation photograph in which a single wire was rotated about its axis. The axis of the wire is parallel to one of the crystallographic *a* axes.

Typical pyrite crystals—cubes modified by octahedral facets—also occur in some of the vesicles, some of the crystals having pyrite needles growing out at right angles to the cube faces.

A vesicle containing several filiform pyrite crystals is shown in Fig. 5.

ACKNOWLEDGMENTS

We wish to thank Elisabeth Godijn for the spectrographic analyses, A. A. Chodos for advice concerning the analyses, R. H. Jahns for criticism of the manuscript, and W. M. Meier for helpful discussion. Figures 1, 4, and 5 were obtained with the help of Hugh S. Baird and William C. Miller. The Division of Chemistry and Chemical Engineering of the Institute kindly made available the *x*-ray facilities used in the investigation. We are indebted to Kenneth Deffeyes for providing us his unpublished data that made possible the identification of the erionite, and to Walter Muffly for providing the specimens studied.

REFERENCES

BARRER, R. M., *et al.* (1959) Hydrothermal Chemistry of the Silicates. Part VIII: *J. Chem. Soc.* **36,** 195–208.

DEFFEYES, K. (1959): *Am. Mineral.* **44,** 501–509.

DENT, L. N., AND SMITH, J. V. (1958) Crystal structure of chabazite, a molecular sieve: *Nature* **131,** 1794–1796.

DONNAY, G., DONNAY, J. D. H., AND KULLERUD, G. (1958a) Crystal and twin structure of digenite, Cu_9S_5: *Am. Mineral.* **43,** 228–242.

——— (1958b) "Bornite": Ann. Rept. Dir. Geoph. Lab., Carnegie Inst. Wash. Yrb. 57 (1957–1958), p. 248.

EAKLE, A. S. (1898) Erionite, a new zeolite: *Am. J. Sci.* **6,** 66.

STRUNZ, H. (1956) Die Zeolithe Gmelinit, Chabasit, Levyn: N. Jb. Min., Mh. 11, 250–259.

——— (1958) *Mineralogische Tabellen:* Leipzig (3d. ed.), p. 344.

WASASTJERNA, J. A. (1923) Soc. Sci. Fenn. Comm. *Phys. Math.* **1,** 37.

Manuscript received May 4, 1959.

THE AMERICAN MINERALOGIST, VOL. 45, JANUARY–FEBRUARY, 1960

DOVERITE, A POSSIBLE NEW YTTRIUM FLUOCARBONATE FROM DOVER, MORRIS COUNTY, NEW JERSEY*

William Lee Smith,[1] Jerome Stone,[2] Daphne R. Ross, and Harry Levine, *U. S. Geological Survey, Washington 25, D. C.*

Abstract

Doverite, a possible new yttrium fluocarbonate, was found at the Scrub Oaks iron mine at Dover, Morris County, New Jersey. The mineral occurs in brownish-red aggregates mixed with xenotime, hematite, and quartz. The aggregates are irregular—some of them as large as 1 inch in diameter—and most of them have rims of bastnaesite.

In parts of the mine, the doverite aggregate constitutes several per cent of the gangue. The aggregate has indices of refraction in the range from 1.700 to 1.685. It is physically inseparable from the other components of the aggregate. Hematite and doverite were leached from the aggregate leaving a residue of quartz and xenotime. From the x-ray powder data, doverite is suggested to be an yttrian analogue of synchisite and to have a general formula $YFCO_3 \cdot CaCO_3$, the Y in the formula including several elements of the rare-earth group.

The x-ray powder pattern of doverite bears a marked similarity to that of synchisite. The powder pattern of synchisite was indexed in terms of a pseudo-orthorhombic C-centered cell with $a=4.10$, $b=7.10$, and $c=9.12$ Å. From these data the cell constants of doverite were calculated to be $a=4.07$, $b=7.06$, and $c=9.12$ Å.

Inasmuch as doverite has not been satisfactorily purified from the aggregate, the possibility remains that doverite may be an yttrium-bearing synchisite. Until it can be proven to be an end-member of a series, its status as a new species is tentative.

Introduction

Ore containing the possible new mineral was found in 1951 in the course of a study of the paragenesis of the ore minerals at Scrub Oaks mine, Dover, New Jersey, by W. L. Smith. It was recognized as an unknown radioactive mineral. In the summer of 1954, Harry Klemic, of the U. S. Geological Survey, collected some of the same material from the Scrub Oaks mine. Analysis of this sample by spectrographic methods showed a high rare-earth content and prompted further studies. The two senior authors visited the deposit in the fall of 1954 to collect more samples and study its geological environment. A preliminary description of doverite was published (Smith and others, 1955).

The brownish-red aggregate containing doverite was found to comprise several per cent of the gangue in some areas of the mine and to occur at several levels. The brownish-red aggregate subsequently has been determined to be a microscopic mixture of doverite, hematite, xenotime, and quartz; some aggregates have rims of bastnaesite, some containing admixed leucoxene. The aggregates are associated with hematite, magnetite, quartz, apatite, albite, zircon, bastnaesite, and rutile. Elsewhere in the mine siderite, calcite, biotite, muscovite, epidote, hornblende, tremolite, sericite, pyrite, chalcopyrite, and bornite were found. Monazite, tourmaline, anatase, sphene, spinel, pumpellyite, chevkinite, garnet, and pyrrhotite have been reported as present in the deposit.

---

* Publication authorized by the Director, U. S. Geological Survey.

[1] Present address: Battelle Memorial Institute, Columbus Ohio.

[2] Present address: 2924 21st Ave., Astoria, N. Y.

The Scrub Oaks mine of the Alan Wood Steel Company is located at Mine Hill, 2½ miles west of Dover, off U. S. route 46. The geology of the Scrub Oaks deposit is described by Roche and Crockett (1933), and Sims (1953, 1958). The deposit lies in the west-central region of the New Jersey highlands. The magnetite body is described by Sims (1953) as an irregular tabular body consisting of several shoots of disseminated ore in albite-oligoclase granite. The granite and ore are of Precambrian age. The doverite aggregates are intimately associated with the ore minerals in the coarser-grained and pegmatitic phases of the ore rather than with the host rock.

MINERALOGY

Separation method

The ore containing the doverite aggregate was crushed by hand rather than by machine to avoid contamination. Because of some inclusions of quartz and iron ores in the mineral fragments, the aggregate concentrates had to be purified by hand picking. Particles greater than 100-mesh size were often attached grains. For ease of handling, the crushed ore was sized in 100- and 200-mesh sieves.

Heavy-liquid separations were made with methylene iodide (sp. gr. 3.33), which produced a light fraction composed primarily of quartz and traces of feldspar and apatite, and a heavy fraction containing the doverite aggregate with attached bastnaesite, magnetite, specular hematite, and zircon. The magnetite was removed from the concentrate by means of a hand magnet. The specular hematite and zircon were removed on a Frantz isodynamic magnetic separator. The doverite aggregate separates on the Frantz separator between 0.30 and 0.45 amp. at horizontal and longitudinal settings of 10°. The magnetic property of the aggregate may be due partly to its rare-earth composition as well as to its hematite component. Hematite occurs both free and as a component of the aggregate. Several grams of the aggregate were concentrated. A 1-gram sample of the purified material was obtained for chemical analysis.

Physical properties

The doverite aggregate is a finely crystalline mixture which may show a platy character. The aggregates range in size from microscopic specks to some approximately 1 inch in diameter. They are irregular, rounded, nodular masses in external form. Doverite is physically inseparable from the other components of the aggregate. Doverite constitutes the more abundant component of the aggregates which have a nometallic luster, are brownish red resembling jasper or red hematite, have a brownish streak, are brittle, and break with an uneven to subconchoidal fracture. The aggregates are somewhat variable in composition, some having appreciably more quartz or hematite than others, and in some the bastnaesite is absent. The hardness of the aggregate is 6.5 and the specific gravity ranges from 3.89 to 4.1+ as the composition of the aggregate varies, as determined by suspension in Clerici solution and checked by pycnometer. Assuming average specific gravities for the other components, the density of doverite was calculated to be in the range of 3.61 to 3.72. The aggregates are moderately radioactive with an equivalent uranium content of 0.5 to 0.6 per cent.

X-ray diffraction data

X-ray powder patterns show the aggregates to be a mixture of doverite, xenotime, hematite, quartz, and in some samples, bastnaesite. The pattern obtained from a sample leached with hot acid shows only xenotime and quartz. A bastnaesite pattern was obtained on a sample of the aggregate rim. The powder pattern of doverite has a marked similarity to that of synchisite. The powder pattern of synchisite was indexed in terms of pseudo-orthorhomic C-centered cell with $a=4.10$, $b=7.10$, and $c=9.12$ Å (Donnay and Donnay, 1953). On the basis of these data, the cell constants of doverite were calculated to be $a=4.07 \pm 0.02$, $b=7.06 \pm 0.02$, $c=9.12 \pm 0.03$ Å. The spacings of the two powder patterns are listed for comparison in Table 1. The cell volume calculated from the constants previously given is 262.1 A^3. If the yttrium end-member were assumed to be $2(YFCO_3 \cdot CaCO_3)$, the calculated density would be 3.40.

Because of the complexity of the doverite pattern, and because of its close similarity to that of synchisite, uncertainty still exists as to the validity of doverite as a new species. It would be expected that an yttrium analogue would have a cell size considerably smaller than the one proposed for doverite. Unless more conclusive evidence can be obtained, it may be that doverite is actually an yttrium-rich synchisite.

Optical properties

The doverite aggregate is brownish red in thin section and in immersions of high-index oils and shows variations in translucency which give the material a streaked or blotchy character. The individual crystal

TABLE 1. COMPARISON OF POWDER DATA FOR DOVERITE AGGREGATE, $YFCO_3 \cdot CaCO_3$, AND SYNCHISITE, $CeFCO_3 \cdot CaCO_3$

(CuKα radiation, λ=1.5418, nickel filter, camera diameter 114.6 mm.)

Doverite aggregate, Dover, N. J. (film T 6391)				Synchisite, Quincy, Mass. (film 6668)	
I	d_{hkl} (Å) (meas.)	d_{hkl} (Å) (calc.)	*hkl*	*I*	d_{hkl} (Å) (meas.)
s	9.1	9.12	001	s	9.1
m	4.55*	4.56	002	m	4.55
s	3.53	3.53	110	s	3.56
		3.53	020		
s	3.45	xenotime		vf	3.49
wb	3.30	3.29	111	m	3.31
		3.29	021		
wb	3.05	3.04	003	w	3.07
				w	3.04
s	2.80	2.79	112	s	2.81
		2.79	022		
vvf	2.75	xenotime			
fb	2.69	hematite			
mw	2.57	xenotime			
vf	2.52	hematite			
w	2.44	xenotime		vvf	2.42
vf	2.30	2.30	113	w	2.31
		2.30	023		
wb	2.28*	2.28	004	w	2.28
vfb	2.21	hematite		vf	2.23
wb	2.15	xenotime		vf	2.15
ms	2.04	2.04	200	ms	2.05
		2.04	130		
vvf	1.995	1.988	131	w	2.002
		1.986	201		
vf	1.935	xenotime			
ms	1.916	1.915	024	m	1.918
		1.915	114		
m	1.863	1.860	132	ms	1.870
		1.858	202		
vfb	1.839	1.824	005	vf	1.821
vf	1.819	xenotime			
m	1.772	1.765	040	w	1.781
		1.763	220		
f	1.768	xenotime			
		1.733	041		
f	1.727	1.731	221	w	1.749

* Lines occur on both xenotime and doverite patterns. s=strong; ms=medium strong; m=medium; mw=medium weak; w=weak; f=faint; vf=very faint; vvf=very very faint; b=broad line.

TABLE 1 (*continued*)

Doverite aggregate, Dover, N. J. (film T 6391)				Synchisite, Quincy, Mass. (film 6668)	
I	d_{hkl} (Å) (meas.)	d_{hkl} (Å) (calc.)	*hkl*	*I*	d_{hkl} (Å) (meas.)
		1.693	133		
f	1.689	1.691	203	w	1.704
w	1.647	1.646	042	m	1.658
		1.645	222		
f	1.544	xenotime			
		1.520	006		
w	1.512	1.518	204		
		1.518	134		
vf	1.487	hematite			
vf	1.457	hematite			
f	1.431	xenotime			
		1.396	116		
		1.396	026		
wb	1.395	1.395	224		
vvfb	1.341	xenotime			
wb	1.282*	1.280	242		
		1.279	312		
fb	1.236	xenotime			
		1.220	313		
fb	1.216	1.218	206		
		1.218	136		
wb	1.153	xenotime			

components of the aggregates are extremely fine grained, approaching the limits of resolution and making detailed optical examination impossible. The doverite aggregate, as distinguished from the other components, is anisotropic and shows indices of refraction in the range from 1.700 to 1.685. The indices of the immersion liquids were measured at the time of examination on an Abbe refractometer. The lighter colored rims around the doverite aggregates, identified to be bastnaesite, are often mixed with leucoxene. Bastnaesite was determined petrographically to approximate ten per cent of the aggregate.

CHEMISTRY

The aggregate, at first thought to be a single mineral species, and subsequently found to be a mixture of doverite, quartz, xenotime, and hematite, rimmed with bastnaesite and leucoxene, was chemically

TABLE 2. CHEMICAL ANALYSIS OF THE DOVERITE AGGREGATE

[Analysts: Harry Levine and Robert Meyrowitz, U. S. Geological Survey]

Constituent	Per cent	Constituent	Per cent
RE oxides*	44.36	TiO_2	0.75
ThO_2	1.62	MgO	0.53
SiO_2	9.70	H_2O (total)	1.35
Fe_2O_3	8.90	CO_2	11.75
CaO	9.80	F	2.87
P_2O_5	8.75		
Al_2O_3	0.54		101.14
UO_3	0.22	$-(O=2F)$	1.21
		Total	99.93

* Includes $Ce_2O_3=7.40$.

analyzed (Tables 2 and 3), and the analysis of the aggregate was computed (table 4).

ACNOWLEDGMENTS

We are indebted to W. P. Schenck of the Alan Wood Steel Company for his cooperation throughout our investigation of doverite. Thanks are also due to the following members of the U. S. Geological Survey: G. E. Ashby and E. A. Cisney for assistance in interpretation of *x*-ray data; and to Michael Fleischer, F. S. Grimaldi, Harry Klemic, E. S. Larsen, Jr., and A. M. Pommer for valuable suggestions helping to determine the constituents of the doverite aggregate.

This work is part of a program conducted by the U. S. Geological Survey on behalf of the Division of Research of the U. S. Atomic Energy Commission.

TABLE 3. SEMIQUANTITATIVE SPECTROGRAPHIC ANALYSIS OF THE DOVERITE AGGREGATE, IN PER CENT

[Analyst: Katherine V. Hazel, U. S. Geological Survey]

Over 10	Y
5 –10	Ca Ce Fe
1 – 5	Si P La Th Gd
0.5 – 1	Dy Er Yb Nd Pr
0.1 –0.5	Ti Al Lu Mg Ho Na
0.05– 0.1	Mn Tm
0.01– 0.05	Ba B Eu Pb Sc Sr

TABLE 4. COMPUTATION OF ANALYSIS OF AGGREGATE, IN PER CENT

Constituent	1	Deduct 2	Deduct 3	4 (=1-2-3)	5[a]
Ce_2O_3, etc.	12.48[b]	—	7.5[c]	5.0	12.1[d]
Y_2O_3, etc.	31.88[b]	17.50[e]	—	14.4	34.8
CaO	9.80	—	—	9.8	23.7
CO_2	11.75	—	1.8[c]	10.0	24.1
F	2.87	—	0.7[c]	2.2	5.3
SiO_2	9.70	9.70[f]	—	—	—
Fe_2O_3	8.90	8.90[g]	—	—	—
P_2O_5	8.75	8.75[e]	—	—	—
TiO_2	0.75	0.75[h]	—	—	—
ThO_2	1.62	1.62[i]	—	—	—
UO_3	0.22	0.22[i]	—	—	—
Al_2O_3	0.54	0.54[i]	—	—	—
MgO	0.53	0.53[i]	—	—	—
H_2O	1.35	1.35[i]	—	—	—
	101.14			41.4	100.0
−(O=2F)	1.21				
	99.93				

[a] Column 4 calculated to 100%.

[b] Column 1 is the analysis of Table 2 with values for Ce earths and Y earths calculated from the averages of the ranges given in Table 3.

[c] Deducting 10% bastnaesite.

[d] Analysis indicates a Y_2O_3 to Ce_2O_3 ratio of approximately 3 to 1.

[e] Deducted as xenotime.

[f] Deducted as quartz.

[g] Deducted as hematite.

[h] Deducted as leucoxene.

[i] Deducted; manner of occurrence unknown. It would be more logical to distribute UO_3 and ThO_2 among bastnaesite, xenotime, and doverite, but the amounts are too small to warrant this refinement.

REFERENCES

DONNAY, G., AND DONNAY, J. D. H. (1953), The crystallography of bastnaesite, parisite, roentgenite, and synchisite: *Am. Mineral.*, **38,** 932–963.

ROCHE, H. M., AND CROCKETT, R. E. (1933), Iron ore mining and milling at Scrub Oaks: *Eng. Mining Jour.*, **134,** 161–164; 197–200.

SIMS, P. K. (1953), Geology of the Dover magnetite district, Morris County, N. J.: U. S. Geol. Survey Bull. 982-G, 298–300.

—— (1958), Geology and magnetite deposits of Dover district, Morris County, N. J.: U. S. Geol. Survey Prof. Paper 287, 116–124.

SMITH, W. L., STONE, J., RISKA, D. D., AND LEVINE, H. (1955), Doverite, a new yttrium mineral: *Science*, **122,** no. 3157, 31.

Manuscript received May 5, 1959.

THE AMERICAN MINERALOGIST, VOL. 45, JANUARY–FEBRUARY, 1960

AUTUNITE FROM MT. SPOKANE, WASHINGTON*

G. W. LEO, *U. S. Geological Survey, Menlo Park, California*

ABSTRACT

Near Mt. Spokane, Washington, coarsely crystalline autunite is developed in vugs, fractures, and shear zones in granitic rock. With the exception of dispersed submicroscopic uraninite particles, autunite is the only ore mineral in the deposits. A study of associated granitic rocks reveals that apatite, the most abundant accessory constituent, has been preferentially leached and corroded in mineralized zones, suggesting that it may have provided a source of lime and phosphate for the formation of autunite. Leaching may have been effected partly by meteoric water, but more probably was due to the action of ascending connate solutions that may also have carried uranium from unoxidized, as yet undiscovered deposits at depth.

Autunite from the Daybreak mine has been studied optically, chemically, and by *x*-ray diffraction. The autunite is commonly zoned from light-yellow margins to dark-green or black cores, and autunite from the inner zone has a higher specific gravity and higher refractive indices than peripheral light material. *X*-ray powder diffraction patterns of dark and light meta-autunite formed from this autunite show no significant differences in the *d* spacings; however, diffraction patterns of nine zoned samples each show uraninite to be present in the dark, and absent from the light, phase. UO_2 and UO_3 determinations range from 0.66–0.70 per cent and 57.9–58.0 per cent, respectively, for light autunite, whereas dark autunite shows a range (in seven determinations) of UO_2 from 1.2 to 4.0 per cent, and UO_3 from 55.1 to 58.8 per cent. The wide range of UO_2 values in dark autunite is tentatively attributed to nonuniform distribution of discrete uraninite particles, which may also account for the dark color and higher density.

Thermogravimetric and differential thermal analyses of autunite suggest discrete water losses at about 90°, 145°, and 220° C. The first water loss probably represents dehydration to meta-autunite II, also recognizable by marked changes in optical properties and the *x*-ray diffraction pattern. The form of the DTA curve above 90° C. resembles that of montmorillonite, suggesting that the dehydrations at about 145° C. and 220° C. may involve interlayer water as in montmorillonites, and the analogy with montmorillonite is further indicated by *x*-ray patterns of meta-autunite II heated just above these temperatures. Autunite heated to red heat shows a diffraction pattern distinct from all others. The cation exchange capacity of autunite, about 2.5 milliequivalents per 100 grams, is substantially lower than that previously reported for artificial material.

INTRODUCTION

Autunite of unusual quality and abundance is developed on the western flanks of Mt. Spokane, about 30 miles northeast of Spokane, Washington (Fig. 1). The autunite deposits occur entirely within granitic rock over an area of about 100 square miles near the eastern limits of the Loon Lake granite.

The present study has a twofold purpose: (1) a consideration of some aspects of the field relations of autunite and the host rocks, in an attempt to shed some light upon the origin of these unusual deposits;

---

* Publication authorized by the Director of the U. S. Geological Survey.

and (2) a detailed study of the mineralogy of autunite from the Daybreak mine, believed to be unique in its relative abundance and fine development.

Much helpful information regarding the geology of the area has been provided by D. C. Alvord and A. E. Weissenborn of the U. S. Geological Survey. Other data have been drawn from an article by H. W. Norman (1957), mining and exploration manager for Daybreak Uranium, Inc.

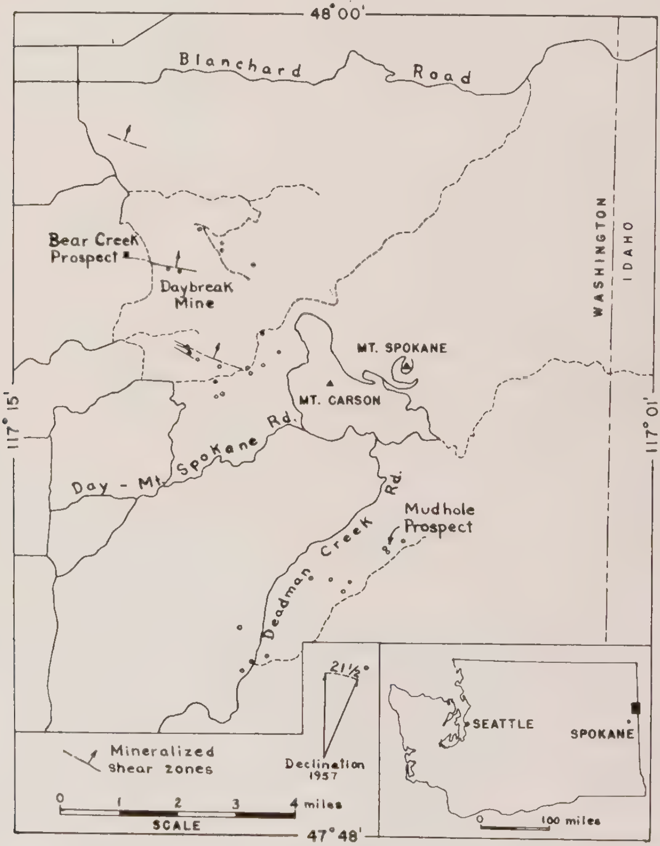

FIG. 1. Location map of the autunite deposits near Mt. Spokane, Washington. Each dot represents an autunite occurrence. Data from D. C. Alvord and A. E. Weissenborn.

After work on this manuscript was nearly complete, the writer learned of a study of meta-autunite from the Daybreak mine by Dr. Alexander Volborth of the University of Nevada (Volborth, 1959). Conversation with Dr. Volborth revealed that the two papers did not overlap appreciably, but rather tended to supplement each other, and it was therefore agreed to publish each paper separately. Dr. Volborth was kind enough to present the writer with a copy of his manuscript, and considerable use has been made of his data.

The autunite deposits

The only uranium mineral in the Mt. Spokane district is the hydrous calcium uranyl phosphate, autunite, which is concentrated along west to northwest striking shear zones with a low northward dip; especially rich concentrations of autunite occur where shear zones are traversed by fractures. Several such zones have been mapped in the vicinity of Mt. Spokane (Fig. 1); by far the most important is the Daybreak mine, which has produced most of the ore from the district. The geologic relations at the Daybreak mine have been well summarized by Norman (1957).

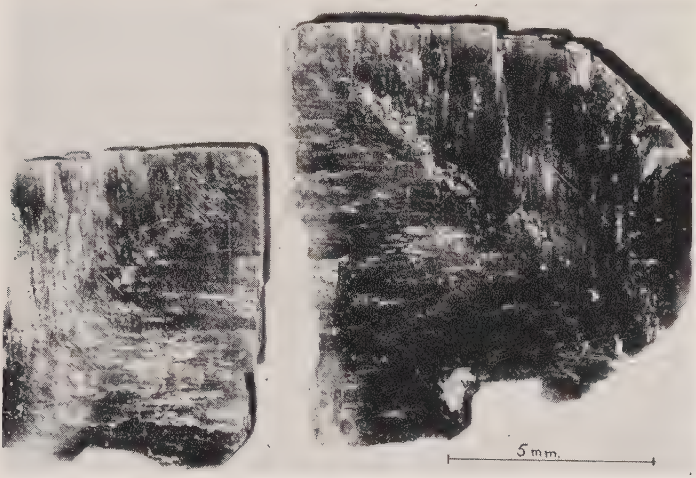

FIG. 2. Individual autunite flakes from Daybreak mine, showing characteristic distribution of dark and light phases.

Autunite occurs in three more or less distinct ways: (1) in veins and fracture fillings, which may locally attain a thickness of twelve to fifteen inches (Fig. 2); (2) in vugs within closely spaced pegmatitic dikes; and (3) disseminated throughout altered granite near fractures and shear zones.

A notable feature of the deposits is their concentration at relatively shallow depth. At the Daybreak mine, production has been almost entirely from a depth of less than 30 feet, and the highest grade ore occurs within 10 feet of the surface; ore of commercial grade, however, has been reported from a depth of 95 feet (Norman, 1957). Total production from the Daybreak mine through May, 1958, is 13,400 tons, with an average grade of 0.24 per cent U_3O_8. This production has been from three distinct pods, now largely mined out, which are generally defined by the intersections of faults with major shear zones. A recently sunk vertical shaft about one-half mile northwest of the Daybreak mine (Bear Creek prospect) has struck autunite at a depth of about 80 feet, apparently on the extension of the Daybreak shear zone (Fig. 1) (A. E. Weissenborn, written communication).

Use of the term autunite

Because of the readiness with which hydrous calcium uranyl phosphate may change from one hydration state to another, in particular between the fully hydrated and meta-I states, the attempt to denote the material precisely at all times becomes cumbersome and leads to ambiguity. The convention has therefore been adopted throughout this paper of using the term autunite, without qualification, to denote hydrous calcium uranyl phosphate in any hydration state. Wherever the precise hydration state is germane to the discussion, the terms, fully hydrated autunite, meta-autunite I, and meta-autunite II are used (see p. 104).

Petrography

The rocks of the Mt. Spokane area range in composition from granite to quartz diorite, and are markedly rich in biotite except near mineralized zones. A typical, fairly fresh quartz monzonite (DB-20) has the following mode: quartz 42, potassium feldspar 24, plagioclase (An_{25-35}) 25, biotite 5, muscovite 2, myrmekite 1, and accessories 1. The rock is medium grained, with a texture ranging from hypidiomorphic to graphic. Highly undulose extinction in quartz, bent twin lamellae in plagioclase, and zones of crushed and shattered grains indicate considerable post-crystallization shearing. The chief varietal mineral is biotite, which forms ragged, partly chloritized plates and shreds associated with anhedral patches of opaque ore; the latter is at least in part a late alteration product. Accessory minerals include apatite, garnet, zircon, monazite, and allanite. The uranium content of this rock and some its constituent minerals are listed in Table 10.

Granite and quartz monzonite alternate irregularly with more mafic rocks corresponding to granodiorite and quartz diorite. Contacts between the different rock types are sharp but irregular; owing to limited exposures, the mutual relations are not clear. Mineral percentages in a typical granodiorite are as follows: quartz 20, plagioclase (An_{28-45}) 40, potassium feldspar 10, biotite 13, and deep blue-green hornblende 14.

Dark fine-grained lamphrophyric dikes and granite pegmatites are widely distributed in the area. The former consist chiefly of quartz, potassium feldspar, biotite, and pale green hornblende, and range up to 15 feet in width. A radioactive but not visibly mineralized rock dike along Deadman Creek Road (Dimitroff claim) has been prospected without known results.

Development of pegmatities is especially conspicuous in mineralized zones, owing perhaps to the better-than-average exposures in these zones along trenches and stripped areas. Pegmatites are commonly sharply bounded and tabular, but may have irregular forms with gradational boundaries into finer-grained rock. Garnet is the predominant accessory constituent.

In general, rock within mineralized zones has a bleached and altered aspect, although examination under the microscope indicates that hydrothermal alteration is not intense. The chief evidence of alteration consists in (1) the relative abundance of muscovite, and almost complete absence of biotite except for local chloritized shreds; (2) cloudiness and moderate sercitization of feldspar, especially plagioclase; and (3) marked leaching of apatite, which is more fully described in the section on origin.

Mineralogy of Autunite

One of the remarkable features of autunite from Mt. Spokane is its coarseness; individual flakes may attain a diameter of one inch, and bonanza specimens of massive autunite clusters measuring two feet across have been preserved intact from the Daybreak mine. The flakes are generally arranged in books parallel to the prominent {001} cleavage which display a characteristic radiating "bow tie" structure. In large specimens, radiating clusters of crystals standing on edge are tightly intergrown and set against each other at diverging angles. The {001} surfaces, though showing perfect cleavage, are characteristically curved and crenulated in larger flakes. Most crystals are bounded by a prominent prismatic cleavage.

Two types of autunite, dark and light, are almost invariably associated. The light type ranges from pale lemon-yellow to light yellow-green, and the dark type is dark green to black. In a given flake the dark material generally forms the core and the light material the rim; this relationship, however, is variable in that cores may be light in part, and small flakes commonly are entirely light (Fig. 2). The transition between light and dark is usually somewhat gradational, and under the microscope small fragments show a continuous range of color from pale yellow to dark green. Under both short- and long-wave ultraviolet light, light colored autunite fluoresces bright yellow-green, whereas the dark cores appear dull with little fluorescence; with long-wave light, however, the contrast between light and dark autunite is more pronounced than with short-wave light.

Hydration states of autunite

Three hydration states are commonly recognized in hydrous calcium uranyl phosphate: fully hydrated autunite, $Ca(UO_2)_2(PO_4)_2 \cdot 10\text{-}12H_2O$; meta-autunite I, $Ca(UO_2)_2(PO_4)_2 \cdot 2\frac{1}{2}\text{-}6\frac{1}{2}H_2O$; and meta-autunite II, $Ca(UO_2)_2(PO_4)_2 \cdot 0\text{-}6H_2O$ (Palache, Berman, and Frondel, 1951, p. 985).

The following observations regarding the nature of successive dehydrations have been previously described (Beintema, 1938, p. 160–163; Palache and others, 1951, p. 985; Donnay and Donnay, 1955, p. 35). Optical changes in autunite with progressive heating were long ago described by Rinne (1901).

Dehydration of fully hydrated autunite to meta-autunite I takes place at room temperature in a dry atmosphere in a few hours; alternately, the dehydration can be brought about much more quickly by moistening fully hydrated autunite with a hygroscopic substance such as acetone and allowing it to dry. Finely divided meta-autunite I may be converted to the fully hydrated form by leaving overnight in an ordinary desiccator with water in the bottom, or, alternately, by boiling briefly in distilled water. Unless a saturated atmosphere is maintained, however, fully hydrated autunite quickly reverts to meta-autunite I, which is clearly the most stable form under ordinary conditions of temperature and humidity.

Irreversible dehydration from meta-autunite I to meta-autunite II takes place at about 80° C.; the dehydration is accompanied by striking changes in optical properties and is, therefore, readily recognizable. Additional dehydrations at higher temperatures are suggested by DTA patterns. When autunite is brought to red heat, a distinct change takes place in the *x*-ray pattern, but the cause for this change was not determined.

It has been suggested that stability of autunite-like minerals in their different hydration states may be controlled by the size of the metal cation (Nuffield and Milne, 1953). The ready transition of autunite between the fully hydrated and meta-I forms is accordingly explained by the size of the Ca^{+2} ion, which is thought to give rise to the approximately equally stable structures in the two hydration states. Minerals with the autunite structure but a smaller metal cation, for example, saléeite (Mg-autunite), are under ordinary conditions stable in the fully hydrated form only, whereas autunite-like minerals with a cation larger than calcium, for example, uranocircite, seem to exist only as the meta-structure.

Optical character of autunite in the various hydration states

Autunite has a tabular habit with a perfect basal {001} cleavage. Another cleavage with two mutually perpendicular directions, here called prismatic, is well developed in Daybreak mine material. The three mutually perpendicular cleavage directions control the shape of even the smallest crushed particles of autunite, so that these are always square or rectangular in outline. A third cleavage, co-zonal with the prismatic cleavages and at 45° to them, can be observed in some tablets. If the prismatic cleavages are regarded as {110}, the third cleavage is {100} or {010}; however, due to a shift in the optic plane, the designations are different for fully hydrated autunite and meta-autunite I (Fig. 3).

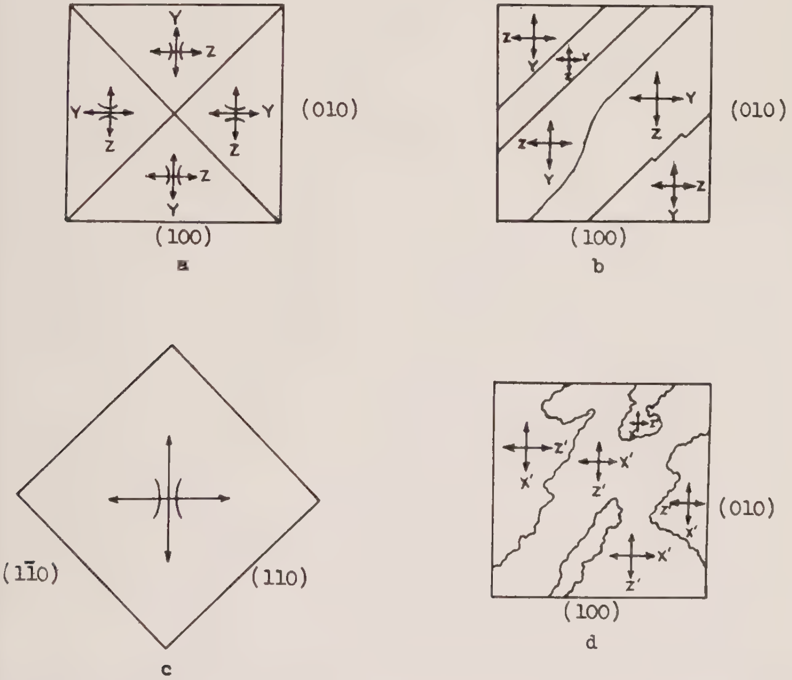

FIG. 3. Optic orientation of autunite in the various hydration states. Idealized cleavage flakes resting on (001).

a. Fully hydrated autunite with very regular sectoral structure on {110}. Optic axial plane always parallel to neighboring cleavage.
b. Fully hydrated autunite; example of less regular sectoral structure.
c. Meta-autunite I; sectoral structure absent. Optic plane diagonal to cleavages.
d. Meta-autunite II; irregular mottling with opposed though parallel vibration directions, which are parallel to bounding cleavages.

X-ray studies by Beintema (1938) and Nuffield and Milne (1953) have shown fully hydrated autunite and meta-autunite I to be structurally tetragonal; an anomalously biaxial character in both phases is attributed to slight distortion in the structure due to variable water content. Meta-autunite II is thought to be orthorhombic (Beintema, 1938, p. 162).

Meta-autunite from the Daybreak mine is always biaxial, and fully hydrated autunite is biaxial except when hydration is brought about by boiling (Table 1). Whenever 2V is not zero, it is necessary to adopt crystallographic notation appropriate to symmetry lower than tetragonal; specifically, in those cases where the optic plane is parallel to the prismatic cleavages, the latter are designated as pinacoids, {100} and {010}, instead of the second-order tetragonal prism, {010}.

TABLE 1. SUMMARY OF OPTICAL DATA ON AUTUNITE FROM DAYBREAK MINE

State of hydration	Indices of refraction[1]		Optical character
	Light	Dark	
1. Fully hydrated autunite (boiled in distilled water for 10 minutes.)	$\beta \simeq \gamma$[2] 1.578±0.003	$\beta \simeq \gamma$ 1.586±0.005	Isotropic or low birefringence, with anomalous blue interference colors, rarely with sectoral arrangement. $2V_X = 0$ to 5°. Dispersion distinct $r > v$, sometimes crossed (?), optic axial plane parallel to cleavage.
2. Fully hydrated autunite (In desiccator with water vapor for several days.)	$\beta \sim \gamma$ 1.579±0.003	$\beta \sim \gamma$ 1.586±0.003	Isotropic or low birefringence; sectoral arrangement. $2V_X = 0$ to 25°. Optic axial plane parallel to cleavage.
3. Meta-autunite I	$\beta \simeq \gamma$ 1.597±0.003	$\beta \sim \gamma$ 1.609±0.005	Usually low birefringence; sectoral character indistinct. $2V_X = 5$ to 20°. Optic axial plane diagonal to cleavage.
4. Meta-autunite II (Heated for approximately ½ hr. at 80° C.)	$\alpha' = 1.610 \pm 0.003$[3] $\gamma' = 1.624 \pm 0.003$	$\alpha' = 1.620 \pm 0.005$ $\gamma' = 1.635 \pm 0.005$	Strongly mottled appearance due to high birefringence and irregular sectoral character. X′ and Z′ in (001) plane, parallel to cleavages.
5. Heated to red heat in platinum crucible.	$\alpha' = 1.68 \pm 0.01$[4] $\gamma' = 1.71 \pm 0.01$	$\alpha' = 1.68 \pm 0.01$ $\gamma' = 1.71 \pm 0.01$	Same as (4).

[1] Only the indices of refraction corresponding to the two orientations of cleavage plates given in each case, since all flakes, however small, rest on (001).

[2] γ-β does not exceed 0.003 in autunite and meta-autunite I.

[3] α' and γ' correspond to X′ and Z′, and are thought to be equivalent to true α and γ.

[4] Values variable and uncertain.

In fully hydrated autunite, $x = c$, and the optic plane is parallel to a prismatic cleavage. The flakes are isotropic or weakly birefringent;

$2V_x = 0-25°$, and dispersion $r>v$, distinct. Individual flakes commonly have a sectoral arrangement (see Beintema, 1938, p. 162); that is to say, the flakes are divided into more or less regular sectors or bands joined on {110} (Fig. 3*a*, *b*). Adjacent sectors have opposed though parallel vibration directions, so that the optic plane is always parallel to the neighboring prismatic cleavage.

In meta-autunite I there is a distinct change in optic orientation, involving a shift of the optic plane through 45° from its original position, so that it bisects the angle between the prismatic cleavages (Fig. 3*c*). Most flakes have $2V_x = 5-20°$, and possess a slight birefringence. A faint and highly irregular sectoral structure with opposed vibration directions persists in light autunite, but is absent in the dark phase.

Upon hydration of flakes to meta-autunite II, sectoral structure reappears, with irregular isotropic boundaries showing slight control by {110} directions (Fig. 3*d*). Adjacent areas have mutually perpendicular virbration directions as before, but now show much higher birefringence, with interference colors up to first-order red. The relatively high birefringence and the appearance of a centered "flash figure" in (001) suggest that the vibration directions in this plane, which corresponded to Y and Z in fully hydrated autunite and meta-autunite I, are now X and Z. An attempt to obtain a Bx_a or optic axis figure by means of sections cut normal to (001) was unsuccessful.

Optical characteristics reported by Beintema (1938, p. 160 162) for synthetic hydrated calcium uranyl phosphate are approximately similar to those in Daybreak mine autunite, except that, in the fully hydrated and meta-I states, the position of the optic plane is reversed relative to that in Daybreak mine autunite. Sectoral structure (interpreted by Beintema as twinning on {110}), furthermore, was noted in the meta-I state only, whereas, in Daybreak mine autunite, sectoral structure is restricted to the fully hydrated form. Beintema also noted (p. 160) a gradual change from biaxial to uniaxial character in synthetic fully hydrated autunite exposed for some time to air, and interpreted this as being due to the gradual attainment of truly tetragonal symmetry of loss of excess water. A similar change could not be detected in Daybreak mine autunite; rather, unaxial crystals were noted only after autunite had been boiled in water and hence most thoroughly hydrated.

All indices of refraction were determined by means of standard immersion oils and sodium light. Because of the strongly preferred orientation of autunite on (001), values for β and γ only were obtained for fully hydrated autunite and meta-autunite I. In accordance with the nearly uniaxial character of these hydrates, β and γ are sensibly equal, and their difference does not exceed the limits of variation between different flakes.

In the case of meta-autunite II, two indices of refraction were determined.

Indices of refraction of dark autunite are consistently higher than those of light autunite (Table 1), although the reason for this is not apparent on the basis of chemical and crystallographic considerations. The values are generally in good accord with published data (Palache, Berman, and Frondel, 1951, p. 985; George, 1949, p. 137–138*). For dark meta-autunite I from the Daybreak mine, Volborth (1959) reports $\alpha = 1.584$, $\gamma = 1.607$; the latter value is in good agreement with that determined by the writer.

TABLE 2. ANALYSIS OF FULLY HYDRATED LIGHT AUTUNITE

Analyst: Blanche Ingram, U. S. Geological Survey

	(1) Weight per cent	(2) Recalculated to 100	(3) Molecular proportions	(4) Combined molecular proportions SiO_2 omitted	(5) Molecular ratios based on (4); (PO_4^{-3}) group = 2.00	(6) $Ca(UO_2)_2(PO_4)_2 \cdot 12H_2O$
UO_3	57.95[1]	58.38	0.204	0.204	1.96	58.00
UO_2	0.68[2]	0.69	0.003			
CaO	5.3	5.34	0.095	0.103	0.99	5.69
SrO	0.52	0.52	0.005			
P_2O_5	14.6	14.71	0.104	2×0.104 = 0.208	2.00	14.39
SiO_2	0.41	0.41	0.007			
H_2O	19.8	19.95	1.107	1.107	10.64	21.92
Total	99.26	100.00				100.00

Formula based on column (5): $(Ca, Sr, U^{+4})_{0.99}(UO_2)_{1.96}(PO_4)_{2.00} \cdot 10.64H_2O$.

[1] Average of two determinations: 57.9 per cent and 58.0 per cent.

[2] Average of two determinations: 0.66 per cent and 0.70 per cent.

Chemical analyses

Chemical analyses of fully hydrated dark and light autunite from the Daybreak mine are recorded in Tables 2 and 3. Preparation of analyzed material required certain precautions. Since intense and prolonged grinding tended to produce irreversible dehydration to meta-autunite II, the necessary reduction in size (to −150 mesh) was accomplished by fine chopping of autunite flakes with a razor blade, followed by gentle grinding under acetone. Separation of the dark from the light phase was then possible, owing to the different densities of the two phases (Table 4). In view of the maximum density of methylene iodide (3.3), autunite in the analyzed samples had to be in the fully hydrated state prior to the

---

* The range, $\gamma = 1.595–1.613$, listed by George (1949) for "autunite," apparently represents determinations of meta-autunite I.

TABLE 3. ANALYSIS OF FULLY HYDRATED DARK AUTUNITE

Analyst: Blanche Ingram, U. S. Geological Survey

	(1) Weight per cent	(2) Molecular proportions	(3) Combined molecular proportions 0.7% UO_2 added to (Ca^{+2}, Sr^{+2})[1]	(4) Molecular ratios based on (3); $(PO_4^{-3}) = 2.00$	(5) $Ca(UO_2)_2(PO_4)_2 \cdot 12H_2O$
UO_3	55.1–58.8[2]	0.193–0.206	0.193–0.206	1.86–1.98	58.00
UO_2	1.2– 4.0[2]	0.004–0.015	0.001–0.012[3] 0.003		
CaO	5.3	0.095	0.095 } 0.101	0.97	5.69
SrO	0.34	0.003	0.003		
P_2O_5	14.8	0.104	0.104×2 = 0.208	2.00	14.39
SiO_2	n.d.				
H_2O	18.3	1.016	1.016	9.77	21.92
Total	95.0–101.5				100.00

Formula based on column (4): $(Ca, Sr, U^{+4})_{0.97}(UO_2)_{1.86-1.98}(PO_4)_{2.00} \cdot 9.77H_2O$.

[1] An amount of UO_2 equal to that added to (Ca^{+2}, Sr^{+2}) group for light autunite.

[2] Values represent a range of seven determinations, two of them on 100 mg. samples, the remainder on 50 mg. samples. The determinations were as follows (first figure UO_3, and second, UO_2, in weight per cent): (1) 58.8, 3.8; (2) 57.5, 3.8; (3) 55.8, 3.2; (4) 55.2, 3.7; (5) 55.1, 4.0; (6) 57.4, 1.8; (7) 58.6, 1.2.

[3] This excess of UO_2 represents uraninite not in the structure.

centrifuging, and it was necessary to rehydrate several times during the course of the separation. The final light concentrate had an overall yellow-green appearance, and consisted of flakes ranging from medium gray-green to pale canary yellow. The dark concentrate had a uniformly dark olive-green color, bordering on black in thicker flakes.

The specific gravity of both the fully hydrated phase and the meta-I phase (Table 4) shows a considerable range of variation, but the values are in general agreement with published data (Palache, Berman, and Frondel, 1951, p. 985; Donnay and Donnay, 1955, p. 34; Volborth, 1959). The value of 3.1, given by George (1949, p. 137) for fully hydrated autunite, seems to be too low.

Of particular interest in the chemical analyses is the presence of U(IV), reported as UO_2, in both dark and light autunite. The U(IV)

TABLE 4. SPECIFIC GRAVITY OF AUTUNITE

	Light	Dark
Fully hydrated autunite[1]	3.18–3.23	3.26–3.28
Meta-autunite I[2]	3.35–3.40	3.45–3.55

[1] Determined by means of heavy liquids checked on a Christian Becker Chainomatic density balance.

[2] Determined by means of a Berman density balance.

content of dark autunite, determined for seven separate samples, is relatively high and shows a wide range of variation. Since each of the seven samples came from the same fraction of carefully purified dark autunite, the variations in U(IV) cannot be ascribed to admixture of unoxidized uranium minerals susceptible to removal by ordinary separatory methods. A possibility that must be considered is differential reduction of U(VI) during analysis, which is especially likely if ferrous iron is present in the sample (Clarke and Altschuler, 1958). However, in view of the small amount of iron in the autunite, especially the dark variety (Table 5), reducing effects were probably not important. In the event of differential reduction of U(VI), moreover, the U(IV):U(VI) ratios in the different samples should be in approximate inverse proportion, and this is definitely not the case. (See Table 3, footnote 2.)

TABLE 5. SEMIQUANTITATIVE SPECTROGRAPHIC DATA[1] ON LIGHT AND DARK AUTUNITE, DAYBREAK MINE

Katherine V. Hazel, analyst, U. S. Geological Survey
L=light autunite, D=dark autunite. Figures represent
number of samples falling in each range

Weight per cent[2]	Si		Al		Fe		Mg		Na[3]		K[3]		Mn		Ba		Be		Pb		Sr	
	L	D	L	D	L	D	L	D	L	D	L	D	L	D	L	D	L	D	L	D	L	D
0.3 –1.0	5	1	7		1																1	
0.1 –0.3	2																				8	9
0.03 –0.1	2	4	1	1	4	1																
0.01 –0.03		4			1								1									
0.003 –0.01			1	2	2	2	9	9		1	1	1	4	6	9	8			9	9		
0.001 –0.003				5		3			1				4	3		1						
0.0003 –0.001																	1					
0.0001 –0.0003																	4					
0.00003–0.0001																	4	9				
0				1	1	3																

[1] Major elements not listed. Elements looked for but not detected: Ag, As, Au, B, Bi, Cd, Ce, Co, Cr, Cs, Cu, Dy, Er, Eu, Ga, Gd, Ge, Hf, Hg, Ho, In, Ir, La, Li, Lu, Mo, Nb, Ni, Os, Pd, Pr, Pt, Rb, Re, Rh, Ru, Sb, Sc, Sn, Sm, Ta, Tb, Te, Th, Ti, Tl, Tm, V, W, Y, Yb, Zn, and Zr.

[2] Comparison of this type of semiquantitative results with the data obtained by quantitative methods, either chemical or spectrographic, show that the assigned group includes the quantitative value about 80 per cent of the time.

[3] Na and K were determined on chemically analyzed samples only.

More probably the variable and relatively high U(IV) content of dark autunite is due to the presence of exceedingly fine, irregularly dispersed uraninite. The presence of uraninite in the dark phase, and its absence in the light phase, is indicated by *x*-ray powder patterns (see p. 115 and 118), although the mineral could not be detected by optical or separatory means. This dispersed uraninite is thought to account for the deep color of dark autunite, and its greater density relative to the light-colored phase.

The presence of U(IV) in light autunite, together with the apparent absence of uraninite from this phase, suggests that U(IV) may be present in the autunite structure, probably as U^{+4} substituting for Ca^{+2}. This substitution, plausible on theoretical grounds because of the closely similar ionic radii of U^{+4} (0.97) and Ca^{+2} (0.99 Å) (Green, 1953), has been recently demonstrated for apatite (Clarke and Altschuler, 1958; Altschuler, Clarke, and Young, 1958). In calculating formulas from the present analyses, it has been arbitrarily assumed that all U(IV) in light autunite, and an equal amount of U(IV) (approximately 0.7%) in dark autunite, substitute in the structure for calcium. A similar substitution is assumed for strontium, which shows higher values than any previously reported autunite.[1]

SiO_2, determined for light autunite only, may be present as SiO_4^{-4} substituting for PO_4^{-3}, and thus balance excess positive charges introduced by U^{+4} in Ca^{+2} positions. Substitution of SiO_4^{-4} for PO_4^{-3} has been proposed for apatite (Borneman-Starinkevitch, 1938), and is also assumed by Volborth (1959, p. 709, Table 5) in dark meta-autunite from Mt. Spokane. The analysis of the latter contains 0.39 per cent SiO_2 (Volborth, 1959), addition of which to P_2O_5 yields molecular proportions close to theoretical values. In the present analysis of light autunite, on the other hand, the molecular proportion for PO_4^{-3} alone (Table 2, column 4) is already somewhat too high, and addition of SiO_4^{-4} to this group would cause further departure of molecular proportions from theoretical values. In view of these considerations, SiO_2 has been omitted in calculating the empirical formula of light autunite (Table 2, column 4), but the possibility of some substitution of SiO_4^{-4} for PO_4^{-3} cannot be disregarded.

An alternate explanation for SiO_2 is that it represents an impurity. The relatively large amounts of Al in light autunite (Table 5) suggest that the contaminating agent may be clay, although contamination was not apparent in the analyzed sample.

Both analyses have been calculated to empirical formulas on the basis of an arbitrary value of 2.00 for PO_4^{-3}. In each case, but especially in dark autunite, the number of water molecules is somewhat low compared to the maximum theoretical value of $12H_2O$ for fully hydrated material. This disparity may probably be ascribed to incipient dehydration to meta-autunite I prior to analysis.

---

[1] After this paper went to press, the writer learned of a determination of 1.38% SrO for dark meta-autunite from Mt. Spokane, Washington, by Volborth (1959).

Spectrographic analyses

Semiquantitative spectrographic analyses of nine samples each of dark and light autunite from different parts of the Daybreak mine (Table 5) show that trace elements are closely similar, both in kind and amount, throughout the suite of analyzed samples. The lack of consistent differences between light and dark material reinforce the suggestion that the color difference is caused primarily by dispersed uraninite in dark autunite, and not by differential distribution of minor and trace elements. Elements that do show systematic fractionation, notably iron, silicon, and aluminum, are all more abundant in light autunite; as mentioned above, the latter two elements may represent clay contamination.

The suite of minor elements generally corresponds to that reported by Emerson and Wright (1957, p. 226) for meta-autunite from the W. Wilson mine in Montana, although these authors list several additional elements (Cu, Co, Li, Ag, B, Ge, and Mo).

Differential thermal analyses

Differential thermal analyses of light and dark autunite are represented in Fig. 4. The curves do not differ greatly from each other, and each is closely similar to the DTA pattern of synthetic autunite (Guillemin and Pierrot, 1956, p. 180).

Each pattern shows three distinct endothermic troughs. The first

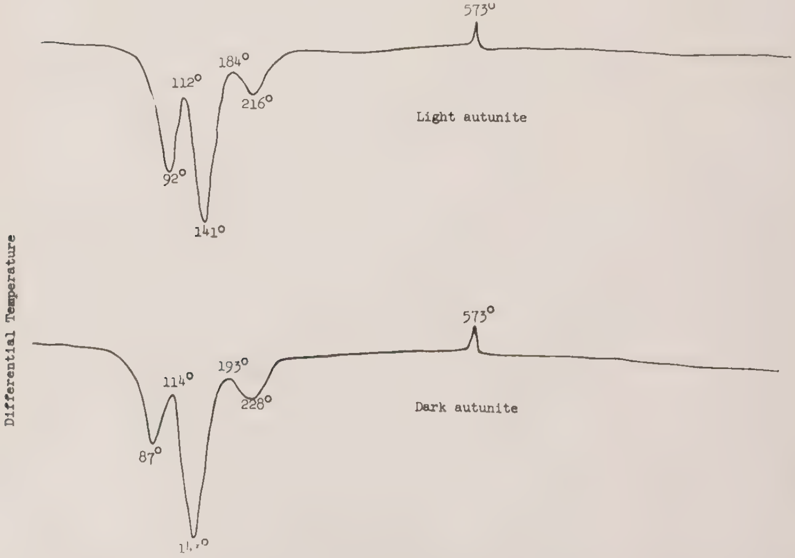

FIG. 4. Differential thermal analyses of light and dark, autunite. Peak at 573° C. is due to quartz standard. Record by George T. Faust.

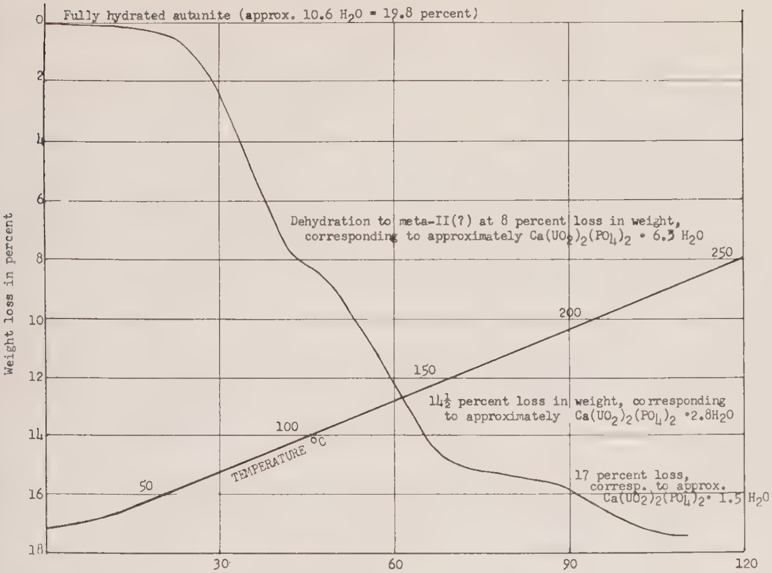

FIG. 5. Thermogravimetric data on light autunite over the range 20°–250° C. Horizontal scale shows time in minutes. Record by Charles A. Kinser.

trough, at 92° C. for light and 87° C. for dark material, probably represents the dehydration of meta-autunite I to meta-autunite II, although the temperatures are slightly higher than that previously determined for this hydration (about 80° C.). On the basis of about ten water molecules per unit formula in fully hydrated autunite (Tables 2 and 3), and a maximum of six water molecules in meta-autunite II, it appears that autunite loses at least four water molecules in the interval between room temperature and about 90° C. (See Brichard and Brasseur, 1958, p. 7.)

The two succeeding endothermic troughs, at 141° and 216° C. for light material, and 143° and 228° C. for dark material, suggest further losses of water. These troughs show a marked similarity to the troughs corresponding to loss of interlayer water in montmorillonites (G. T. Faust, written communication; Grim, 1953, p. 197; Greene-Kelly, 1957, p. 140–164), and may, hence, be analogous. The analogy with montmorillonite is borne out by *x*-ray powder patterns of meta-autunite II heated above 90° C. (Table 8).

Thermogravimetric analyses

As an additional method of determining the nature of progressive dehydration of autunite, thermogravimetric analyses were obtained for dark and light autunite from the Daybreak mine (Figs. 5, 6). The procedure involves a constantly recording balance. The sample is placed in a crucible which is suspended from a balance pan and is enclosed in a furnace which heats the sample either at a uniform rate or in discrete steps, while the resulting loss in weight is continuously recorded on a graph. This technique is similar to that employed in the study of dehydration of clays. (See, for example, Ross and Hendricks, 1945, p. 49–51.)

A slightly modified reproduction of the dehydration curve for light autunite (Fig. 5) represents the course of dehydration at a uniform temperature rise of 2° per minute. The curve shows three more or less distinct inflection points, at temperatures fairly similar to those corresponding to endothermic troughs in the DTA patterns (Fig. 4). The first inflection point, at a weight loss of about 8 per cent, corresponds to about 6.3 water molecules per unit formula, which is in satisfactory agreement with the theoretical maximum of six water molecules in meta-autunite II. The temperature at the inflection point, about 97° C., is in good agreement with that of the first endothermic trough in the DTA patterns.

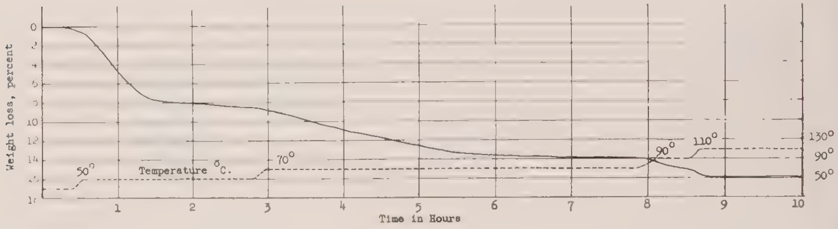

a. Light Autunite

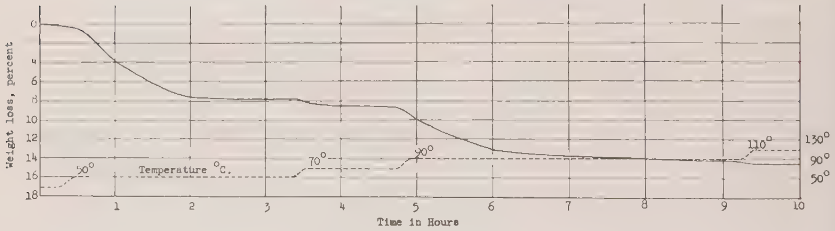

b. Dark Autunite

FIG. 6. Thermogravimetric data on light and dark autunite over the range 20°–110° C. Record by Charles A. Kinser.

The second and third inflection points, less well defined than the first, occur at approximately 15 and 17 per cent loss in weight; each point appears to mark the beginning of a finite water loss, and they may correspond to the last two endothermic troughs in the DTA patterns. In view of the previously noted similarity between the dehydration relationships of autunite and those of montmorillonite, these inflection points may be interpreted as representing loss of interlayer water The above data are in good accord with those of Brichard and Brasseur (1958, p. 7), who depict breaks in the dehydration curve of autunite at about 90° and 215° C.

Dehydration of dark and light autunite over a lower temperature range (20°–110° C.) are represented in Fig. 6. In these runs the temperature was raised in steps of 20°, and was held at each step until constant weight was attained. For reasons that are not apparent, the two curves are markedly different, although both reflect progressive loss of water over the temperature range involved.

Cation exchange capacity

Determination of base (cation) exchange capacity of four 0.5 gram samples (−20 mesh) of mixed light and dark autunite (DB-31) by the Bower and Truog colorimetric manganese method (Bower and Truog, 1940) gave values of 2.3–2.7 milliequivalents/100 grams, with an average value of 2.5 milliequivalents/100 grams. The determinations were made by J. C. Hathaway and H. C. Starkey of the U. S. Geological Survey.

Fairchild (1929) showed that artificial autunite may readily undergo base (cation) exchange with Na, K, Ba, Mn, Cu, Ni, Pb, and Mg; in some cases the exchange with original calcium was complete, indicating a cation exchange capacity much greater than that reported for Daybreak mine autunite. The difference may probably be explained by the fact that at least some of Fairchild's experiments were conducted by elevated temperatures over periods of several days, and that the artificial autunite crystals used by him were much finer—on the order of 0.2 mm. across—than the flakes of Daybreak mine autunite on which cation exchange determinations were carried out. The great difference in the experimental procedure in the two cation exchange experiments, thus makes it difficult to evaluate the small measured value of the cation exchange of the natural material.

X-ray determinations

X-ray powder films of nine different samples of dark and light meta-autunite I, prepared by Betsy Levin, U. S. Geological Survey, corresponded closely to published data for synthetic autunite (Frondel and others, 1956, p. 120). There was no significant or consistent difference between light and dark meta-autunite I, except that every pattern of dark material showed the strongest uraninite line ($d = 3.13$–3.14 Å), whereas that of the light material did not.

Diffraction patterns were also run on a single sample (DB-31) using the Norelco x-ray diffractometer, taking special precautions to obtain a randomly oriented sample (McCreery, 1949). Some degree of preferred orientation was nevertheless noted, as was the failure of a distinct uraninite line to appear in the pattern of dark autunite, presumably because of the relatively low intensity of the diffracted beam. From the standpoint of number and clarity of reflections, however, the patterns obtained by means of the diffractometer were superior to film data, and are hence reported in preference to the latter. Diffraction patterns were obtained of autunite in the fully hydrated, meta-I and meta-II forms, and also of material heated to higher temperatures, including red heat. The purpose of the latter experiments was an attempt to correlate the pronounced endothermic peaks in the DTA patterns with any possible related changes in the crystal structure. Separate patterns for light and dark material were obtained only for meta-autunite I, and these patterns were so similar that all other x-ray work was done with composite material, that is, the natural mixture of light and dark autunite.

Fully hydrated autunite

Some difficulty was experienced in the x-ray diffraction of fully hydrated autunite, because, if wetted excessively, the mineral assumes a highly preferred orientation in the sample holder. If insufficiently moistened, on the other hand, fully hydrated autunite tends to dehydrate to meta-autunite I during the period required for irradiation. A reliable pattern based on repeated runs (Table 6) is in good agreement with data for synthetic autunites (Frondel and others, 1956, p. 98; Brichard and Brasseur, 1958, Table IV), except for the rather strong reflection in the pattern of Daybreak mine autunite at $d = 5.19$, corresponding to (004); the same reflection is designated as weak by Brichard and Brasseur, and is lacking altogether from the pattern of Frondel and others. The strength of this reflection in the pattern of Daybreak mine autunite suggests a degree of preferred orientation. Another fairly strong line in the Daybreak pattern, at $d = 2.08$, is absent from the pattern of Frondel and others, but is listed by Brichard and Brasseur as (028), and also corresponds to (0, 0, 10). Other disparities between the three patterns are minor, and involve weak reflections only.

Meta-autunite I

In order to establish the difference in structure, if any, between dark and light autunite, the meta-I hydrates of the two phases were x-rayed separately. Comparison of the d-spacings of the two phases (Table 7), however, show that they are virtually identical, with no large or consistent differences. Some of the peaks in the range $2\theta = 60° - 90°$ are rather indefinite, and lack of close correspondence in this range is not considered significant.

The patterns of both dark and light meta-autunite correspond rather closely to published data (Frondel and others, 1956, p. 120; Brichard and Brasseur, 1958, Tables I and III; Volborth, 1959), except for minor disparities similar to those in fully hydrated autunite.

TABLE 6. *X*-RAY POWDER DIFFRACTION DATA FOR FULLY HYDRATED AUTUNITE[1]

d (Å)	I[2]	*hkl*[3]	*d* (Å)	I[2]	*hkl*[3]
10.4	160±	002	2.17	9	312
8.72	2		2.15	12	217
8.24	4		2.08	24	028; 0, 0, 10
6.67	10	011	2.039	9	314
5.19	84	004	1.918	7	029
4.96	39	110	1.834	2	
4.48	29	112	1.787	4	0, 2, 10
3.58	70	015	1.761	4	325
3.51	31	020	1.73	8b	
3.33	28	022	1.637	12	
2.91	8	024	1.551	6	
2.86	12	213	1.515	6	
2.73	17	017	1.484	4	
2.60	3	008	1.419	7	
2.50	5	215	1.365	8	
2.48	5	220	1.271	3	
2.41	8	222	1.232	4	
2.30	5	009	1.202	3	
2.22	8	140	1.138	3	
2.19	10	311			

[1] Undifferentiated autunite, i.e., the natural mixture of light and dark material, specimen DB-31. CuKα radiation, $\lambda = 1.5418$ Å; Ni filter; 40 KV, 15 MA; scale factor 8, time constant 4; range 2°–90° 2θ, at 1° 2θ per minute.

[2] Intensities correspond to actual peak heights. Value of $I = 160$ is extrapolated off the chart and hence approximate.

[3] Data after Brichard and Brasseur (1958, Tables II and IV).

b = broad.

Autunite heated at different temperatures

Powder data of meta-autunite II heated at 110°, 170°, and 225° C. are compared in Table 8. These temperatures represent arbitrary points between the pronounced endothermic peaks on the DTA pattern of autunite (Fig. 4), and powder patterns of the different stages were expected to reveal any changes in crystal structure accompanying the endothermic

Table 7. X-Ray Powder Diffraction Data for Light and Dark Meta-Autunite I[1]

Light meta-autunite		Dark meta-autunite		hkl[3]
d (Å)	I[2]	d (Å)	I[2]	
8.59	160±	8.57	125±	001
5.45	38	5.44	25	221
5.01	10	4.98	12	040
4.26	32	4.28	22	002
3.64	73	3.64	46	222
3.52	20	3.51	29	440
3.25	17	3.25	18	042
—		3.14*		
2.95	7	2.95	8	621
2.71	3	2.71	3	213
2.64	23	2.63	13	641
2.53	6	2.52	5	323
2.48	5	2.47	2	080
2.46	5	2.45	3	740
2.38	4	2.38	5	423
2.26	3	2.25	4	523
2.22	6	2.22	8	480
2.15	7	2.14	6	613
2.12	26	2.12	14	911
2.10	10	2.10	9	623
2.045	6	2.045	6	633
2.032	6	2.027	5	832
—		1.978	2	
1.952	9	1.948	5	941
1.90	2b	1.89	2b	653
1.815	6	1.814	4	942
1.767	5	1.762	4	10, 2, 2
—		1.752	4	
1.717	2	1.715	3	923, 763 (?)
1.695	5	1.70	2	
1.604	13	1.604	7	10, 2, 3
—		1.573	2	
—		1.566	2	
1.530	7	1.53	5b	12, 1, 2
1.413	3	—		13, 2, 2
1.400	2	1.397	2	
1.384	4	1.384	2	10, 4, 4
1.347	5	1.346	3	12, 7, 2
1.255	2b	1.256	2	
1.234	2	1.238	1b	
—		1.208		
1.191	3	1.193	2	
1.181	2	—		
1.151	2	—		
1.130	2b	1.129	3	

[1] Specimen DB-31. CuKα radiation; $\lambda = 1.5418$ Å; Ni filter; 40 KV, 15 MA; scale fac tor 8, time constant 4; range 2°–90° 2θ, at 1° 2θ per minute.

[2] Intensities correspond to actual peak heights. Values of I greater than 100 are extrap olated off the chart and hence approximate.

[3] Data after Brichard and Brasseur (1958, Tables I and III) and Volborth (1959).

* Strongest uraninite line; on X-ray powder films only.

b = broad.

TABLE 8. *X*-RAY POWDER DIFFRACTION DATA FOR META-AUTUNITE II HEATED AT 110°, 170°, 225° C., AND TO RED HEAT[1]

Meta-autunite II (Heated at 110° C.)		Heated at 170° C.		Heated at 225° C.		Heated to redness	
d (Å)	I[2]	*d* (Å)	I	*d* (Å)	I	*d* (Å)	I
						11.12	12
8.21	150±	8.20	165±	8.20	175±	8.28	115±
6.58	9	6.55	7	6.57	7	6.39	4
5.33	9	5.34	6	5.34	9	5.59	140±
4.81	11	4.81	11	4.80	8	4.96	12
4.08	70	4.08	100	4.07	150±	4.13	28
3.60	5	3.60	5	3.60	6	3.72	63
3.53	17	3.52	15	3.52	15	3.51	6b
3.27	8	3.27	8	3.27	6	2.95	4
3.21	6	3.21	5	3.22	5	2.88	4
3.12	2b			3.10	3	2.79	18
2.97	10	2.97	10	2.97	7	2.22	24
2.72	16	2.72	18	2.71	33	1.657	3
—		2.58	2	2.58	3	1.588	7
2.21	5	2.20	4	2.18	3		
—		—		2.13	2		
2.04	7	2.04	7	2.04	16		
—		—		1.99	3		
1.90	2	1.91	3	1.90	3b		
—		—		1.76	3		
1.63	5	1.630	4	1.63	5		
1.61	3	1.613	2	—			
1.48	3	—		—			

[1] Undifferentiated autunite, i.e., the natural mixture of dark and light material. Specinen DB-31. CuKα; $\lambda = 1.5418$ Å; Ni filter; 40 KV, 15 MA: scale factor 8, time constant 4; ange 2°–90° 2θ, at 1° 2θ per minute.

[2] Intensities correspond to actual peak heights. Values of I greater than 100 are extraplated off the chart and hence approximate.

b = broad.

eactions. The diffraction patterns of heated meta-autunite II in each ase were made after the sample had cooled to room temperature in the xpectation that any structural changes induced by heating would be naintained upon cooling. This assumption is based only upon the known rreversibility of the dehydration to meta-autunite II.

Comparison of the diffraction patterns corresponding to 110°, 170°, nd 225° C. indicates no fundamental differences in structure, and the lifferent peaks and their relative spacings are closely similar in the three atterns. The only progressive variation lies in the increasing relative intensities of some of the peaks, namely, $d=4.08$, 2.72, and 2.04, which may be ascribed to progressive loss of water between layers with increasing temperature, in a manner similar to that exhibited by montmorillonite (George T. Faust, written communication).

There is only limited correspondence between the above three patterns and that given by Frondel (1951, p. 677) for the meta-II hydrate of sabugalite, which is said to be "virtually identical with that of the meta-II hydrate of autunite." Marked disparities are found particularly in the lines falling in the range $2\theta=0°-25°$, which are especially well defined in the patterns of the Daybreak material.

The pattern of meta-autunite II heated to red heat (Table 8) is markedly different from that of material heated to lower temperatures, indicating that a distinct change in the structure occurs at some temperature above 225° C.

ORIGIN OF THE DEPOSITS

The Mt. Spokane deposits are strikingly different from other uranium deposits in granitic rocks, for example, within the Boulder batholith (Thurlow and Reyner, 1951; Wright and Emerson, 1957; Emerson and Wright, 1957), or at Marysvale, Utah (Kerr and others, 1952). In the latter cases, autunite is but one of a complex suite of secondary uranium minerals, and is closely related to primary unoxidized ore, notably uraninite; sulfides and oxides of copper, lead and iron are usually also present. The overwhelming preponderance of autunite in the Mt. Spokane area suggests a free supply of lime and phosphate, to the exclusion of other substances that could complex with uranium; the absence of known reserves of unoxidized uranium ore raises a baffling problem concerning a source of uranium to give rise to the large quantities of autunite.

A possible source of lime and phosphate is suggested by a study of the accessory constituents in twenty-seven samples of granitic rock, partly within and partly outside of mineralized zones. Results for representative samples are summarized in Table 9. The most striking observation is that apatite, by far the most abundant accessory constituent in most samples, is notably corroded and leached in specimens from mineralized zones (Fig. 7), whereas, in rocks at some distances from mineralized areas, apatite appears relatively fresh (Fig. 8). The indication is that apatite has been preferentially leached from granite in mineralized zones, releasing lime and phosphate which may have contributed toward the formation of autunite.

Fresh apatite may occur in rocks relatively close to mineralized zones (*e.g.*, DB-3, DB-56), whereas apatite from rocks at some distance from known mineralization (*e.g.*, DB-57C, DB-79, DB-83A) may show signs of

TABLE 9. ACCESSORY MINERALS IN SOME ROCKS FROM THE MT. SPOKANE AREA, WASHINGTON

Percentages based on visual estimates only

Sample No.	Sample location and description	Accessory minerals		Condition of apatite	Remarks
DB-3	Fairly fresh fine-grained granite three feet above horizontal gouge zone, east of main mineralized zone, Daybreak mine.	Apatite Zircon Opaques	95 2 3	Most grains smooth and euhedral; some etching on larger grains.	Zircon forms tiny fresh euhedral prisms.
DB-4	Altered gouge from ore zone, Daybreak mine.	Apatite Garnet Opaques Monazite and zircon	64 20 15 1	Generally corroded and embayed, irreguular outlines.	Garnet has pitted surfaces, some grains deeply embayed.
DB-5	Altered medium-grained muscovite granite 50 ft. west of main ore zone, Daybreak mine.	Apatite Garnet Opaques	90 5 5	Grains uniformly corroded and dirty, with irregular outlines and occasional embayments.	Garnet partly etched and pitted, partly fresh.
DB-12	Somewhat altered fine-grained granite in mineralized zone, Daybreak mine.	Apatite Opaques	95 5	Most grains corroded with rough surfaces, sharp irregular edges; rare smooth prisms.	
DB-20	Fairly fresh quartz monzonite aboue one mile northwest of Daybreak mine.	Apatite Monazite Zircon	95 4 1	Grains mostly clean, unetched, prismatic.	Lead-alpha age on monazite found to be 75 ± 10 m.y.[1]
DB-36	Fine-grained autunite-bearing pegmatite, Lehmbecker Claim.	Garnet	100		Garnet forms fresh, light orange-red euhedral grains up to 0.25 mm. in diameter.
DB-40	Medium- to coarse-grained altered muscovite-bearing granite, adjacent to zone of intense shearing; Kessler property.	Apatite Garnet	95 5	Grains uniformly etched; rough surfaces, irregular jagged outlines, some development of spines.	
DB-50	Sheared and foliated biotite granite along Deadman Creek road near summit of Mt. Spokane.	Apatite Monazite Garnet Zircon and Allanite (?)	85 10 3 2	Grains mostly clean, unetched, prismatic; slight pitting in some cases.	Monazite in rounded prisms; some grains slightly etched.
DB-54	Altered granite next to autunite stringer in mineralized zone; Mudhole prospect on Deadman Creek.	Apatite Garnet Sphene, Monazite and Zircon	90 10	Highly corroded; rough and dirty looking surfaces, extremely irregular outlines; spines and deep embayments on many grains (See Fig. 8.)	Garnet, sphene, and monazite slightly etched; zircon completely fresh.

---

[1] Analyst, T. W. Stern, U. S. Geological Survey.

TABLE 9 (*continued*)

Sample No.	Sample location an description	Accessory minerals		Condition of apatite	Remarks
DB-56	Fine-grained biotite granite from end of trench, approximately 10 yards from autunite mineralization; Mudhole prospect.	Apatite Zircon and Allanite (?)	95 5	Nearly all grains clean, fresh, euhedral; slight etching on larger grains only. (See Fig. 9.)	One of the freshest concentrates examined.
DB-57C	Fresh biotite granite 7 miles north of Daybreak mine.	Apatite Opaques (mostly pyrite) Sphene, monazite and zircon	80 15 5	Most grains fresh and euhedral, but some etching and pitting, especially on larger grains.	
DB-64	Altered medium-grained muscovite granite cut by pegmatites. From trench, Dahl property. No visible autunite.	Apatite Garnet Monazite Pyrite and misc.	65 15 10 10	Most grains corroded, with jagged outlines, spines, and embayments.	Monazite partly etched though less than apatite; garnet fairly fresh
DB-73A	Fairly fresh biotite granite, Deadman Creek road, 0.1 mile west of Mudhole prospect.	Apatite Allanite Zircon Misc.	90 7 2 1	Fresh clean euhedral or slightly rounded prisms, no sign of etching.	Allanite forms irregular grains and subhedral prisms, partly etched. Zircon forms sharply euhedral prisms.
DB-79	Slightly altered biotite granite, Deadman Creek road at junction of north and south forks of Deadman Creek.	Apatite Monazite and misc.	98 2	Most grains slightly etched and pitted; generally euhedral but some with embayments and irregular outline.	
DB-83A	Slightly altered medium-grained muscovite-bearing granite along Blanchard Creek road 1½ miles northwest of Daybreak mine.	Apatite Monazite	98 2	Most grains etched and pitted, though less strongly than apatite from mineralized zones. Shapes of grains often irregular.	Monazite shows slight etching.
DB-83B	Fine-grained aplite dike in granite DB-83A	Garnet Apatite	90 10	Most grains prismatic, slightly etched.	Garnet in euhedral or slightly rounded grains 0.1–0.2 mm. in diameter.

corrosion. The first observation suggests that intense leaching of apatite is a rather localized process, evidently restricted to immediate shear zones, and thus closely related in space to development of autunite. Corrosion of apatite in relatively unaltered rocks, on the other hand, may perhaps be attributed to normal weathering, unrelated to the active leaching that apparently prevailed in shear zones. The number of specimens studied is insufficient to warrant generalization on these points; the above observations, however, must be considered in any discussion regarding the origin of these deposits.

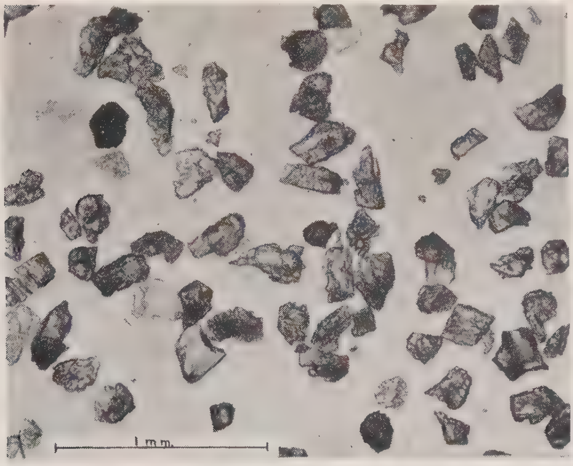

FIG. 7. Apatite from specimen DB-54, altered granite from mineralized zone at Mudhole prospect, Mt. Spokane area.

Leaching of apatite with subsequent crystallization of autunite has been proposed as a weathering process by Frondel (1951b, p. 685). In the western part of the Wind River district, Wyoming (R. G. Coleman, U. S. Geological Survey, written communication), incrustations of autunite have formed on nodules and stringers of apatite, apparently as the result of reaction of apatite with weakly acid groundwater. Apatite in water solution dissolves appreciably below pH 8 (Kazakov, 1950), and

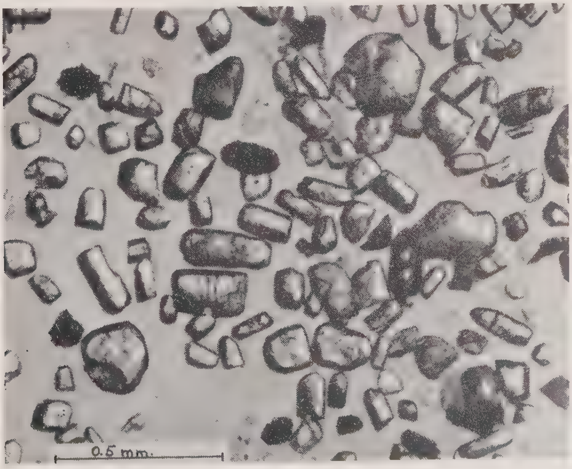

FIG. 8. Apatite from specimen DB-56, fairly fresh biotite granite about 30 feet distant from most intense autunite mineralization, Mudhole prospect.

its solubility increases markedly below pH 4 (Stelly and Pierre, 1942, p. 140). Leaching of apatite in the Mt. Spokane area may have been effected by near-surface meteoric waters, but for reasons considered below, it appears more probable that ascending juvenile waters were more important. A possible indication of a generally acid environment in this area is the absence of uranophane and phosphuranylite, which are thought to form by reaction of autunite with silica-bearing solutions above pH 7 (Shcherbina and Ignatova, 1956). Noticeable decomposition of autunite at room temperature in solutions of HCl with pH 5 or lower, on the other hand, indicates an effective lower limit of pH during and after mineralization.

TABLE 10. URANIUM CONTENT OF QUARTZ MONZONITE AND SOME CONSTITUENT MINERALS FROM MT. SPOKANE, WASHINGTON
In parts per million[1]

Quartz monzonite (DB-20)[2]	2.1
Apatite[3]	23
Biotite[3]	10

[1] Each figure represents the average of two determinations.
[2] Analyst, Wendell P. Tucker, U. S. Geological Survey.
[3] Analyst, Joseph Budinsky, U. S. Geological Survey.

Whereas lime and phosphate for autunite formation appears to be potentially abundant, an adequate source of uranium is much less apparent. Some uranium, like calcium and phosphorus, may have been derived from the granitic rocks by leaching. Relatively unaltered quartz monzonite about one mile north of the Daybreak mine (DB-20) contains about 2 ppm. uranium (Table 10), about one-half of which might be leached from the rock (Larsen and others, 1955, p. 68). Even on the assumption, however, that this figure represents an average for the granitic rocks of the area, the amount of uranium derived by leaching would be scarcely adequate to account for the known autunite deposits.* It is therefore necessary to look for additional sources of uranium. One possibility is that the deposits represent originally unoxidized veins almost entirely converted to autunite; alternately, uranium may have been transported from depth by oxidizing solutions.

---

* A phosphate determination for specimen DB-20 indicated a P_2O_5 content of 0.14 per cent. Assuming all P_2O_5 to be in apatite, and apatite to be 20 per cent leached, it is estimated that available lime and phosphate from a ton of rock could yield about 1,500 grams of autunite, whereas available uranium (assuming 50 per cent leaching) would yield less than two grams of autunite.

As evidence for the first origin may be cited the presence of finely dispersed uraninite throughout cores of autunite clusters, which might be interpreted as remnants of incompletely converted uraninite veins. However, there are important differences, already alluded to, between the deposits of Mt. Spokane and many other oxidized vein deposits in granitic rocks. At the W. Wilson mine south of Helena, Montana (Wright and Emerson, 1957), a complex suite of secondary uranium minerals, mainly meta-autunite, meta-uranocircite, uranophane, and phosphuranylite, is developed above the water table within a few feet of uraninite-bearing veins. Meta-autunite is disseminated in the wall rock up to four and one-half feet from veins; direct replacement of uraninite by autunite or other secondary minerals, although noted, is very rare. In the Marysvale district (Kerr and others, 1952), autunite, torbernite, and schroeckeringite are disseminated in the oxidized zone, above unoxidized veins containing sooty uraninite, pyrite, and fluorite. These and other pitchblende-bearing vein deposits in felsic intrusive rocks (Everhart and Wright, 1953) are furthermore characterized by a variety of other ore minerals, predominantly base-metal sulfides, and commonly show hematite alteration. Since the above features are essentially lacking in the Mt. Spokane district, the latter can certainly not be regarded as typical of uraninite-bearing vein deposits.

An alternate explanation for accumulation of uranium is that the latter may have been leached from unoxidized deposits at depth by oxidizing, slightly acid juvenile waters. The uranyl-bearing solutions, ascending along structurally controlled channels, may have leached apatite and subsequently deposited autunite along shear zones and fractures.

As pointed out earlier, the chief difficulty with the above hypothesis is the apparent absence of significant amounts of unoxidized ore, at least within a depth of about 100 feet. Much deeper drilling at mineralized sites may be required to locate primary sources of uranium that gave rise to the autunite deposits.

Origin of uraninite

No obvious explanation is apparent for the occurrence of uraninite in submicroscopic particles throughout the inner portions of autunite flakes. One possibility, that the uraninite represents unoxidized remnants of original uraniferous veins, seems improbable because of the complete absence of larger remnants of unoxidized ore in the process of replacement. Alternately, it is suggested that uraninite may have been precipitated within autunite during and following crystallization of the latter. The solutions depositing autunite were probably mildly oxidizing, with a pH of about 5 to 7. According to the diagrams of Garrels (1955, Fig. 5), under the above conditions a very small quantity of U^{+4} ions would be in equilibrium with uranyl-bearing solutions, and the amount of U^{+4} would increase greatly with a moderate drop in Eh. If, after initial crystallization of autunite, the environment for a period became more reducing, uraninite might have been precipitated.* In the event of fluctuation of Eh across the boundary of stability of U(IV) relative to U(VI), alternate crystallization of autunite and uraninite might have taken place.

Because of limited evidence for such a mechanism, especially with regard to the likelihood of a fluctuating oxidation-reduction environment in the Mt. Spokane area, the above idea is put forward only speculatively. However, such a mechanism, if tenable on theoretical grounds, would be in better accord with the observed occurrence of uraninite than to suppose the latter to represent remnants of unoxidized veins.

ACKNOWLEDGMENTS

Acknowledgments for various analytical services and other specialized work are made throughout the text. Thanks are due Mr. Kae Sowers of Daybreak Uranium, Inc., for permission to visit the Daybreak mine and to collect valuable autunite specimens. In addition, the writer wishes to thank the various claimholders in the Mt. Spokane area for their cooperation, as well as geologists of the Atomic Energy Commission and various private companies for providing helpful information and stimulating discussions.

George T. Faust, David B. Stewart, and Z. S. Altschuler of the U. S. Geological Survey critically read the manuscript and offered many valuable suggestions. Finally, special appreciation is expressed to Robert G. Coleman of the U. S. Geological Survey for his sustained interest and much helpful advice throughout the study. This work was done by the U. S. Geological Survey partly on behalf of the Division of Raw Materials, U. S. Atomic Energy Commission.

REFERENCES

ALTSCHULER, Z. S., CLARKE, R. S., JR., AND YOUNG, E. J. (1958), The geochemistry of uranium in apatite and phosphorite: *U. S. Geol. Survey Prof. Paper* **314-D,** 45–90.

BEINTEMA, J. (1938) On the composition and the crystallography of autunite and the meta-autunites: *Rec. travaux Chim. Pays-Bas* **57,** 155–175.

---

* The possibility of precipitating sooty uraninite at low temperatures and pressures by means of a reducing agent such as H_2S has been demonstrated by Gruner (1952) and Miller and Kerr (1954). McKelvey and others (1955, p. 490) state that "Precipitation of primary uranium minerals may be caused solely by a decrease in temperature and/or pressure, or may be the result of chemical interaction with the host rock."

Borneman-Starinkevitch, I. D. (1938), On some isomorphic substitutions in apatite: *Acad. Sci. U.R.S.S., Comptes rendus (Doklady)* **19,** no. 4, 253–255.

Bower, C. A., and Truog, E. (1940), Base exchange capacity determination of soils and other materials using colorimetric manganese method: *Indus. and Eng. Chemistry, Anal. Ed.* **12,** 411–413.

Brichard, H., and Brasseur, H. (1958), Sur les autunites naturelles et synthétiques: *Soc. française minéralogie et crystallographie Bull.* **81,** 4–10.

Clarke, R. S., Jr., and Altschuler, Z. S. (1958), Determination of the oxidation state of uranium in apatite and phosphorite deposits: *Geochim. et Cosmochim. Acta* **13,** 127–142.

Donnay, G., and Donnay, J. D. H. (1955), Contribution to the crystallography of uranium minerals: *U. S. Geol. Survey* **TEI-507**, 42 p., issued by U. S. Atomic Energy Comm. Tech. Inf. Service Extension, Oak Ridge, Tenn.

Emerson, D. O., and Wright, H. D. (1957), Secondary uranium minerals at the W. Wilson mine in the Boulder batholith, Montana: *Am. Mineral.* **42,** 222–239.

Everhart, D. L., and Wright, R. J. (1953), The geologic character of typical pitchblende veins: *Econ. Geology* **48,** 77–96.

Fairchild, J. G. (1929), Base exchange in artificial autunites: *Am. Mineral.* **14,** 265–275.

Frondel, C. (1951a), Studies of uranium minerals (VIII): Sabugalite, an aluminum-autunite: *Am. Mineral.* **36,** 671–679.

——— (1951b), Studies of uranium minerals (IX): Saléeite and novacekite: *Am. Mineral.* **36,** 680–686.

Frondel, C., Riska, D., and Frondel, J. W. (1956), *X*-ray powder data for uranium and thorium minerals: *U. S. Geol. Survey Bull.* **1036-G,** 91–153.

Garrels, R. M. (1955), Some thermodynamic relations among the uranium oxides and their relation to the oxidation states of the uranium ores of the Colorado Plateaus: *Am. Mineral.* **40,** 1004–1021.

George, D'Arcy (1949), Mineralogy of uranium and thorium bearing minerals: *U. S. Atomic Energy Comm.* **RMO-563,** 198 p., issued by U. S. Atomic Energy Comm. Tech. Inf. Service Extension, Oak Ridge, Tenn.

Green, Jack (1953), Geochemical table of the elements for 1953: *Geol. Soc. Am. Bull.* **64,** 1001–1012.

Greene-Kelly, R. (1957), The montmorillonite minerals (smectites), *in* Mackenzie, R. C., ed., The differential thermal investigation of clays: Miner. Soc. (Clay Miner. Group) London, 140–164.

Grim, R. E. (1953), Clay mineralogy: New York, McGraw-Hill Book Co., Inc., 384 p.

Gruner, J. W. (1952), New data for syntheses of uranium minerals, *in* Annual report for July 1, 1951, to June 30, 1952, pt. 1: *U. S. Atomic Energy Comm.* **RMO-983,** 26 p., issued by U. S. Atomic Energy Comm. Tech. Inf. Service Extension, Oak Ridge, Tenn.

Guillemin, C., and Pierrot, R. (1956), La sabugalite du gite de Margnac II. Haute-Vienne: *Soc. française minéral. et cryst. Bull* **79,** 179–182.

Kazakov, A. V. (1950), The fluorapatite system of equilibria in the conditions of formation of sedimentary rocks: *Akad. Nauk SSSR, Inst. Geol. Nauk* **114,** Geol. ser. no. 40, 1–21. (Unpublished translation, 1951, by V. L. Skitsky.)

Kerr, P. F., Brophy, G., Dahl, H. M., Green, J., and Woolard, L. E. (1952), A geologic guide to the Marysvale area, Annual report for July 1, 1951, to June 30, 1952, pt. 1: *U. S. Atomic Energy Comm.* **RMO-924,** 57 p., issued by U. S. Atomic Energy Comm. Tech. Inf. Service Extension, Oak Ridge, Tenn.

Larsen, E. S., Jr., Phair, G., Gottfried, D., and Smith, W. L. (1955), Uranium in magmatic differentiation, *in U. S. Geol. Survey Prof. Paper* **300,** 65–74.

McCreery, G. L. (1949), Improved mount for powdered specimens used on the Geiger counter x-ray spectrometer: *Am. Ceramic Soc. Jour.* **32,** 141–146.

McKelvey, V. E., Everhart, D. L., and Garrels, R. M. (1955), Origin of uranium deposits: *Econ. Geology,* **50th Anniversary Volume,** pt. 1, 464–533.

Miller, L. J., and Kerr, P. F. (1954), Progress report on the chemical environment of pitchblende, *in* Annual Report for June 30, 1953, to April 1. 1954, pt. 2: *U. S. Atomic Energy Comm.* **RMO-3096,** p. 72–99, issued by U. S. Atomic Energy Comm. Tech. Inf. Service Extension, Oak Ridge, Tenn.

Norman, H. W. (1957), Uranium deposits of northeastern Washington: *Mining Eng.* **9,** 662–666.

Nuffield, E. W., and Milne, I. H. (1953), Studies of radioactive compounds: VI. Meta-uranocircite: *Am. Mineral.* **38,** 476–488.

Palache, Charles, Berman, Harry, and Frondel, Clifford (1951), Dana's system of mineralogy, 7th ed., **2**: New York, John Wiley and Sons, Inc., 1124 p.

Rinne, F. (1901), Kalkuranit und seine Entwaesserrungsprodukte (Metakalkuranite): *Centralbl. Mineral. Geol. und Palaeontl.,* 709–713.

Ross, C. S., and Hendricks, S. B. (1945), Minerals of the montmorillonite group, their origin and relation to soils and clays: *U. S. Geol. Survey Prof. Paper* **205-B,** 23–77.

Shcherbina, V. V., and Ignatova, L. I. (1956), Formation and dissolution of autunite: *Geokhimiya,* no. 2, 56–61.

Stelly, M., and Pierre, W. H. (1942), Forms of inorganic phosphorus in the C horizons of some Iowa soils: *Soil Sci. Soc. Am. Proc.* **7,** 139–147.

Thurlow, E. E., and Reyner, M. L. (1951), Preliminary report on uranium-bearing deposits of the northern Boulder batholith region, Jefferson County, Montana: *U. S. Atomic Energy Comm.* **RMO-800,** 62 p., issued by U. S. Atomic Energy Comm. Tech. Inf. Service Extension, Oak Ridge, Tenn.

Volborth, A. (1959), Strontian meta-autunite from the Daybreak mine, Mt. Spokane, Washington: *Am. Mineral.* **44,** 702–711.

Wright, H. D., and Emerson, D. O., 1957, Distribution of secondary uranium minerals in the W. Wilson deposit, Boulder batholith, Montana: *Econ. Geology* **52,** 36–59.

Manuscript received May 8, 1959.

THE AMERICAN MINERALOGIST, VOL. 45, JANUARY-FEBRUARY, 1960

METAMORPHISM OF LOWER PALEOZOIC ROCKS IN THE VICINITY OF THE TACONIC RANGE IN WEST-CENTRAL VERMONT[1]

E-AN ZEN

Department of Geology and Geography, University of North Carolina, Chapel Hill, North Carolina

ABSTRACT

Rocks from the Taconic Range and adjacent areas, near Castleton in west-central Vermont, have been studied for their mineral assemblages. Most of the rocks are argillaceous or arenaceous, of Early Cambrian to Middle Ordovician age, and are from the Taconic allochthone. A number of samples, including carbonates, are from the Lower Ordovician to Middle Ordovician rocks of the surrounding autochthonous marble belt. Regional metamorphism was later than the emplacement of the Taconic allochthone; the metamorphic grades in the Taconic sequence cut across structures, and conform to the trend in the surrounding autochthone. The grade decreases from east to west, and the rocks range correspondingly from phyllites to slates and shales.

Study of the mineralogy of the samples made use both of the *x*-ray diffractometer and the petrographic microscope. Two chlorite samples, one from a slate and one from a phyllite and a chloritoid sample from a phyllite, in addition to four rock samples, were chemically analyzed.

The most significant mineral assemblages found are:

(1) muscovite-chlorite-quartz
(2) muscovite-paragonite-chlorite-chloritoid-quartz
(3) muscovite-chlorite-chloritoid-epidote-hematite-magnetite-quartz
(4) muscovite-stilpnomelane-chlorite-albite-microcline-quartz
(5) muscovite-biotite-quartz-graphite
(6) calcite-dolomite-chlorite-muscovite
(7) calcite-zoisite-chlorite

The prevalence of assemblage (1), with its simple mineralogy, indicates that chlorite may be variable in the (Fe, Mg)/Al ratio in addition to the Fe/(Fe+Mg) ratio. This is borne out by the chemical analyses; the analyzed chlorites are among the highest reported in their Al/(Fe, Mg) ratios.

The basal spacings of coexistent muscovite and paragonite in assemblage (2), found in the phyllites, are 9.97(5) Å and 9.62(3) Å, respectively, indicating very limited solid solution between these phases at this metamorphic grade. No paragonite has been found in the slates; it is suggested that paragonite may possess a lower limit of stability, with the more hydrous assemblage, kaolinite plus albite, taking the place of paragonite plus quartz.

Rocks relatively rich in Al contain chloritoid (2,3), and the chloritoid-chlorite association is common even in slates. The chlorite is always more Mg-rich although the analyzed chloritoid also shows significant solid solution of Mg for Fe. The only sodic phase found with chloritoid is paragonite. Rocks relatively poor in Al do not have chloritoid but contain stilpnomelane (4), in addition to microcline which is incompatible with high-Al phases. The location of stilpnomelane on the low-Al part of the A-F-M diagram is based on regarding all Fe‴ in stilpnomelane as subsequently oxidized Fe″; this is justified by an analysis of the available chemical data on this mineral. Stilpnomelane- and chloritoid bearing as-

---

[1] Contribution No. 390 from the Department of Mineralogy and Petrography, Harvard University.

semblages are mutually incompatible in the area; that the control is chemical composition rather than physical conditions of metamorphism is borne out by field mapping of the lithologic units. The stilpnomelane-microcline-chlorite assemblage rules out the chlorite-Fe biotite pair, which in fact is not found in the area although biotite does occur (5).

Data pertaining to phases in the A-C-F diagram are scanty. The mineral assemblages show, however, that chlorite may be the first mineral to form upon metamorphism of a quartzose and aluminous dolostone (6). The presence of the zoisite-calcite pair (7) indicates that the calcite-kaolinite pair, found in sedimentary rocks, ceases to be stable in the rocks of this area.

The analysis of the mineral assemblages in the Castleton area indicates that these rocks by and large have attained chemical equilibrium during metamorphism. The assemblages obey the Phase Rule, and no incompatible mineral pair has been found. Textural data on the rocks also suggest extensive recrystallization has occurred. Both H_2O and CO_2 may be treated as mobile components without violating the Phase Rule. Evidence, however, is inconclusive on the status of O_2.

Introduction

In the course of geological mapping at the north end of the Taconic Range and adjacent areas around the town of Castleton in west-central Vermont (Zen, in preparation), a large number of specimens of metamorphosed sedimentary rocks of Cambro-Ordovician age were collected. These rocks are predominantly argillites, but also include quartzites, graywackes, arkoses, and carbonates. Owing to regional metamorphism, the argillites now range from phyllites or fine-grained schists in the Taconic Range along the east side of the area, where the grade of metamorphism is the highest, to virtually unmetamorphosed shales in the Champlain Valley to the west. The other lithologic types show corresponding mineralogical and textural changes. With the stratigraphic succession and the nature of the geological structure fairly well known, it has become possible to study the metamorphism of these rocks.

The only extensive petrographic study of rocks of the Castleton area is that of T. N. Dale (1898). Dale made detailed microscopic studies of the slates, and published a number of chemical analyses of rocks from this area, as well as one mineral analysis, that of a pyrophyllite. No correlation was made by Dale between the results of chemical and microscopic investigations, however; and so the former are not very useful for modern petrological discussions.

In this paper, the observed mineralogical and petrographic details of the various minerals or mineral groups are first given, supplemented by chemical data. The mutual relationships of these minerals are then considered in the second section. Instead of considering each individual rock type as such, however, the various mineral assemblages are considered in terms of ternary or pseudoternary phase diagrams, and the mutual relation of the various mineral assemblages discussed in the light of these diagrams. In this manner, it is hoped, the dependence of the observed assemblages on the bulk chemical composition, for a given metamorphic environment, will be emphasized. The phase-diagram approach also makes it more easy to apply the principles of physical chemistry to the study of the mineral assemblages, such as predicting the direction of changes upon given changes in the environment, and understanding the mutual stability relationships of the mineral phases in a given assemblage. Lastly, the phase diagram approach, in one form or another, has been traditional for the study of metamorphic rocks of higher grades (see, for instance, Turner, 1948; Thompson, 1957; Korzhinskii, 1959); it is hoped that the present study may be easily integrated with these others in its present form.

ACKNOWLEDGMENTS

Much of the material in this paper was drawn from a doctoral dissertation submitted to Harvard University. For the critical guidance of its writing, I would like to thank Professors M. P. Billings, C. Frondel, and J. B. Thompson, Jr. The manuscript in its present form was read by Professors Billings and Thompson; for their extensive comments and critical discussions I am much indebted. The imprint of Thompson's teaching can probably be recognized in the approach adopted in this paper. I would also like to acknowledge the helpful discussions of other fellow petrologists among whom I should especially mention Arden L. Albee and Priestley Toulmin III, both of the U. S. Geological Survey. Numerous grants from the Division of Geological Sciences, Harvard University, and part of one from the Geological Society of America, have largely paid for the cost of chemical analyses and thin-section preparation. A grant from the Research Council of the University of North Carolina has helped to defray the cost of typing.

RESUME OF REGIONAL GEOLOGY

As the full report on the geology of the Castleton area will be published elsewhere (Zen, in preparation; 1959b), only a brief summary is given here. The following is a simplified description of the stratigraphic succession in the area, the units being arranged from younger to older.

Lower to Middle Ordovician: Red, green, gray, and black, hard, quartzose slates, with interbedded fine, cherty quartzites, massive ankeritic quartzites, and thin, ribbony limestones. Some of the red slates are soft and of commercial value. The name "Poultney River group" is used informally for this group of rocks.

Lower Cambrian:

1. West Castleton formation. Black slate, with black, fossiliferous limestone near its base. The slate ranges from soft, fissile and pyritiferous to hard and sandy.

2. Bull formation. Mainly the Mettawee slate facies, consisting largely of purple,

green, and gray slate and argillite. Included also in the Bull formation are a fossiliferous intraformational conglomerate and a vitreous orthoquartzite near the top of the formation; a graywacke, the Zion Hill quartzite, near the middle of the formation; and the Bomoseen graywacke, a massive, olive-drab, areally extensive facies in the middle and lower part of the formation.

3. Biddie Knob formation. A purple to green, highly aluminous, chloritoid- and paragonite-bearing slate or phyllite.

These rocks, together, constitute an allochthonous unit, originally deposited perhaps at the site of the present Green Mountain anticlinorium. They were moved into the present position as a series of imbricate thrust plates, each of which is internally intricately and recumbently folded. The emplacement of the allochthone was an Upper Trenton event. The regional metamorphism was later superimposed on the complex regional structure, and has simple regional patterns, conforming to the grade and trend in the surrounding autochthonous units. The metamorphic grade generally decreases from east to west, so that, while at the eastern edge of the area the argillaceous rocks are phyllites and the carbonates contain actinolite and zoisite, at the western margin of the map area the rocks are barely metamorphosed.

The place names referred to in the text are located, to the nearest 1′ of latitude and longitude, in Appendix I at the end of the paper.

METHOD OF STUDY

The slates of the Castleton area are commonly so fine-grained that microscopic examinations do not always yield definitive results. Because of this fact, considerable reliance has been placed on *x*-ray methods of mineral identification. Due to the sensitivity of the results of such studies to the laboratory procedure, a brief description of the method used follows.

A Norelco high angle Geiger-counter diffractometer, equipped with Cu tube and Ni filter, was used in most of the work. The sample was ground fine and molded into standard aluminum holders by the use of a hand press. Such a method gives preferred orientation to inequidimensional minerals, particularly the platy minerals; however, for the purpose of identification of phases this fact presents no problem. For routine work, the following instrumental settings are used on the diffractometer: goniometer speed, 1° 2θ per minute, chart speed, $\frac{1}{2}''$ per minute; divergent, scatter, and receiving slits, 1°, 1°, and 0.003″, resp.; scale factor, multiplier, and time constant, 8, 1, 4, or 4, 1, 4, resp. The resulting charts are compared with prepared standards and the minerals thus identified. For careful measurements of line positions, a goniometer speed of $\frac{1}{4}°$ 2θ per minute is used with quartz added as an internal standard.

A simple scheme of mineral identification by the *x*-rays such as outlined above does not, of course, always yield clear-cut results. Despite the existence of such reference data as the A.S.T.M. file, the identification of an unknown phase often rests, in the last analysis, on evidence not intrinsic to the *x*-ray records. For instance, a study of the literature on the mineralogy of similar rocks may be helpful; or the thin section might yield clues to the mineral identities. One of the major drawbacks to the x-ray method is the possibility of line interference by several different phases in the sample; however, in most cases the combination of lines, rather than a single line, is used for identification, and such combinations are generally enough to define a phase. Nonetheless, the microscope has to be depended upon almost exclusively for the detection of minute amounts of a mineral, and for the study of the textural relations of the minerals. In all, about 200 thin sections have been examined.

MINERALOGY

Chlorite

Petrography and association. Chlorite is a common mineral in the rocks of the Castleton area; it is nearly ubiquitous in the argillaceous rocks and has been found in association with every other mineral except biotite. It occurs either in the bulk of the rock, or as irregular vein fillings, by itself or in association with quartz, quartz and albite, or quartz, albite, and carbonate.

Chlorite appears microscopically either as tiny scales, about 10μ in long dimensions, or as randomly oriented microporphyroblasts up to 0.5 mm. in size. As microporphyroblasts, it is commonly intergrown with muscovite and occasionally with stilpnomelane (?). The existence of chlorite in a specimen is easily checked by the x-ray diffraction pattern. The $(00l)$ reflections are generally sharp to the fifth order. The only possible source of confusion comes from the 7 Å clay minerals such as kaolinite, but the latter lacks the reflection at about 14 Å.

Chemical analysis. Data on the composition of chlorites from low-grade rocks are scarce; yet such data are essential in discussions of the phase relations of the host rocks. Two chlorites, accordingly, have been separated and analyzed, and a third one computed from a rock analysis of known mineralogy. The two analyzed chlorites are given in Table 1, together with their optical properties and calculated formulae, taking the number of oxygens per formula as 18. Chlorite no. 197-2 was from a fracture filling in a soft, green slate of the Bull formation on the east side of Crystal Ledge $\frac{1}{2}$ mile north of Bull Hill, and was virtually free of impurities, the small amount of alkali in the analysis having been computed as white mica, a trace of which was visible under the microscope. Chlorite no. 212-2A was from a paragonite phyllite found in the vicinity of Ben Slide north of Herrick Mountain, and the analyzed sample had 2% of quartz and 1.5% of muscovite and paragonite according to a point-count of the analyzed material. These impurities have been corrected for, but the chlorite composition is necessarily less reliable than no. 197-2.

TABLE 1. MINERAL ANALYSES

(Booth, Garrett and Blair, analysts)

Sample number	197-2 (chlorite)	212-2A (chlorite)	213-1A (chloritoid)
SiO_2	23.62	25.92	25.18
TiO_2	0.04	0.13	0.40
Al_2O_3	23.04	23.74	39.48
Fe_2O_3	2.20	1.70	2.00
FeO	31.18	27.67	22.26
MgO	8.64	8.66	1.25
MnO	0.15	0.30	1.32
CaO	none	0.36	0.06
Na_2O	0.12	0.30	0.15
K_2O	0.03	0.27	0.43
H_2O (1150°C)	11.00	10.65	7.30
H_2O (105°C)	0.20	0.00	0.06
Total	100.22	99.70	99.89
Optical properties: (sodium light)			
α	1.640 ± 0.001	-----	1.720 ± 0.002
β	1.642 ± 0.001	1.636 ± 0.001	1.722 ± 0.002
γ	-----	same	1.725 ± 0.002
2V	(-?) small	0°	(+) moderate
	X ⊥ (001)	-----	Y ∧ (001) ≈ 20°
Pleochroic formula	Y ≈ Z = deep green X = light yellow	Y = Z = deep green X = straw yellow	X = Y = indigo-green Z = straw yellow
Anomalous extinction?	blue	blue	bronze to lavender
			polysynthetic twinning with composition plane (001)
X-ray data:	d (001) 14.113 ± 0.002A	d (001) 14.113 ± 0.002A	d (001) 17.801 ± 0.002A

Calculated formula:

Chlorite no. 197-2

(a) All Fe''' grouped with Fe'' in the calculations

$$(\underbrace{\mathrm{Fe}_{3.08}\mathrm{Mg}_{1.43}\mathrm{Mn}_{0.01}\mathrm{Al}_{1.46}}_{5.98})(\underbrace{\mathrm{Al}_{1.46}\mathrm{Si}_{2.53}}_{3.99})\mathrm{O}_{18}\mathrm{H}_{8.07}$$

$$(\mathrm{Fe}'' + \mathrm{Mn})/(\mathrm{Fe}'' + \mathrm{Mn} + \mathrm{Mg}) \approx 0.68$$

(b) All Fe''' grouped with Al in the calculations

$$\underbrace{(\underbrace{\mathrm{Fe}''_{2.88}\mathrm{Mg}_{1.42}\mathrm{Mn}_{0.01}}_{4.31})(\underbrace{\mathrm{Al}_{1.36}\mathrm{Fe}'''_{0.18}}_{1.54})}_{5.85}(\underbrace{\mathrm{Al}_{1.55}\mathrm{Si}_{2.52}}_{4.07})\mathrm{O}_{18}\mathrm{H}_{8.03}$$

$$(\mathrm{Fe}'' + \mathrm{Mn})/(\mathrm{Fe}'' + \mathrm{Mn} + \mathrm{Mg}) \approx 0.67$$

$$(\mathrm{Fe}_{\mathrm{total}} + \mathrm{Mn})/(\mathrm{Fe}_{\mathrm{total}} + \mathrm{Mn} + \mathrm{Mg}) \approx 0.68$$

(c) According to the method of Brindley and Gillery (1956):

$$(\mathrm{Fe}_{4.0}\mathrm{Mg}_{0.7}\mathrm{Al}_{1.3})(\mathrm{Al}_{1.3}\mathrm{Si}_{2.7})\mathrm{O}_{18}\mathrm{H}_{8}$$

Name [Hey, 1954, p. 280]: ripidolite

Chlorite no. 212-2A (corrected for quartz and sericite)

(a) All Fe''' calculated as Fe''

$$(\underbrace{\mathrm{Fe}_{2.85}\mathrm{Mg}_{1.51}\mathrm{Mn}_{0.03}\mathrm{Ca}_{0.05}\mathrm{Al}_{1.47}}_{5.91})(\underbrace{\mathrm{Al}_{1.47}\mathrm{Si}_{2.52}}_{3.99})\mathrm{O}_{18}\mathrm{H}_{8.08}$$

$$(\mathrm{Fe} + \mathrm{Mn})/(\mathrm{Fe} + \mathrm{Mg} + \mathrm{Mn} + \mathrm{Ca}) \approx 0.65$$

(b) All Fe''' calculated as Al

$$\underbrace{(\underbrace{\mathrm{Fe}''_{2.71}\mathrm{Mg}_{1.51}\mathrm{Mn}_{0.03}\mathrm{Ca}_{0.05}}_{4.30})(\underbrace{\mathrm{Al}_{1.38}\mathrm{Fe}'''_{0.15}}_{1.53})}_{5.83}(\underbrace{\mathrm{Al}_{1.53}\mathrm{Si}_{2.53}}_{4.06})\mathrm{O}_{18}\mathrm{H}_{8.10}$$

$$(\mathrm{Fe}'' + \mathrm{Mn})/(\mathrm{Fe}'' + \mathrm{Mg} + \mathrm{Mn} + \mathrm{Ca}) \approx 0.62$$

$$(\mathrm{Fe}_{\mathrm{total}} + \mathrm{Mn})/(\mathrm{Fe}_{\mathrm{total}} + \mathrm{Mg} + \mathrm{Mn} + \mathrm{Ca}) \approx 0.65$$

Name [Hey, 1954, p. 280]: ripidolite

Chloritoid no. 213-1A (all alkali computed as mica, titania as rutile)

(a) All Fe''' calculated as Fe''

$$(\mathrm{Fe}_{0.88}\mathrm{Mg}_{0.08}\mathrm{Mn}_{0.05}\mathrm{Ca}_{0.00})\mathrm{Al}_{1.94}\mathrm{Si}_{1.00}\mathrm{O}_{7}\mathrm{H}_{2.10}$$

$$(\mathrm{Fe} + \mathrm{Mg})/(\mathrm{Fe} + \mathrm{Mn} + \mathrm{Mg}) \approx 0.92$$

(b) All Fe''' calculated as Al

$$(\mathrm{Fe}''_{0.82}\mathrm{Mg}_{0.08}\mathrm{Mn}_{0.05}\mathrm{Ca}_{0.00})(\mathrm{Al}_{1.94}\mathrm{Fe}'''_{0.07})\mathrm{Si}_{1.00}\mathrm{O}_{7}\mathrm{H}_{2.10}$$

$$(\mathrm{Fe}'' + \mathrm{Mn})/(\mathrm{Fe}'' + \mathrm{Mn} + \mathrm{Mg}) \approx 0.92$$

$$(\mathrm{Fe}_{\mathrm{total}} + \mathrm{Mn})/(\mathrm{Fe}_{\mathrm{total}} + \mathrm{Mn} + \mathrm{Mg}) \approx 0.92$$

In Table 2 is presented the rock analysis for specimen 212-2 from which, knowing the chlorite composition, the compositions of the white micas can be estimated.

In Tables 1 and 2 are presented the analysis for rock no. 213-1, and

TABLE 2. ROCK ANALYSES

(Booth, Garrett, and Blair, analysts)

Sample number	212-2	213-1	392-1	648-1
SiO_2	42.42	39.41	49.46	78.86
TiO_2	1.10	0.66	1.02	0.70
Al_2O_3	33.89	31.21	25.36	8.85
Fe_2O_3	2.40	2.10	1.96	1.86
FeO	4.87	10.36	6.33	1.63
MgO	1.93	3.41	2.01	0.76
MnO	0.08	0.16	0.08	0.02
CaO	0.12	0.14	0.22	0.56
Na_2O	2.40	1.55	4.25	1.69
K_2O	5.07	4.01	4.14	2.37
H_2O (1000° C.)	5.80	6.54	4.90	1.97
Total	100.14	99.55	99.73	99.27
Modal mineralogy:	Muscovite Paragonite Chlorite Quartz Rutile	Muscovite Paragonite Chloritoid Chlorite Quartz Rutile	Albite Muscovite Chlorite Quartz Rutile	Muscovite Chlorite Stilpnomelane Plagioclase (albite) Microcline Quartz
Weight % norms (based on identified mineralogy):				
(a) All Fe′′′ as Fe′′	Muscovite 42.9 Paragonite 29.6 Margarite 0.8 Chlorite 21.6 Quartz 4.0 Rutile 1.1	Muscovite 34.2 Paragonite 19.2 Margarite 1.0 Chloritoid 8.7 Chlorite 31.2 Quartz 5.1 Rutile 0.7	Muscovite 35.4 Chlorite* 23.1 Albite 36.6 Anorthite 1.1 Quartz 2.7 Rutile 1.1	
(b) All Fe′′′ as Al	Muscovite 43.2 Paragonite 29.8 Margarite 0.8 Chlorite 17.4 Quartz 7.6 Rutile 1.1			
(c) *X*-ray mode			Chlorite 23 Muscovite 30 Plagioclase 43 Quartz 3† Rutile 1†	

Calculated chlorite composition: (Number 213-1)

(a) All Fe′′′ calculated as Fe′′, both in chlorite and chloritoid

$(Fe+Mn)/(Fe+Mn+Mg+Ca) \approx 0.62$

(b) All Fe′′′ calculated as Al, both in chlorite and chloritoid

$(Fe''+Mn)/(Fe''+Mg+Mn+Ca) \approx 0.51$

$(Fe_{total}+Mn)/(Fe_{total}+Mg+Mn+Ca) \approx 0.56$

(c) According to Winchell and Winchell (1951, p. 385) and the "$\frac{1}{3}$ substitution" formula:

$(Fe+Mn)/(Fe+Mg+Mn) \approx 0.67$

---

* Chlorite based on "$\frac{1}{3}$ substitution" formula.

† Presence assumed in the computations.

for the chloritoid separated therefrom. The rock is from a locality about 500 feet due east of the locality for specimen 212-2. From the composition of the chloritoid, the Fe/(Fe+Mg+Mn) ratio in the coexistent chlorite has been computed, as given in Table 2.

Calculation of the chlorite formula. The calculated composition of a chlorite depends on the structural nature to be assigned to the ferric iron given in the chemical analysis. On the one hand, it might be substituting for aluminum, and must be reckoned therewith; on the other hand, it might be ferrous iron that has undergone oxidation after the formation of the chlorite. The corresponding chlorite formulae constitute limits of variation between which the true composition must lie. These calculated formulae are presented in Table 1.

Discussion. Both chlorite analyses show considerable excess of Al over the ideal Pauling formula of 2 Al's per 18 oxygen (Pauling, 1930). This indicates that an added compositional variation exists in chlorite, in that the Al^{iv}/Si ratio is variable, a fact familiar to the mineralogists (Winchell, 1926; Orcel, 1927; Brindley and Robinson, *in* Brindley, 1951; Hey, 1954).

Thompson (1952, lecture notes) suggested that, in order to achieve local valence saturation in the chlorite structure, $\frac{1}{3}$ additional Al per 18 oxygen, in each of the octahedral and tetrahedral positions of the talc-type layers, may be expected. The calculated formulae just given exceed even this value. The following schemes of atomic substitution are tentatively suggested to account for the excess Al.

First there is the possibility of a random mixed-layer structure between talc-type and pyrophyllite-type layers sandwiched in between the brucite-type layers. Against this hypothesis, however, may be cited the lack of evidence for the completely analogous mixed-layer structure between biotite and muscovite (Yoder and Eugster, 1953, p. 67); this lack of solid solution may be explained by the strain that would be induced in the lattice due to differences in the *a* and *b* dimensions of the dioctahedral and trioctahedral layers.

Second, the excess Al in chlorite may be accommodated, again with local valence balance, by the simultaneous replacement of a divalent atom in the brucite-type layer and a silicon atom in the tetrahedral position to yield a chlorite having the following formula as a component:

$$(Fe, Mg)_2Al(OH)_6(Fe, Mg)_2AlAl_2Si_2O_{10}(OH)_2.$$

Indeed, Nelson and Roy (1958, p. 712) have found experimentally that a complete solid solution apparently exists between chlorite with the above formula and with the Pauling formula.

Finally, it is possible to accommodate some extra Al within the octahedral layer by the simple scheme

$$2Al \rightarrow 3(Fe, Mg).$$

This scheme is impossible to differentiate, by chemical data alone, from the first one; it should, however, be limited in extent since it implies strong local bond-strength variations leading to a less stable structure.

Problems in the identification of chlorite. The problem of determination of the chemical composition of chlorites by means of physical measurements has long interested the mineralogist. Hey (1954) recently summarized the data to date and attempted to establish regression equations between the composition and the indices of refraction, cell dimensions, and the bulk density of the chlorites. Many other attempts also exist at relating some specific compositional variation with certain cell-dimension changes (see, for instance, Brindley and Robinson, *in* Brindley, 1951; Mikheev, 1953; Nelson and Roy, 1958), and Brindley and Gillery (1956) recently advocated the use of *x*-ray line intensities for the same purpose.

Hey's method is based on the assumption of the existence of five independent compositional variables, which he chose to be Si, Fe''', Fe^{total}, Mn, and Cr. To use his relations, one must assume (1) that there is no hydrogen-deficiency in the structure, and (2) that ferric iron occupies either only 4-fold or only 6-fold positions, for otherwise there is no unique solution to the Mg and Al contents in the mineral.

The defects of earlier attempts at the determination of chlorite composition by *x*-ray have been summarized by Brindley and Robinson (*in* Brindley, 1951). The method of Brindley and Gillery, based on a combination of cell-dimension and intensity studies, so far seems to give only qualitative information (1956, p. 182, fig. 3), as is shown by their own results. Chlorite no. 197-2 was studied this way and the results are incorporated in Table 1 for comparison with direct chemical analysis.

In the following discussions, unless otherwise specified, a "$\frac{1}{3}$ substitution" formula is assumed for chlorite. The FeO/(FeO+MgO) ratio is then determined by using the chart given by Winchell and Winchell (1951).

Chloritoid

Petrography and association. Chloritoid has been reported from low-grade rocks of various areas; as examples may be cited the Tintagel district (Tilley, 1925), Cornwall (Phillips, 1928), the Gotthard area (Niggli, 1912), southeastern Pennsylvania (Agron, 1950), and the Berkshire Hills of Massachusetts (Balk, 1953). In the Castleton area, chloritoid occurs abundantly not only in the phyllites of the Taconic Range, but even in the purple and green slates in the vicinity of Lake Bomoseen.

On the *x*-ray diffractometer, chloritoid is distinguished by a sharp line pair, corresponding to the (004) and (006) reflections, at about 20° and 30° 2θ, respectively. Microscopically, chloritoid typically occurs as lath-shaped, euhedral, polysynthetically twinned crystals, about 0.1 mm. in length. The crystals are randomly oriented in the rocks, and commonly cluster together in sheaves. The high relief, low birefringence, and segmented appearance, coupled with pleochroism from indigo to yellow, are diagnostic. Chloritoid commonly intergrows with muscovite, occupying the centers of the "sandwiches." The effect is most striking in hematitic rocks, as the compound porphyroblasts show up as clear areas in a pasty, translucent background. The size of the porphyroblasts, about 0.1 mm., affords a minimum measure of the distance of material transport during recrystallization.

In the Castleton area, chloritoid has been found to coexist with the following minerals: muscovite, paragonite, chlorite, epidote, hematite, magnetite, rutile, and quartz. Albite has not been found with chloritoid; this may be due in part to low sodium content of the aluminous pelites in the area so that no distinct sodic phase is formed; however, it may also reflect the low metamorphic grade, so that this mineral pair is unstable, a point to be considered later. Chloritoid has not been found with biotite in the present study, but the evidence is inconclusive due to the rarity of biotite. Hietanen (1941, p. 144, 146) reported chloritoid with albite and biotite in the Wissahickon schist in Pennsylvania.

Chemical analysis. Table 1 gives a chemical analysis of chloritoid from specimen 213-1, from a locality east of Ben Slide. The analyzed sample had 0.4% of sericite and 0.1% of quartz as impurities (point-count analysis) and was full of tiny rutile inclusions. In the calculations of chloritoid formula, therefore, all alkali has been taken as white mica and all titanium oxide as rutile. The resulting formulae are given in Table 1, both when the analyzed Fe''' is taken as original Fe''' and when it is taken as oxidized Fe''. Both formulae are so close to the ideal formula of $(Fe, Mg)Al_2SiO_7H_2$ that they are equally likely. The analysis shows that 8% of the octahedral, divalent position in chloritoid is taken by magnesium. This is a minimum measure of the amount of Mg that chloritoid can dissolve in an environment represented by the rocks of this vicinity, and shows that even at such low metamorphic grades chloritoid cannot be taken as a purely ferrous mineral.

Muscovite and Paragonite

Muscovite and paragonite occur in slates and phyllites typically as microscopic flakes, about 20μ long (in the *ab* plane). They are distinguished from other platy minerals by the relatively high birefringence and lack of color and pleochroism. The flakes are commonly oriented parallel to one of the rock cleavages.

Muscovite also occurs as bulbous microporphyroblasts about 0.1 mm. across, cross-cutting the rock cleavage directions and commonly interleaved with chlorite and less commonly with chloritoid. This textural feature demonstrates that the minerals are the results of recrystallization, and not detrital in origin.

On the *x*-ray diffractometer, the pattern of muscovite is distinctive. The most useful reflections are the strong basal lines; the exact *d* spacings of which are a measure of the amount of sodium (and possibly calcium) in solution in muscovite. The one possible source of confusion is biotite, which has the same basal spacing. Iron-bearing biotite is generally pleochroic and readily identified with the microscope, though pure Mg biotite (phlogopite) could escape notice. For most of the rocks, however, there is commonly an iron-bearing chlorite, hence it is not likely that any coexisting biotite could be purely magnesian.

Paragonite is microscopically indistinguishable from muscovite in the rocks studied. Rosenfeld (1956, p. 144) reported differences in the 2V values and in refractive indices; the method is not adaptable to very fine-grained samples. On the *x*-ray diffractometer, however, the two phases are readily differentiated by their basal spacings. Although the strong 3.2 Å line of paragonite coincides with the (002) reflection of albite, the over-all pattern of paragonite is sufficient for its certain identification.

Muscovite is found in the Castleton area in association with all minerals. In fact, rarely is there a rock that does not carry muscovite. In the majority of the rocks studied, this mineral represents the principal potassic phase; only a few rock types, notably the Bomoseen greywacke, a few slates of the Poultney River group, and a few limestones, carry a potassic feldspar as well as muscovite.

In contrast, paragonite is rare in rocks of this region and has not been found in the true slates. It is found in significant amounts only from a low outcrop at 2000′ level, about $\frac{1}{4}$ mile east of Ben Slide (specimen 212-2). The rock is a highly micaceous phyllite, containing also muscovite, chlorite, and a little quartz and rutile. The basal spacings of the two micas in this rock are as follows:

Paragonite, *d*(001)	9.62(3) Å
Muscovite, *d*(001)	9.97(5) Å

Traces of paragonite have also been found, in this area and near Biddie Knob, in the Biddie Knob formation, in coexistence with chloritoid as well as the above-mentioned minerals.

In recent years paragonite has become increasingly recognized, thanks to the *x*-ray diffractometer, as an important mineral in low- to medium-grade metamorphic rocks high in aluminum. The various mineral associations of paragonite have been described (Rosenfeld, 1956; Harder, 1956; Dietrich, 1956; Eugster and Yoder, 1955; Albee, 1957b). A study of the paragonite-muscovite pair has been published (Rosenfeld, Thompson, and Zen, 1958) and the mineral assemblages will be considered in a separate paper by the same authors. From the *x*-ray lattice spacing data, the paragonite and its coexistent muscovite from the Castleton area represent nearly pure sodic and potassic micas, respectively; and with the possible exception of the brammallite reported by Bannister (1943), the occurrence of paragonite at Ben Slide may represent the lowest-grade assemblage yet recorded.

Stilpnomelane and Biotite

Petrography and association. The micaceous mineral stilpnomelane has been found commonly in the Bomoseen greywacke member of the Bull formation in the Castleton area. It is found in the most easterly areas of the greywacke outcrop, just west of the main Taconic Range; it is also found in the most westerly area, at Mill Pond near Benson. Since the metamorphic grade generally decreases westward, this mineral appears to occur over the entire range of metamorphic grade in the Castleton area.

The Bomoseen greywacke is a fine-grained, olive-drab, poorly-cleaved rock with occasional grains of quartz, feldspar, muscovite, and rock fragments visible in the hand specimen. Stilpnomelane cannot be seen even with the aid of a hand lens.

Under the microscope, stilpnomelane is seen as tiny scales, generally less than 0.02 mm. in their long dimensions, interstitial to and wrapping around quartz and feldspar grains, as well as in separate sheaves. The scales may be interleaved with muscovite or chlorite, demonstrating that they are the results of recrystallization and not detrital in origin. The scales are strongly pleochroic, and resemble brown biotite closely except for the occasional segmented appearance and lack of mottling between crossed nicols, in agreement with Hutton's observations (1938, p. 182). Optical data on stilpnomelane and coexisting chlorite from one of the specimens are given on page 163. The basal spacing, 12.1 Å, agrees with those of Gruner (1944, p. 298) and Hutton (1938) and proves its identity. The 12.1 Å line is not shifted by treatment with ethylene glycol. On the basis of its pleochroic color and index of refraction, the stilpnomelane may be rather rich in ferric iron according to the data of Hutton (1938, p. 177, 182, 184, 187). This is in agreement with the rather high ferric-ferrous ratio (about 1:1 atomic ratio) in the rock analysis for specimen 648-1 (Table 2), which contains stilpnomelane.

The correlation of the indices of refraction of stilpnomelane with composition is uncertain. Hutton (1938, p. 187) and Winchell and Winchell (1951, p. 390) give regression charts. Winchell and Winchell, however, take into account only the effect of oxidation of iron and manganese, whereas Hutton assumes that ferric iron and aluminum have the same effect on the indices of refraction, which is probably not true.

Stilpnomelane has been found in association with the following minerals in the same rock: plagioclase (nearly pure albite by extinction-angle and $\Delta 2\theta$ measurements; the latter based on data of Tuttle and Bowen, 1958, p. 12), microcline, muscovite, quartz, chlorite, and hematite. Microcline and hematite are rare, but the associations with the other phases are common. These phase relations will be discussed in a later section.

Besides stilpnomelane, a number of rocks in the Castleton area carry a pleochroic, micaceous mineral, probably biotite or stilpnomelane, which because of its extreme rarity in the specimens cannot be definitely identified. Two characteristic appearances of the mineral(s) are described below.

1. Small (about 0.05 mm.) scales, in green, grey, and purple slates and greywackes, found as far west as the neighborhood of Glen Lake. These are pleochroic, with X = light green, Y = Z = dark green. The grains look like stilpnomelane. Due to rarity of grains, the indices of refraction have not been ascertained. For the same reason this mineral cannot be observed on the *x*-ray diffraction chart. The mineral association is quartz, albite, chlorite, muscovite, and hematite.

2. Tiny books, characteristically in graphitic black slates or quartzose nodules therein. Y = Z = light olive brown, X = light yellow. Between crossed nicols this mineral appears mottled. It is most probably biotite. Associated minerals are quartz, muscovite, and graphite.

Problem of stilpnomelane. Special interest is attached to the mineral association of stilpnomelane because of the rather uncertain composition and structure of this phase. The mineralogy has been summarized elsewhere (Hutton, 1938; Gruner, 1944); it seems certain that structurally this mineral is related to the micas. The chemical analyses of stilpnomelane (Hutton, 1938, 1956; Gruner, 1944; Kojima, 1944; Shirozu, 1955) are difficult to interpret because apparently the composition is independently variable along several coordinates, a point which, however, cannot be established. The chemical analyses, compared with the analyses of biotite and minnesotaite, consistently run relatively high in silica and calcium. The role of ferric iron in the analyses presents additional difficulties. To see in what manner these factors affect the field of composition of stilpnomelane, and in what ways the compositions may be related to those of iron biotite and minnesotaite, the best published chemical analyses are plotted in Fig. 1 under three different assumptions: (1) all of the ferric iron is original and structurally substitutes for Al; (2) all ferric iron represents oxidized ferrous iron of the original mineral;

and (3) ferric iron plays a distinct and independent role in the structure and therefore does not plot on the diagram. One could also make different plots by assigning to Ca different structural roles, for instance substituting for the alkalis, substituting for the divalent metal atoms, and having its own structural position and therefore not plotting on the diagrams at all. The amount of Ca is so small, however, that these different plots appear sensibly the same. In Fig. 1, Ca is ignored.

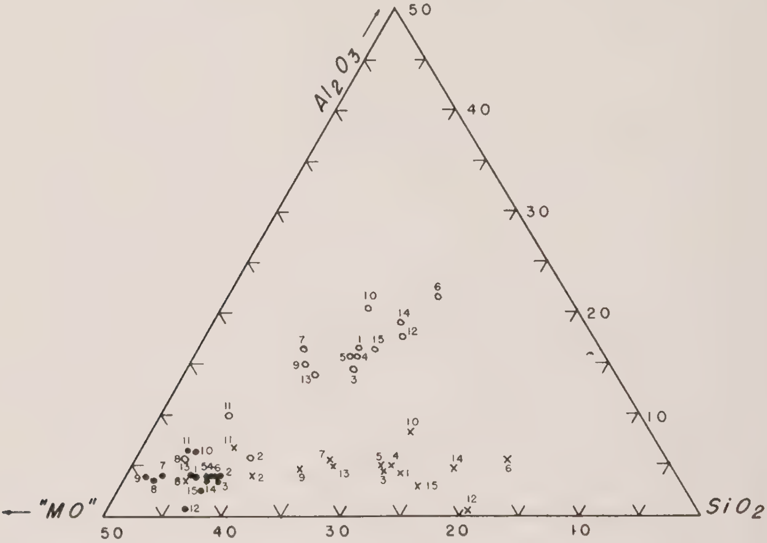

FIG. 1. SiO_2-Al_2O_3-"MO" plot of analyzed stilpnomelane.

Open circles: data analyzed according to assumption (1), using the following coordinates:

$$Al_2O_3 + Fe_2O_3 - Na_2O - K_2O; \quad FeO + MnO + MgO; \quad SiO_2 + 2K_2O + 2Na_2O$$

Solid circles: data analyzed according to assumption (2), using the following coordinates:

$$Al_2O_3 - Na_2O - K_2O; \quad FeO + MnO + MgO + 2Fe_2O_3; \quad SiO_2 + 2K_2O + 2Na_2O$$

Crosses: data analyzed according to assumption (3), using the following coordinates:

$$Al_2O_3 - Na_2O - K_2O; \quad FeO + MnO + MgO; \quad SiO_2 + 2Na_2O + 2K_2O$$

Sources of data:

Numbers 1 through 6, Hutton, 1938; p. 184, nos. B through G, resp.;
Numbers 7, 8, and 9, *ibid.*, p. 185, nos. B-2, C-1, and E-1, resp.;
Numbers 10 and 11, Kojima, 1944, p. 328, nos. I and II, resp.;
Number 12, Shirozu, 1955;
Numbers 13, 14, and 15, Hutton, 1956, p. 611, nos. A, B, and C, resp.

The results are interesting in that the points show enormous scatter except when ferric iron is treated as oxidized ferrous iron. Shirozu's analysis is the only one which may require calculation of Fe''' as Al, depending on the structural position assigned to Ca. It is interesting to note that, on the basis of microscopic evidence, Hutton (1938, p. 181) also suggested that ferric stilpnomelane may be due to later oxidation of the ferrous component.

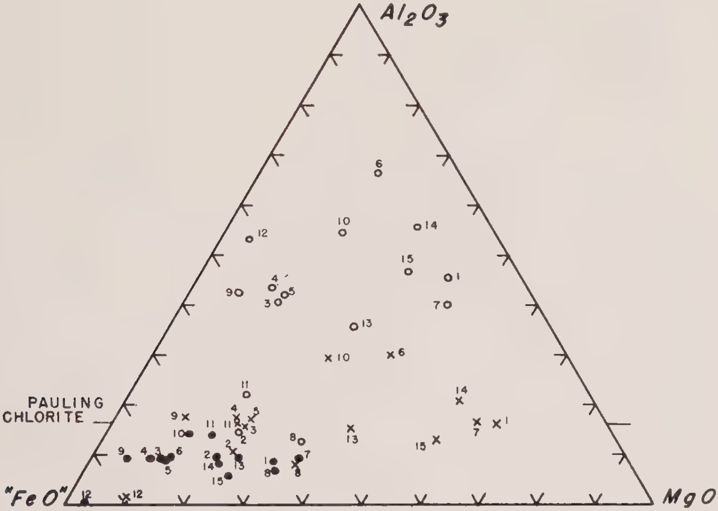

FIG. 2. A-F-M plot of analyzed stilpnomelane. The position of chlorite according to Pauling's ideal formula is indicated; biotite according to the ideal formula would plot along the base of the diagram.

Open circles: data analyzed according to assumption (1), using the following coordinates:

$$Al_2O_3 + Fe_2O_3 - Na_2O - K_2O; \quad FeO + MnO; \quad MgO$$

Solid circles: data analyzed according to assumption (2), using the following coordinates:

$$Al_2O_3 - Na_2O - K_2O; \quad FeO + MnO + 2Fe_2O_3; \quad MgO$$

Crosses: data analyzed according to assumption (3), using the following coordinates:

$$Al_2O_3 - Na_2O - K_2O; \quad FeO + MnO; \quad MgO$$

The numbers have the same significance as in figure 1.

Ignoring calcium, the results are also plotted on an A-F-M diagram, with (Al_2O_3-Na_2O-K_2O), FeO+MnO, and MgO as the apices, under the same set of three assumptions. The results are given in Fig. 2. Assumption (2) gives good coherence to the data. All the points plotted under assumption (2), significantly, fall below the $Al_2O_3/(Al_2O_3+FeO+MgO+MnO)$ line for chlorite according to the Pauling formula, and in fact fall between this and the line for biotite, due allowance being made for the "$\frac{1}{3}$ substitution" analogous to that for chlorite (Thompson, 1952, lecture notes). The stilpnomelane analyses, under assumption (2), are also plotted on the A-K-F(M) diagram, Fig. 5.

Carbonate

Two carbonates are found in rocks from the Castleton area: calcite and dolomite. Both occur as beds, lenses, and nodules, as well as subsidiary constituents in slates, quartzites, greywackes, and so forth. East of the Taconic Range in Whipple Hollow, the Ordovician limestones (Zen, 1959b) are sugary-textured marbles although the dolomitic beds may remain fine-grained; the average grain size decreases westward across the slate belt, paralleling the lowering of regional metamorphic grade in that direction, so that at the western margin of the map area the limestone rarely shows visible calcite grains in a hand specimen.

Calcite, under the microscope, generally is anhedral and tends to be considerably coarser grained than the coexisting dolomite, which commonly is in rhombs. The identities of these two carbonates have been checked by *x*-rays, making use of the strong and distinctive (10.4) reflections.

In the Castleton area, both dolomite and calcite have been found with the following minerals: quartz, muscovite, chlorite, albite, a potassic feldspar which is at least in some cases microcline, hematite, and possibly chloritoid. The association of microcline with carbonates occurs commonly in limestones, where the amount of argillaceous matter is low and thus microcline is presumably stable. The single occurrence of zoisite, in the marble at West Rutland, is associated with calcite.

Aside from quartz and the feldspars, chlorite and muscovite are the most common accessory phases in the carbonate rocks. Muscovite is commonly in euhedral, thin books, slender and lath-shaped in thin section and cross-cutting the carbonate grain-boundaries; chlorite may assume the same textural relations and is strongly colored due to its iron content. Less commonly, it is nearly colorless, with positive optical sign, and occurs as clots of delicate scales between carbonate grains, apparently as a magnesium-rich phase (Albee, 1957a, p. 80) resulting from reaction between the carbonate and an aluminum-rich phase during metamorphism. The textural relations also suggest that muscovite and chlorite are not metastable detrital grains.

Feldspar

Only two feldspars are known from the Castleton area: albite and potassic feldspar, some samples of which are definitely identified as microcline.

Albite is a fairly common accessory in slates and phyllites that do not carry chloritoid. It is the major mineral in many albite-phyllites, found sporadically along the contact of the green and black phyllites east of Taconic Range. As what appears to be detrital grains, it is a common mineral in greywackes and arkoses and in various limestones.

Albite in slates and phyllites is difficult to identify microscopically, as it is generally fine grained and untwinned. The albite from porphyroblastic phyllites is commonly also untwinned, typically occurring as round grains up to 0.5 mm. across, and showing, under the microscope, numerous helicitic inclusions of the mica and carbonaceous material of the matrix, indicating bodily rotation of the grains during growth. Detrital albite is generally polysynthetically twinned according to the albite law. Such albite, especially in greywackes, is commonly sericitized. The nature of the sericite is uncertain due to the very small amounts.

The composition of the albite is deduced from a combination of refractive index measurement, extinction-angle measurement according to the method of Michel-Lévy (when feasible), and *x*-ray lattice spacing measurement. The first two methods, especially the index of refraction, are sensitive to calcium content, which is found to be negligible. The potassium content is then estimated by the angular separation of the $(\bar{2}01)$ and the quartz (10.0) lines, using the regression relation now published by Tuttle and Bowen (1958, p. 13). These data are strictly applicable only to high temperature, synthetic feldspars, and show decreasing angular separation with increasing potassium content. Albite from the Castleton area shows this angular separation to a degree exceeding that of pure high-temperature albite ($\Delta 2\theta = 1.14°$), but agrees exactly with that of Amelia albite ($\Delta 2\theta = 1.18°$ according to the data of Smith, 1956, p. 52) which is generally accepted to have the low-temperature feldspar structure. The albite samples from the Castleton area, accordingly, are nearly pure $NaAlSi_3O_8$; this is true even of the albite in carbonate rocks. Combined with the observation of sericitization, it shows that even large detrital grains closely approached chemical equilibrium during regional metamorphism. That albite is the product of low-grade metamorphism of plagioclase feldspar is also demonstrated by the work of Coombs (1954).

In the Castleton area, albite is found to coexist with most other minerals. The exceptions are chloritoid, paragonite, and epidote (or zoisite). Imperfect sampling may account for the last two relations; the absence of the albite-chloritoid pair may be due to the low metamorphic grade.

A potassic feldspar is abundant in limestones in the Castleton area. In most cases it is definitely microcline, showing quadrille twinning; it is angular and commonly fragmentary, indicating a detrital origin. Microcline probably is present also as porphyroblasts in a few albite phyllites from the eastern slopes of the Taconic Range. Such porphyroblastic "microcline" shows at most simple Carlsbad twin, and is identified chiefly on the basis of its optical properties: 2V (−) large, $\gamma <$ balsam. X-ray evidence is inconclusive, as the amount of this is small, and the diffraction peak at 27.5° 2θ would be weak and interfered with by the rutile peak. Staining of the feldspars by sodium cobaltinitrite solution, according to the simplified technique of Chayes (1952), is equally inconclusive largely due to the fine grain size.

Microcline, showing quadrille twinning, occurs in the Bomoseen greywacke and occasionally, as detrital grains, in other greywacke and arkose beds. A potassic feldspar was also identified by x-rays in some of the Poultney River slates; but here the feldspar grains are too fine for microscopic identification.

Other Minerals

Pyrophyllite. Dale (1898, p. 191; 1900, p. 19) reported pyrophyllite from the phyllite of Ben Slide, north of Herrick Mountain. Enough sample was purified for a chemical analysis. Dale (1898, p. 191) described the mineral as "bright green . . . in thin scales." The rocks found today at Ben Slide are purple and green phyllite carrying muscovite, chlorite, chloritoid, quartz, and exceptionally paragonite. The writer has collected some 50 likely-looking samples from Ben Slide and studied them by x-rays. Not a trace of pyrophyllite has been found, and so its mineral association here remains unknown.

Epidote and zoisite. In the Castleton area, a mineral of the epidote group is found in a purple phyllite, specimen 29-4-1, from the west slope of Clark Hill, northeast of Herrick Mountain. It occurs as rare, large (about 0.4 mm. across), randomly oriented euhedral grains. Due to its rarity, however, the precise nature of the mineral cannot be determined. Associated phases are chloritoid, chlorite, muscovite, quartz, rutile, hematite, and traces of probable magnetite.

Zoisite is definitely found in a Beekmantown marble at West Rutland. It is colorless and euhedral, in slender prisms up to 3 inches long. Its identity is established by both x-ray and microscopic methods. The associated minerals are calcite and chlorite.

Quartz. Quartz is practically ubiquitous in the Castleton area. With few exceptions, it shows clear-cut extinction between crossed nicols. Especially in phyllitic rocks, it is commonly sufficiently recrystallized to give polygonal outlines in a thin section, with straight contacts between neighboring grains. The longest dimensions parallel the rock foliation. This relation shows that the grains have approached textural equilibrium through recrystallization.

Tourmaline. Tourmaline is a very common accessory in slates of the Castleton area. It characteristically forms euhedral crystals cross-cutting the rock cleavage. In some specimens the amount of tourmaline may be up to 1% of the rock by volume.

Sphene. Sphene is found only in specimen 29-4-1, which also carries epidote. Apart from rutile, it is the only titanium mineral found in the area.

Rutile. Rutile is the common titanium mineral found in the area. It characteristically forms minute needles randomly distributed in a thin section, and is microscopically discernible only under extreme magnification. Rutile is found in all assemblages in this area.

Iron oxides. Two iron oxides have been observed: hematite, found in the slates and much of the phyllites, and magnetite, rarely found in the slates (specimen 233-1-2), and more commonly in the phyllites of the Taconic Range. Hematite and magnetite are found together only in specimen 29-4-1, already described.

Hematite has been found to coexist with every known mineral in the Castleton area except paragonite. Under the microscope, it is readily recognized by the red color, high relief, and translucency; moreover, under high magnification the hexagonal outline of the basal plates can usually be seen, showing that it is not goethite.

Magnetite is recognized mainly in reflected light under the microscope, as very fine and rare grains in thin sections. Its identity therefore is not beyond doubt; the amount is commonly too small for checking with a magnet. It is observed in coexistence with the same minerals as hematite.

PETROLOGY

Mineral Assemblages

Before embarking on a discussion of the mutual relations of the minerals, it is convenient to list all the observed mineral assemblages. In the list that follows, no regard is paid to the relative *amounts* of the phases present, although differences in amounts may result in rocks of very different appearances and may even imply significantly different origins. For these gross lithological differences, the reader is referred to the field report (Zen, in preparation). The accessory minerals that might be described as the "heavy mineral suite" are also ignored. These minerals have not been studied as such and in all probability do not participate in any important way in the phase equilibrium relations to be considered in this part of the paper. Phases that are listed in parentheses are subsidiary in amount and may or may not be present in any given specimen.

1. Muscovite-chlorite-quartz (rutile, carbonate)
2. Muscovite-chlorite-paragonite-quartz (rutile)

3. Muscovite-chlorite-albite-quartz (rutile, carbonate)
4. Muscovite-chlorite-hematite-quartz (rutile, albite, carbonate)
5. Muscovite-chlorite-magnetite-quartz (rutile, albite)
6. Muscovite-biotite-quartz-graphite
7. Muscovite-stilpnomelane-chlorite-albite-quartz (rutile)
8. Muscovite-chlorite-stilpnomelane-albite-microcline-quartz-hematite (rutile)
9. Muscovite-chlorite-potassic feldspar-quartz
10. Muscovite-chlorite-chloritoid-quartz (rutile)
11. Muscovite-chlorite-chloritoid-paragonite-quartz (rutile)
12. Muscovite-chlorite-chloritoid-hematite-quartz (rutile)
13. Muscovite-chlorite-chloritoid-epidote-hematite-magnetite-quartz (rutile)
14. Muscovite-chlorite-albite-potassic feldspar-quartz (rutile, graphite)
15. Quartz
16. Calcite (quartz, albite, microcline, muscovite, chlorite, hematite)
17. Dolomite (quartz, albite, microcline, chlorite, muscovite)
18. Calcite-dolomite (quartz, albite, microcline, muscovite, chlorite)

The following assemblages are found in boudinage fillings:

19. Calcite
20. Quartz
21. Chlorite
22. Quartz-chlorite
23. Quartz-chlorite-albite
24. Quartz-chlorite-albite-ankerite

ROCK ANALYSES

In Table 2 are given four analyses of rocks from the Castleton area. The following brief descriptions and discussions may be helpful.

Rock no. 212-2. This rock, from which the chlorite 212-2A of Table 1 was extracted, is a highly micaceous, lustrous, medium-coarse grained, green-grey phyllite of the Biddie Knob formation. The outcrop from which the specimen was collected is at 2000′ elevation, about 1000 feet east of Ben Slide, and S75°W from the 1930′ knob west of Clark Hill. The rock contains, on the basis of *x*-ray data, muscovite, paragonite, chlorite, quartz, and rutile. Knowing the composition of the chlorite, it is possible to calculate both the composition and amounts of the white micas. It turns out, unfortunately, that the results of this calculation depend on whether the Fe‴ in the analysis is assumed to be oxidized Fe″ or if it is truly trivalent iron substituting for Al in the minerals. Accepting these two assumptions as limits, the calculated percentages of these minerals are given in Table 2. The β index of the muscovite, using Na light, was 1.604 ± 0.001.

Rock no. 213-1. This rock, from which the chloritoid 213-1A of Table 1 was separated, is a green, friable, lustrous phyllite of the Biddie Knob formation, collected from a small northeast-trending ravine, at 1850′ level about 1500 feet east of Ben Slide. Besides chloritoid, the rock contains chlorite, muscovite, quartz, rutile, and some paragonite. Knowing the chloritoid composition, and assuming an ideal formula of $(Na,K)Al_3Si_3O_{10}(OH)_2$ for the white micas and the "$\frac{1}{3}$ substitution" formula for chlorite, the latter has been calculated to have the following alternative formulae, depending on the structural role of ferric iron:

(1) All Fe‴ calculated as Fe″, both in chlorite and in chloritoid:

$$\{(Fe, Mn)_{2.9}(Mg, Ca)_{1.8}Al_{1.3}\}^{vi}\{Al_{1.3}Si_{2.7}\}^{iv}O_{18}H_{7.9}$$

$$(Fe + Mn)/(Fe + Mn + Mg + Ca) = 0.62$$

(2) All Fe‴ calculated as Al

$$\{(Fe, Mn)_{2.4}(Mg, Ca)_{2.3}(Al,Fe''')_{1.3}\}^{vi}\{Al_{1.3}Si_{2.7}\}^{iv}O_{18}H_8$$
$$(Fe'' + Mn)/(Fe'' + Mg + Mn + Ca) = 0.51$$
$$(Fe^{total} + Mn)/(Fe^{total} + Mg + Mn + Ca) = 0.56$$

and the calculated weight norms, for Fe‴ as oxidized Fe″, are given in Table 2.

Other pertinent petrographic data on this rock follow.

Muscovite: d (001) = 9.98 A
Paragonite: d (001) = 9.62 Å
Chlorite: d (001) = 14.11 Å
β (Na light) = 1.642 ± 0.001

Rock no. 392-1. This rock is from a local 730′ prominence 0.6 mile S69°W of the 661′ benchmark near Butler Pond in Whipple Hollow, immediately west of the local road. It is mapped as the West Castleton(?)-Hortonville(?) formation (Zen, 1959b). In the hand specimen, it is a grey, massive rock with minute porphyroblasts of a feldspar studded throughout the sample. Thin section and x-ray analysis show the mineralogy to be albite, chlorite, muscovite, quartz, and rutile. On the muscovite, $d(001) = 10.00$ Å; β (Na light) $= 1.601 \pm 0.001$. The albite is untwinned and shows rounded outline; $\Delta 2\theta_{CuK}((\bar{2}01) - (10.0)_{Qtz}) = 1.17°$, near that for Amelia albite, $\Delta 2\theta = 1.18°$ and therefore presumably nearly pure $NaAlSi_3O_8$ since both calcium (Smith, 1956, p. 52) and potassium (Tuttle and Bowen, 1958, p. 13) tend to decrease this angular separation. This is confirmed by the value of $\alpha, < 1.540$, showing that it is substantially free of calcium.

The calculated mode, on the basis of pure potassic muscovite and no potassium in the feldspar, is given in Table 2; an Fe/(Fe+Mg) ratio of 0.64 is computed for the chlorite. The results tally with an x-ray mode, based on calibration curves and technique developed by the writer and described elsewhere (Schmalz and Zen, in preparation).

Rock no. 648-1. Specimen 648-1, from an outcrop of the Bomoseen greywacke at 1490′ elevation on a small terrace 1.6 mile N22°W of Biddie Knob, is a dark grey, massive mudstone showing occasional rock chips up to 3 mm. across and grains of quartz and feldspar as well. Thin section and x-ray studies show the following mineral assemblage: stilpnomelane, chlorite, muscovite, plagioclase, microcline, quartz. The stilpnomelane has these properties:

$$2\ V = 0°;\quad \beta \text{ (Na light)} = \gamma = 1.687 \pm 0.002;\quad d\ (001) = 12.1\ \text{Å}.$$

Using the Michel-Lévy method, the albite turns out to be nearly calcium-free.

Because of the uncertain composition of both chlorite and stilpnomelane in this rock, it has not been feasible to calculate a norm for it.

REPRESENTATION OF MINERAL ASSEMBLAGES BY PHASE DIAGRAMS

Introduction. To study the mutual relations of the various minerals and mineral groups found in the slates, two possible approaches may be chosen. The first is to study each mineral assemblage as it is found, and attempt to see how it reflects the physical and chemical environment of formation; different assemblages may then be compared for the causes of the divergences. On the other hand, the mineral assemblages may also be studied by constructing multicomponent, isothermal, and isobaric phase diagrams, and correlating the observed associations with the various phase assemblages indicated by the diagrams. This second approach, though less direct, has many advantages. It emphasizes the compositional relationships among the minerals as well as the control of bulk composition on the mineralogy. It enables one to predict the changes in the mineralogy and compositions of individual phases with changing physical variables. Most significant, however, is its ability to bring together the different mineral assemblages, observed or as yet undiscovered, and exhibit their mutual relationships—which differences may reflect merely compositional variations, and which must reflect changing external factors such as temperature and pressure.

Because of these reasons, the second method is adopted in this study. A number of excellent general treatises of the method in the literature (Thompson, 1957; Korzhinskii, 1959) makes this feasible. Graphical methods will be used extensively. Because of the practical difficulty of representing multicomponent systems in two dimensions, where only three components can be conveniently depicted, standardized methods of selection of components are employed; the scheme is considered with each diagram. The diagrams to be considered are the following, in that order:

1. The A-N-K diagram: Al_2O_3; Na_2O; K_2O
2. The A-C-F(M) diagram: Al_2O_3; CaO; $FeO+MgO$
3. The A-K-F-M tetrahedron:
    a) The A-K-F(M) projection
    b) The A-F-M projection.

In the study of fine-grained rocks, it is not often possible to ascertain the exact compositions of all phases in a specimen, nor even always to identify all the phases present, so that one may be forced to use the bulk chemical analysis to estimate the composition of one phase when those of the other phases are known; indeed one may have to resort to this method to detect unsuspected phases. It is thus necessary to devise schemes for plotting a bulk chemical analysis onto any given ternary diagram. The particular scheme adopted depends of course on the nature of the other phases present and might change with each crossing of an isograd.

The A-N-K diagram. As no mineral found in the Castleton area has its gram-formula ratio of alkali to aluminum in excess of unity, corresponding to the alkali feldspars, the following values may be assigned to the apices of this ternary diagram: "A" = (Al_2O_3-K_2O-Na_2O); "N" = $NaAlO_2$; "K" = $KAlO_2$. The diagram, Fig. 3, is valid for quartz-bearing rocks and at some particular values of temperature, pressure, and the chemical potential of H_2O.

The proper aluminum silicate phase to place at the "A" corner, for the

Castleton area, is uncertain. As discussed before, Dale's report of pyrophyllite (1898, p. 191) from this area cannot be verified. The x-ray pattern of pyrophyllite is such that it should be easily detected even in small amounts. The writer suspects that in many slates kaolinite is the "A" phase. Kaolinite is difficult to ascertain in the presence of chlorite (Bradley, 1954), especially in small amounts, and could have escaped notice in many samples where it is expectable by the mineral association. Until more data exist, this phase is assumed to be appropriate for the "A" corner in the Castleton area; as we shall see, this does not affect any of the equilibrium arguments to be presented.

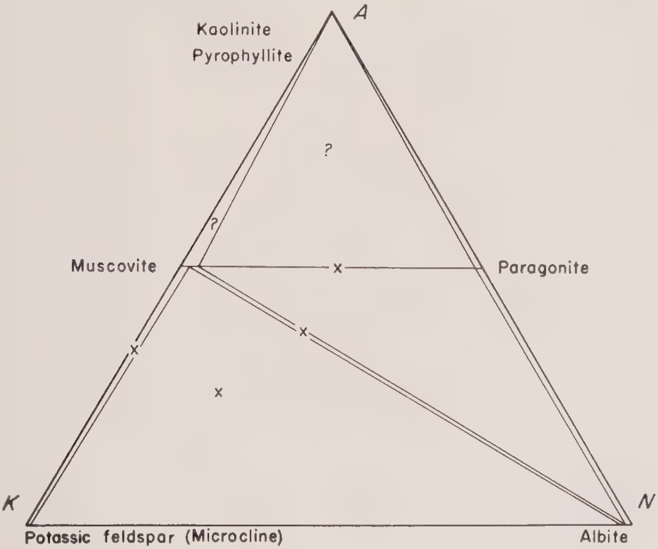

FIG. 3. The A-N-K diagram for rocks with free quartz and under particular values of the external conditions, appropriate to the Castleton region. Crosses indicate assemblages found in the Castleton area. If Dale's report of pyrophyllite is accepted, then one of the two assemblages marked with a question mark probably should be added. In this and in the ensuing diagrams, the position of all the phases are calculated according to the formula proportions of the oxide components.

In the Castleton area, the following mineral assemblages, appropriate to this diagram, have been found:

Muscovite-albite-potassic feldspar (at least in part microcline)
Muscovite-albite
Muscovite-paragonite

In addition, x-ray data on the slates of the Poultney River group indicate the muscovite-potassic feldspar assemblage, although due to interference by the muscovite pattern the presence of small amounts of albite in the samples cannot be disproved.

The muscovite-albite-potassic feldspar association defines a 3-phase field which under particular temperatures and pressures is invariant. The muscovite from the Bomoseen greywacke, which supplies this assemblage (at 1370′ level south of 1444′ knob near Walker Pond), has basal spacing of 10.00 ± 0.02 Å and so is virtually pure $KAl_2AlSi_3O_{10}(OH)_2$. Unfortunately, no good *x*-ray method exists for the determination of the Na/K ratio of low-temperature potassic feldspar; its amount in a specimen is commonly so low or the size of the grains so fine that no reliable refractive index can be measured. It seems certain, however, that the feldspars must be nearly pure potassic and sodic phases, without appreciable solid solution.

The muscovite-paragonite relations have been considered in an earlier section. The muscovite in coexistence with paragonite in the Castleton area has a basal spacing of 9.975 Å; between this muscovite and those with 10.00 Å basal spacing, therefore, must lie all muscovites in the 2-phase muscovite-albite field, the 3-phase muscovite-albite-potassic feldspar field, and the 2-phase muscovite-potassic feldspar field. The determined spacings from these assemblages are given in Table 3. The data are consistent except those from specimens 100-3, 648-1, and 1219-1. The last specimen, from the Bascom formation at Halls Island near Brandon (Cady and Zen, in press), is a rock of considerably higher metamorphic grade and so its muscovite spacing may not be comparable with the rest. The low values for the other two samples, however, are not readily explained.

Many slates exist which do not have an essential sodic phase. This does not necessarily mean that the rock has no sodium in it; rather if the amount is sufficiently small it is easily camouflaged in muscovite.

Although in Fig. 3 paragonite is shown to be stable, the lowest-grade metamorphic rocks from which it is known are phyllites; in the Castleton area these rocks are confined to the Taconic Range. No paragonite has been found in the true slates despite systematic search. While possibly due to inadequate sampling, this fact could, in view of the coexistence of kaolinite and albite in sedimentary rocks (see, for instance, Coombs, 1954, p. 81), be due to a reaction of the sort:

$$\text{albite} + \text{kaolinite} = \text{paragonite} + \text{quartz} + H_2O$$

$$NaAlSi_3O_8 + Al_2Si_2O_5(OH)_4 = NaAl_2AlSi_3O_{10}(OH)_2 + 2SiO_2 + H_2O$$

where the second, balanced equation would apply to stoichiometric phases only. The reaction to the right generates free H_2O (either vapor or liquid water), and suggests a net entropy gain; paragonite is on the high-grade side of the reaction.[2] Whether this hypothesis is correct, or whether the recorded occurrence of sodic illite or brammellite (Bannister, 1943) in certain sedimentary rocks bespeaks to the contrary, only additional petrographic data can settle.

On the other hand, under similar conditions microcline and kaolinite are probably unstable together and muscovite should exist instead. Careful petrographic work by Sand (1956) shows that a potassic mica always intervenes between kaolinite and potassic feldspar in weathering, although Coombs (1954, p. 81) reports kaolinite and potassic feldspar, both as pseudomorphs after analcite in the same specimen, in the altered Triassic sediments in New Zealand.

TABLE 3. BASAL SPACINGS OF MUSCOVITE IN VARIOUS ASSEMBLAGES IN THE A-N-K DIAGRAM

Specimen No.	Locality and Formation (See Appendix I)	d (001) muscovite, ±0.005A	Assemblage
100-3	South end of Graham Hill (Bull formation)	9.96	Quartz, *muscovite*, chlorite, *albite*
111-2	Southeast side of Zion Hill, above the cliff (Bull formation)	9.98	Quartz, *muscovite*, chlorite, *albite*
126-1	Southeast side of Sargent Hill (West Castleton formation)	9.98	*Muscovite*, *albite*, chlorite, quartz
137-2	960′ WSW of Eagle Rock, east of Beebe Pond (Poultney River group)	9.98	*Muscovite*, *albite*, *potassic feldspar*, chlorite, dolomite, quartz
182-1	Cut on Route 30, near Crystal Ledge (West Castleton formation)	9.98	*Muscovite*, *albite*, quartz, chlorite (?)
212-2	2000′, about 1000 feet east of Ben Slide (Biddie Knob formation)	9.975	*Muscovite*, *paragonite* (d (001) $=9.62(3)$), chlorite, quartz, rutile
213-1	1850′ in small ravine, 1500 feet east of Ben Slide (Biddie Knob formation)	9.98	*Muscovite*, *paragonite* (d(001) $=9.62$) chloritoid, chlorite, quartz, rutile
392-1-2	730′ knob, 0.6 mile SWof Butler Pond in Whipple Hollow (West Castleton formation (?))	9.99	*Muscovite*, *albite*, chlorite, quartz, rutile
648-1	1490′, 1.6 miles NNW of Biddie Knob (Bomoseen greywacke)	9.95	*Muscovite*, *microcline*, *albite*, chlorite, stilpnomelane, quartz
722-1	1170′, north of Eagle Rock near Beebe Pond (Poultney River group)	9.97	*Muscovite*, *potassic feldspar*, quartz
982-1	650′, east of Scotch Hill Road, 0.6 mile north of 424′ BM along the road (Poultney River group)	9.98	*Muscovite*, *albite*, *potassic feldspar*, dolomite, chlorite, quartz
1219-1	East side of Halls Island near Brandon (Bascom formation)	9.95	*Muscovite*, *microcline*, *plagioclase*, chlorite, biotite (?), calcite, quartz
1747-1	600′, east side of ridge due east of 424′ BM, Scotch Hill Road (Poultney River group)	9.98	*Muscovite*, *potassic feldspar*, *albite*, chlorite, hematite, quartz

The A-C-F(M) diagram. The A-C-F(M) diagram has, for its apices, CaO, FeO+MgO+MnO, and (Al_2O_3-Na_2O-$3K_2O$). It is thus analogous to the original A-C-F diagram of Eskola (1915), and presupposes the presence of all K in muscovite and all Na in albite. Thus constructed, the diagram suffers the disadvantage, namely possible incompatible phases such as kaolinite and albite are not automatically excluded, where assemblages with potassic feldspar are not included. On the other hand, if the diagram is properly projected from albite such that paragonite occupies the "A" corner, phases like chloritoid may become "inaccessible" to the diagram and more than one projection, from different essential sodic phases, would be necessary. Such a procedure would be justified, however, only with more petrographic data than are now available. The pseudo-projection is therefore used with the reservations stated above. The diagram is shown in Fig. 4, in which the chemical potentials of CO_2 and H_2O are supposed to be such that calcite and dolomite, as well as the hydrous silicates, are stable. Unfortunately, our knowledge of the phases along the A-C boundary of the diagram is very poor. Calcite is certainly found in many samples; a mineral of the epidote group is found in one sample in the phyllites of the Taconic Range and zoisite in the marbles of West Rutland; but no other phase is known.

---

[2] Although analcite and quartz are stable together under certain conditions (Coombs, 1954; Fenner, 1936; Milton and Eugster, 1959), analcite is not found in the Castleton area and will not be considered further.

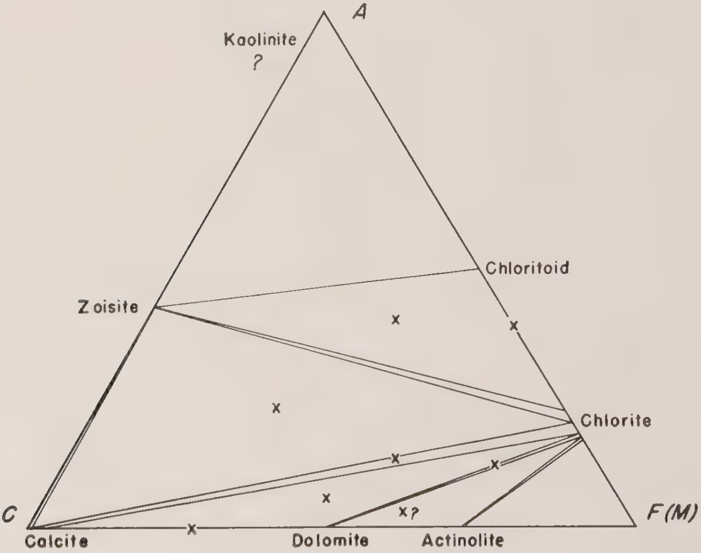

FIG. 4. The A-C-F(M) diagram for rocks with free quartz, under particular values of the external conditions appropriate to the Castleton area. Crosses indicate assemblages found in the Castleton area.

The mineral assemblages found in the Castleton area that belong to the diagram are as follows:

Chlorite-chloritoid-epidote[3]
Chlorite-calcite-dolomite
Chlorite-calcite
Dolomite-chlorite
Chlorite-chloritoid

In the adjacent marble belt of West Rutland, in addition, these associations are also found:

Calcite-chlorite-actinolite
Calcite-chlorite-zoisite

Since the "F(M)" corner is a superposition of at least two independent components, at least one more phase than shown on the diagram involving these components should be possible under arbitrary external conditions[4] without violating the Phase Rule. Unfortunately, *no* 4-phase assemblage belonging to this diagram has been found in the Castleton area and so the correct tie lines cannot be drawn.

In an earlier paper (Zen, 1959a) it was suggested that calcite and kaolinite could, under proper conditions, form a compatible pair in sediments and sedimentary rocks. The existence of zoisite rules out this pair, however, for rocks metamorphosed under conditions then prevailing in the West Rutland area. The formation of zoisite may be represented by the following reaction:

$$\text{calcite} + \text{kaolinite} = \text{zoisite} + CO_2 + H_2O$$
$$4CaCO_3 + 3Al_2Si_2O_5(OH)_4 = 2Ca_2Al_3Si_3O_{12}(OH) + 4CO_2 + 5H_2O,$$

the balanced equation being applicable if all the phases correspond to pure components. The reaction to the right entails a large increase in entropy due to the evolution of the volatiles, and (neglecting the volume of the volatiles) a volume decrease, so that this reaction is favored by increasing grade of metamorphism.

The assemblage calcite-dolomite-chlorite is a fairly common one in the Castleton area. From indices of refraction and x-ray data, the dolomite in coexistence with chlorite is sensibly free of iron, whereas the chlorite is relatively rich therein, as the following data for sample no. 102-2, from the south slope of Bull Hill, demonstrate:

Chlorite: $\beta = 1.630 \pm 0.003$ $\quad$ $Fe/(Fe + Mg) \approx 0.56$
Dolomite: $\omega = 1.862 \pm 0.002.$

---

[3] Although this mineral may be ferriferous, the rock contains hematite and therefore this mineral belongs to the present diagram. The possible complication due to manganese is not considered.

[4] By "external conditions" is meant the collection of such independent variables as temperature, total pressure, and the chemical potentials of the mobile components. These are all intensive variables.

Actinolite is another phase belonging to the A-C-F(M) diagram. This mineral was reported by Dale (1898, p. 191) to occur extensively in the pelitic "Berkshire schist" of the northern Taconic Range; in the present study, however, chloritoid instead of actinolite is found in these areas, including those specifically mentioned by Dale. This is clearly a case of misidentification under the microscope. The only verified occurrence of actinolite is in the autochthonous Ordovician marbles of the West Rutland marble belt, coexisting with chlorite and calcite, and without dolomite.

Bowen (1940) predicted that for the metamorphism of a purely magnesian dolomite in the presence of quartz, tremolite is the first phase to form, and marks the disappearance of dolomite. Although this fits the observed association, dolomite is known to depart from the ideal formula of $CaMg(CO_3)_2$ both in the Ca/Mg ratio and in taking ferrous iron into solution. The need for dolomite to disappear at the tremolite-actinolite isograd, then, is no longer true and actinolite and dolomite of different Fe/Mg ratios may coexist. Indeed, in adjacent beds in the West Rutland area the quartz-dolomite-calcite assemblage is very common.

Another point to be remembered is that calcite itself could dissolve $MgCO_3$ and $FeCO_3$. Thus even if the rock is not sufficiently (Mg, Fe) rich to form the phase dolomite, actinolite might still form with progressive metamorphism by the reaction of quartz with calcite. This, however, will occur always at a higher metamorphic grade than the reaction involving dolomite, since the chemical potential of Mg in a calcite must be lower than in a dolomite under the same physical conditions. On the other hand, the occurrence, near the actinolite marble, of dolomitic marbles suggests that this is not the mechanism by which actinolite is formed in the West Rutland area, provided of course that the effects of possible variations in the bulk Fe/Mg ratios in these rocks are negligible. The need for caution in interpreting the actinolite isograd, however, is evident.

The assemblages (1) calcite-dolomite-chlorite; (2) calcite-kaolinite-chlorite; (3) calcite-dolomite-kaolinite; and (4) dolomite-chlorite-kaolinite have all been reported from unmetamorphosed sediments and sedimentary rocks (Zen, 1959a). In the A-C-F-M tetrahedron, in fact, all four phases may coexist, in the presence of quartz, under arbitrary values of the external conditions. For a particular Fe/Mg ratio, however, only three of these phases will in general obtain; for these four phases are related by a reaction of the sort

$$\text{calcite} + \text{chlorite} + CO_2 = \text{dolomite} + \text{kaolinite} + \text{quartz} + H_2O,$$

with more carbon dioxide released per unit reaction to the left than H_2O

consumed. We might thus expect the calcite-chlorite side to be relatively more stable at higher metamorphic grades. Rocks are found in the Castleton area which show the calcite-chlorite assemblage, with the chlorite, a high-Mg variety (optically positive and colorless), ramifying through the rock and apparently a result of metamorphic reaction between a carbonate and some pre-existing aluminum-rich phase (see the section on carbonate). It is possible that the above reaction is the correct one, although no dolomite is found in the rock today.

The A-K-F-M tetrahedron. For the A-K-F-M tetrahedron, the following coordinates have been used for the apices: A = (Al_2O_3-K_2O-Na_2O); K = $KAlO_2$; F = FeO + MnO; M = MgO. This construction then corrects for the presence of albite when a rock analysis is plotted; however, due to the possible incompatibility of albite and pyrophyllite (or kaolinite), the "A" corner should, in some instances, be paragonite; the difficulties are the same as has been discussed under the A-C-F(M) diagram.

In practice, this difficulty can be circumvented. The nature and relative amounts of the normative sodic phases can be estimated by plotting the "A" corner both as given above and as (Al_2O_3-$3Na_2O$), corresponding to paragonite, and noticing the relative proportions of these two versions at which the plot of the rock composition crosses the muscovite-chlorite join. This procedure is justified since below this join stilpnomelane, biotite, or microcline is a stable phase, none of which has been found with paragonite; and above this join chloritoid is stable, which so far is not found with albite in the Castleton area.[5]

In order to simplify the problem of graphical representation, two pseudoternary projections of the A-K-F-M system will be discussed.

1. A-K-F(M) diagram. This is the standard diagram suggested by Eskola (1915), wherein FeO and MgO are represented at the same apex. The phases that appear in this diagram, for rocks of the Castleton area, are shown in Fig. 5.* Among these phases, biotite and stilpnomelane alone show compositional variations *in* the pseudoternary system. However, biotite has not been found in enough samples and in sufficient quantities to permit a study of its phase relations in the Castleton area. Stilpnomelane, on the other hand, occurs abundantly and must be considered in some detail.

The projection of the stilpnomelane composition onto the A-K-F(M) diagram remains problematic. Although the alkali and alkaline earth oxides in the chemical analyses of this mineral are dominantly potash, soda and lime do occur in variable amounts. In the section on the mineralogy of stilpnomelane it was seen that the best clustering of data results from assuming all the ferric iron as ferrous iron oxidized after the crystal had formed (although Shirozu's analysis clearly shows that this is not always true and some stilpnomelane has ferric iron playing the role of aluminum), and that generally the amount of calcium is so low that changing assumptions on its structural role affects the scatter of the plotted points but slightly. The hypothesis of total Fe as ferrous iron is therefore adopted, and on an A-K-F(M) projection all the analyses, whatever the role of Ca, loosely cluster below the biotite-chlorite join. Despite the higher SiO_2 content of stilpnomelane compared to chlorite and biotite, in the presence of quartz and albite, stilpnomelane may, to a good approximation, be taken as a phase on the A-K-F(M) diagram at approximately the indicated position.

---

[5] This procedure cannot be strictly correct since the muscovite-chlorite join is not a surface but a volume in the tetrahedron. This difference, however, will be overlooked.

* Note added in proof: Due to a drafting error, the chlorite-stilpomelane 2-phase field is shown to converge upon a fixed stilpomelane composition. In fact, stilpomelane in equilibrium with different chlorites should show different compositions also.

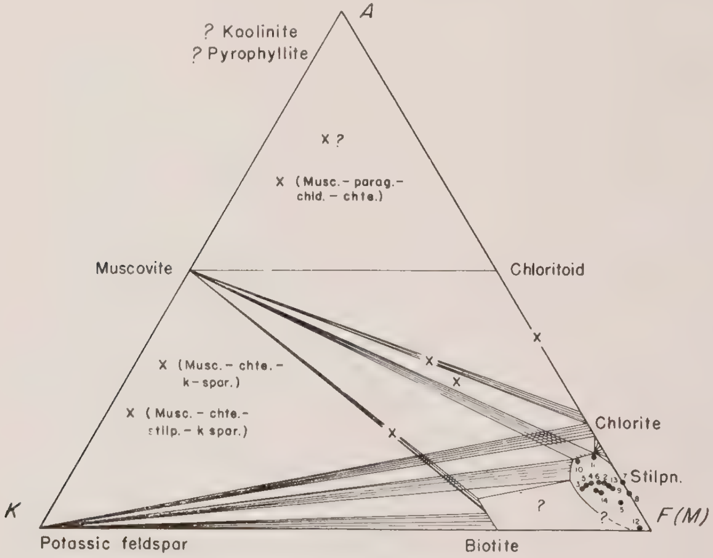

FIG. 5. The A-K-F(M) diagram for rocks with free quartz, under particular values of the external conditions, appropriate to the Castleton area. The numbers attached to the analyzed stilpnomelane have the same significance as in figure 1. Crosses indicate assemblages found in the Castleton area. Notice the apparent crossing of the tie-lines; this is due to the lumping of FeO and MgO as one component.

Since the "F(M)" corner is a superposition of two components, at least one additional phase (except along the A-K edge) may be expected in the diagram. Rocks from the Castleton area have yielded the following assemblages:

Muscovite-chlorite
Chlorite-chloritoid
Muscovite-chlorite-chloritoid
Muscovite-chlorite-potassic feldspar (in at least some cases definitely identified as microcline)
Muscovite-chlorite-stilpnomelane-potassic feldspar
Muscovite-biotite.

In addition, the assemblage muscovite-chlorite-dolomite-calcite is common among the two-carbonate marbles; when projected from calcite it properly belongs to the diagram. Since the assemblage muscovite-chlorite-potassic feldspar-stilpnomelane would exclude the association of muscovite and dolomite in the presence of calcite (provided that CO_2 does not act as an "inert" component), this might indicate that stilpnomelane does not truly belong to the diagram and calcium and/or ferric iron plays an essential role in its phase relations. That this is not always the case, however, is shown by the occurrence of hematite and calcite in a few stilpnomelane-bearing rocks; for these it must be reckoned as truly belonging to the A-K-F-M tetrahedron.

An alternative explanation is that stilpnomelane is stable with muscovite only at sufficiently high Fe/Mg ratios; at low ratios muscovite and dolomite become stable together instead. This idea is supported by the optically determined Fe/Mg ratio of stilpnomelane; in the Castleton area, also, the dolomite found with muscovite is always iron poor, judging by the index of refraction (see p. 155).

Mineral assemblages containing a potassic feldspar are rare in the Castleton area. These are found principally in the Bomoseen greywacke, associated with stilpnomelane; or in the Poultney River group and the Zion Hill quartzite, with muscovite, chlorite, and quartz. This scarcity of potassic feldspar is probably due to the fact that the bulk of the rocks have sufficiently high Al/alkali ratio so that muscovite is the stable potassic phase, rather than due to the intrinsic instability of potassic feldspar.

The muscovite-chlorite assemblage is a very common one in the slates of the Castleton area. Since the only other phases present in these rocks are quartz, albite, and rutile, four components, K_2O, Al_2O_3, FeO and MgO (ignoring any MnO that may be present) must be reckoned with. This suggests that for arbitrary values of the external conditions, the phases muscovite and chlorite must have a total of two independent means of compositional variation. One of these is accounted for by Fe-Mg substitution in chlorite; probably Al-Fe, Mg variation in chlorite accounts for the other degree of freedom.

As albite is known to coexist with muscovite and chlorite, without potassic feldspar, the chlorite apex, along the Al-Fe, Mg coordinate, of the albite-chlorite-paragonite 3-phase field must be at a higher Al/Fe, Mg ratio than the corresponding apex of the chlorite-muscovite-potassic feldspar 3-phase field.

2. The A-F-M diagram. The A-F-M diagram is constructed by projecting from muscovite which thus is assumed to be ubiquitously present (Thompson, 1957). The diagram thus constructed takes no account of calcic phases, and so is applicable only to calcium-free rocks, or to rocks in which no calcic phase involves the above components. The situation, where this is not valid, is complicated and data are very poor. Such rocks, luckily, are not important in the Castleton area.

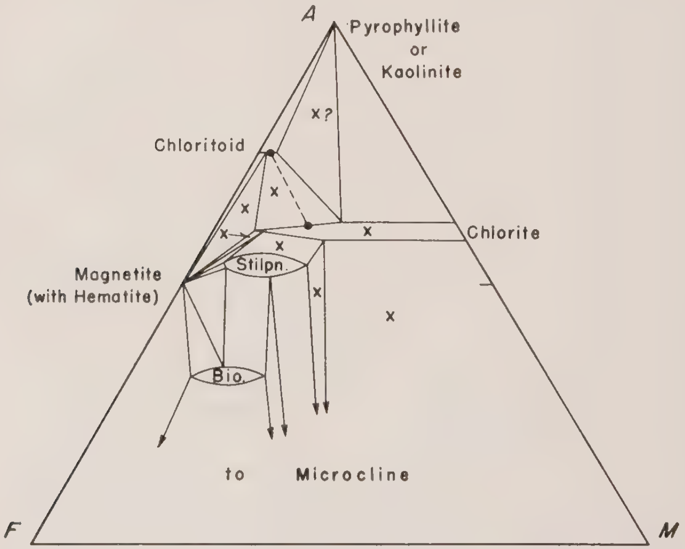

FIG. 6. The A-F-M diagram for rocks with free quartz and muscovite, under particular values of the external conditions, appropriate to the Castleton area. The diagram is a projection from muscovite composition in the A-K-F-M tetrahedron, according to the method of Thompson (1957). For rocks containing magnetite, an additional projection is made from hematite; this part of the diagram is thus strictly valid only where the rock contains both iron oxides. The lower portion of the diagram refers to rocks with negative values of "A"; it appears incomplete due to the method of projection. Crosses indicate assemblages found in the Castleton region. The dashed line from chlorite to chloritoid connects the analyzed chloritoid (no. 213-1A) with the calculated composition of the chlorite which is actually found in coexistence with the chloritoid. See text for details.

The diagram is given in Fig. 6, with quartz, muscovite, and a sodic phase to be added to those shown. Calcite or dolomite, but not both, may also be present. The lower side of the diagram is shown as unfinished; this is due to the geometry of the construction (Thompson, 1957). This fact does not, of course, preclude such assemblages as microcline-chlorite-stilpnomelane even on this projection; merely microcline is located at the unfinished lower boundary of the diagram.

The assemblages found in the Castleton area are listed below:

Chlorite-chloritoid
Chlorite-chloritoid-magnetite (ilmenite?), with hematite and rutile
Chlorite-stilphomelane
Chlorite-stilpnomelane-potassic feldspar (microcline in some samples)
Chlorite-potassic feldspar
Chlorite-magnetite
Chlorite
Biotite

If Dale's report of pyrophyllite from Ben Slide, in rocks now known to contain chloritoid and chlorite, is correct, another 3-phase assemblage would obtain.

It will be noticed that magnetite, and probably also stilpnomelane, contain ferric iron and therefore do not belong to this diagram. However, there exists stilpnomelane whose analysis shows virtually no ferric iron (Hutton, 1938, p. 184, 185); and as earlier discussed, the ferric iron in stilpnomelane may be due to later oxidation. As to magnetite, the one specimen that contains the indicated 3-phase assemblage also has hematite and rutile, and so even if the "magnetite" should turn out to be ilmenite (only a few specks exist and the amount was too small for specific identification), it still plots at the indicated position on the diagram. The diagram would then be a projection from rutile as well as from hematite.

On the other hand, large numbers of rocks from the Castleton area are without magnetite or indeed other phases appropriate to the "F" corner. Measured β of chlorites have not gone beyond 1.66, and with the exception of one specimen, beyond 1.64; the latter value corresponds to an Fe/(Fe+Mg) value of about 0.66. Thus the nature of the phase for the "F" corner of the diagram, in equilibrium with quartz and muscovite, remains in doubt. It might be iron-biotite, iron-chlorite, or an oxide; minnesotaite is unlikely with muscovite, as chlorite and potassic feldspar is a more probable alternative. Nor has any almandite been found in the Castleton area; this is presumably due to the low metamorphic grade.

The association of chlorite and chloritoid is a very common one in the Castleton region. One analysis of chloritoid was presented in Table 1; from this and the analysis of the rock the calculated approximate chlorite composition is given in Table 2. The values of β of chlorite from other, similar assemblages are given in Table 4, together with the estimated Fe/(Fe+Mg) ratios; the data indicate that chloritoid is always more ferroferrous than the coexisting chlorite.

TABLE 4. β-INDEX OF COEXISTENT CHLORITE AND CHLORITOID

Specimen number	β of chlorite, Na light, ± 0.002	Est. Fe/(Fe+Mg) atomic*	β of chloritoid, Na light, ± 0.002	Additional phases
6-3	1.630	0.56	1.718	Muscovite, quartz (G)
14-1	1.633	0.59	1.715	Muscovite, hematite, quartz (P)
19-1	1.632	0.58		P
24-1	1.635	0.61	1.718	G
25-2	1.634	0.59		P
36-1	1.634	0.59	1.72	G
43-1	1.640	0.66		G
55-1	1.630	0.56	1.722	G
213-1	1.642	0.67 0.62‡	1.722†	Muscovite, paragonite, quartz, rutile
217-1	1.628	0.54	1.72	Muscovite, paragonite, quartz, rutile
228-1-2	1.635	0.61		P
228-2	1.631	0.57		G
253-1	1.633	0.59	1.721	P
253-2	1.634	0.59		G
262-1	1.633	0.59		P
262-1	1.628	0.54	1.720	G
314-1-3	1.634	0.59		P
393-3	1.640	0.66	1.72	P
393-6	1.636	0.62	1.720	G
440-1	1.630	0.56		G
441-1	1.629	0.55		P
453-1	1.628	0.54	1.725	G
698-1	1.634	0.59		Muscovite, paragonite, quartz
726-1	2.638	0.64	1.720	G
726-2	>1.66§	>0.84	1.721	P
751-1	1.633	0.59		G

* Using Winchell and Winchell (1951, p. 385) and "$\frac{1}{3}$ substitution" formula.

† $(Fe+Mn)/(Fe+Mn+Mg) \approx 0.92$. See Table 1.

‡ According to normative calculation from rock analysis, assuming the "$\frac{1}{3}$ substitution" formula. See Table 2.

§ On one grain only. Data poor due to rarity of chlorite in the sample.

The chlorite-chloritoid 2-phase region is bounded on the two sides by two 3-phase regions. Unfortunately, no data on these 3-phase fields exist to set limits to the 2-phase region, nor the rate of movement of the limiting boundaries with metamorphic grade. The lowest grade rock containing the chlorite-chloritoid association (plus hematite, quartz, and muscovite), from near Lake Bomoseen, gives, on one grain of chlorite, $\beta > 1.66$, or an $Fe/(Fe+Mg)$ ratio >0.84; this suggests that the 2-phase field may approach the pure iron end. At the high Mg side, a minimum estimate of the extension of the 2-phase field may be gotten by the index of refraction of the chlorite from this association, assuming that the lowest value of β for chlorite corresponds to the highest Mg content. The lowest value from table 4, 1.628 ± 0.002, corresponds to an Fe/(Fe+Mg) ratio of about 0.53, using the chart in Winchell and Winchell (1951) and assuming the "$\frac{1}{3}$ substitution" formula. The specimens, no. 262-1 and 453-1, respectively, came from 1630′ elevation on the southwest slope of Biddie Knob, and in the mountain brook at its crossing with Belgo Road, south of Grandpa Knob. Comparison with the index of 1.66 shows that the chlorite-chloritoid 2-phase field is fairly wide along the Fe-Mg coordinate for the Castleton area as a whole, although at any given locality this width may be considerably more restricted.

At the high Mg side of this 2-phase region, the limit being the 3-phase field chlorite-chloritoid-kaolinite or chlorite-chloritoid-pyrophyllite, the shift in the boundary with metamorphism may be given by the reactions

$$\text{kaolinite} + \text{chlorite} = \text{chloritoid} + \text{quartz} + H_2O$$

or

$$\text{pyrophyllite} + \text{chlorite} = \text{chloritoid} + \text{quartz} + H_2O.$$

The reactions to the right represent large entropy increases and net dehydration, as well as net volume decreases (ignoring the volatiles); thus they are favored by rising metamorphic grade. With rising grade, then, the chlorite-chloritoid-kaolinite (or pyrophyllite) 3-phase field will move to the high Mg side. This agrees with Hietanen's data (1951, p. 862, 867) from the Wissahickon schist, which is of higher metamorphic grade than the present slates. Hietanen's rock gives the mineral assemblages: albite-chlorite-chloritoid-muscovite, and the chloritoid analysis gives an Fe/(Fe+Mg) ratio of about 0.76. Assuming that all K occurs in muscovite and Na in albite, the normative chlorite calculated from the rock analysis gives for this same ratio a value of about 0.3.

The next 3-phase field shown on the diagram, chlorite-chloritoid-magnetite, cannot be discussed now because of insufficient data. Similarly, doubt exists as to the reality, in the Castleton region, of the 3-phase field magnetite-chlorite-stilpnomelane.

The association of chlorite and stilpnomelane is a fairly common one, albeit limited geologically to the Bomoseen greywacke. Accurate indices of refraction are difficult to obtain because of the fine grain size; correlation of indices of stilpnomelane with composition is uncertain due to lack of regression equations. One pair that has been measured, however, gives the following data:

Stilpnomelane: 2V(−) small; fast ray normal to cleavage.
Pleochroic, X = pale golden yellow
Y and Z = dark olive brown
$\beta = \gamma = 1.700 \pm 0.005$ (Na light)
Chlorite: $\beta = 1.648 \pm 0.003$.

Thus the stilpnomelane is probably more Fe rich than the coexisting chlorite. If Fe and Mg approximate ideal solution behaviors in both phases, this property may be expected to hold through the entire composition range over which the pair is stable.

Stilpnomelane-bearing rocks are of interest also in that these are among the few types in the Castleton area wherein a potassic feldspar occurs. Stilpnomelane, thus, might be regarded as the counterpart of chloritoid in low-Al rocks.

The assemblage of potassic feldspar and chlorite, with quartz and muscovite, is found in a few specimens of the Poultney River group argillites of Ordovician age, as well as in the Zion Hill quartzite. These, as well as those with stilpnomelane, are in fact the only instances of potassic feldspar in the area. From Fig. 6 it is seen that chlorite in coexistence with potassic feldspar may be expected to show the highest Fe, Mg-Al ratio in the presence of muscovite; however, chlorite-potassic feldspar assemblage without muscovite may give even higher ratios (see Fig. 5).

Many rocks in the Castleton area carry only muscovite, chlorite, and quartz, in addition to rutile, as detectable phases. As pointed out before, the frequency of such an assemblage suggests that it is not due to chance occurrence of proper bulk compositions but due to Al/(Fe+Mg) and Al/Si variabilities of such values as to remain in equilibrium with quartz (more formally,

$$\sum_{k} \frac{\partial \mu_{\mathrm{Si}}}{\partial \mathrm{N}_{k \neq \mathrm{Si}}} \Delta \mathrm{N}_{\mathrm{k}} = 0$$

for a given set of external conditions, where μ_k is the chemical potential of component k and N_k its mole fraction), in addition to a variable Fe/(Fe+Mg) ratio in chlorite. On the A-F-M diagram, therefore, chlorite is shown as a region rather than a line; the variable Si content is not shown, but its chemical potential is fixed by that in quartz.

Difficulties are introduced in the treatment of the A-F-M diagram through uncertainties in the status of ferric iron. Since Fe''' and Fe'' may be related by an equation involving oxygen,

$$2\mathrm{FeO} + \tfrac{1}{2}\mathrm{O}_2 = \mathrm{Fe}_2\mathrm{O}_3,$$

they must be regarded as two independent components *if* oxygen were an inert component and is not counted as one itself. If, however, the chemical potential of oxygen is controlled by external conditions, it is mobile and Fe''' and Fe'' are to be regarded as a single independent component (Thompson, 1955, p. 81). Hematite, in this latter case, would plot on the A-F-M diagram and count toward 3-phase assemblages there.

If phases like magnetite and hematite coexist commonly in a given area, this fact would constitute powerful argument for regarding oxygen as inert, for an externally controlled value of μ_{O_2} would, in general, not correspond to the buffered μ_{O_2} value of the hematite-magnetite pair. On the other hand, to have only one of these phases, in particular hematite, could be due either to mobile oxygen or to excess oxygen.

In the Castleton area, hematite is the most common iron oxide phase and generally occurs without magnetite. Though suggestive of mobile oxygen, thus, the evidence is far from conclusive. Accordingly, indices of refraction of chlorite from the chloritoid-chlorite-hematite assemblage (purple) and *adjacent* (the distance varying, generally, from a few inches to a few feet) chloritoid-chlorite (green) assemblage were measured, as chlorite with hematite should be more Fe rich if hematite belongs to the A-F-M diagram, but not necessarily so otherwise. The results are given in Table 5. Although suggestive of a systematic variation with association, the data are not definite.

Recent studies of the iron formations of the Great Lakes region (James and Howland, 1955) show that for these rocks the mineralogy of the iron oxides indicates inertness of oxygen during metamorphism (Thompson, 1957, p. 855). Without further evidence to the contrary, this is the hypothesis tentatively adopted for rocks of the Castleton area.

Finally, the trace of the paragonite-albite boundary on the A-F-M diagram will be considered. Since both phases are known to coexist with chlorite, this trace must cross the chlorite field. In the presence of muscovite and quartz and under given external conditions, moreover, the system is univariant (four components and three phases) and so the trace may traverse the chlorite field in some arbitrary manner. Albite alone is found with stilpnomelane, and paragonite alone, to date, is found with chloritoid. Thus although the chlorite-stilpnomelane and chlorite-chloritoid 2-phase fields constitute limits between which the paragonite-albite boundary trace must lie in the Castleton area, nothing more definite can be said.

In the Wissahickon schist of Maryland, Hietanen (1941, p. 146; 1951, p. 862) reported the albite-chloritoid pair. The reaction

$$\text{paragonite} + \text{chlorite} + \text{quartz} = \text{albite} + \text{chloritoid} + H_2O$$

goes to the right with increasing metamorphic grade and so Hietanen's data from rocks of higher grade than those of Castleton are consistent with predictions. This also agrees with the higher Mg content in Hietanen's analyzed chloritoid. It should be noted that the system chloritoid-chlorite-paragonite-albite is invariant under specified external conditions and so the trace of the paragonite-albite field boundary must follow one of the chloritoid-chlorite tie lines. For this reason also, this boundary will always "jump" 3-phase fields on the A-F-M diagram. In general, with

TABLE 5. β-INDEX OF CHLORITE IN GREEN VS. PURPLE SLATES FROM THE SAME LOCALITY

Specimen number	Locality (See Appendix I)	Assemblage	β, ± 0.002 (Na light)	$Fe/(Fe+Mg)$*
14-1	1650′ terrace, south of Biddie Knob	Chlorite, chloritoid, muscovite, hematite, quartz (P, purple)	1.633	0.59
217-1	1450′ in trail SSW of Biddie Knob, W of crest of Taconic Range	Chloritoid, chlorite, muscovite, paragonite, quartz, rutile (green)	1.628	0.54
262-1	1580′, WSW slope of Biddie Knob	Chloritoid, chlorite, muscovite, quartz, rutile (G, green)	1.628	0.54
262-1	Same specimen	P	1.633	0.59
6-3	1200′, pasture due west of Biddie Knob	G	1.630	0.56
253-2	1130′, same pasture	G	1.634	0.59
253-1	Same	P	1.633	0.59
228-1-2	990′, S. of Giddings Brook, just S. of 971′ road junction, N. of Sargent Hill	P	1.635	0.61
228-2	960′ in Giddings Brook, same locality	G	1.631	0.57
751-1	700′ in Giddings Brook	G	1.633	0.59
698-1	910′ in pasture S. of Giddings Brook, ⅛ mile NE of 1010′ knob just S. of Monument Hill Road	G	1.634	0.59
726-1	540′, due W. of 800′ knob just southeast of the village of Hubbardton	G	1.638	0.64
726-1	Same locality	P	>1.66†	>0.84
440-1	Small knob north of Castleton River, ½ mile SW of 1918′ knob, 5 miles east of Castleton	G	1.630	0.56
441-1	1405′ knob 200 feet south of last locality	P	1.629	0.55
393-6	1800′, west slide, Ben Slide	G	1.636	0.62
393-3	Same locality	P	1.640	0.66

* Using Winchell and Winchell (1951, p. 385) and "⅓ substitution" formula.

† On one grain only. Data poor due to rarity of chlorite in the sample.

increase in metamorphic grade the trace of the paragonite-albite boundary on the A-F-M diagram moves towards the "A" corner, and the field of albite expands at the expense of the field of paragonite.

EVIDENCE FOR PHASE EQUILIBRIUM

The foregoing discussions of mineral reactions in the rocks of the Castleton areas, based on phase diagrams derived ultimately on thermodynamic principles, assume chemical equilibrium among the phases under the physical and chemical conditions of metamorphism. It is necessary, therefore, to present evidence that such equilibrium is indeed attained in the rocks.

One of the most powerful criteria for chemical equilibrium in any system is its obedience to Gibbs' Phase Rule. Obedience of this Rule is a necessary, though not a sufficient, condition for equilibrium. The test consists simply of counting the number of components and phases, such that

$$\phi \leq c + 2$$

where ϕ is the number of phases and c the number of independent components; if mobile components obtain, of which there are c' in number,

$$\phi' \leq c + 2 - c'$$

(Thompson, 1955, p. 81). For arbitrary values of temperature and hydrostatic pressure, a condition applicable to a randomly chosen sample, we have

$$\phi' \leq c - c'.$$

In rocks of the Castleton region, even assuming H_2O and CO_2 to be mobile components, this restricted version of the Phase Rule is never violated.

Even so, however, a rock may be out of chemical equilibrium if phases, empirically determined to be mutually incompatible, are found together. Such incompatibility would be demonstrated if, for example, two phases striding the composition of some intermediate phase, known to be stable, are found together. In the presence of quartz, this might be, for instance, microcline and pyrophyllite instead of microcline-muscovite or muscovite-pyrophyllite. Such incompatible phases are not found together in the Castleton area.

In many purple and red slates, there are thin beds of pyritic quartzite or of limestone, as well as pebbles of limestone in a slaty matrix. In all instances, except where the limestone itself is salmon-colored and carries hematite, there is a layer, though possibly an extremely thin one, of green slate between the two lithologies. This relation is so consistent as to suggest some incompatible relation between some phases of the two rock types. The nearly ubiquitous presence of rims like this implies the existence of chemical reaction among the minerals, and at least locally the attainment of equilibrium.

The argument for phase equilibrium would be more persuasive if it can be demonstrated that the phase relations depicted in the previous diagrams are obeyed *in detail.* For example, consider the relative Fe/(Fe+Mg) ratio in the chlorite-chloritoid 2-phase field vs. the Na/(Na+K) ratio in the albite-muscovite-microcline 3-phase field. If equilibrium obtains, adjacent rocks of presumably identical metamorphic grade should show variation in the ratio of the 2-phase assemblage corresponding to bulk compositional variations, but invariant ratios for phases in the 3-phase assemblage. At the same time, adjacent beds should show different phase assemblages corresponding to appropriate bulk compositional differences. Unfortunately, lack of sufficiently coarse mineral grains suitable for chemical analysis greatly hampers the use of the test. Moreover, refractive indices of chlorite and especially of chloritoid, even if correlated directly with Fe/(Fe+Mg) ratios, show rather narrow ranges of variation and cannot be used confidently to check, for instance, if the 2-phase compositional tie lines "cross" from one sample to another, thus suggesting possible disequilibrium. Finally, there are relatively few 3-phase assemblages in the rocks for such a study.

On the other hand, there is no evidence to refute the idea of equilibrium, and the mineral associations observed do "make sense." Thus one of the few associations of potassic feldspar found, in the Bomoseen greywacke, is with stilpnomelane and albite -where (for example, near Brandon Mountain Road) nearby on *both sides* of this rock unit the Biddie Knob formation carries no feldspar but does carry chloritoid and locally paragonite. This is clearly a case of mineralogical variation due to bulk composition; such consistent results are not to be expected from chance collection of detrital material.

The compositional arguments of phase equilibrium may be supplemented by textural data. Clearly, porphyroblasts in a rock demonstrate recrystallization during metamorphism and thus probably in equilibrium with its surroundings during some stage. Feldspar, mainly untwinned albite, and chloritoid porphyroblasts are abundant in the Castleton area. Recrystallized limestone and dolomite, as well as minerals in fracture and boudinage fillings, again testify to mineralogical and textural response to metamorphism and involve chemical reconstitution.

The platy minerals also show definite evidence of recrystallization. Microporphyroblasts of chlorite and of muscovite, or intergrowth of these two, on the order of 0.1 mm. across, or of either of these with chloritoid, are extremely common in the slate. These crystals are randomly oriented but generally cut across the slaty cleavage as well as lying within the cleavage surface. The orientations are also random with respect to the bedding, where this is visible. Compositionally, there is no measurable difference between the porphyroblastic chlorite and chlorite in the groundmass and suggests that all the crystals are recrystallized, the difference in size being controlled by growth rate or surface tension.

Stilpnomelane in the Bomoseen greywacke tends to be extremely fine-grained, on the order of 20μ; these are thin books which commonly wrap around larger grains of quartz and feldspar, as well as occurring in sheaves. Such textures are unlikely due to primary sedimentation and/or deformation alone and probably result from recrystallization.

Some phyllites from the Taconic Range show segregation of the platy minerals and quartz into distinct bands on a microscopic scale. The platy minerals show parallel orientation with the basal planes in the plane of foliation. The quartz grains show roughly rectangular outlines in thin sections, with two edges parallel to the foliation. Such a geometric relation cannot be altogether primary and must be due to recrystallization with approach to textural equilibrium. Chemical readjustment clearly also took place, with chances of attainment of equilibrium.

Summary and Conclusions

Perhaps the single most important conclusion to be drawn from the present investigation is the fact that rocks at the lower end of the metamorphic spectrum are amenable to phase-equilibrium studies. With the aid of modern x-ray techniques, the mineralogy of even the slates can generally be ascertained to a fair degree; the grain sizes are not so small as to bring in uncertainties due to poor crystal quality, as is commonly the case with sediments. What data the x-ray method fails to furnish can commonly, though not always, be furnished by microscopic examinations; among these are textural information on the rocks.

Not only is the mineralogy of a rock determinable, but the results can be analyzed in terms of phase diagrams. The relation among the various minerals and mineral assemblages can be understood and can be compared directly with similar results from rocks of higher metamorphic grades. Despite the fact that an observed mineral assemblage generally comprises too many independent components to make possible a complete graphical representation of the phase relations, it has been found possible, by and large, to eliminate enough of them by proper projections, so that only three or four of these appear in any one diagram and so can be graphically shown. The limitations imposed by these simplifying assumptions do not vitiate their usefulness.

The second conclusion that might be drawn concerns the existence and nature of isograds in the low-grade argillites. Chloritoid seems to be one of the best isograd-indicators; indeed it was used by Balk (1953) south of the present area. In the present area, this mineral is confined to east of Lake Bomoseen, and is most widespread in the lustrous, relatively coarse-grained phyllites of the Taconic Range. However, the fact that this mineral is not found in *all* pelites east of its first appearance, but is confined to a stratigraphically mappable unit, bespeaks the importance of the bulk composition in its existence, for a given set of conditions. Thus its non-existence in the western part of the area might be due as much to rock composition as to lack of the proper physical environment.

Stilpnomelane has been found throughout the area regardless of the metamorphic grade; if a lower isograd exists for it, this must occur in rocks of even lower grade. For the same reason, little can be said at the moment of the biotite isograd.

Chlorite is found throughout the area and no isograd exists for this phase. Recent studies of sediments and sedimentary rocks show that this is one of the commonest ferromagnesian phases and it is questionable whether chlorite, as a phase, has any lower stability limit at all within the accessible part of the earth's surface.

A third general conclusion that might be drawn is the essential simplicity of the mineral assemblages. With few exceptions, the minerals are well-known, and they occur in combinations each of which includes a small number of phases. This indicates, first, that the systems are in mutual equilibrium, for it is not likely that a chance collection of detrital grains will give such ordered simplicity; second, that many of the phases must have solid solubility along one or more compositional coordinates, to rather extensive degrees. This is in fact borne out by the mineralogical studies. Finally, the mineralogical compositions of the rocks are quite consistent with those of higher metamorphic grades and there is no evidence for breaks in the nature of the metamorphism at lower grades nor any unusual trends.

A fact of some interest is that chloritoid and stilpnomelane are found in the same metamorphic belt. Both minerals have been commonly reported from areas of low grade metamorphism —however, as a rule, from different areas. In the Castleton area, the stilpnomelane-bearing Bomoseen greywacke occurs not only side by side, but repeatedly interfolded, with the chloritoid-bearing Biddie Knob formation (Zen, 1959*b*). The physical conditions of metamorphism could not have been very different, and the existence of these two phases must be controlled by chemical compositions of the rocks. As has been indicated earlier, this is borne out by their respective mineral assemblages.

The discussions also make clear the fact that our information on the low-grade metamorphism of argillaceous sediments is far from adequate; much more data are needed, from this general area as well as from other regions, before many questions can be answered. For example, many mineral assemblages have been predicted by the diagrams but are not yet observed. The projection of the paragonite-albite transition on the A-F-M diagram is only partly defined. The phase occupying the "A" corner of the diagrams in the presence of quartz is not certain. The role of stilpnomelane on the A-F-M diagram, if it belongs there at all, is far from fully understood. We need more information to check if paragonite has a lower limit of stability, giving way to kaolinite and albite. The whole problem of the A-F-M projection for calcareous rocks has been sidestepped for lack of data. Few of the "3-phase assemblages" in the pseudoternary projections have had their apices pinned down and their rates of change with progressive metamorphism delimited. Finally, the part played by redox reactions in the mineral assemblages remains obscure, *i.e.*, we do not know for sure what is the best way to treat oxygen as a component, whether as a mobile component, and therefore treating ferric phases as if they were ferrous phases in the A-F-M diagram, or as an inert component, so that ferric and ferrous iron must be regarded as independent components. Although present indications are in favor of the latter, the situation is by no means unequivocal.

APPENDIX I. LOCATION OF GEOGRAPHICAL NAMES MENTIONED IN THE TEXT

(All locations given to the nearest 1′ of latitude and longitude. Names in parentheses refer to names of U. S. Geological Survey topographic sheets.)

Name	*Longitude* (73° W+)	*Latitude* (43° N+)
Beebe Pond (Bomoseen)	11′	44′
Belgo Road (Bomoseen; Proctor)	06′–08′	38′
Ben Slide (north side of 2390′ knob) (Castleton)	06′	34′
Benson (Benson)	19′	42′
Bird Mountain (Castleton)	07′	35′
Brandon (Brandon)	06′	48′
Brandon Mountain Road (Bomoseen)	08′	44′
Biddie Knob (Proctor)	06′	43′
Bull Hill (Bomoseen)	11′	38′
Butler Pond (Proctor)	05′	42′
Castleton (Castleton)	10′	37′
Castleton River (Castleton; Thorn Hill)	04′–17′	36′
Clark Hill (Castleton)	04′	34′
Crystal Ledge (780′ knob) (Bomoseen)	11′	39′
Eagle Rock (Bomoseen)	11′	44′
Giddings Brook (Bomoseen)	08′–11′	42′–43′
Glen Lake (Bomoseen)	14′	40′
Graham Hill (Castleton)	11′	37′
Grandpa Knob (Proctor)	06′	40′
Gully Brook (Castleton)	08′	36′
Halls Island (Brandon; Sudbury)	07′	47′
Herrick Mountain (Castleton)	06′	33′
Hubbardton (Bomoseen)	11′	42′
Lake Bomoseen (Bomoseen; Castleton)	11′–14′	36′–42′
Mill Pond (Benson)	17′	42′
Monument Hill Road (Bomoseen)	10′	43′
Sargent Hill (Bomoseen)	09′	43′

Scotch Hill Road, 424′ Benchmark (Bomoseen)	15′	38′
Taconic Range (Castleton; Bomoseen; Proctor; Sudbury)	05′–10′	37′–47′
Walker Pond (Bomoseen)	08′	44′
West Rutland (Castleton)	03′	36′
Whipple Hollow (Proctor)	04′–05′	36′–42′
Zion Hill (Bomoseen)	09′	41′
1405′ knob north of Castleton River (Castleton)	07′	37′
1930′ knob west of Clark Hill (Castleton)	05′	35′
2035′ knob (Proctor)	07′	41′

APPENDIX II. LOCATION OF SPECIMENS MENTIONED IN THE TEXT

(Names in parentheses refer to names of the formations)

6-3	1100′ in pasture 1.0 mile northwest of Biddie Knob, near 1007′ benchmark (green; Biddie Knob)
14-1	1650′ on terrace 0.3 mile due south of Biddie Knob (purple; Biddie Knob)
19-1	1300′, east slope of 1630′ peak at the north end of Bird Mountain (purple; Biddie Knob)
24-1	1750′, north of topographic saddle, 1.2 miles north-northeast of Herrick Mountain (green; Biddie Knob)
25-2	760′ in major north-flowing brook east of Bird Mountain (purple; Biddie Knob)
29-4-1	1400′ on the west slope of Clark Hill (purple; Biddie Knob)
36-1	1630′ knob 0.6 mile east of Grandpa Knob (green; Biddie Knob)
43-1	620′ in Gully Brook, at junction with tributary from the west (green; Biddie Knob)
55-1	1240′ on ridge, 0.6 mile northwest of 635′ road corner 1.3 miles northeast of Biddie Knob (green; Biddie Knob)
100-3	480′, 0.2 mile south-southwest of Graham Hill (green; Mettawee slate, Bull)
102-2	600′, 0.7 mile south-southwest of 905′ top of Bull Hill (green reaction rim between purple Mettawee slate and dolomitic nodule)
111-2	1010′ knob due west of 816′ benchmark east of Zion Hill (green; Mettawee slate, Bull)
126-1	1250′, about 0.2 mile south of 1360′ knob of Sargent Hill (West Castleton)
137-2	960′ west-southwest of Eagle Rock, east of Beebe Pond (black slate; Poultney River group)
182-1	Cut on Route 30, west of Crystal Ledge (West Castleton)
197-2	720′, 0.2 mile south-southeast of top of Crystal Ledge (green; Mettawee slate, Bull)
212-2	2000′, 1000′ east of Ben Slide, S75°W from 1930′ knob west of Clark Hill (green; Biddie Knob)
213-1	1850′, in northeast-trending ravine 1500′ east of Ben Slide (green; Biddie Knob)
228-1	990′, south of Giddings Brook, just south of 971′ road junction, north of Sargent Hill (purple; Biddie Knob)
228-2	960′ in Giddings Brook, same locality (green; Biddie Knob)
233-1-2	1270′, 0.2 mile southeast of 1360′ knob of Sargent Hill (green; Mettawee slate, Bull)
253-1	1130′, in pasture 0.9 mile northwest of Biddie Knob, near 1007′ benchmark (purple; Biddie Knob)
253-2	same locality (green; Biddie Knob)
262-1	1580′ on west-southwest slope of Biddie Knob (purple and green; Biddie Knob)

314-1	1990′ knob in Taconic Range, 0.5 mile south-southeast of 2035′ knob (purple) Biddie Knob)
392-1	730′ prominence, 0.6 mile S69°W of 661′ benchmark near Butler Pond (West Castleton?)
393-3	1800′, west slide, Ben Slide (purple; Biddie Knob)
393-6	same locality (green; Biddie Knob)
440-1	small knob 200′ north of 1405′ knob north of Castleton River (green; Biddie Knob)
441-1	1405′ knob north of Castleton River (purple; Biddie Knob)
453-1	860′ in brook just south of Belgo Road (green; Biddie Knob?)
648-1	1490′ on small terrace 1.6 mile N22°W of Biddie Knob (Bomoseen)
698-1	910′ in pasture south of Giddings Brook, $\frac{1}{8}$ mile northeast of 1010′ sharp knob just south of Monument Hill Road (green; Biddie Knob)
722-1	1170′, north of Eagle Rock near Beebe Pond (black slate; Poultney River group)
726-1	540′ due west and on slope of 800′ knob just southeast of the village of Hubbardton (green; Biddie Knob)
726-2	same locality (purple; Biddie Knob)
751-1	700′ in Giddings Brook (green; Biddie Knob)
982-1	650′, east of Scotch Hill Road 0.6 mile north of 424′ benchmark along the road (green slate; Poultney River group)
1219-1	470′ knob at east end of Halls Island (Bascom)
1747-1	600′, east side of ridge, due east of 424′ benchmark, Scotch Hill Road (purple slate; Poultney River group)

References

Agron, S. L. (1950), Structure and petrology of the Peach Bottom slate, Pennsylvania and Maryland, and its environment. *Geol. Soc. America Bull.* **61,** 1265–1306.

Albee, A. L. (1957a), Geology of the Hyde Park Quadrangle, Vermont. Harvard University Thesis. 139 p.

——— (1957b), Bedrock geology of the Hyde Park Quadrangle, Vermont. *U. S. Geol. Survey Map* **GQ 102**.

Balk, R. (1953), Structure of greywacke areas and Taconic Range, east of Troy, New York. *Geol. Soc. America Bull.* **64,** 811–864.

Bannister, F. H. (1943), Brammallite (soda illite), a new mineral from Llandebie, South Wales. *Mineralog. Mag.* **26,** 304–307.

Bowen, N. L. (1940), Progressive metamorphism of siliceous limestone and dolomite. *Jour. Geol.* **48,** 225–274.

Bradley, W. F. (1954), *X*-ray diffraction criteria for the characterization of chloritic material in sediments. *In* Clay and clay minerals, Publ. **327,** *Nat. Acad. Sci. and Nat. Res. Council.* 324–334.

Brindley, G. W., ed. (1951), *X*-ray identification and crystal structures of clay minerals. Mineralogical Society, London. 345 p.

——— and Gillery, F. H. (1956), *X*-ray identification of chlorite species. *Am. Mineral.*, **41,** 169–186.

Cady, W. M., and Zen, E. (in press), Stratigraphic relationships of the Lower Ordovician Chipman formation in western Vermont. *Amer. Jour. Sci.*

Chayes, F. (1952), Notes on the staining of potash feldspar with sodium cobaltinitrite in thin section. *Am. Mineral.*, **37,** 337–340.

Coombs, D. S. (1954), The nature and alteration of some Triassic sediments from Southland, New Zealand. *Royal Soc. New Zealand Trans.*, **82,** 65–109.

Dale, T. N. (1898), The slate belt of eastern New York and western Vermont. *U. S. Geol. Survey Ann. Rept.* **19,** Part 3. 163–307.

——— (1900), A study of Bird Mountain, Vermont. *U. S. Geol. Survey Ann. Rept.* **20,** Part 2. 15–23.

Dietrich, R. V. (1956), Trigonal paragonite from Campbell and Franklin counties, Virginia. *Am. Mineral.*, **41,** 940–942.

Eskola, P. (1915), On the relation between chemical and mineralogical composition in the metamorphic rocks of the Orijärvi region. *Comm. Géol. Finlande, Bull.* no. **44,** 145 p.

Eugster, H. P., and Yoder, H. S., Jr. (1955), Paragonite. *In* Ann. Rept. Director of the Geophysical Lab., *Carnegie Inst. Wash. Yearbook* no. **54,** 124.

Fenner, C. N. (1936), Bore-hole investigations in Yellowstone Park. *Jour. Geology,* **44,** 225–315.

Grunner, J. W. (1944), The structure of stilpnomelane reëxamined. *Am. Mineral.*, **29,** 291–298.

Harder, H. (1956). Untersuchungen an Paragoniten und an natriumhaltigen Muscoviten. *Heidelberger Beiträge zur Mineral. und Petrog.*, **5,** 227–271.

Hey, M. H. (1954), A new review of the chlorites. *Mineralog. Mag.*, v. **30,** 277–292.

Hietanen, A. (E. Cloos and) (1941), Geology of the "Martic Overthurust" and the Glenarm series in Pennsylvania and Maryland. *Geol. Soc. America Special Papers* no. **35,** 207 p.

——— (1951), Chloritoid from Rawlinsville, Lancaster county, Pennsylvania. *Am. Mineral.* **36,** 859–868.

Hutton, C. S. (1938), The stilpnomelane group of minerals. *Mineralog. Mag.*, **25,** 172–206.

——— (1956), Further data on the stilpnomelane mineral group. *Am. Mineral.*, **41,** 608–615.

James, H. L., and Howland, A. L. (1955), Mineral facies in iron- and silica-rich rocks. *Geol. Soc. America Bull.*, **66,** 1580–1588.

Kojima, J. (1944), Stilpnomelane in green schists of Japan. *Imperial Acad. Proc.*, **20,** 322–328.

Korzhinskii, D. S. (1959), Physico-chemical basis of the analysis of the paragenesis of minerals. Consultants Bureau, Inc., New York. 142 p.

Mikheev, V. I. (1953), Determination of the minerals of the chlorite group by *x*-ray methods. *Mem. Soc. Russe. Mineral.* (*Vsesoyuz. Mineralog. Obshchestva*), **82,** 214–217.

Milton, C., and Eugster, H. P. (1959), Mineral assemblages of the Green River formation. *In* Researches in Geochemistry. P. H. Abelson, ed. John Wiley and Sons, Inc., New York. p. 118–150.

Nelson, B. W., and Roy R. (1958), Synthesis of the chlorites and their structural and chemical constitution. *Am. Mineral.*, **43,** 707–725.

Niggli, P. (1912), Die Chloritoidschiefer des nordöstlichen Gotthardmassives. *Beiträge zur Geol. Karte der Schweiz, Neue Folge.* 17–95.

Orcel, M. J. (1927), Recherches sur la composition chimique des chlorites. *Soc. France Min. Bull.*, **50,** 75–454.

Pauling, L. (1930), Structure of chlorites. *Nat. Acad. Sci. Proc.*, **16,** 578–582.

Phillips, F. C. (1928), Metamorphism in the upper Devonian of north Cornwall. *Geol. Mag.*, **65,** 541–556.

Rosenfeld, J. L. (1956), Paragonite in the schist of Glebe Mountain, southern Vermont. *Am. Mineral.*, **41,** 144–147.

—, Thompson, J. B., Jr., and Zen, E. (1958), Data on coexistent muscovite and paragonite (abstract), *Geol. Soc. America Bull.*, **69,** 1637.

Sand, L. B. (1956), On the genesis of residual kaolins. *Am. Mineral.*, **41,** 28–40.

SCHMALZ, R. F., AND ZEN, E. (in preparation), Quantitative modal analysis of sediments by *x*-ray diffraction.

SHIROZU, H. (1955), A stilpnomelane like mineral from the skarn of the Obira Mine, Oita Prefecture, Japan. *Kobutsugaku Zasshi*, **2,** 115–120.

SMITH, J. V. (1956), The powder patterns and lattice parameters of plagioclase felspars. I. The soda-rich plagioclases. *Mineralog. Mag.*, **31,** 47–68.

THOMPSON, J. B., JR. (1955), The thermodynamic basis for the mineral facies concept. *Amer. Jour. Sci.* **253,** 65–103.

——— (1957), The graphical analysis of mineral assemblages in pelitic schists. *Am. Mineral.*, **42,** 842–858.

TILLEY, C. E. (1925), Petrographical notes on some chloritoid rocks. *Geol. Mag.*, **62,** 309–319.

TURNER, F. J. (1948), Mineralogical and structural evolution of the metamorphic rocks. *Geol. Soc. America Mem.* **30.** 342 p.

TUTTLE, O. F., AND BOWEN, N. L. (1958), Origin of granite in the light of experimental studies in the system $NaAlSi_3O_8$-$KAlSi_3O_8$-SiO_2-H_2O. *Geol. Soc. America Mem.*, **74.** 153 p.

WINCHELL, A. N. (1926), Chlorite as a polycomponent system. *Amer. Jour. Sci.*, **211,** 283–300.

——— AND WINCHELL, H. (1951), Elements of optical minerlaogy, Part 2. John Wiley and Sons, Inc., New York. 551 p.

YODER, H. S., JR., AND EUGSTER, H. P. (1953), Phase relations in the micas. Ann. Rept. Director of the Geophysical Lab., *Carnegie Inst. Wash. Yearbook* no. **52,** 64–69.

ZEN, E. (1959a), Clay mineral—carbonate relations in sedimentary rocks. *Amer. Jour. Sci.* **257,** 29–43.

——— (1959b), Geology of the north end of the Taconic allochthone and surrounding areas. Guidebook to the 51st annual meeting of the New England Intercollegiate Geological Conference. p. 1-16.

——— (in preparation), Stratigraphy and structure at the north end of the Taconic Range in west-central Vermont.

Manuscript received May 18, 1959.

THE AMERICAN MINERALOGIST, VOL. 45, JANUARY–FEBRUARY, 1960

STUDIES OF THE MANGANESE OXIDE MINERALS. III. PSILOMELANE*

MICHAEL FLEISCHER, *U. S. Geological Survey, Washington 25, D. C.*

ABSTRACT

Study of 14 analyses of psilomelane, including 7 new ones, verifies Wadsley's formula, $(Ba,H_2O)_4Mn_{10}O_{20}$. *X*-ray study of the products of dehydration shows that the water is lost zeolitically up to 500° C. and that the mineral is converted to hollandite at about 550° C. Thermogravimetric and differential thermal analysis curves are given for two analyzed samples.

INTRODUCTION

"The mineralogical determination of those species, the chief constituent of which is Manganese, has been for a long time destitute of that precision at which other species had long arrived, whose chemical constitution was better known." This is the opening sentence of a most remarkable paper by W. Haidinger, read by him on December 17, 1827, and published in 1831 (Haidinger, 1831). In it and the accompanying chemical report by Edward Turner (Turner, 1831), the minerals pyrolusite, manganite, hausmannite, braunite, and psilomelane were named and characterized; the descriptions, with the exception of the chemical composition of braunite, are still valid. When the U. S. Geological Survey began in 1941 a detailed study of the manganese oxide minerals, their determination was still destitute of precision. A preliminary report of our work (Fleischer and Richmond, 1943) partly corrected this, but other commitments have for a long time prevented the publication of the data on which the conclusions of the 1943 report were based.

The name psilomelane was given by Haidinger to the smooth black uniform and botryoidal mineral, which he stated to be "a pretty common species" and for which he lists many localities. He gave the hardness as 5–6, sp. gr. 4.145, 4.079, 4.004. Turner's analysis of a sample from Schneeberg (Table 1, A) gave BaO 16.36%; another sample, from Romanèche, France, sp. gr. 4.365, which he thought contained some pyrolusite (Table 1, B) contained 16.69% BaO.

Later workers, unfortunately, used the name psilomelane to refer to any hard, botryoidal manganese oxide, regardless of composition or density, until the term had practically come to mean any hard, unidentified manganese oxide, soft samples being referred to wad. The data in the literature on psilomelane therefore refer in part to cryptomelane, hollandite, coronadite, and lithiophorite, and probably to other minerals as well. One cannot be sure what mineral was studied unless *x*-ray powder data were given for the material described as "psilomelane"; on the other hand, some samples that differ in appearance from the usual hard botryoidal psilomelane have been described under other names. A good example is the "varvacite" of Walker (1888), Table I C, which is soft, fibrous, and radiating and which would be unhesitatingly identified by sight as pyrolusite.

---

* Publication authorized by the Director, U. S. Geological Survey.

Psilomelane was redefined as a single species by Vaux (1937), who made an *x*-ray study of samples from Schneeberg and Romanèche, reporting it to be orthorhombic with a_0 9.1, b_0 13.7, c_0 2.86 Å, and found from four new analyses that the composition could be expressed as $H_4(Ba, Mn)_2 Mn_8^{+4}O_{20}$ with Ba:Mn close to 1:1. His chemical results were confirmed by Fleischer and Richmond (1943), who followed him in restricting the name psilomelane to this species, the formula of which they gave in the slightly different form $BaR_9O_{18} \cdot 2H_2O$, ($R = Mn^{+4}$, Mn^{+2}, Co, etc.). Palache, Berman, Frondel (1944) likewise restrict the name to this species; they give the formula in a third modification, $BaMn^{+2}Mn_8^{+4}O_{16}(OH)_4$.

Later *x*-ray work by Wadsley (Wadsley 1952, 1953) has shown that psilomelane is monoclinic, space group *A* 2/*m*, with a_0 9.56, b_0 2.88, c_0 13.85 Å, β 92°30′. His structural study showed that Ba and H_2O occupy positions that are crystallographically indistinguishable, although they are very probably in an ordered sequence. On the basis of the structural data, he gave the formula (here doubled for comparison with those above) as $(Ba, H_2O)_4Mn_{10}O_{20}$ with Ba:H_2O approximately 1:2, and Mn including Mn^{+4}, Mn^{+2}, and other elements.

The present paper gives new analyses, dehydration curves, and differential thermal analyses of psilomelane.

CHEMISTRY

In Table 1 are given 17 analyses of psilomelane, 10 from the literature (lettered) and 7 new analyses made in the laboratories of the U. S. Geological Survey (numbered). These include every analyzed sample whose identity has been proved by *x*-ray study. Analyses A, B, and D, included because of their historical interest, are of samples that have not been studied by *x*-rays, although other samples from the same localities have been shown to be psilomelane. Many older analyses, some of which agree closely with those listed here, are given in Doelter's Handbuch der Mineralchemie, Bd. III, Pt. 2, p. 863 881, but these samples as well as one analyzed by Koch and Grasselly (1951) have not been studied by *x*-ray methods.

It will be noted in Table 1 that several of the samples contained large amounts of WO_3, one had a high content of V_2O_5, and three of As_2O_5.

TABLE 1. CHEMICAL ANALYSES OF PSILOMELANE

(arrangement chronological)

	A	B	C	D	1	E
MnO_2	66.98	66.40	68.86	66.87	59.65	66.73
MnO	10.18	11.83	7.51	8.23	6.70	7.12
CuO	—	—	—	0.10[a]	0.25	0.31
CoO	—	—	—	—	—	1.00
MgO	—	—	—	0.20	trace	0.13
BaO	16.36	16.69	14.42	16.20	14.40	17.48
CaO	—	—	—	0.40	0.05	0.26
K_2O	—	—	—	0.10	0.11	trace
Na_2O	—	—	—		0.42	trace
H_2O^-	6.22	4.13	5.08	4.65	0.49	0.50
H_2O^+					3.78	4.41
Al_2O_3	—	—	2.23		0.55	0.35
Fe_2O_3	—	—		1.45	3.27	0.20
As_2O_5	—	—	—	1.50	—	—
V_2O_5	—	—	—	—	—	—
WO_3	—	—	—	—	—	0.68
SiO_2	0.26	0.95	1.98	0.40[b]	9.25[c]	0.51
Others	—	—	—	—	0.37[d]	trace[e]
Total	100.00	100.00	100.08	100.10	99.29	99.68
G.	4.004 to 4.079	4.365	3.27	4.21	4.48 (corr. for SiO_2)	

	F	G	H	I	2	3
MnO_2	66.62	68.00	70.38	65.31	69.00	68.40
MnO	7.09	10.70	7.90	7.83	6.99	7.02
CuO	0.48	trace	0.38	—	none	0.03
CoO	0.90	—	0.48	—	—	none
MgO	0.15	0.30	0.13	1.68	trace	none
BaO	17.46	15.73	12.38	14.02	17.84	14.91
CaO	0.19	—	0.66	0.38	none	0.72
K_2O	trace	0.08	0.42	0.11	0.07	0.59
Na_2O	trace	0.02	trace	0.19	0.05	0.48
H_2O^-	0.48	0.48	1.88	4.69	0.07	0.63
H_2O^+	0.48	3.82	4.18		4.46	4.43
Al_2O_3	0.37	—	0.73	—	0.43	0.12
Fe_2O_3	0.15	0.30	0.18	0.84	0.14	0.15
As_2O_5	—	—	—	—	—	2.15
V_2O_5	—	—	—	—	—	—
WO_3	0.89	0.28	—	4.88	0.63	none
SiO_2	0.52	0.59	0.09	0.38	0.85[h]	0.13
Others	trace[f]	trace	0.03[g]	—	—	—
Total	99.68	100.30	99.82	100.31	100.53	99.76
G.	4.71	4.70	—	—	4.74	4.45

TABLE 1 (*continued*)

	4	5	6	7	J
MnO_2	70.85	67.10	70.52	67.91	74.36
MnO	6.87	7.46	6.10	7.62	6.10
CuO	0.03	—	—	0.11	—
CoO	0.03	0.26	0.01	0.07	—
MgO	0.22	0.26	0.22	0.11	—
BaO	14.99	14.59[j]	13.56	13.68	13.49
CaO	none	1.84[j]	0.27	0.07	—
K_2O	0.27	0.48	0.35	0.43	0.81
Na_2O	0.13	0.35	0.29	none	—
H_2O^-	0.37	0.70	—	0.90	—
H_2O^+	4.39	4.75	4.03[k]	5.00	5.14
Al_2O_3	0.29	none	0.27	none	0.59
Fe_2O_3	0.09	0.28	1.12	0.20	
As_2O_5	—	—	—	0.36	—
V_2O_5	—	1.13	—	—	—
WO_3	0.36	—	1.32	2.92	—
SiO_2	0.83	0.48	0.40	0.14	—
Others	0.09[i]	—	1.24[l]	0.17[m]	
Total	99.81	99.68	99.70	99.69	100.49
G.	4.56	4.41	4.44	4.43	4.61

Notes to Table 1—(a) $=CuO+PbO$; (b) $=SiO_2$ 0.25, gangue 0.15; (c) insol. SiO_2 8.35, sol. SiO2 0.90; (d) $=PbO$ 0.32, P_2O_5 0.05; (e) traces NiO and Li_2O; (f) trace NiO; (g) $=NiO$; (h) insol. SiO_2 0.41, sol. SiO_2 0.44; (i) $=ZnO$ 0.07, PbO 0.02; (j) includes some SrO; (k) sample dried at 110° before analysis; (l) $=SrO$ 1.19, P_2O_5 0.05; (m) $=ZnO$ 0.14, PbO 0.01, P_2O_5 0.02.

A-B Turner (1831), A. from Schneeberg, Saxony, B. from Romanèche, France, C. Walker (1888), fibrous, radiating; "varvacite" from near Austinville, Wythe Co., Virgina; *x*-ray identification by U. S. Geological Survey laboratory on type material from U. S. National Museum, G. evidently incorrect. D. Gorgeu (1890), from Romanèche; (1) Analyst-Charles Milton, 1933. Exact locality unknown, sample submitted from Tucson, Arizona; E-H. Quoted by Vaux (1937). (E, F, and H.) Hilda Bennett, analyst; (G) H. J. Hallowell, analyst; E. from Spitzleite, Eibenstock, Saxony; F-G. from Schneeberg; H. from Restormel Mine, Lostwithiel, Cornwall, England. I. Quoted by Kerr (1940); from Sodaville, Nevada; analyst F. A. Gonyer; *x*-ray identification by U. S. Geological Survey laboratory on material supplied by P. F. Kerr. (2) Analyst—W. T. Schaller, 1940. From Mayfield prospect, Chispa Siding, Jeff Davis Co., Texas. Collected by S. G. Lasky. (3) Analyst—M. Fleischer, 1941. From Romanèche, France, U. S. National Museum No. R 2232. (4) Analyst—M. Fleischer, 1941. From Tolbard Mine, Paymaster district, Imperial Co., California, collected by J. B. Hadley. (5) Analyst—M. Fleischer, 1942. Exact locality unknown, sample U. S. National Museum No. 94, 341, sent in from Manila, Utah. (6) Analyst—M. Fleischer, 1943. From Hoggett manganese group, Hidalgo Co., New Mexico, collected by Sherman K. Neuschel. (7) Analyst—M. Fleischer, 1943. From Talamantes Mine near Parral, Chihuahua, Mexico, collected by P. D. Trask; a photograph of this sample is given by Wilson and Rocha (1948), Plate 37 A. (J) Wadsley (1950), massive, from Pilbara, W. Australia.

TABLE 2. UNIT CELL CONTENTS OF PSILOMELANES, O=20.00

Analysis	C	1	E	F	G	H	I
Mn^{+4}	8.68	8.31	8.54	8.53	8.52	8.67	8.18
Mn^{+2}	1.16	1.14	1.12	1.11	1.64	1.19	1.20
Others[a]	0.31	0.67	0.37	0.38	0.13	0.32	0.79
R	10.15	10.12	10.03	10.02	10.29	10.18	10.17
Ba, etc.[b]	1.03	1.36	1.32	1.31	1.15	1.09	1.17
H_2O	3.09	2.54	2.73	2.71	2.31	2.49	2.84
$Ba+H_2O$	4.12	3.90	4.05	4.02	3.46	3.58	4.01
G. calcd.	4.66	4.70	4.76	4.77	4.69	4.49	4.72
G. meas.[c]	3.27	4.48[d]	—	4.71	4.70	—	—
Mn^{+4}/Mn^{+2}	7.48	7.29	7.63	7.68	5.20	7.29	6.82
	2	3	4	5	6	7	J
Mn^{+4}	8.69	8.50	8.73	8.42	8.66	9.58	9.00
Mn^{+2}	1.08	1.07	1.05	1.15	0.92	1.18	0.90
Others[a]	0.14	0.25	0.16	0.29	0.33	0.28	0.08
R	9.91	9.82	9.94	9.86	9.91	10.04	9.98
Ba, etc.[b]	1.31	1.50	1.28	1.63	1.29	1.09	1.08
H_2O	2.71	2.66	2.62	2.88	2.39	3.05	2.98
$Ba+H_2O$	4.02	4.16	3.90	4.51	3.68	4.14	4.06
G. calcd.	4.73	4.64	4.67	4.66	4.60	4.70	4.56
G. meas.[c]	4.74	4.45	4.56	4.41	4.44	4.43	4.61
Mn^{+4}/Mn^{+2}	8.05	7.94	8.31	7.32	9.41	7.27	10.00

[a] Includes Fe, Al, Cu, W, V, As, etc.

[b] Includes Ba, Sr, Ca, Pb, K, Na.

[c] Not corrected for SiO_2 except analysis 1.

[d] Corrected for SiO_2.

The Romanèche sample with 2.15% As_2O_5 (no. 3) and that from Chihuahua with 2.92% WO_3 (no. 7) were of ideal purity, as judged from optical and *x*-ray study, and there can be little doubt that these constituents were present in the manganese oxide mineral and not in any impurity. Tungsten, arsenic, and vanadium are characteristic constituents of manganese oxide minerals, and especially of psilomelane, from many localities in the southwestern United States and Mexico. Their genetic significance is discussed elsewhere by Hewett and Fleischer (1960), who give many additional partial analyses.

In Table 2 are given the calculated unit cell contents, assuming

$O = 20.00$, and using the unit cell dimensions of Wadsley (1953). All constituents reported in the analyses, with the exception of SiO_2, have been assumed to be part of the mineral. This is undoubtedly incorrect, especially for at least part of the Al_2O_3 and Fe_2O_3. SrO is reported in only one analysis, but is known to be a characteristic constituent of psilomelanes from many deposits in the southwestern United States and is probably present in some of the other samples of Table 1.

It is interesting to compare the calculations of Table 2 with the requirements of the four formulas that have been suggested in recent years for psilomelane:

1. Vaux	$H_4(Ba, Mn^{+2})_2Mn_8^{+4}O_{20}$
2. Fleischer and Richmond	$Ba(Mn^{+4}, Mn^{+2})_9O_{18} \cdot 2H_2O$
3. Palache, Berman and Frondel	$BaMn^{+2}Mn_8^{+4}O_{16}(OH)_4$
4. Wadsley	$(Ba, H_2O)_4Mn_{10}O_{20}$

All the formulas are fairly good approximations, but that of Wadsley clearly fits the analyses best. The first three formulas give for the sum of the cations 10, whereas Wadsley's formula gives 10+Ba; the 14 analyses give 11.06 to 11.49, average 11.3. Formulas 2 and 3 require $Ba = 1$; the analyses show Ba 1.03 to 1.63, average 1.26. Formula 3 requires $Mn^{+2} = 1$ and all but one of the analyses are in the range 0.90 to 1.20; it also requires the ratio $Mn^{+4}/Mn^{+2} = 8$; the analyses show the range 5.20 to 10.00, but 11 of the 14 are in the range 6.8–8.4, which may indicate some sort of Eh-pH control of the formation of the mineral. It should be noted, however, that cryptomelane and hollandite, which are commonly associated with psilomelane, show much higher Mn^{+4}/Mn^{+2} ratios.

The first three formulas require $2H_2O$, whereas Wadsley's require $H_2O + Ba = 4$. The calculations show H_2O^+ 2.31 to 3.09, average 2.71, but the dehydration studies discussed below show that some of this water is probably adsorbed. The sum of $Ba + H_2O$ ranges from 3.46 to 4.51, average 3.97; 10 of the 14 are between 3.90 and 4.16. Considering the massive nature of most samples and the difficulty of detecting small amounts of opaque admixtures such as pyrolusite, the over-all constancy of composition is surprising.

The calculated specific gravities are in general higher than those determined, as would be expected because the errors in the determination all give low results. They range from 4.49 to 4.77, average 4.67, and only one departs from the average by more than 0.11. There is, however, considerable uncertainty in the calculation because the presence of adsorbed water has not been taken into account; some arbitrary asumption as to how much of the water is adsorbed would have to be made. The data in the next section show that such an assumption would be very uncertain.

STUDY OF DEHYDRATION

Fleischer and Richmond (1943) found that psilomelane was converted to hollandite by heating at 550° C. (this was confirmed on synthetic material by Wadsley (1950)) and concluded that the water was essential. Wadsley (1953) stated that a temperature vs. weight curve recorded by A. J. Gaskin showed no abrupt transition and that powder photographs of material heated to 400° C. showed no change, despite the fact that at least 60% of the water was lost; further that material heated to 400° C. could be dehydrated by exposing the sample to the atmosphere at room temperature. It seemed desirable, therefore, to study the dehydration in more detail. The samples studied were Nos. 6 and 7 of Table 1 from the Hoggett Mine (H_2O^+ 4.03%, sample had been dried at 110° C.), and from Talamantes Mine, Parral, Chihuahua (H_2O^- 0.90, H_2O^+ 5.00%).

TABLE 3. DEHYDRATION OF PSILOMELANE

Temperature ° C.	Loss of Weight—in %			
	Talamantes Mine		Hoggett Mine (sample dried at 110°)	
	M.F.	C.A.K.	M.F.	C.A.K.
400	3.92	2.70	1.09	0.50
500	0.83[a]	1.20	1.15[b]	0.40
600	2.62	1.40	3.53	0.75
700	0.04	0.70	0.00	2.25
800	0.65	1.20	0.47	0.90
900	0.91	1.50	1.29	1.90
Total	8.97	8.70	7.53	6.70
H_2O^+	5.00		4.03	
H_2O^-	0.90		—	

[a] Another sample heated directly and held at 500° C. for 14 days lost 5.12%.
[b] Another sample heated directly and held at 500° C. for 14 days lost 1.90%.

The results are given in Table 3. The losses in weight recorded in the columns headed M.F. were determined by heating weighed samples in platinum dishes at the temperature indicated for 24 hours. The temperatures were held to ±10°. The data marked C.A.K. were determined by C. A. Kinser of the U. S. Geological Survey and are shown in Fig. 1

The data by Kinser were obtained on a thermogravimetric balance modified from that described by Mauer (1954), which continuously records the weight of a sample as the temperature of the sample is raised at a pre-determined uniform rate.

It will be noted from Table 3 and Fig. 1 that the two samples lost water at very different rates. The total loss in weight exceeds by a good deal the water content; evidently oxygen was driven off above 500° C. in the static dehydrations, and at 700° and above in the rapid heating of the thermogravimetric apparatus.

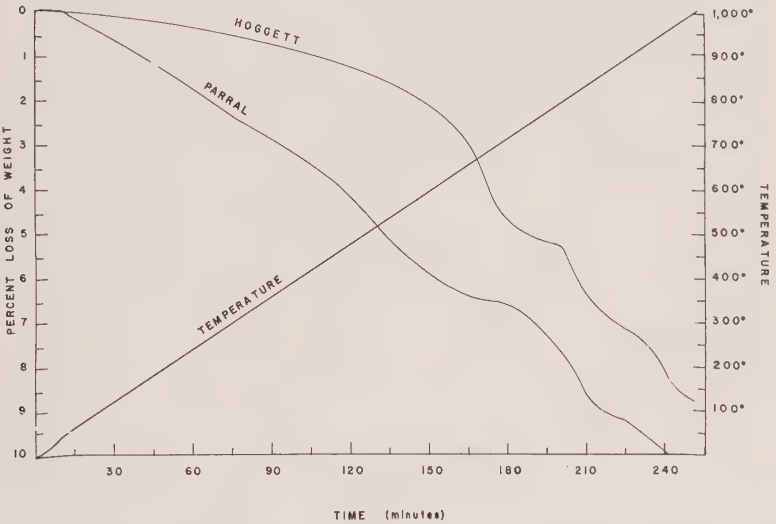

FIG. 1. Thermogravimetric dehydration curves by C. A. Kinser of psilomelanes from the Hoggett Mine, New Mexico, and the Talamantes Mine, Parral, Chihuahua. The loss in weight is read directly from the scale at the left. The temperature for any point on the curves is obtained by drawing a vertical line to the temperature curve and reading from the scale at the right.

X-ray powder patterns were made by E.C.T. Chao of the samples run by Fleischer. For the sample from the Hoggett Mine, the pattern of material heated at 400° was unchanged; the pattern of material heated at 500° C. was still that of psilomelane, but the lines at 3.88, 3.30, 3.21, 2.97, 2.36, and 1.82 had become diffuse and that at 2.25 Å had become markedly weaker; the pattern of samples heated at 600°, 700°, and 800° C. was that of hollandite with perhaps small amounts of bixbyite, as indicated by lines at 2.72 and 1.67 Å; the pattern of material heated at 900° C. was still mainly hollandite, but the broad band at 3.12 Å had changed to a doublet at 3.08 and 3.16 Å, and hausmannite was present in place of bixbyite.

The *x*-ray study of the heated samples from the Talamantes Mine, Parral, showed slightly different behavior. The pattern of material heated at 400° was diffuse with only lines at 6.87, 3.46, 2.40, 2.18, and 2.14, and diffuse bands at 1.82, 1.56, and 1.42 Å; the pattern of material heated at 500° C. was even weaker. The patterns of material heated at 600°, 700°, 800° and 900° C. showed hollandite plus small amounts of hausmannite. The broad band of hollandite at 3.13 changed in the samples heated at 800° and 900° C. to a doublet at 3.10 and 3.18 Å.

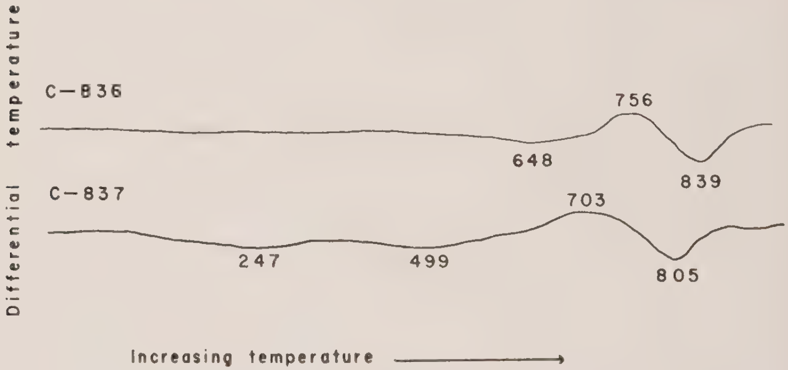

FIG. 2. D.T.A. curves by George T. Faust for psilomelanes from Hoggett Mine, New Mexico (C-836) and from Talamantes Mine, Parral, Chihuahua (C-837).

Thus the results on the two samples confirm Wadsley's findings that heating at 400° C. produced no structural change and the report by Fleischer and Richmond that there is a change at 550° C. to hollandite. Wadsley's statement that the structural change is accompanied by a period of marked crystal disorder is confirmed. The sample from the Talamantes Mine lost its water more readily and showed signs of disorder at lower temperatures than the sample from the Hoggett Mine. We have no explanation for this, nor for the fact that the latter sample gave a small amount of bixbyite first, then hausmannite, whereas the former sample gave hausmannite directly.

DIFFERENTIAL THERMAL ANALYSIS

Figure 2 shows the D.T.A. curves for the same two samples, kindly run by George T. Faust of this laboratory. Each curve shows one exothermal break (at 703° and 756° C.) and one endothermal break (at 805° and 839° C.) for the Parral and Hoggett samples, respectively. The exothermic breaks correspond approximately to the short plateaus on Kinser's thermogravimetric curves, but the endothermal breaks do not correspond closely to decided breaks in Kinser's curves.

Curves have previously been published for "psilomelane" in four papers, but none of these gave *x*-ray data for the samples. Kulp and Perfetti (1950) gave a curve for a sample from Cuba, which showed a broad endothermic peak at 900–1000°. Kauffman and Dilling (1950, p. 229) gave a curve for a sample from California, which showed an endothermic peak at about 840°. Heystek and Schmidt (1953, p. 165) gave a curve for a sample from Frischgewaagd, Waterberg District, South Africa, which showed two large endothermic breaks at 620° and 840° C. There is no way in which one can guess as to what manganese oxide minerals these curves actually represent, in the absence of *x*-ray and chemical data. Rode (1955), on a sample from Schneeberg containing BaO 10.45%, found a sharp exothermic peak at about 750° and an exothermic peak at 1050° C. The analysis indicates that the sample could not have been pure psilomelane.

In view of the differences in behavior of the two samples we have studied, we expect to continue our studies of the thermal behavior of samples for which chemical and *x*-ray data are available.

NOMENCLATURE

The early history of the nomenclature of this mineral was summarized in the Introduction. The name romanèchite was proposed by Lacroix (1910, p. 6) for the same mineral (he quotes Turner's analysis!) and this name has been used, especially in France, up to the present. It has been favored mainly because of the feeling that psilomelane has been used for so many different minerals that the name has ceased to be well-defined. The name romanèchite has, however, also suffered in this way; it has unfortunately also been applied to the potassium manganese oxide cryptomelane by Gruner (1943), who found that the latter occurred at Romanèche and assumed that this was the mineral named by Lacroix. This was unjustified, because it ignored the fact that Lacroix cited six analyses, showing BaO 13.50 to 16.84%.

On the whole, it seems best to retain the name psilomelane for the specific mineral here described and to relegate romanèchite to the synonymy. This nomenclature has been adopted by Palache, Berman, and Frondel (1944), by Hey (1955), and by Strunz (1947).

ACKNOWLEDGMENTS

I am deeply indebted to many colleagues of the U. S. Geological Survey: to W. T. Schaller and Charles Milton for permission to use their

unpublished analyses; to W. E. Richmond, J. M. Axelrod, and E. C. T. Chao for *x*-ray powder determinations; to M. D. Foster, who aided in the colorimetric V_2O_5 determinations; to C. A. Kinser for the thermogravimetric curves; to George T. Faust for the D.T.A. curves; to John P. Marble, who prepared the figures; to J. B. Hadley, S. G. Lasky, Sherman K. Neuschel, and P. D. Trask who collected some of the samples; to the late W. F. Foshag for his loan of samples from the U. S. National Museum. The work was begun under the urging of D. F. Hewett and C. F. Park, Jr., who along with T. A. Hendricks, were sources of much helpful advice and encouragement throughout.

REFERENCES

FLEISCHER, MICHAEL AND RICHMOND, W. E. (1943), The manganese oxides: a preliminary report. *Econ. Geol.*, **38,** 269–286.

GORGEU, A. (1890), Sur les oxydes de manganèse naturels: *Soc. franc. mineral., Bull.* **13,** 21–31.

GRUNER, J. W. (1943), The chemical relationship of cryptomelane (psilomelane), hollandite, and coronadite: *Am. Mineral.*, **28,** 497–506.

HAIDINGER, W. (1831), Mineralogical account of the ores of manganese: *Roy. Soc. Edinburgh, Trans.*, **11,** 119–142.

HEWETT, D. F. AND FLEISCHER, MICHAEL (1960), Deposits of the manganese oxides: *Econ. Geol.* **55,** 1–55.

HEY, M. H. (1955), An index of mineral species and varieties arranged chemically, 2nd Ed. British Museum, 728 p.

HEYSTEK, H. AND SCHMIDT, E. R. (1953), The technique of differential thermal analysis and its application to some South African minerals: *Geol. Soc. S. Africa, Trans. and Proc.*, **56,** 149–176.

KAUFFMAN, A. J. JR. AND DILLING, E. D. (1950), Differential thermal curves of certain hydrous and anhydrous minerals, with a description of the apparatus used: *Econ. Geol.*, **45,** 222–244.

KERR, P. F. (1940), Tungsten-bearing manganese deposit at Golconda, Nevada: *Geol. Soc. Am., Bull.*, **51,** 1359–1390.

KOCH, S. AND GRASSELLY, G. (1951), The manganese ore mineral occurrences of Hungary: *Acta Univ. Szegediensis, Acta Mineralog. Petrog.*, **5,** 1–14.

KULP, J. L. AND PERFETTI, J. N. (1950), Thermal study of manganese oxide minerals: *Mineralog. Mag.*, **29,** 239–251.

LACROIX, A. (1910), Minéralogie de la France et de ses colonies; **4:** Paris, 923 p.

MAUER, F. A. (1954), An analytical balance for recording rapid changes in weight: *Rev. Sci. Instruments*, **25,** 598–602.

PALACHE, C., BERMAN, H. AND FRONDEL, C. (1944), Dana's System of Mineralogy, 7th Ed., v. 1, p. 668–671. John Wiley and Sons, New York.

RODE, E. YA. (1955), Thermography of manganese oxides: Trans. 1st Congress Thermography 1953, p. 219–238 (in Russian).

STRUNZ, HUGO (1957), Mineralogische Tabellen, 3rd ed.: Akad. Verlagsgesellschaft, Leipzig, 448 p.

TURNER, EDWARD (1831), Chemical examination of the oxides of manganese: *Roy. Soc. Edinburgh, Trans.*, **11,** 143–174.

Vaux, George (1937), *X*-ray studies on pyrolusite (including polianite) and psilomelane: *Mineralog. Mag.*, **24,** 521–526.

Wadsley, A. D. (1950), Synthesis of some hydrated manganese minerals: *Am. Mineral.*, **35,** 485–499.

Wadsley, A. D. (1952), Role of water in the structure of psilomelane $(Ba, H_2O)_2Mn_5O_{10}$: *Nature*, **170,** 973–974.

Wadsley, A. D. (1953), The crystal structure of psilomelane $(Ba, H_2O)_2 Mn_5O_{10}$: *Acta Cryst.*, **6,** 433–438.

Walker, P. H. (1888), Analysis of varvacite from Wythe County, Virginia. *Am. Chem. Jour.*, **10,** 41–42.

Wilson, I. F. and Rocha, V. S. (1948), Manganese deposits of the Talamantes district near Parral, Chihuahua, Mexico: *U. S. Geol. Survey Bull.*, **954-E,** 181–208.

Manuscript received May 29, 1959.

THE AMERICAN MINERALOGIST, VOL. 45, JANUARY–FEBRUARY, 1960

REEDMERGNERITE, $NaBSi_3O_8$, THE BORON ANALOGUE OF ALBITE, FROM THE GREEN RIVER FORMATION, UTAH*

CHARLES MILTON, E. C. T. CHAO, JOSEPH M. AXELROD,† AND FRANK S. GRIMALDI, *U. S. Geological Survey, Washington 25, D. C.*

ABSTRACT

Reedmergnerite, $NaBSi_3O_8$, is a boron analogue of albite, occurring with eitelite, shortite, nahcolite, searlesite, leucosphenite, acmite, analcite, and magnesioriebeckite in unmetamorphosed dolomitic oil shales of the Green River formation in several oil wells in Duchesne County, Utah. It is triclinic, colorless, in stubby prisms with characteristic wedge-shaped ends; biaxial, negative, $2V=80°$, indices of refraction α 1.554, β 1.565, γ 1.573, all ±0.001. *X*-ray diffraction and crystallographic data are given.

INTRODUCTION—NAME ACKNOWLEDGMENTS

The discovery of leucosphenite in 1953 (Milton, Axelrod, and Grimaldi, 1954) in brown dolomitic core from the Sinclair Company Senior Mortenson No. 1 wildcat oil well near Duchesne, Duchesne County, Utah (Fig. 1) led to a careful search for other unusual minerals. A thin section of leucosphenite-bearing rock (Figs. 2 and 3) showed crystals evidently different; these were isolated (Fig. 4) and from them an *x*-ray diffraction pattern was obtained which could not be identified with that of any known mineral. Further investigation showed that the crystals were $NaBSi_3O_8$, isostructural with albite, $NaAlSi_3O_8$, and were a new species which was then named reedmergnerite.

The name was given to honor two outstanding technicians of the U. S. Geological Survey, Frank S. Reed (1894–) and John L. Mergner (1894) who for almost half a century have prepared thin and polished sections for several generations of Survey geologists. Through their skill, and willingness to use it generously, they have made possible much of the petrological and mineralogical research of their better-known colleagues.

For most of the core and cutting material on which this study is based, we are indebted to the generous co-operation of Mr. J. C. McCulloch and Mr. Verne E. Farmer, Jr., geologists of the Carter Oil Company.

OCCURRENCE AND LOCALIZATION

Following the initial discovery in the Sinclair Mortenson well, the mineral was found in relative abundance in cores and cuttings from five other wells within an area of 20 miles west and 10 miles south. The wells

---

* Publication authorized by the Director, U. S. Geological Survey.

† Present address: Hughes Aircraft Corp., Box 90427, Airport Station, Los Angeles, California.

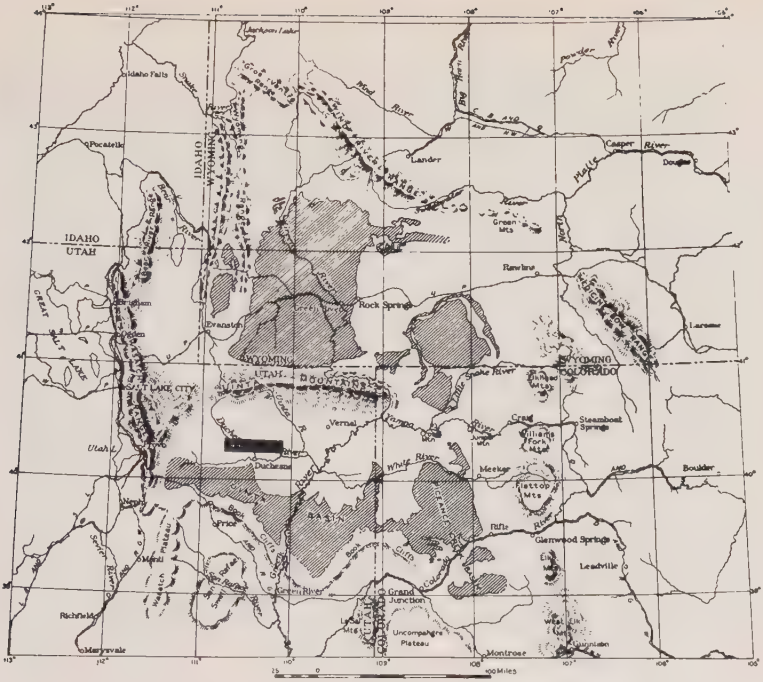

FIG. 1 (From Bradley, 1931). Map showing outcrop (shaded) of Green River formation in Utah, Colorado, and Wyoming. In Utah the Green River formation continues northward underground from the shaded area to the Uinta Mountains, and reedmergnerite occurs at depths of two thousand or more feet. The six wells in which reedmergnerite was found are in the rectangle just north of Duchesne, Utah.

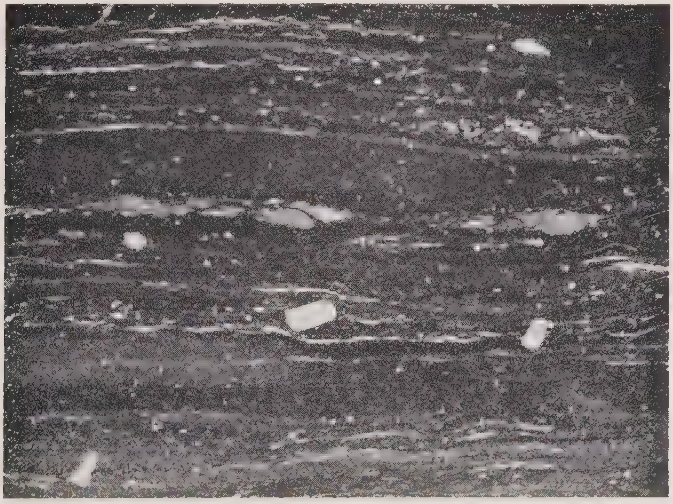

FIG. 2. Reedmergnerite crystals with band of lenticular aggregates of blue magnesioriebeckite (across middle, gray), in black oil shale. Thin section, ordinary light. ×7.5

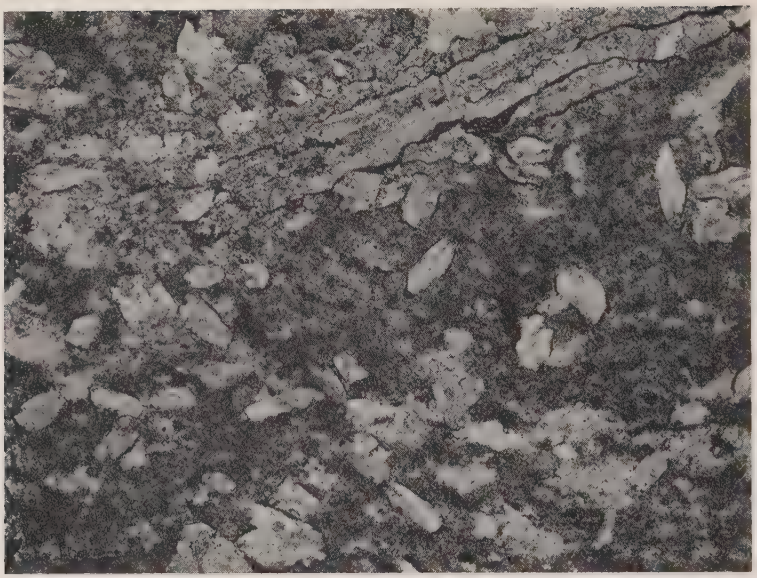

FIG. 3. Reedmergnerite in black oil shale. The diagonal wide band across the upper right is nahcolite. The oriented inclusions almost invariably present are shown in many crystals. Thin section, ordinary light. ×20.

in which reedmergnerite has been found are:

Sinclair Senior Mortenson No. 1	Sec. 7, T. 3 S., R. 2 W.
Carter Oil Co.	
Willis Moon No. 1	Sec. 13, T. 4 S., R. 4 W.
Elmer Moon No. 1	Sec. 8, T. 4 S., R. 3 W.
Duchesne County No. 1	T. 3 S., R. 5 W.
Joseph Smith No. 1	Sec. 16, T. 3 S., R. 5 W.
Kermit Poulson No. 1	Sec. 31, T. 3 S., R. 4 W.

The general area in which these wells were drilled is shown in Fig. 1.

The mineral occurs as mentioned in a brown dolomitic rock, and also, especially in the Joseph Smith, in black oil shale. In addition to leucosphenite, nahcolite, $NaHCO_3$, and shortite, $Na_2Ca_2(CO_3)_3$, are abundantly present; also eitelite, $Na_2Mg(CO_3)_2$, searlesite, $NaBSi_2O_6 \cdot H_2O$, acmite, $NaFeSi_2O_6$, analcite, $NaAlSi_2O_6 \cdot H_2O$, and magnesioriebeckite, $Na_2(Mg,Fe)_3Fe_2^3Si_8O_{22}(OH)_2$; all of which are likewise authigenic, not detrital.

Later papers will describe leucosphenite, eitelite, acmite, and magnesioriebeckite in the Green River formation.

Reedmergnerite seems to be restricted in the Green River to the single Utah area of the six wells indicated in Fig. 1, and albite is similarly restricted, having been found only in the oil shale mine near Rifle, Colorado.

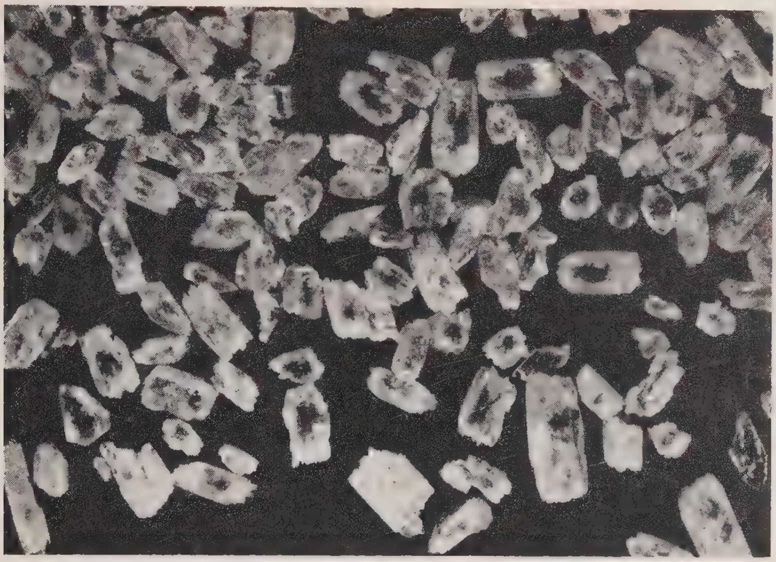

FIG. 4. Reedmergnerite crystals, isolated from oil shale. ×10.

Yet searlesite and analcite are almost ubiquitous in the Utah-Wyoming areas of the Green River so far studied. (Note—recently authigenic albite has been found fairly widely in the Wyoming Green River.)

CRYSTALLOGRAPHY

Optical and physical data

Reedmergnerite is colorless with a vitreous luster. It is easily fusible, insoluble in nitric or hydrochloric acid, but decomposed by hydrofluoric acid. The hardness is about 6 to 6.5. The specific gravity is 2.69 (observed), 2.77 (calculated). Crystals are usually microscopic; the largest being about 0.2 cm.

The indices of refraction, optic sign, and optical orientation were determined on the Federov universal stage. Indices were determined using white light at 28° and corrected to 25° C. Immersion liquids in 0.002 steps were checked by refractometer at time of use. The data are:

α 1.554 ± 0.001
β 1.565 ± 0.001
γ 1.573 ± 0.001

2V (measured) 80°
optic sign (−)
Δ0.019

Reedmergnerite has a perfect {001} cleavage. Crushed fragments therefore tend to lie on this cleavage; indices of such flat lying grains will be

$$\alpha' = 1.558 \quad \text{and} \quad \gamma' = 1.567 \text{ at } 25° \text{ C.}$$

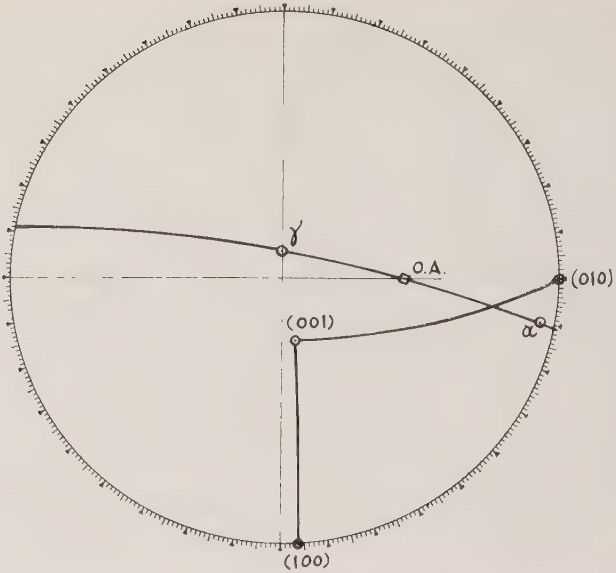

FIG. 5. Stereographic projection of reedmergnerite crystal, showing optic orientation.

Figure 5 is a stereographic projection, showing the relations of optics to morphology, based on the feldspar orientation.

X-ray single crystal data

Precession photographs of the *h*0*l* and 0*kl* nets of reedmergnerite, taken with Mo/Zr radiation (λ Mo$K\alpha$=0.7107 Å), were used to measure the cell dimensions. Reedmergnerite is triclinic and the presence of a center of symmetry is assumed from sudy of the morphology. Two descriptions of the direct cell of reedmergnerite are given in Table 1, one for a primitive cell, and one for the conventional feldspar orientation. The transformation matrix from primitive to feldspar-type cell is 110/110/001. Crystallographic data for albite are given for comparison.

The observed density of reedmergnerite 2.69 (determined on a portion of the sample chemically analyzed) is appreciably lower than the calculated 2.77. The discrepancy can probably be explained by the numerous fluid inclusions characteristically present in these crystals (Fig. 3). The formula, $NaBSi_3O_8$, suggests the possible analogy with albite. Although the powder patterns are complex and not notably similar, comparison of precession photographs reveals an isostructural relationship. Crystal structure studies of reedmergnerite are now in progress by Joan R. Clark and D. E. Appleman of the U. S. Geological Survey.

TABLE 1. CRYSTALLOGRAPHIC ELEMENTS OF REEDMERGNERITE AND ALBITE

	Reedmergnerite		Albite	
	Primitive cell[1]	Feldspar orientation[1,2]	Present study[1,3]	Cole, Sörum, and Taylor (1951)[4]
a	7.21 Å	7.85 Å	8.14 Å	8.1353 Å
b	7.44	12.38	12.79	12.7883
c	6.81	6.81	7.15	7.1542
α	100°37′	93°27′	94°10′	94°13.6′
β	107°04′	116°23′	116°36′	116°31.2′
γ	115°16′	91°57′	87°43′	87°42.5′
Space Group	$P\bar{1}$	$C\bar{1}$	$C\bar{1}$	
Z	$2[NaBSi_3O_8]$	$4[NaBSi_3O_8]$	$4[NaAlSi_3O_8]$	
Volume	294.8 Å^3	589.6 Å^3	663.5 Å^3	664.16 Å^3
Density (calc.)		2.77_0 g.cm.$^{-3}$		2.6241 g.cm.$^{-3}$
(obs.)		2.69		2.6280

Axial ratio $a:b:c=0.634:1:0.550$ for feldspar orientation.
$a:b:c=0.969:1:0.915$ for primitive cell.

[1] Axial lengths all ±0.03 Å; axial angles all ±10′.

[2] Transformation matrix $P\bar{1}$ to $C\bar{1}$: $\bar{1}\bar{1}0/\bar{1}10/00\bar{1}$.

[3] Albite from Amelia, Virginia.

[4] Albite from Kodarma, Bihar, India.

X-ray powder data

The x-ray powder diffraction patterns were taken with a Debye-Scherrer camera (114.59 mm. diameter) with Cu/Ni radiation ($\lambda CuK\alpha = 1.5418$ Å). Patterns made using a rolled cylindrical mount (film 7180) show definite, but not extreme, preferred orientation, and patterns made using a spherical mount (film 7179) show no evidence of preferred orientation. Measurements from the films were indexed down to $d=2.5$ Å (Table 2). The lower limit of 2θ measurable on both films is approximately 7°(=13 Å). Intensity measurements are given for both patterns to facilitate future identification by comparison with patterns made by techniques which, respectively, permit or eliminate preferred orientation (Hildebrand, 1953). The marked differences in strong line intensities are shown in Fig. 6.

Morphology

The characteristic and almost invariable shape of the crystals is shown in the feldspar orientation in Fig. 7. Forms commonly present

TABLE 2. *X*-RAY POWDER DATA FOR REEDMERGNERITE, $NaBSi_2O_8$

Triclinic $P\bar{1}$: $a=7.21$, $b=7.44$, $c=6.81$ Å (all ±0.03 Å);
$\alpha=100°37'$, $\beta=107°04'$, $\gamma=115°16'$ (all ±10')

Measured[1]			Calculated[2]		Measured[1]			Calculated[2]	
I[3]	I[4]	d_{hkl}	d_{hkl}	*hkl*	I[3]	I[4]	d_{hkl}	d_{hkl}	*hkl*
12	3	6.28	6.28	010	70	25	3.08	3.08	$2\bar{2}0$, 112
9	13	6.16	6.16	$1\bar{1}0$	25	100	3.03	3.04	002
15	18	5.55	5.56	$10\bar{1}$	18	18	2.96	2.96	200
100	60	3.87	3.88	$11\bar{1}$	9	35	2.94	2.93	$\bar{1}21$
6	13	3.75	3.75	011	40	25	2.84	2.85	$\bar{2}21$
35	15	3.65	3.66	$1\bar{2}0$				2.82	$\bar{1}12$
18	50	3.57	3.56	101	2	2	2.77	2.78	$20\bar{2}$
14	18	3.45	3.44	$2\bar{1}0$	15	18	2.68	2.68	$2\bar{1}1$
4	9	3.33	3.33	$10\bar{2}$	3b	3b	2.53	2.54	$1\bar{2}2$
25	25	3.23	3.22	$01\bar{2}$				2.53	$21\bar{1}$
30	18	3.14	3.14	020					

Measured[1]			Measured[1]			Measured[1]		
I[3]	I[4]	d_{hkl}	I[3]	I[4]	d_{hkl}	I[3]	I[4]	d_{hkl}
18	4	2.441	6	4m	1.860	2	1	1.538
6	6	2.403	6	3	1.828	4	2	1.523
20	18	2.383	2	—	1.800	5b	4b	1.485
6	6	2.369	6	6	1.775	7	4	1.445
2	—	2.269	4	7	1.752	4	3	1.420
13	9b	2.238	—	2	1.728	2	2	1.414
5	5	2.162	3	9	1.707	3	3	1.388
—	1	2.130	9	18	1.698	3b	3b	1.376
3	1	2.111	2	2	1.678	1	—	1.365
14	6	2.061	6	4	1.655	—	1	1.350
4	3	2.015	4	6b	1.623	6	3	1.341
6	4	1.992	4	4	1.599	3	4	1.328
4	2	1.940	2	—	1.571	plus additional lines,		
5	3m	1.900	6	13	1.562	all with I≤3		

[1] No correction for film shrinkage; b=broad, m=incompletely resolved multiplet. Radiation: Cu/Ni, λ CuKα=1.5418 Å. Lower limit of 2θ measurable: approximately 7° (13 Å).

[2] Calculated and indexed from direct cell elements given above.

[3] Intensities read from film no. 7179, preferred orientation minimized.

[4] Intensities read from film no. 7180, preferred orientation present.

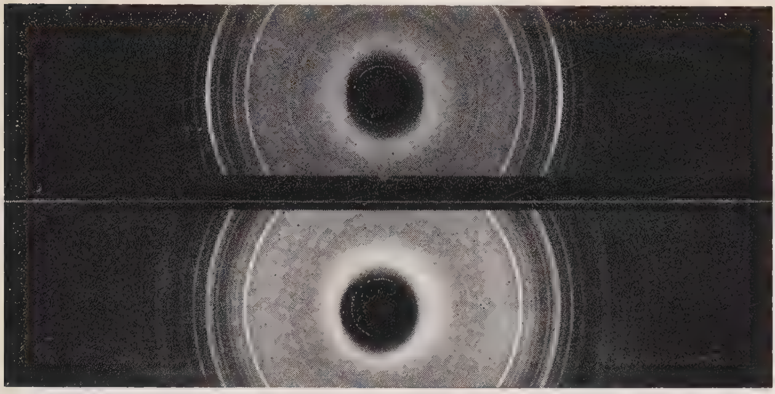

FIG. 6. *X*-ray powder diffraction patterns of reedmergnerite. Film 7180 (above) shows effects of preferred orientation; rolled cylinder mount. Film 7179 (below) shows minimization of preferred orientation; spherical mount.

are *a* {100}, *b*{010}, *c*{001}, *m*{110}, *o*{$\bar{1}\bar{1}1$} and δ {$\bar{1}\bar{1}2$}. The measured interfacial angles are as follows:

$(001)\wedge(110)=65°04'$
$(\bar{1}\bar{1}2)\wedge(001)=29°17'$
$(\bar{1}\bar{1}2)\wedge(\bar{1}\bar{1}1)=29°21'$
$(010)\wedge(110)=57°30'$
$(100)\wedge(110)=28°57'$

In some crystals, especially in larger ones, there are jagged ends (skeletal growth) replacing the two terminal faces (100) and (010) (Fig. 4). The natural crystals are always single, never twinned or composite, and the largest are about 2 mm. long. Cleavage is perfect parallel to {001}.

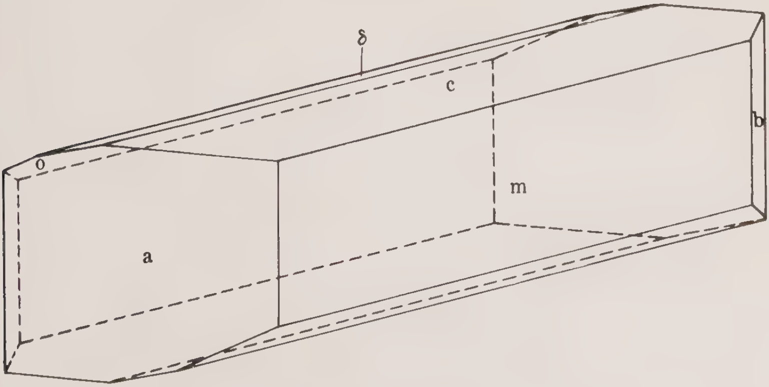

FIG. 7. Reedmergnerite, Duchesne County, Utah. Forms indicated are conventional ones of albite. *a* 100, *b* 010, *c* 001, *m* 110, *o* $\bar{1}\bar{1}1$, *θ* $\bar{1}\bar{1}2$.

Most crystals show oriented inclusions concentrated along the apparent growth traces of crystal edges, giving rise to a flattened cross in section (Figs. 3 and 4). The (010) face is very small or absent so it is not clear whether the inclusions are along the growth trace of the whole face or only along the trace of one edge. With this reservation, the inclusions are present along the following edges in decreasing amount: (010) to (110); (100) to (001), $(\bar{1}\bar{1}2)$, and $(\bar{1}\bar{1}1)$; (110) to (001) and $(11\bar{1})$.

TABLE 3. CHEMICAL COMPOSITION OF REEDMERGNERITE

	Chemical analysis[1]	Theoretical composition $Na_2O \cdot B_2O_3 \cdot 6SiO_2$
SiO_2	73.13	73.25
B_2O_3	14.27	14.15
Na_2O	12.15	12.60
Al_2O_3	0.15	
MgO	0.09	
BaO	0.09	
Fe_2O_3	0.08	
TiO_2	0.03	
K_2O	0.03	
H_2O (−)	0.00	
H_2O (+)	0.08	
Total	100.10	100.00

[1] Analyst, Frank S. Grimaldi.

CHEMICAL STUDY

Reedmergnerite is insoluble in nitric or hydrochloric acids, which permits its removal from its dolomitic or carbonaceous matrix. The mineral is decomposed by $HF + H_2SO_4$. Approximately one-half gram of handpicked crystals of reedmergnerite was chemically analyzed. The chemical composition is given in Table 3. The sum of determined oxides other than the three essential being but 0.55 per cent, the analyzed sample contained less than 1 per cent impurities and closely approximated the theoretical composition.

A semiquantitative spectrographic analysis by Charles Annell, U. S. Geological Survey, showed more than 10 per cent Si, Na, 1 to 5 per cent B; 0.1 to 0.5 per cent Al, Ba; 0.05 to 0.1 per cent Fe, Ti; 0.01 to 0.05 per cent Zr, K, Mg; and 0.001 to 0.005 per cent V.

Method of chemical analysis

A 0.2-gram portion was treated with $HF-H_2SO_4$, brought to fumes of sulfuric acid, diluted and digested with water, filtered, and barium was determined gravimetrically as $BaSO_4$. The filtrate from $BaSO_4$ was treated with 8-hydroxyquinoline in ammoniacal solution to precipitate and isolate magnesium, aluminum, iron, titanium, and zirconium as oxinates.

Sodium was determined in the filtrate by evaporating and igniting to destroy 8-hydroxyquinoline, and the salts were weighed as $Na_2SO_4 + K_2SO_4$. Potassium was determined flame photometrically, and the sodium calculated from the combined $K_2SO_4 + Na_2SO_4$ by deducting the K_2SO_4.

The oxine precipitate was ignited under cover of oxalic acid and weighed and then dissolved by fusing with a small amount of $K_2S_2O_7$ and leaching with a small amount of (1+9) HCl. The iron, zirconium, and titanium were precipitated with cupferron, and the combined cupferrates were filtered, ignited, and weighed. The residue was brought in solution with a small amount of $K_2S_2O_7$ and titanium was determined colorimetrically with H_2O_2 and iron colorimetrically with *o*-phenanthroline.

The filtrate from the cupferron separation was evaporated and excess cupferron destroyed by HNO_3 followed by gentle ignition. This filtrate contained aluminum and magnesium. Aluminum was precipitated with NH_4OH and determined gravimetrically. The magnesium in the filtrate was precipitated as magnesium ammonium phosphate and ignited to $Mg_2P_2O_7$ which was weighed. Weighings were made on a semi-micro balance.

Silica was determined on a separate (0.2 gm.) portion by fusing with a small amount of Na_2CO_3 and treating the melt with HCl. Three dehydrations with HCl in the presence of methyl alcohol were made to isolate the SiO_2 free from boron.

A separate sample (0.15 gm.) was used for the boron determination which followed essentially the method of Allen and Zies (1918) involving distillation of methyl borate and titration of boric acid with NaOH after the addition of mannitol. The blank in the procedure amounted to 0.10 ml. of 0.1*N* NaOH. Of this blank about 0.08 ml. was due to the difference in end point between the paranitrophenol and phenolphthalein indicators. Thus, only 0.02 ml. blank was due to the distilling operation.

$H_2O(+)$ is ignition loss at 800° C. Iron was calculated as Fe_2O_3.

THERMAL STUDY

Morey (1951) had previously studied the system Na_2O-B_2O_3-SiO_2, (Fig. 8) and found only one ternary compound $Na_2O \cdot B_2O_3 \cdot 2SiO_2$, *n* 1.572. It was first prepared hydrothermally, using very low water pressure, but later was crystallized dry, and found to melt congruently at 766° C. Morey (written communication) found that the natural crystals

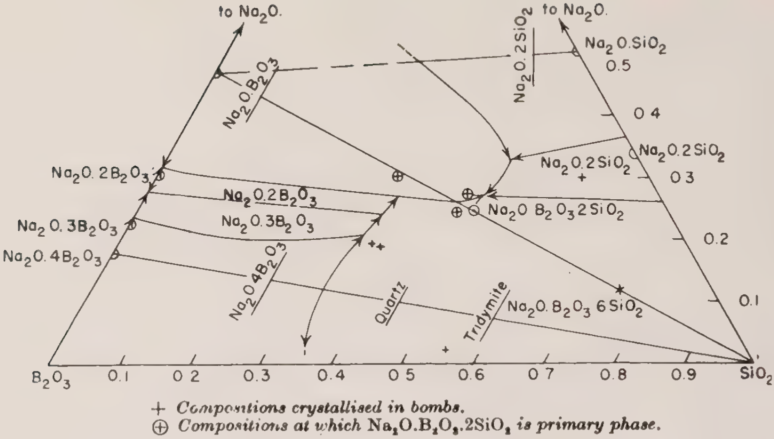

FIG. 8 (Adapted from Morey, 1951). System Na_2O-B_2O_3-SiO_2 liquidus diagram, incomplete in high silica end. Compositions of ternary compounds $Na_2O \cdot B_2O_3 \cdot 2SiO_2$ and $Na_2O \cdot B_2O_3 \cdot 6SiO_2$ reedmergnerite are shown. The field of the congruently melting compound $Na_2O \cdot B_2O_3 \cdot 2SiO_2$ was not determined. Reedmergnerite has been crystallized under hydrothermal conditions. One quaternary compound in the H_2O-Na_2O-B_2O_3-SiO_2 system exists (searlesite, $Na_2O \cdot B_2O_3 \cdot 4SiO_2 \cdot 2H_2O$).

of reedmergnerite melted incongruently at 862° C. in 44 hours to form a glass crowded with crystals of quartz and tridymite. The glass obtained from the natural crystals, containing the inclusions noted, had an index of refraction of 1.48, which is lower than that of a glass of exact $Na_2O \cdot B_2O_3 \cdot 6SiO_2$ composition, made by Morey. This had an index of refraction 1.505 ± 0.003. Attempts to crystallize this glass under hydrothermal conditions yielded quartz and other unidentified crystalline phases, none of them reedmergnerite.

Subsequently using considerably higher pressures (30,000 psi) Hans Eugster prepared crystals with the optics and *x*-ray diffraction pattern of reedmergnerite. A later paper will present his data on synthetic reedmergnerite and other boron analogues of feldspars and feldspathoids.

References

ALLEN, E., AND ZEIS, E. G. (1918), Methods of glass analysis with special reference to broic acid and the two oxides of arsenic: *Am. Ceramic Soc. Journ.*, **1**, 739–786.

BRADLEY, W. H. (1931), Origin and microfossils of the oil shale of the Green River formation of Colorado and Utah: *U. S. Geol. Survey Prof. Paper* **168**, 58 p.

COLE, W. F., SÖRUM, H., AND TAYLOR, W. H. (1951), The structures of the plagioclase felspars. I: *Acta Cryst.* **4**, 20–29.

HILDEBRAND, F. A. (1953), Minimizing the effects of preferred orientation in x-ray powder diffraction patterns: *Am. Mineral.*, **38**, 1051–1056.

MILTON, CHARLES, AXELROD, J. M., GRIMALDI, F. S. (1954), New minerals, reedmergnerite ($Na_2O \cdot B_2O_3 \cdot 6SiO_2$) and eitelite ($Na_2O \cdot MgO \cdot 2CO_2$), associated with leucosphenite, shortite, searlesite, and crocidolite in the Green River formation, Utah (abstract): *Geol. Soc. America Bull.*, **65**, 1286–1287.

MOREY, G. W. (1951), The ternary system Na_2O-B_2O_3-SiO_2: *Soc. Glass Technology Jour.* **35**, 270–283.

Manuscript received June 1, 1959.

THE AMERICAN MINERALOGIST, VOL. 45, JANUARY–FEBRUARY, 1960

X-RAY STUDY OF ALTERATION IN THE URANIUM MINERAL WYARTITE*

JOAN R. CLARK, *U. S. Geological Survey, Washington 25, D. C.*

ABSTRACT

X-ray examinations of the mineral wyartite, assigned the chemical formula $UO_2 \cdot 6UO_3 \cdot 2CO_2 \cdot 3CaO \cdot 12\text{-}14H_2O$ by Guillemin and Protas (1959), show that with passage of time the mineral is altering. Up to the present time two phases, both orthorhombic, have been found from repeated precession *x*-ray examination of a single crystal: wyartite I (comparable to "ianthinite" described by Bignand, 1955), $a = 11.25 \pm 0.03$, $b = 7.09_8 \pm 0.03$, $c = 20.80 \pm 0.06$ Å, space group $P2_12_12_1\text{-}D^4_2$ (no. 19), pseudo space-groups $P2_1cn\text{-}C^9_{2v}$ (no. 33) or $Pmcn\text{-}D^{16}_{2h}$ (no. 62); wyartite II (not previously described), $a = 11.25 \pm 0.03$, $b = 7.09_8 \pm 0.03$, $c = 16.83 \pm 0.05$ Å, space groups $P2_1cn\text{-}C^9_{2v}$ (no. 33) or $Pmcn\text{-}D^{16}_{2h}$ (no. 62), pseudo space-group $Pbcn\text{-}D^{14}_{2h}$ (no. 60). Indexed *x*-ray powder diffraction data for both phases are given. The alteration occurs without visible external change in the crystals, so that interpretation of chemical analyses on macroscopic samples may be open to question. The precise nature of the alteration is still unknown, although oxidation of U^{+4} to U^{+6}, with formation of uranyl ions, possibly also accompanied by some dehydration, seems to be a plausible explanation.

INTRODUCTION

In the course of studies in this laboratory on uranyl oxide hydrates and related compounds (Christ and Clark, in press), interest in ianthinite led to *x*-ray examination of the uranium mineral described as "ianthinite" (Bignand, 1955). The material of Bignand was later said to be distinct from ianthinite (Destas, Vaes, and Guillemin, 1958) and has recently been named wyartite (Guillemin and Protas, 1959).

The wyartite crystals used in the present study are from the sample originally described as "ianthinite" by Bignand (1955). The crystals occur on Shinkolobwe specimen no. 2222, Museum of the Belgian Congo, Tervuren, Belgium (M.C.B. no. 2222) and were made available to the author through the courtesy of Dr. Claude Guillemin, Bureau de Recherches Géologiques, Géophysiques, et Minières, Paris, France.

SINGLE-CRYSTAL STUDIES

X-ray examinations of single crystals were made on a quartz-calibrated precession camera with both Mo/Zr and Cu/Ni radiations ($\lambda MoK\alpha = 0.7107$ Å; $\lambda CuK\alpha = 1.5418$ Å). Film measurements were corrected for both horizontal and vertical film shrinkage.

Crystallographic data found in this study for one crystal at different times are given in Table 1. The phase associated with crystal data found in August, 1956, is referred to in this paper as wyartite I, and the later phase, associated with data of January, 1959, is referred to as wyartite

---

* Publication authorized by the Director, U. S. Geological Survey.

TABLE 1. CRYSTALLOGRAPHIC DATA FOR WYARTITE I AND WYARTITE II†

	Wyartite I	Wyartite II
a	11.25 ± 0.03 Å	11.25 ± 0.03 Å
b	$7.09_8\pm0.03$	$7.09_8\pm0.03$
c	20.80 ± 0.06	16.83 ± 0.05
a:*b*:*c*	1.585:1:2.930	1.585:1:2.371
Cell Volume	1661 Å^3	1344 Å^3
True Space-Groups	$P2_12_12_1-D^4_2$ (no. 19)	$P2_1cn-C^9_{2v}$ (no. 33) or $Pmcn-D^{16}_{2h}$ (no. 62)
Pseudo Space-Groups	$P2_1cn-C^9_{2v}$ (no. 33) or $Pmcn-D^{16}_{2h}$ (no. 62)	$Pbcn-D^{14}_{2h}$ (no. 60)

† All measurements are from patterns obtained of one crystal; patterns for wyartite I were taken in August, 1956; patterns for wyartite II were taken in January, 1959. See also Figs. 1 and 2.

II. Wyartite I data correspond to those given by Bignand (1955) for "ianthinite"; the two sets of data are compared in Table 2. The crystal under present examination is tabular on {001} and nearly square, being only slightly elongated [010]; at one end the crystal has the {110} forms as shown on a sketch of an "ianthinite" crystal by Bignand (1955). The color of the crystal is dark violet in reflected white light, pale violet in transmitted white light.

During the observation interval of slightly more than two years a

TABLE 2. COMPARISON OF CRYSTAL DATA FOR WYARTITE I AND IANTHINITE

	Wyartite I		Ianthinite
	Present Study	Bignand (1955)	Guillemin and Protas (1959)
a (Å)	11.25 ± 0.03	11.25 ± 0.03	11.52 ± 0.05
b (Å)	$7.09_8\pm0.03$	7.08 ± 0.02	7.15 ± 0.02
c (Å)	20.80 ± 0.06	20.98 ± 0.05	30.3 ± 0.1
Cell Volume (Å^3)	1661	1671.06	2496*
Space Group	$P2_12_12_1-D^4_2$		
Chemical Formula	—	$UO_2\cdot6UO_3\cdot2CO_2\cdot3CaO\cdot10H_2O$	$UO_2\cdot5UO_{+3}\cdot10\cdot56H_2O$
Z	†	2	4
Density, g.cm.$^{-3}$			
(calc.)	—	4.81*	5.03*
(obs.)	—	4.94 ± 0.03‡	5.16 ± 0.05

* Calculated by present author from data of original investigator.

† Space group $P2_12_12_1$ contains positions of fourfold multiplicity only.

‡ Guillemin and Protas (1959) point out that for this determination wyartite crystals were dried at 50° C.; they find 4.69 ± 0.05 g.cm.$^{-3}$ for crystals not subjected to heat.

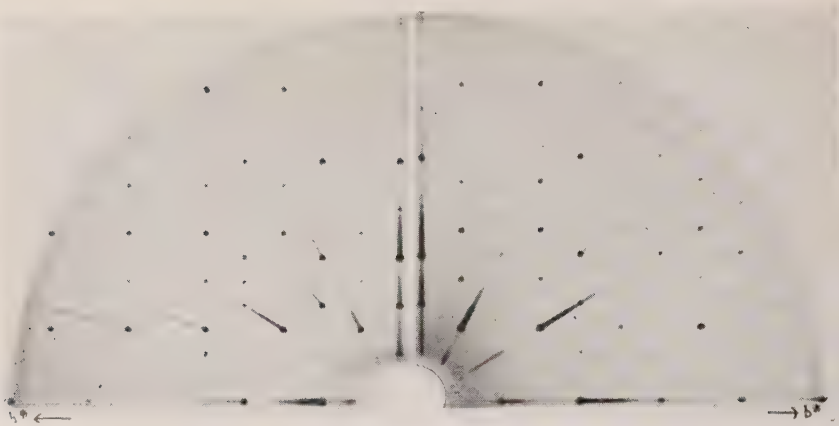

FIG. 1. (Left) Precession *hk*0 pattern of wyartite I crystal, taken August, 1956, with Mo/Zr radiation. (Right) Precession *hk*0 pattern of same crystal, now altered to wyartite II, as shown by the changed intensity distribution. Film taken January, 1959, with Mo/Zr radiation.

shrinkage of about four Ångstroms has occurred in the *c*-length; the shrinkage is accompanied by a change in space group (Table 1). In addition, extensive changes in the overall intensity distribution have taken place (Fig. 1) indicating that shifts in atomic positions have occurred. Taken together, the evidence shows that alteration on an atomic scale is in progress within the crystal; yet its external appearance is unchanged except for a slight splitting-apart of the (001) plates. The color of the crystal is unchanged from the violet originally described for "ianthinite" by Bignand (1955) and illustrated in Destas, Vaes, and Guillemin (1958).

No *x*-ray patterns of this crystal were ever obtained without appearance of some wyartite II reflections (Fig. 2). Patterns taken in 1956 of another wyartite crystal were later interpreted as showing both phases approximately equally represented. Comparison with results from previous study of schoepite alteration products (Christ and Clark, in press) shows that the stage of alteration present in any one crystal can be determined only by *x*-ray examination, preferably by precession camera techniques. It follows that chemical analyses and density determinations carried out to date on macroscopic samples cannot be directly correlated with the crystal data for either one of the phases.

X-RAY POWDER DIFFRACTION DATA

In August, 1956, a powder spindle (no. 8596) of wyartite was prepared from the crystals of M.C.B. no. 2222. An *x*-ray powder pattern was taken with a 114.59 mm. diameter powder camera using Cu/Ni radiation

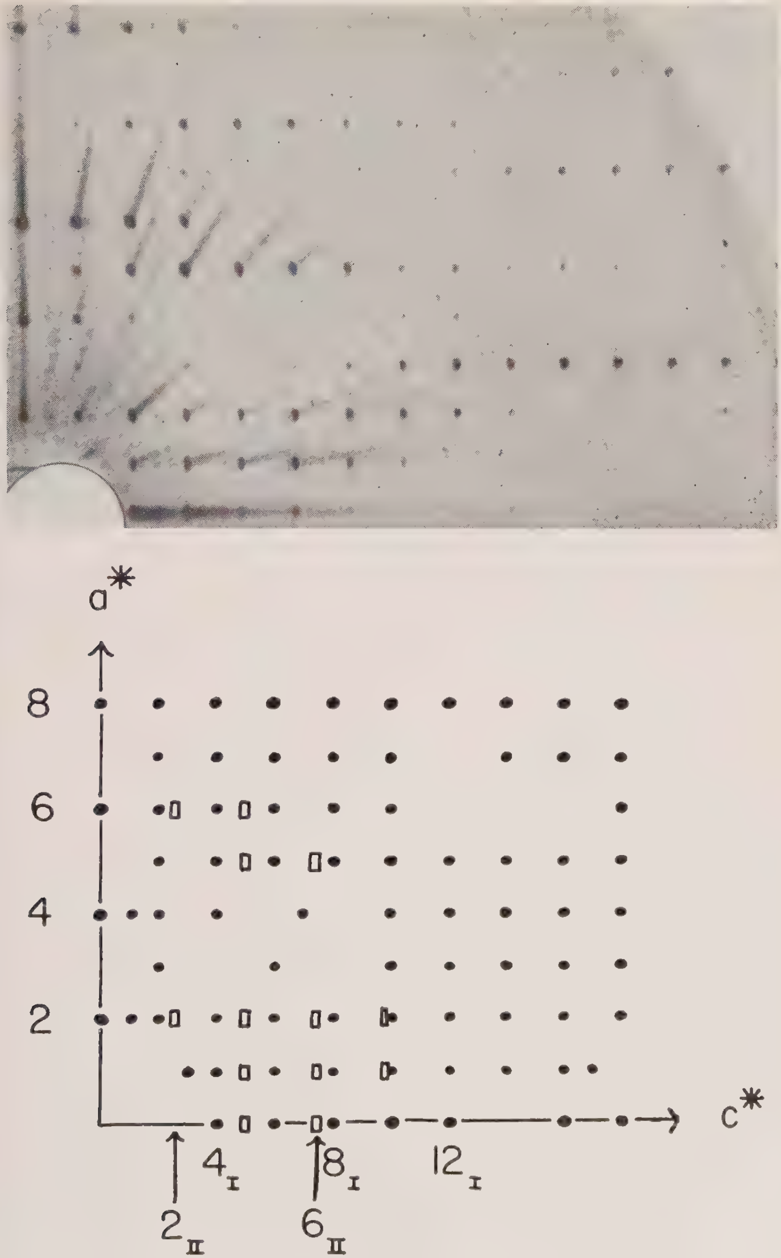

FIG. 2. (Above) Precession *h0l* net of wyartite, showing dominant wyartite I pattern appearing together with diffuse reflections of wyartite II. Mo/Zr radiation. (Below) Indexed *h0l* net for wyartite. Dots correspond to reflections of wyartite I, rectangles to wyartite II.

TABLE 3. *X*-RAY POWDER DATA FOR WYARTITE I

($UO_2 \cdot 6UO_3 \cdot 2CO_2 \cdot 3CaO \cdot 12\text{–}14\ H_2O$, according to Guillemin and Protas, 1959)

Present Study: Film no. 11454, taken August 3, 1956; powder spindle no. 8596. Orthorhombic: $P2_12_12_1-D^4_2$ (no. 19), with pseudo space-groups $P2_1cn-C^9_{2v}$ (no. 33) or $Pmcn-D^{16}_{2h}$ (no. 62); $a=11.25\pm0.03$, $b=7.09_8\pm0.03$, $c=20.80\pm0.06$ Å.

Measured[1]						Calculated[2]		
Bignand (1955)[3]		Guillemin and Protas (1959)[4]		Present Study[5]				Single Crystal Intensity[6]
I[7]	d_{hkl}	I[7]	d_{hkl}	I	d_{hkl}	d_{hkl}	*hkl*	
FF	10.29	FF	10.39	100	10.3	10.40	002	*
		fff	8.57	30	8.5_4	(8.42	002 W-II)[8]	*
ff	7.60	ff	7.63	3	7.6_4	7.64	102	m
				<1	6.7_7	(6.74	102 W-II)[8]	vw
						6.72	011	a
						6.00	110	*
						5.86	012	a
				<1	5.77	5.77	111	m
						5.62	200	m
mF	5.19	F	5.18	30	5.19	5.20	004	s
						5.20	112	a
						4.96	013	a
						4.95	202	m
		ff	4.68	3	4.72	4.72	104	m
						4.54	113	a
		ff	4.33			4.31	211	*
				4d[9]	4.26	(4.21	004 W-II)[8]	m
						4.20	014	a
m	4.07					4.06	212	*
				<1	3.98	(3.941	104 W-II)[8]	vw
						3.930	114	a
				<1	3.83	3.818	204	m
		ff	3.745	<1	3.72	3.720	213	*
						3.589	015	a
		m	3.53	4	3.55	3.549	020	s
						3.528	302	vw
						3.498	021	m

[1] Wyartite from M.C.B. specimen no. 2222 (Shinkolobwe, Katanga) was used to obtain each of the patterns. Radiation in each case, Cu/Ni: λCuKα=1.5418 Å.

[2] Interplanar spacings are given for all *hkl* permitted by the pseudo space-groups and having $d_{hkl}\geq 2.750$ Å. The few additional *hkl* of the true space-group have intensities too weak for their appearance on the powder films.

[3] Camera diameter, 240 mm. Interplanar spacings converted from kX to Ångstrom units by present author.

[4] Camera diameter not given.

[5] Camera diameter, 114.59 mm. Film shrinkage negligible; lower limit of 2θ measurable, approximately 7° (13 Å). Film no. 11454 taken August 3, 1956, with powder spindle no. 8596. Compare to data in Table 4 for film no. 14253 taken January 9, 1959, of the same powder spindle.

[6] Intensities estimated visually from precession films of varying exposure times; radiation, Mo/Zr, λMoKα=0.7107 Å. * means no observation could be made for a given reflection, either because an appropriate film was not available or because of the large low-angle cut-off for MoKα radiation. Other abbreviations are: vs, very strong; s, strong; m, medium; w, weak; vw, very weak; a, absent.

[7] FF=very strong, F=strong, mF=medium strong, m=medium, mf or fm=medium weak, f=weak, ff=very weak, fff=very very weak.

[8] Line identified as wyartite II; see Table 4.

[9] d=diffuse.

TABLE 3 (*continued*)

Measured[1]						Calculated[2]		
Bignand (1955)[3]		Guillemin and Protas (1959)[4]		Present Study[5]				Single Crystal Intensity[6]
I[7]	d_{hkl}	I[7]	d_{hkl}	I	d_{hkl}	d_{hkl}	*hkl*	
		m	3.46	10	3.47	3.467	006	vs
						3.419	115	vw
						3.363	214	a
						3.359	022	s
f	3.35	m	3.35	7	3.36	3.341	121	w
						3.316	310	s
						3.313	106	m
mF	3.28	F	3.27	10	3.28	3.274	311	*
						3.218	122	m
		f	3.16	3	3.16	3.159	312	*
						3.159	023	m
						3.115	016	a
				<1	3.08$_1$	(3.085	312 W-II)[8]	*
						3.042	304	a
				5d[9]	3.03$_5$ to 2.976	3.042	123	vw
						3.026	215	s
m	3.01					3.002	220	vw
						3.002	116	vw
						2.991	313	*
						2.971	221	vw
		m	2.93	4	2.945	2.951	206	m
						2.931	024	s
		f	2.91			2.884	222	m
						2.837	124	m
						2.812	400	s
						2.796	313	*
						2.754	223	w
m	2.59	fm	2.59	5	2.592			
f	2.52	ff	2.52	4	2.532			
f	2.46	f	2.46	4	2.470			
				<1	2.420			
				<1	2.363			
f	2.20	f	2.21	<1	2.206			
				<1	2.095			
mf	2.03	f	2.05	5	2.047			
ff	2.00	ff	1.995	4	1.999			
ff	1.96	ff	1.963	1	1.969			
				<1	1.955			
		ff	1.922	1	1.928			
plus additional weak lines								

(λCuKα = 1.5418 Å). The interplanar spacings and intensities of the lines observed on this pattern are given in Table 3, together with data for material from M.C.B. no. 2222 reported by Bignand (1955) and by Guillemin and Protas (1959). All the experimental observations are in good agreement and most of the observed lines can be indexed from the single-crystal data for wyartite I. All calculated interplanar spacings for $d \geq 2.750$ Å are given in Table 3.

TABLE 4. X-RAY POWDER DATA FOR WYARTITE II

Film no. 14253, taken January 9, 1959; powder spindle no. 8596.

Orthorhombic: $P2_1cn - C^9_{2v}$ (no. 33) or $Pmcn - D^{16}_{2h}$ (no. 62), with pseudo space-group $Pbcn - D^{14}_{2h}$ (no. 60); $a = 11.25 \pm 0.03$, $b = 7.09_8 \pm 0.03$, $c = 16.83 \pm 0.05$ Å.

Measured[1]			Calculated[2]	
I[3] (Single Crystal)	I (Powder)	d_{hkl}	d_{hkl}	hkl
*	13	10.7	(10.40	002 W-I[4])
*	100	8.4_6	8.42	002
m	3	6.7_5	6.74	102
*		6.08	6.00	110
	1d[5]	to		
vw		5.66	5.65	111
vw			5.62	200
w	3	5.18	(5.20	004 W-I[4])
*			4.89	112
s	2	4.68	4.68	202
w			4.26	211
vs	18	4.22	4.21	004
*			4.10	113
s	6	3.94	3.941	104
s			3.905	212
s	9	3.56	3.549	020
vs	21	3.47	3.473	021
s			3.466	213
a			3.445	114
vw			3.425	302
m		3.37	3.369	204
w		↑	3.318	121
vs	6b[6]	3.31	3.316	310
m		↓	3.270	022
vs		3.24	3.253	311

[1] Wyartite from M.C.B. specimen no. 2222, originating in Shinkolobwe, Katanga. Camera diameter, 114.59 mm; radiation, Cu/Ni: $\lambda \text{CuK}\alpha = 1.5418$ Å. Film shrinkage negligible; lower limit of 2θ measurable, approximately 7°(13 Å).

[2] Interplanar spacings are given for all hkl permitted by the pseudo space-group and having $d_{hkl} \geq 2.700$ Å. The few additional hkl of the true space-group have intensities too weak for their appearance on the powder film.

[3] Intensities estimated visually from precession films of varying exposure times; radiation, Mo/Zr, $\lambda \text{MoK}\alpha = 0.7107$ Å. *means no observation could be made for a given reflection, either because an appropriate film was not available or because of the large low-angle cut-off for MoKα radiation. Other abbreviations are: vs, very strong; s, strong; m, medium; w, weak; vw, very weak; a, absent.

[4] Line identified as wyartite I; see Table 3.

[5] d = diffuse.

[6] These three lines are unresolved on the pattern; measurements were taken at end points of the broad intensity band and at the central strong region; b = broad.

TABLE 4 (*continued*)

Measured[1]			Calculated[2]	
I[3] (Single Crystal)	I (Powder)	d_{hkl}	d_{hkl}	*hkl*
vw	1	3.16	3.140	122
s	2	3.09_2	3.085	312
w			3.044	214
a			3.002	200
vs	9	3.00_2	2.999	023
w			2.955	221
w	1	2.934	2.936	115
m			2.898	123
s	2	2.858	2.854	313
vw			2.827	222
s			2.812	400
s	2	2.802	2.805	006
vw			2.799	304
m	2	2.723	2.722	106
vw			2.713	024
	2	2.602		
	1	2.512		
	2	2.442		
	2	2.377		
	1	2.243		
	1	2.221		
	1	2.189		
	2	2.102		
	3	2.068		
	6	2.000		
	1	1.966		
	3	1.944		
	3	1.880		
	plus additional lines, all with I (powder) ≤ 2			

After alteration of the single crystal was observed in the present study, another *x*-ray powder pattern of spindle no. 8596 was taken in January, 1959. This pattern is strikingly different from the original one and yields data that apparently have not been previously reported. Most of the observed lines can be indexed from the single-crystal data for wyartite II, and in Table 4 observed data are listed together with all calculated interplanar spacings for $d \geq 2.700$. The wyartite II data also permit indexing of the lines previously unaccounted for on the original pattern, and these lines are identified in Table 3. A few lines corresponding to the presence of wyartite I still occur on the more recent pattern, and in

Table 4 these lines are identified. Approximate intensities for single-crystal reflections, listed in Tables 3 and 4, were estimated visually from precession films to verify indexing of the powder patterns. The powder diffraction data for wyartite I and for wyartite II are distinctive from those reported for ianthinite and epi-ianthinite (Frondel, 1958; Guillemin and Protas, 1959).

At present the nature of the alteration that has occurred in wyartite is unknown, although it is undoubtedly connected, at least in part, with the oxidation of U^{+4} to U^{+6} and formation of the $[O\text{-}U\text{-}O]^{+2}$ uranyl ion. Some dehydration may also be taking place. It is not yet certain whether the alteration process is complete or will continue, so the crystal and the powder spindle will be kept under observation and any future developments of interest will be reported.

ACKNOWLEDGMENTS

I am deeply indebted to Dr. Claude Guillemin for providing the crystals from M.C.B. no. 2222, and to Dr. Guillemin and Dr. J. Protas for letting me see their manuscript in advance of publication. This study is part of a program being conducted by the U. S. Geological Survey on behalf of the Division of Research, U. S. Atomic Energy Commission.

I am grateful to several colleagues at the U. S. Geological Survey for assistance in the course of this study. Mary E. Mrose made available the crystals supplied by Dr. C. Guillemin, took *x*-ray powder pattern no. 14253, and provided helpful discussion. Other *x*-ray powder patterns were taken by F. A. Hildebrand who also prepared powder spindle no. 8596. Calculations of interplanar spacings were carried out by D. E. Appleman on a digital computer. C. L. Christ and H. T. Evans, Jr., contributed valuable suggestions in the course of numerous discussions.

REFERENCES

BIGNAND, C. (1955), Sur les propriétés et les synthèses de quelques minéraux uranifères: *Soc. française Minéral. et Crist. Bull.* **78,** 1–26.

CHRIST, C. L., AND CLARK, JOAN R. (in press), Crystal chemical studies of some uranyl oxide hydrates: *Am. Mineral.* (in press).

DESTAS, A., VAES, J. F., AND GUILLEMIN, C. (1958), Minéraux d'uranium du Haut Katanga: "Les Amis du Musée royal du Congo Belge," Tervuren, Belgium.

FRONDEL, CLIFFORD (1958), Systematic mineralogy of uranium and thorium: *U. S. Geol. Survey Bull.* **1064,** 62–91.

GUILLEMIN, C., AND PROTAS, J. (1959), Ianthinite et wyartite: *Soc. française Minéral. et Crist. Bull.* **82,** 80–86.

Manuscript received June 8, 1959.

THE AMERICAN MINERALOGIST, VOL. 45, JANUARY–FEBRUARY, 1960

THE CRYSTAL CHEMISTRY OF DAHLLITE

DUNCAN MCCONNELL,* *Ohio State University, Columbus, Ohio*

ABSTRACT

Chemical and powder diffraction data are given for fossilized dental enamel from a mastodon tooth. The specific gravity is 2.968 (20°/4° C.) and $a_0=9.454$, $c_0=6.892$ Å.

Calculations, analogous to those previously made for francolite, indicate that the carbonate groups enter the structure as substitutions for phosphate groups. However, (CO_3OH) does not appear to be an accurate representation. The recent supposition that carbonate groups can substitute for (F, OH) groups of normal apatite is untenable.

INTRODUCTION

Through personal conversations with several mineralogists, it has become evident that they regard the problem of the carbonate apatites as solved. They find such formulations as $Ca_5F/(PO_4, CO_3OH)_3$ in recent reference books, and are quite willing to accept this representation as a close approximation, at least. However, they are not mindful of the reluctance of the physiological chemists to accept any portion of the mineralogical investigations as analogous to the problem of tooth and bone composition.

Certain chemists are more than mildly perturbed about "amorphous $CaCO_3$", various synthetic concoctions which produce apatitelike diffraction patterns but show a range of Ca/P ratios, how the carbonate ions can substitute for phosphate ions in the structure whereas citrate ions cannot, and numerous *non-sequiturs* that have been presented as "conclusions" after heating and dissolving various solid materials, both natural and synthetic and with or without other treatment. A summary of most of these views, including an extensive bibliography, has been presented by Carlström (1955), who states: "Summarizing the views on the structure of the carbonate-apatites, it may be concluded that they do not exist as homogeneous single phase compounds but are composed of a microcrystalline, somewhat 'impure,' fluorapatite with 'amorphous' carbonate mainly in the form of $CaCO_3$, and from that point of view they are of great interest in relation to the state of the carbonate in calcified tissues." Although this statement will astonish numerous mineralogists who have had first-hand experience with carbonate apatites (see: McConnel and Gruner, 1940), it is more or less typical of numerous "mineralogical" interpretations by persons completely unfamiliar with mineralogical methods of investigation.

Being familiar with the fundamental principles of solid-state physics and chemistry, mineralogists raise questions which are quite different from those which disturb the physiological chemists, and there is no need to explain to the former group that the "citrate ion" (containing seven oxygens) cannot enter the apatite crystal structure to produce an isomorphic variant whereas the carbonate group can do precisely this. Furthermore, crystal chemists quickly recognize that some minor changes in the structure would necessarily result as a consequence of the introduction of carbonate groups:

---

* Public Health Service Research Fellow, National Institute of Dental Research.

(1) The optical properties, particularly the birefringence, might be altered.
(2) The cell dimensions, intensities of diffraction from certain planes, and specific gravity might be altered.
(3) The structure might be converted from hexagonal to lower symmetry and the optical properties and twinning might reveal that the structure is merely pseudohexagonal.

All of these criteria are satisfied in the case of francolite, but the data for dahllite are not nearly so adequate.

A recent book, *The Chemical Dynamics of Bone Mineral*, for example, states: "It is difficult to attain a clear-cut comprehension of the crystallography of hydroxy apatite when the mineralogists themselves do not agree on rather fundamental interpretations." The authors, Neuman and Neuman (1958), also refer to such substances as phosphorite as forming at "high temperatures," apparently without realizing that the temperatures need be no greater than temperatures encountered in present-day oceans. Certain portions of their chemistry are as confused as their geology and mineralogy, particularly such statements as: "One cannot approach the same *equilibrium* from the two directions—precipitation and dissolution." (Italics added.) It is to be remembered that the title of this book contains the word "mineral." Although it seems unlikely that workers in these areas can be expected to consult mineralogical literature with comprehension, there is good reason for recording the fundamental data and interpretations, nevertheless.

Accordingly, certain fundamental investigations have been carried out on a sample of post-Wisconsin fossilized dental enamel from a mastodon, found near Bluffton, Ohio. It was furnished through the courtesy of Dr. Mildred Marple of the Geology Department. The *x*-ray diffraction data were supplied by Dr. Leslie C. Coleman of the Mineralogy Department. The chemical analysis was made at the Laboratory for Rock Analysis at the University of Minnesota under the direction of Dr. S. S. Goldich. Most of the remaining sample has been deposited with the National Museum (U.S.N.M. 113977).

EXPERIMENTAL DATA AND INTERPRETATIONS

Shown in Table 1 are the results of chemical analysis and the calculations used to determine the contents of the unit cell. From the "molec-

TABLE 1. SUMMARY CALCULATIONS ON ANALYSIS OF DENTAL ENAMEL FROM MASTODON TOOTH

(C. O. Ingamells, Analyst)

Oxides	Weight per cent	Oxide ratios	Relative charges of cations	Cation charges $\Sigma=53.0$	Atoms per unit (cations)	Structural locations*	
CaO	51.44	.9173	1.835	18.21	9.11	Ca, Mg, Na	9.45
MgO	0.34	.0084	.017	.17	.08	C	[.19]
Na_2O	0.80	.0129	.026	.26	.26	H_3	.55
						Ca Positions	10.00
CO_2	2.72	.0618	.247	2.45	.61	H_2O (excess)	.24
H_2O+	2.83	.1570	.314	3.12	4.00		
H_2O-	0.80	.0444	.089	.88			10.24
						P	5.58
P_2O_5	39.92	.2812	2.812	27.91	5.58	C	.42
						P Positions	6.00
Cl	0.42	.0118‡					
F	0.03	.0016‡					
Others†	0.19	—				Cl, F	.13
						OH	1.87
						F Positions	2.00
	99.49						
Less O	.10						
	99.39			53.00§			

* The method of calculation, which includes assignment of H_3O^+ and C structurally replacing Ca (although the H_3O^+ and C are not additive), causes the accumulated error to occur in the summation of the Ca positions. There is an excess of 0.24 expressed as H_2O.

† Others: Al_2O_3 0.07, Fe_2O_3 0.03, K_2O 0.05, Insoluble 0.04, SO_3 trace, and N_2O_5 trace.

‡ Chlorine and fluorine must be adjusted by the same factor that was applied to other oxide ratios, namely 9.925.

§ The summation of cationic charges is taken as 53.0. To the usual 26 large anions (O+F+Cl) must be added any oxygens which occur as H_3O^+ (see first note above) but compensating deductions must be made for Cl and F.

ular" weight, the specific gravity is calculated to be 3.062, whereas the experimental value with reference to water at 4° C. was found to be 2.968 by means of a Roller-Smith torsion balance. The disagreement is attributed to porosity of the fossilized dental enamel; it is approximately three per cent.

No difficulty was encountered in separating an adequate sample of pure dental enamel from the dentin, and microscopic examination failed to reveal any lack of homogeneity (Fig. 1). Ingamell's analysis does not show a particularly satisfactory summation despite repetition of most of the determinations. It is assumed that the explanation lies in the tenacity of hydroxyl ions, even at high temperatures. The calculations have been made, of course, on the actual analytical constituents reported and, of necessity, would be subject to slight modification if more water were assumed to be present.

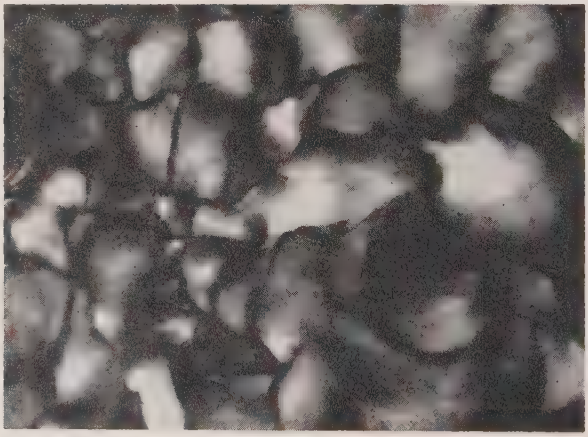

FIG. 1. Fossilized dental enamel of mastodon in section cut approximately parallel with the enamel surface. Shown are the peculiar convolutions (bending and grouping) of the enamel rods (bundles or aggregates of crystal with their *c* axes more or less parallel). Mag. 30×; polarizing prisms slightly rotated from "crossed" position.

The calculations indicate, as has been shown previously for francolite, that $(CO_3)^{-2}$ groups enter the structure in substitution for $(PO_4)^{-3}$ groups. The data on francolite do not fit the assumption that $(CO_3OH)^{-3}$ substitutes for $(PO_4)^{-3}$ because there is not a straightforward relation between the water and the carbon dioxide contents. The best interpretation still postulates (CO_3) groups entering the structure in such a manner that some Ca ions are omitted, i.e. some (CO_3) groups lie parallel to (00.*l*), whereas approximately three times as many CO_3 groups are essentially perpendicular to (00.*l*) and are distributed symmetrically about an axis which has essentially (pseudo) threefold symmetry (McConnell, 1952A and 1952B).

Powder diffraction data obtained goniometrically are contained in Table 2, which also gives supplementary data on precise measurements made with the North American Philips goniometric apparatus.

TABLE 2. X-RAY POWDER DIFFRACTION DATA FOR DAHLLITE

(Dental Enamel of Mastodon)

Line number	hk.l	I	$d_{\text{calc.}}$	$d_{\text{exp.}}$
1	20.0	1	4.094	4.092
2	11.1	2	3.899	3.897
3	00.2	3	3.446	3.446
4	12.0	3	3.095	3.096
5	12.1 11.2	>10	2.823 2.785	2.811
6	30.0	8	2.729	2.730
7	20.2	2	2.636	2.627
8	30.1	<1	2.537	2.533
9	13.0	3	2.271	2.270
10	11.3	1	2.066	2.056
11	22.2	3	1.950	1.947
12	13.2	1	1.896	1.893
13	23.0	1	1.878	1.878
14	23.1	1	1.812	1.808
15	14.0	1	1.787	1.785
16	40.2 30.3	1	1.760 1.758	1.757
17	00.4	1	1.723	1.723

Precision measurements made with North American Philips apparatus:

$d_{12.0}=3.0959\pm.0021$
$d_{13.0}=2.2696\pm.0006$
$d_{30.0}=2.7295\pm.0004$
$d_{00.2}=3.4460\pm.0013$
$a_0=9.454\pm<.004$
$c_0=6.892\pm.0025$
Cu*K* radiation, Ni filter

Wallaeys (1954) has described a synthetic carbonate apatite for which he concludes that the (CO_3) groups are all arranged in such positions as to substitute for (OH) ions, i.e. arranged essentially parallel to (00.*l*) but on the 6_3 axes. His cell dimension for the *a* direction greatly exceeds any previously reported for any carbonate-containing apatite. He reports $a=9.518$ *kX* as compared with 9.454 Å obtained in the present work for a substance containing more than an adequate amount of (OH, F) to fill these positions. Again, as was the situation with francolite, it seems highly improbable that (CO_3) groups would enter this structure in positions on the 6_3 axes—other monovalent anions being present in excess. The larger *a* dimension obtained by Wallaeys may be the result of (O_4H_4) groups substituting for (PO_4) groups; neither the precise composition of his original synthetic "hydroxyapatite" nor its carbonated product were determined by direct analytical methods.

SUMMARY

Despite what may be a slight increase in chlorine content brought about during the process of fossilization, the dahllite sample investigated still deserves every consideration as a carbonate apatite analogous to the inorganic substance of teeth and bones. Reference to the substance of teeth and bones as "hydroxyapatites" is a misnomer; statements concerning the non-existence of carbonate apatites are absurdities based solely upon conjecture.

TABLE 3. RATIOS OF LARGE CATIONS TO PHOSPHORUS FOR CARBONATE-APATITE MINERALS

Mineral	Locality and reference	Ratio Atomic Ca′/P′	Ca′	P′
Dahllite	Bluffton, Ohio present work	1.69	Ca, Mg, Na	P
Dahllite	Mouillac, France McConnell (1938)	1.72	Ca, Na, K*	P, S
Francolite (Quercyite)	François Lake, B.C. Poitevin (1927)	1.82	Ca†	P
Francolite	Busumbu, Uganda Davis (1947)	1.77	Ca, Mg	P
Francolite	Staffel, Germany Gruner & McConnell (1937)	1.85	Ca, Mg	P, V
Francolite	Richtersveld, So. Africa de Villiers (1942)	2.02	Ca, Mg, Na	P
Francolite	Yorkshire, England Deans (1938)	1.81	Ca, Sr	P
Francolite	Tavistock, Devon Sandell, *et al.* (1939)	1.80	Ca, Mg	P

* Oxides disregarded as "impurities" were Fe_2O_3, Al_2O_3, SiO_2.

† Disregarded were: FeO, Fe_2O_3, Mn_2O_3, Al_2O_3, MgO, SiO_2 and organic C.

Most of the investigations of synthetic "hydroxyapatites," particularly those showing an appreciable range of Ca/P, can be dismissed as meaningless with respect to crystal chemical interpretation because of inadequate evidence that the preparations consisted of a single, homogeneous crystalline phase. One of Carlström's precipitates for example, contains diffraction lines that cannot be attributed to apatite. Also, it is particularly noteworthy that mineral carbonate apatites, like teeth and bones, do not tend to have Ca/P ratios below the theoretical value (1.667) provided other divalent and monovalent cations are taken with calcium (Table 3). To be sure, the reason for these higher values depends upon the proportionally greater substitution of carbon for phosphorus. No constancy would be expected for this ratio, and this prediction is entirely consistent with the experimental results given in Table 3.

That several persons are pretending to have a knowledge of crystallography is evident from the fact that they have copied the atomic parameters of Náray-Szabó (1930) without discovering an obvious error. The literature (Carlström lists 195 references) is burdened with meaningless data, faulty logic and *non sequiturs*. Many papers which have been written on the problem of the carbonate apatites show no evidence that the authors were cognizant of previous investigations on closely related segments of the problem. The earliest reference to the problem seems to be a statement by Haüy (1822) in which Werner is taken to task for assuming that phosphorite is not merely impure apatite.

Supplementary Discussion

Subsequent to the preparation of the manuscript of this paper, an important contribution on the laboratory synthesis of carbonate apatite has appeared (The genesis of carbonate apatites, L. L. Ames, Jr., *Econ. Geol.* 54, 829–841, 1959). The author states therein (p. 837): "The reaction equilibrium data and structural formulae indicate that this carbonate can be entirely present in the apatite lattice when the apatite contains less than 10 per cent by weight of CO_3^{-2}." The substance of teeth and bones, to be sure, is always far below this limit so there is no need for assuming any type of adsorptive process peculiar to the surfaces of the crystallites even for dentin and bone.

Ames concludes, furthermore, that the "structural formulae, equilibrium data, and C^{14} tracing show no indications of the carbonate being present in Hendricks' 'voids' or adsorbed to any great extent on apatite surfaces . . . ," and "the variable composition of the apatite phase, even in this relatively simple system, shows the fallacy of attempting to apply the laws of sparingly soluble compounds to apatite." Not only do Ames' opinions coincide with my opinions based upon my investigations of mineral carbonate apatites, but they are consistent with my interpretations of certain phenomena observed during synthesis and dissolution studies by other investigators.

REFERENCES

CARLSTRÖM, DIEGO (1955), *X*-ray crystallographic studies on apatites and calcified structures: *Acta Radiol.*, Supplement **121,** 59 pages.

DAVIS, K. S. (1947), The phosphate deposits of the Eastern Province, Uganda: *Econ. Geol.* **42,** 137–146.

DEANS, T. (1938), Francolite from sedimentary ironstones of the Coal Measures: *Mineral. Mag.* **25,** 135–139.

GRUNER, J. W., AND McCONNELL, D. (1937), the problem of the carbonate apatites. The structure of francolite: *Zeits. Kristallogr.* **97**A, 208–215.

HAÜY, L'ABBÉ (1822), *Traité de Minéralogie*, **I,** p. 503, Paris.

McCONNELL, DUNCAN (1938), The problem of the carbonate apatites; a carbonate oxyapatite (dahllite): *Am. Jour. Sci.* **236,** 296–303.

——— (1952A), The problem of the carbonate apatites. IV. Structural substitutions involving CO_3 and OH: *Bull. Soc. Franç. Min. Crist.* **75,** 428–445.

——— (1952B), The Crystal chemistry of carbonate apatites and their relationships to the composition of calcified tissues: *Jour. Dental Res.* **31,** 53–63. (See also: The crystal chemistry of francolite and its relationship to calcified animal tissues: *Trans. Macy Conference on Metabolic Interrelations* **4,** 169–184 (1952).)

———, AND GRUNER, J. W. (1940), The problem of the carbonate apatites. III. Carbonate apatite from Magnet Cove, Arkansas: *Am. Mineral.* **25,** 157–167.

NEUMAN, W. F., AND NEUMAN, M. W. (1958), The Chemical Dynamics of Bone Mineral. Univ. Chicago Press, 209 pages.

POITEVIN, E. (1927), A new Canadian occurrence of phosphorite from near François Lake, British Columbia: *Canada Dept. Mines, Geol. Sur. Bull.* **46,** 2–13.

SANDELL, E. B., HEY, M. H., AND McCONNELL, D. (1939), The composition of francolite: *Mineral. Mag.* **25,** 395–401.

DE VILLIERS, J. E. (1942), The carbonate apatites; francolite from the Richtersveld, South Africa: *Am. Jour. Sci.* **240,** 443–447.

Manuscript received June 4, 1959.

THE AMERICAN MINERALOGIST, VOL. 45, JANUARY–FEBRUARY, 1960

NOTES AND NEWS

A VERY HIGH PRESSURE–HIGH TEMPERATURE RESEARCH APPARATUS AND THE SYNTHESIS OF DIAMOND*

A. A. Giardini, J. E. Tydings and S. B. Levin, *U. S. Army Signal Research and Development Laboratory, Fort Monmouth, N. J.*

Introduction

The mineralogical significance of research at elevated pressures and temperatures is obvious. As striking also are the implications in the field of special electronic, magnetic and optical materials. The following is a brief report on one aspect of such a program.

A description is given of a research apparatus capable of reproducible* sustained near-hydrostatic pressures to at least 100,000 atmospheres concurrent with temperatures exceeding 3000° C. An experimental example, namely, the synthesis of diamond, also is included.

The Supported Stepped Piston–Cylinder Apparatus

Since operating pressures to 100,000 atmospheres far exceed the maximum strengths of construction materials, existing values must be extended. This can be accomplished by providing auxiliary external support to overstressed components. This principle is generously applied to the apparatus under discussion.

A cross sectional schematic of the pressure apparatus with an exploded view of critical internal components is shown in Fig. 1. Essentially the apparatus consists of two sets of symmetrically opposed stepped cemented carbide pistons,† labeled A, B, and C, and a cylinder assembly consisting of a double bore cemented carbide set, numbered 1 and 2, surrounded by a series of hardened steel bands.‡ The latter are fitted at maximum permissible interference. An outer band of mild steel is included to protect against possible fracture of the hardened steel components. The series of steel prestressing bands and the protection band are labeled 3, 4, 5 and 6. Rigid steel plates, item 7, are used to counter lateral shear tendencies in the carbide cylinder assembly.

Working force can be applied to the piston assembly by a hydraulic press of suitable capacity. Part of the force exerted on piston B is directly applied to the high pressure piston C which in turn bears upon the

---

* A reproducibility of 5% at room temperature can be achieved relative to electrical resistance discontinuities as a function of pressure for pure bismuth and barium as reported by P. W. Bridgman (1, 2, 3).

† All cemented carbides used consist of tungsten carbide with 6% cobalt.

‡ All hardened steel used is A.I.S.I. 4340 hardened to RC 52 and triple tempered.

sample volume. The remaining force is exerted (neglecting frictional losses) on the annular volume bearing against the tapered surface of B. The annular space is filled with a compressible pressure transmitting solid, generally pyrophyllite. The compressible segment permits the piston assembly to advance. The high pressure piston can thus compress the sample volume, and at the same time the resulting compressional stress in the annular cavity is transmitted to the exposed wall of the high pressure piston and to the exposed end faces of the high pressure cylinder. The transmitted pressure provides external support to these normally overstressed components, and when properly balanced, no failure occurs.

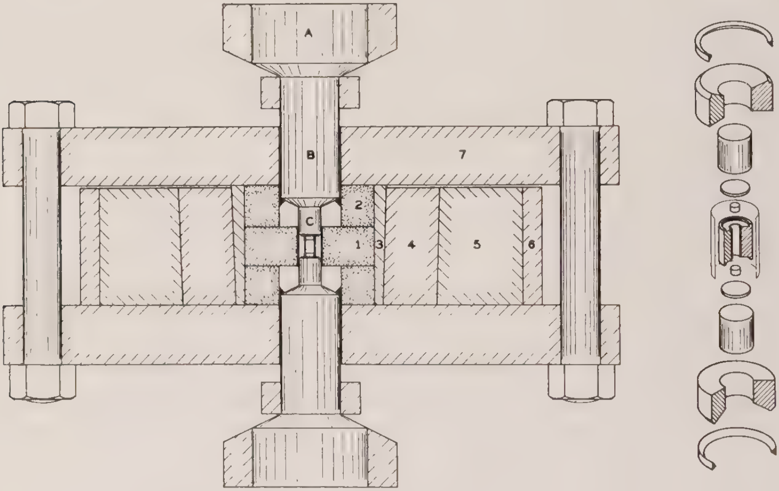

Fig. 1. A cross sectional schematic of the Very High Pressure—High Temperature Apparatus. Also included on the right is an exploded view of critical internal components. For scale, the diameter of the high pressure piston, C, is ½ inch.

The exploded view of internal components of the apparatus shown on the right of Fig. 1 consists of the following from top to bottom: (1) hardened steel seal ring in order to prevent extrusion of pyrophyllite between the piston and cylinder which might cause them to jam. (2) machined pyrophyllite support segment, (3) high pressure carbide piston, (4) metal electrical contact disk used to provide broadest coverage of the 6% cobalt content of the carbide, (5) thin electrical insulation sheath to isolate the high pressure piston from the carbide cylinder bore, (6) metal plugs to compact and contain the sample within the electrical resistance heating tube shown along the axial bore of the pyrophyllite specimen cylinder. The remaining items are symmetrical analogues.

Low voltage electrical power leads are attached to pistons A. Pistons B are insultated from their cyclinder walls by a thin sheet of suitable dielectric material. Temperature measurements are made under specific pressures by means of a thermocouple placed into the sample volume through a small axial bore through a special set of B and C pistons. Calibration data are obtained on the basis of power input for given temperatures for fixed experimental systems. Data can be extrapolated to higher pressures by use of the Simon melting equation (4).

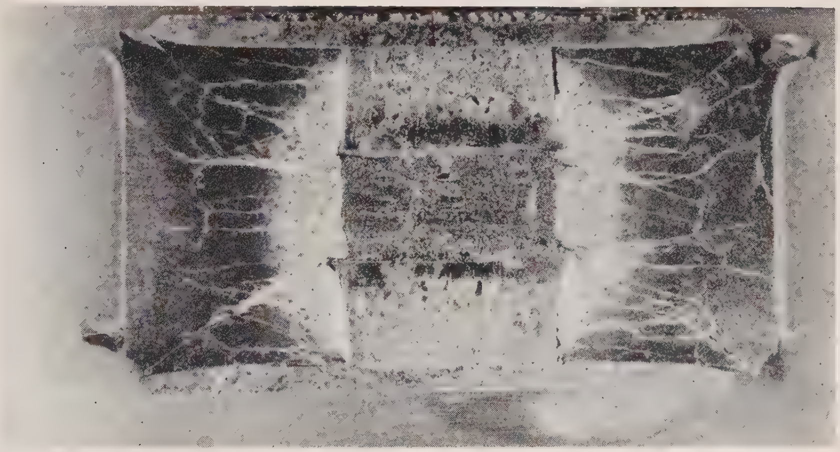

FIG. 2. A cross section of an actual pyrophyllite cylinder containing nickel-carbon-nickel from top to bottom, respectively, which has been stressed to 85,000 atmospheres at approximately 1560° C. for 3 minutes. Note the diamond growth at the top center of the graphite section. Scale is ½ inch for the horizontal width of the cylinder.

DIAMOND SYNTHESIS

Although the first diamond synthesis was achieved by man in 1955 (5), it has been only recently that details on the method have been made available to the public (6, 7). With the proper apparatus, diamond synthesis is remarkably simple.

An appreciable part of our studies in the metal-carbon system have been carried out with pure graphite and nickel at a pressure of 85,000 atmospheres and approximately 1560° C. The elements were chosen on the basis of ready availability. The pressure was chosen because it produced no undue hardships upon the apparatus. Pyrophyllite was used to contain the Ni-C system within the high pressure volume. No contamination of the system has been noticed.

Figure 2 shows an actual cross section of a pyrophyllite cylinder containing a Ni-C system which has been subjected to the above P-T conditions for 3 minutes. The arrangement of items from top to bottom, respectively, are: Ni electrical contact disk, Ni plug, graphite plug, Ni plug and other contact disk. The metal has been etched with HNO_3 to show the recrystallization which has occurred. One diamond can be quite clearly seen protruding from the top center of the graphite section. Others can just barely be detected to the left and above the latter. The color discontinuity at the upper Ni-graphite boundary shows a saturated Ni-carbon area and one of incipient diamond formation. Unfortunately details are not as clear along the lower boundary. X-ray diffraction analysis of the Ni at the carbon contact showed no evidence of nickel carbide formation. The white colored area surrounding the Ni-C system graphically illustrates the thermal gradient present during the experiment. The many cracks along the pyrophyllite clearly show the stress distribution upon the specimen. Note that other than initial tolerance adjustments to sample configuration, essentially no deformation has occurred.

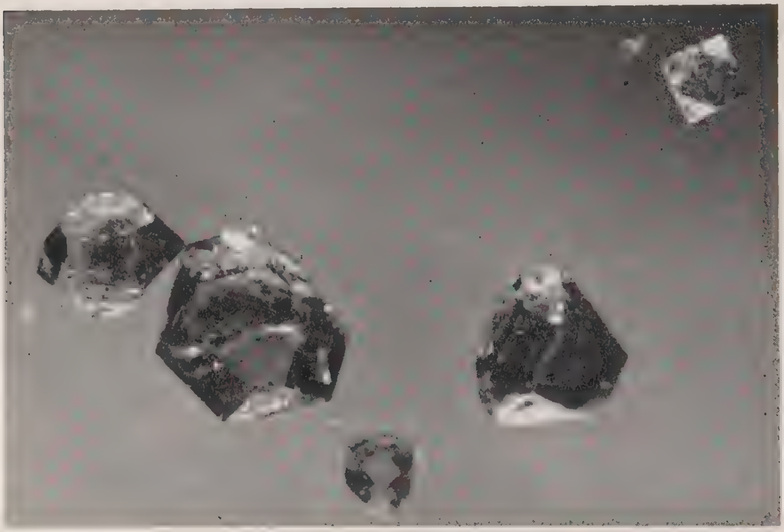

FIG. 3. Yellow diamond crystals grown in nickel under a pressure of 87,000 atmospheres and a temperature of approximately 1560° C. for a period of 5 minutes. Longest dimension of the largest crystal is 0.5 mm.

Figure 3 illustrates several diamond crystals grown in nickel at approximately 87,000 atmospheres and 1560° C. They are colored a bright yellow. Colors have been observed from green to yellow to colorless. The largest dimension observed thus far is 0.8 mm. Crystals are generally well formed giving good optical goniometric reflections. Combination cube-octahedron forms have been most commonly observed thus far, although some octahedra and a few cubes have been found; and dodecahedron faces noted. Twinning according to the spinel law is very common. Although the adamantine luster and typical habit of diamond aided in the initial identification, positive evidence was obtained from single crystal *x*-ray diffraction analysis. A rotation pattern about [001] gave $a_0 = 3.57$ Å, in good agreement with the literature value.

ACKNOWLEDGMENTS

The authors would like to express deep gratitude to Dr. J. A. Kohn for many helpful discussions and *x*-ray diffraction studies during the course of this work, and to Pfc. Wm. McGraw, Gene Hagaman and Frank Becker for their many contributions.

REFERENCES

1. P. W. BRIDGMAN, *Proc. Am. Acad. Arts Sci*, **81,** 228 (1952).
2. ———, *Proc. Am. Acad. Arts Sci.*, **74,** 438 (1942).
3. ———, The Physics of High Pressure; G. Bell and Sons, Ltd., London (1949).
4. L. SALTER, *Philosophical Mag.*, **45,** 369 (1954).
5. "Man Made Diamonds," General Electric Res. Info Serv., March, 1955.
6. Chem. Engr. News, Nov., 1959.
7. H. P. BOVENKERK, *et al.*, *Nature*, 1094, Oct. 10, 1959.

THE AMERICAN MINERALOGIST, VOL. 45, JANUARY–FEBRUARY, 1960

IDENTITY OF CALCIUM RINKITE AND GÖTZENITE

TH. G. SAHAMA
Institute of Geology, University of Helsinki, Finland

From a lava of the extinct volcano Mt. Shaheru in the Belgian Congo, a triclinic F-bearing Na-Ca-Ti-silicate was described by Sahama and Hytönen (1957 *a*) and named götzenite. It was realized that the mineral was related to calcium rinkite that occurs in the lovchorrite-bearing veins of Mt. Yukspor in Kola Peninsula and which has been briefly reviewed by P. Chirvinsky and I. Borneman-Starynkevich (in Fersman, 1937). The data presented for calcium rinkite were, however, not sufficient for an accurate comparison of the two minerals with each other. For that reason and, further, because of the entire absence of the rare earths, niobium and strontium in the Shaheru mineral, this mineral was distinguished from calcium rinkite.

The unit cell dimensions of götzenite as originally published by Sahama and Hytönen are as follows: $a = 10.93$, $b = 7.32$, $c = 5.74$, $\alpha = 90°$,

$\beta=100°$, $\gamma=120°$, volume 389 (all based on $\lambda_{\text{CuK}\alpha_1}=1.54050$ Å). This cell is very oblique. In a personal communication addressed to the author, Professor Horace Winchell, of Yale University, very kindly drew the author's attention to the fact that the base-diagonal [110] is shorter than the *a* axis given above. He suggested the transformation: [110] (old)→*a*(new), −*b*(old)→*b*(new), *c*(old)→*c*(new) thus giving a new cell with the following dimensions: $a=9.65$, $b=7.32$, $c=5.74$, $\alpha=90°$, $\beta=101.3°$, $\gamma=101.1°$. The volume of this new cell is the same as that of the old one. The new cell is less oblique and should be preferably adopted for götzenite. The author is grateful to Professor Winchell for this suggestion.

During the Inaugural Meeting of the International Mineralogical Association held in April, 1958, in Madrid, Professor Clifford Frondel, of the Harvard University, kindly informed the author about the existence of a paper by Slepnev (1957) that deals with the minerals of the rinkite group. Dr. Michael Fleischer, of the U. S. Geological Survey, very helpfully placed an English translation of this paper at the author's disposal. The paper by Slepnev contains some new data for calcium rinkite, the most important of which is the tabulation of the powder pattern previously not recorded. During the same Madrid meeting, Professor K. A. Vlasov, of Moscow, very generously gave the author a beautiful specimen of calcium rinkite from the original Kola locality to be used for comparison with the African götzenite.

Through the courtesy of the three gentlemen mentioned above—Frondel, Fleischer, Vlasov—an accurate comparison of calcium rinkite with götzenite has now become possible. From the specimen handed over by Vlasov a pure fraction of calcium rinkite was extracted by heavy liquids. The material was chemically analyzed by Mr. Pentti Ojanperä, of the Geological Survey of Finland, with the following result: SiO_2 32.34, TiO_2 8.74, ZrO_2 0.19, Nb_2O_5 3.36, Al_2O_3 0.45, rare earth oxides 1.84, Fe_2O_3 0.02, FeO 0.14, MnO 0.62, MgO 0.04, CaO 38.95, BaO 0.00, SrO 0.87, Na_2O 6.32, K_2O 0.09, P_2O_5 0.00, SO_3 0.00, F 9.15, Cl 0.00, H_2O+ 0.57, H_2O^- 0.04, −0 for F 3.85, total 99.88. Spectroscopic test for Ta negative. Under the microscope, the needle-like mineral appears to be multiply twinned with very strong dispersion. Optical α is subparallel to the needle axis, here taken as *b*. $2V_\gamma=$ ca. 60°. The refractive indices and the specific gravity determined by Mr. Kai Hytönen, of this Institute, are: $\alpha=1.651$, $\beta=1.653$, $\gamma=1.659$, sp. gr. = 3.106 (pycnometer). A *b*-axis rotation photograph yielded $b=7.34\pm0.02$ Å with a very strongly pronounced sub-cell with $b/2$. Zero and second layer *b*-axis Weissenberg photographs were found to be virtually identical with those for götzenite. Accordingly, it seems justified to conclude that the unit cells of the two minerals are identical. The unit cell content of calcium rinkite was calculated as follows: Si 3.92, Ti 0.80, Zr 0.01, Nb 0.18, Al 0.06, rare earth metals ca. 0.08, Fe 0.01, Mn 0.06, Mg 0.01, Ca 5.06, Sr 0.06, Na 1.49, K 0.01, F 3.51, OH 0.46, O 14.09. The powder pattern data recorded with the Philips Norelco Diffractometer are reproduced below, compared with the data published by Slepnev for calcium rinkite and those for götzenite by Sahama and Hytönen (Table 1).

Table 1. Powder Photograph Data for Calcium Rinkite and Götzenite

Calcium rinkite (Slepnev)		Calcium rinkite (this paper)		Götzenite (Sahama-Hytönen)	
I	d	I	d	I	d
—	—	15	3.988	15	3.994
w	3.58–3.40	—	—	5	3.601
m	3.265	5	3.286	—	—
s	3.07	100	3.099	100	3.100
s	2.97	50	2.982	100	2.986
—	—	15	2.863	10	2.859
—	—	10	2.828	7	2.822
m	2.625	25	2.653	40	2.648
m	2.48	15	2.522	25	2.511
—	—	15	2.324	10	2.323
vw	2.25	5	2.263	15	2.261
—	—	—	—	7	2.214
w	2.15	5	2.171	5	2.152
vw	2.04	—	—	5	2.059
—	—	—	—	7	1.989
s	1.93	20	1.915	50	1.911
m	1.87	15	1.879	15	1.876
m	1.834	10	1.834	15	1.833
m	1.81	5	1.806	10	1.798
s	1.685	10	1.680	25	1.690
w	1.64	5	1.680	7	1.646
—	—	—	—	10	1.594
m	1.563	—	—	10	1.573
vw	1.537	—	—	10	1.543
vw	1.49	—	—	15	1.482
vw	1.457	—	—	—	—

The information summarized above seems to justify the conclusion that calcium rinkite and götzenite do represent the same species, found so far only in Kola and in the Belgian Congo. As has been remarked by Fleischer (1958 *a*), götzenite is closer to a pure end-member and, accordingly, calcium rinkite may be termed a rare earth- and niobium-bearing strontian götzenite.

The unit cell dimensions of götzenite separate it from the minerals of the mosandrite-rinkite group. Based on some differences in powder pattern between mosandrite (johnstrupite) on the one hand and rinkite on the other, Sahama and Hytönen (1957 *b*) considered rinkite to represent a species separate from mosandrite (johnstrupite). As very truly was remarked by Flesicher (1958 *b*), the differences may be caused by the less pronounced metamict alteration of rinkite. Both Slepnev and Fleischer agree in considering mosandrite (johnstrupite) and rinkite one single species. As mentioned by Fleischer, the name mosandrite has the priority and, accordingly, names like rinkite, johnstrupite, rinkolite and lovchorrite should be dropped in mineralogical nomenclature. If this is accepted, then also the name calcium rinkite should be dropped in favor of götzenite.

REFERENCES

Fersman, A. E. (1937), Minerals of the Khibina and Lovozero Tundras; Lomonossov Inst. Acad. Sci. USSR.

Fleischer, Michael (1958 *a*), Abstract in *Am. Mineral.*, **43,** p. 790.

——— (1958 *b*), Abstract in *Am. Mineral.*, **43,** 795–796.

Sahama, Th. G. and Hytönen, Kai (1957 *a*), Götzenite and combeite, two new silicates from the Belgian Congo; *Min. Mag.*, **31,** 503–510.

——— (1957 *b*), Unit cell of mosandrite, johnstrupite and rinkite; *Geol. För. Stockholm Förh.*, **79,** 791–796.

Slepnev, Yu. S. (1957), The minerals of the rinkite group: *Izvestiya Akad. Nauk. USSR, Ser. Geol.*, No. 3, 63–75.

THE AMERICAN MINERALOGIST, VOL. 45, JANUARY-FEBRUARY, 1960

A PLASTIC UNIVERSAL STAGE FOR STUDENT USE

R. H. Clark* and W. J. Clarke†

For many optical techniques a clear understanding of the indicatrix is essential. This concept is fundamental in the use of convergent light figures, in refractive index measurements, in the relation of vibration axes to crystallographic directions, and in similar techniques.

Geology students frequently encounter difficulty in fully understanding the indicatrix. The "three-dimensional thinking" involved is aided by use of the universal stage before the student is introduced to convergent light, but unfortunately, it is generally impracticable to provide junior students with expensive multi-axis stages.

---

* Geology Department, Victoria University of Wellington, Wellington, New Zealand.

† The British Petroleum Company Limited, Exploration Division, BP Research Centre, Chertsey Road, Sunbury-on-Thames, Middlesex, England.

The authors have overcome this difficulty by designing a low cost, 3 axis universal stage, of simplified construction. It may be produced in a small workshop with the minimum of equipment, and can be made in sufficient quantity to be used with large classes. Being small, it can be fitted to most microscopes with little difficulty. Special objectives are not necessary, a standard low power (e.g., Swift 32 mm., ×4) is quite satisfactory.

The perspex stage is not intended for precise measurement, but it has been found possible to make reasonably accurate measurements of 2V.

Material

The stage described was made from perspex, but any similar reasonably durable, non brittle and easily machined plastic (Leucite; Plexiglas) would be suitable.

Construction

The component parts are shown in the "exploded" diagram (Fig. 1), and an assembled stage, mounted on a Swift Model P polarizing microscope, appears in Fig. 2.

Quarter inch sheet perspex was used for all parts except the inner rotating stage (D, Fig. 1) which was cut from $\frac{1}{16}$ inch perspex, and the upper segment holder (E), of $\frac{1}{8}$ inch perspex. The rings were cut with a trepanning bit; few other tools are necessary.

Considerable variation in dimensions and detail is possible. Measurements indicated below are those used in construction of the stage illustrated in Fig. 2. The basal ring (A, Fig. 1) and main ring (B) have an outside diameter of $3\frac{5}{16}$ inch and $3\frac{3}{16}$ inch respectively, each ring being $\frac{13}{32}$ inch wide. Supports F and G are cemented to the basal ring and the main ring mounted between them, with a vertical gap of $\frac{3}{4}$ inch between the rings.

The inner ring (C) has an outside diameter of $2\frac{5}{16}$ inch, is $\frac{5}{16}$ inch wide, and is recessed to carry the inner rotating stage with a cut $\frac{1}{16}$ inch wide and $\frac{1}{16}$ inch deep. The inner rotating stage (D), with a diameter of $1\frac{13}{16}$ inch, fits snugly into the recess in C, and yet is free to rotate.

The quadrants, H and I, were cut from a ring of the same outside diameter as B, but to permit clearance of C when rotated about the horizontal N—S axis, only $\frac{11}{32}$ inch in width. A maximum quadrant height of $1\frac{1}{4}$ inches above the thin section is sufficient to clear the revolving nosepiece of a Swift microscope when a $1\frac{1}{2}$ inch objective is used.

Any type of bearing may be used. In the original prototype $\frac{3}{32}$ inch

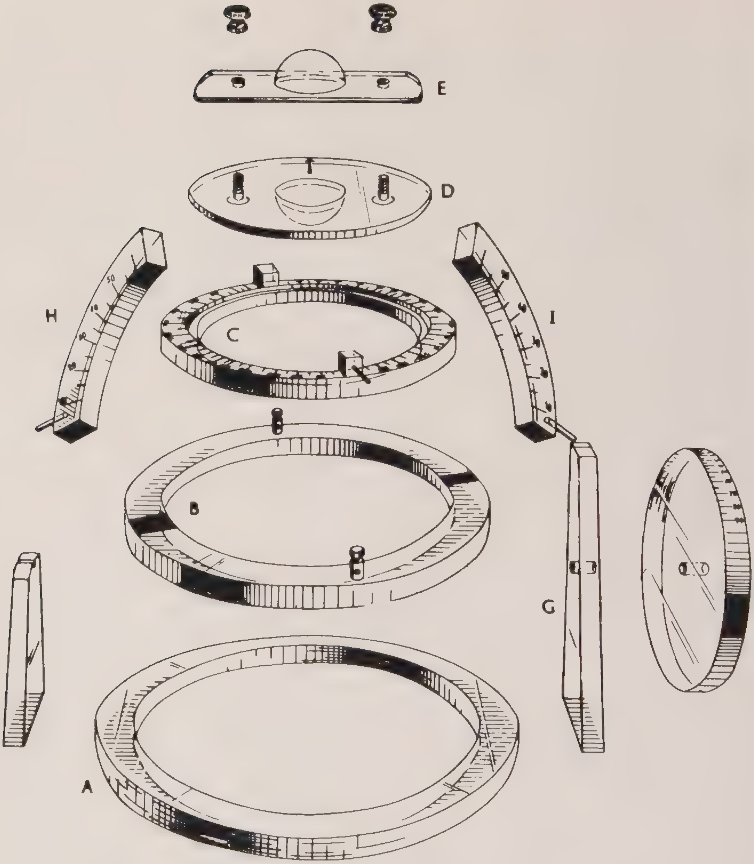

FIG. 1. The perspex stage, "exploded" to show details of components.

steel rod and small brass electrical terminals were used (Fig. 1). Those in Fig. 2 are threaded brass, and have proved particularly satisfactory as they permit the amount of friction between the moving parts to be adjusted.

Perspex cement was used in assembly. Especial care is necessary to align both sets of horizontal bearings so that the axes of rotation are level with the rock slice in an average thin section above the inner rotating stage D.

Glass hemispheres

Small hemispheres (diameter about $\frac{3}{4}$ inch) were made by heating soda glass rod free from air bubbles in a glassworking lathe. Alternatively they

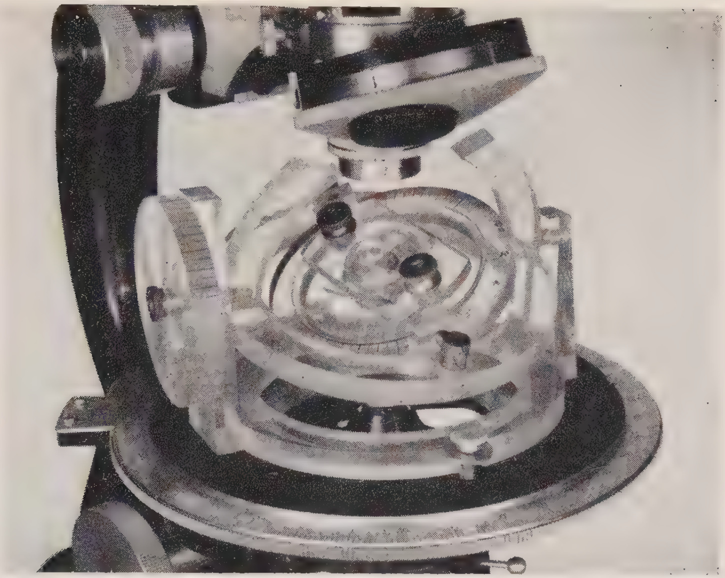

FIG. 2. The perspex stage, mounted on a Swift Model P microscope.

can be ground fairly cheaply, as precision is not essential, and all that is required is moderately clear vision through the upper segment.

Cost

Perspex stages, quite suitable for student use, were produced for the Victoria University of Wellington at a cost, including labor and glass segments, of approximately $25 per stage.

Use of Perspex Stages

Any suitable mineral may be measured in thin section on the perspex stage. Augite has been found to be convenient for introducing students to biaxial minerals. Grains giving under the conoscope a slightly off center acute bisectrix figure may be previously selected. Use of these grains ensures that both optic axes, Y, and the obtuse bisectrix are accessible without excessive tilt.

Students with some previous experience of the stereographic projection can rapidly acquire the necessary technique to enable them to find and plot the X and Y vibration axes of such suitably oriented augite crystals. They can then locate the optic axes and measure 2V directly.

This leads to a comprehension of the indicatrix which enables students to proceed to the study of convergent light interference figures with understanding.

ACKNOWLEDGMENTS

The writers wish to acknowledge technical advice received from Mr. G. N. Newell of the University of Edinburgh. The photograph (Fig. 2) is by Mr. M. D. King.

THE AMERICAN MINERALOGIST, VOL. 45, JANUARY–FEBRUARY, 1960

VERMICULAR GIBBSITE IN THE PENSAUKEN OF NEW JERSEY

WILLIAM LODDING, *Rutgers State University, New Brunswick, N. J.*

Vermiforms found near South River, New Jersey and in at least five other localities in the Pensauken formation of the New Jersey coastal plain were definitely identified as mainly composed of gibbsite by differential thermal analysis, *x*-ray diffraction, and chemical analysis. They occur in coarse sand, average 0.5 to 2.0 mm. in length, but a few specimens were as long as 6 mm. (Fig. 1). Gibbsite is also found there as whitish aggregates cementing coarse quartz grains. The veriforms are very similar in aspect to those found in South Carolina, California, and other localities and identified as kaolinite (1). A hand picked sample from South River showed the following mineral composition:

gibbsite	87%
kaolinite	6%
goethite	5%
other	2%

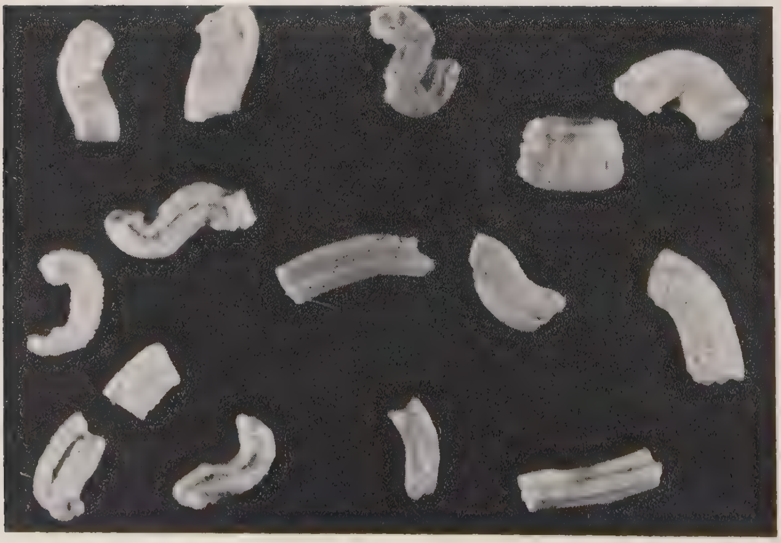

FIG. 1. Microphotograph of vermicular gibbsite, South River, New Jersey. ×14

A more detailed paper on the occurrence and genesis of these vermiforms is in preparation.

Reference

Ross, C. S. and Kerr, P. F., "The Kaolin Minerals," professional paper 165-E 1930.

THE AMERICAN MINERALOGIST, VOL. 45, JANUARY–FEBRUARY, 1960

LOW TEMPERATURE PHASE TRANSITION OF COLEMANITE

A. Perloff and S. Block, *National Bureau of Standards, Washington 25, D. C.*

In recent years several workers (1, 2, 3) by means of pyroelectric, ferroelectric, and nuclear magnetic resonance measurements have obtained evidence that colemanite, $CaB_3O_4(OH)_3 \cdot H_2O$, room temperature space group $P2_1/a$ (4, 5), undergoes a transition near 0° C. to a noncentrosymmetric phase. This phase change can also be observed with x-ray diffraction techniques.

Precession photographs of the $h0l$ and $0kl$ reciprocal lattice nets at room temperature and at −30° C. were taken using MoK_α radiation with a Zr filter. The single crystal fragment was from a colemanite specimen from Death Valley, California, kindly supplied by Dr. C. L. Christ of the U. S. Geological Survey.

Within the limits of error there was no change in the cell dimensions, which agree with the published values (5), and no changes were observed on the $0kl$ net. However, the low temperature $h0l$ net contained very weak reflections from the $70\bar{1}$, $50\bar{2}$, $90\bar{5}$, and $70\bar{6}$ planes which establishes that the glide plane does not exist in the low temperature form. The transition between the room temperature $P2_1/a$ phase and the low temperature $P2_1$ phase is readily reversible.

References

1. Davisson, J. W. (1956), *Acta Cryst.* **9,** 9.
2. Goldsmith, G. J. (1956), *Bull. Am. Phys. Soc. Ser II* **1,** 322.
3. Holuj, F. and Petch, H. E. (1958), *Can. J. Phys.* **36,** 145.
4. Christ, C. L. (1953), *Am. Mineral.* **38,** 411.
5. Christ, C. L., Clark, J. R. and Evans, H. T., Jr. (1958), *Acta Cryst.* **11,** 761.

THE AMERICAN MINERALOGIST, VOL. 45, JANUARY–FEBRUARY, 1960

X-RAY CRYSTALLOGRAPHY AND CRYSTAL CHEMISTRY OF GOWERITE, $CaO \cdot 3B_2O_3 \cdot 5H_2O$*

C. L. CHRIST AND JOAN R. CLARK, *U. S. Geological Survey, Washington 25, D. C.*

The new mineral gowerite, $CaO \cdot 3B_2O_3 \cdot 5H_2O$, was recently described by Erd, McAllister, and Almond (1959). The present note gives the results obtained from an *x*-ray study of single crystals of gowerite. The crystals were examined on a quartz-calibrated precession camera, using Cu/Ni radiation ($\lambda CuK\alpha = 1.5418$ Å); film measurements were corrected for both horizontal and vertical shrinkage. The following crystallographic data were obtained: monoclinic, $P2_1/n$-C_{2h}^5 (no. 14), $a = 11.03 \pm 0.04$, $b = 16.40 \pm 0.05$, $c = 6.57_7 \pm 0.02$ Å, $\beta = 90°56' \pm 05'$, $a:b:c = 0.673:1:0.401$; cell volume 1190 Å^3; calculated density 1.98_2 g. cm.$^{-3}$ for cell contents $4[CaO \cdot 3B_2O_3 \cdot 5H_2O]$, observed specific gravity 2.00 ± 0.01 (Erd *et al.*, 1959). An alternative description of the unit cell is $P2_1/a$, $a = 12.93$, $b = 16.40$, $c = 6.57_7$ Å, $\beta = 121°30'$, $a:b:c = 0.788:1:0.401$. The transformation from the $P2_1/a$ to the $P2_1/n$ setting is given by the matrix 101/010/001.

The morphology of gowerite crystals and a sketch of a typical crystal are given by Erd *et al.* (1959). The crystals used in the present study can be described, in accordance with either the $P2_1/a$ or $P2_1/n$ setting, as follows: prismatic needles, elongated [001], flattened on {010}, with small {100}, {110}, {140}, and terminating form, for $P2_1/n$, {111}, optical orientation $Y = b$, $Z \wedge c = 27°$. The present description is the same as that given by Erd *et al.* (1959), except that these authors called the terminating form {001?}.

An *x*-ray powder pattern of gowerite was taken with Cu/Ni radiation in a 114.59 mm. diameter camera and the measurements from the resulting film were corrected for shrinkage. Interplanar spacings were calculated from the single crystal data for $d \geq 2.250$ Å and indexed on the $P2_1/n$ orientation; the powder film results, and the diffractometer results of Erd *et al.* (1959) are compared in Table 1.

It has been pointed out (Christ, 1959) that crystals of formula $MO \cdot 3B_2O_3 \cdot xH_2O$ (where M represents a bivalent cation) may be explained by postulating either discrete polyions of composition $[B_3O_3(OH)_4]^{-1}$, or polymerization products resulting from these polyions by the splitting out of water. This structural unit, consisting of two boron-oxygen triangles and a boron-oxygen tetrahedron linked at corners

---

* Publication authorized by the Director, U. S. Geological Survey.

TABLE 1. *X*-RAY POWDER DATA FOR GOWERITE, $CaO \cdot 3B_2O_3 \cdot 5H_2O$

Monoclinic $P2_1/n-C_{2h}^5$: $a=11.03\pm0.04$, $b=16.40\pm0.05$,
$c=6.57_7\pm0.02$ Å; $\beta=90°56'\pm05'$

Measured				Calculated[1]	
Erd *et al.* (1959)[2]		Present Study[3]			
I	d_{hkl}	I	d_{hkl}	d_{hkl}	*hkl*
2	9.18	25	9.2_0	9.15	110
10	8.23	100	8.2_3	8.20	020
<1	6.61	5	6.5_7	6.58	120
		2	6.0_7	6.10	011
<1	5.64	2	5.64	5.689	$\bar{1}01$
				5.608	101
<1	5.52			5.513	200
1	5.40	5	5.37	5.374	$\bar{1}11$
				5.306	111
				5.225	210
1	5.15	5	5.13	5.130	021
1	4.91	5	4.89	4.898	130
				4.674	$\bar{1}21$
				4.629	121
				4.575	220
				4.204	031
				4.122	$\bar{2}11$
5	4.11	20	4.09_4	4.100	040
2	4.07			4.061	211
<1	3.95	10b	3.94_5	3.942	$\bar{1}31$
1	3.92		to	3.914	131
1	3.88			3.882	230
2	3.85		3.83_6	3.843	140
				3.779	$\bar{2}21$
<1	3.74	2	3.72_4	3.732	221
				3.586	310
				3.479	041
				3.360	$\bar{2}31$
1	3.36	10	3.34_5	3.354	320
<1	3.32			3.326	231, $\bar{1}41$
				3.310	141
				3.290	240
				3.288	002
1	3.23	2	3.22_8	3.230	$\bar{3}01$
				3.224	012

[1] All calculated interplanar spacings listed for $d_{hkl}\geq 2.250$ Å.

[2] *X*-ray diffractometer data, unfiltered Fe radiation, only lines due to FeKα, $\lambda=1.9373$ Å, are given.

[3] Corrected for shrinkage; b=broad. Radiation: Cu/Ni, λCuKα=1.5418 Å. Lower limit of 2θ measurable, approximately 7° (13 Å). Film no. 13540. Camera diameter, 114.59 mm.

TABLE 1 (*continued*)

Measured				Calculated[1]	
Erd *et al.* (1959)[2]		Present Study[3]		d_{hkl}	*hkl*
I	d_{hkl}	I	d_{hkl}		
6	3.19	45	3.18_6	3.186	301
				3.170	$\bar{3}11$
2	3.15	2	3.13_9	3.144	150
				3.128	311
				3.108	$\bar{1}12$
				3.081	112
1	3.06	5	3.04_9	3.052	022
				3.050	330
<1	3.01			3.006	$\bar{3}21$
1	2.97			2.970	321
<1	2.96	10	2.960	2.954	$\bar{2}41$
				2.953	$\bar{1}22$
1	2.93			2.935	051
				2.931	241
				2.930	122
				2.844	$\bar{2}02$
				2.841	$\bar{1}51$
				2.831	151
1	2.82	10	2.816	2.819	250
				2.818	032
				2.804	202
				2.802	$\bar{2}12$
				2.781	$\bar{3}31$
1	2.77	10	2.768	2.764	212
				2.756	400
				2.753	331
				2.739	$\bar{1}32$
				2.737	340
4	2.73	25	2.728	2.733	060
				2.721	132
				2.718	410
				2.687	$\bar{2}22$
2	2.65	10	2.648	2.653	160, 222
				2.613	420
				2.599	$\bar{2}51$
				2.583	251
				2.565	042
1	2.54	5	2.531	2.537	$\bar{3}41$
				2.526	$\bar{4}11$
				2.524	061
				2.523	$\bar{2}32$
				2.516	341
<1	2.50			2.505	$\bar{1}42$
				2.498	411
				2.495	232
				2.491	142

TABLE 1 (*continued*)

Measured				Calculated[1]	
Erd *et al.* (1959)[2]		Present Study[3]			
I	d_{hkl}	I	d_{hkl}	d_{hkl}	*hkl*
				2.464	$\bar{1}61$
<1	2.46	2	2.458	2.461	430
				2.457	161
				2.449	260
				2.447	350
				2.443	$\bar{3}12$
				2.441	$\bar{4}21$
				2.415	421
				2.405	312
				2.365	$\bar{3}22$
		2	2.334	2.337	$\bar{2}42$
				2.331	322
				2.322	052
				2.316	$\bar{4}31$
				2.314	242
				2.302	$\bar{3}51$
				2.300	$\bar{2}61$
1	2.29	10	2.294	2.294	431
				2.292	170
				2.289	261
				2.287	440
				2.285	351
				2.278	$\bar{1}52$
				2.267	152
				2.251	$\bar{3}32$
1	2.17	5	2.165		
1	2.13	5	2.128		
<1	2.11	5	2.109		
<1	2.08	2	2.079		
1	2.06	5	2.060		
<1	2.05				
<1	2.00	5	2.015		
<1	1.995	5	1.998		
		2	1.966		
<1	1.946	2	1.942		
<1	1.924				
<1	1.896	5b	1.895		
<1	1.868				
<1	1.865	2b	1.861		
1	1.797	5b	1.795		
<1	1.755	2	1.756		
1	1.730	5b	1.726		
1	1.590	plus additional lines, all with $I \leq 2$			
plus additional lines all with $I<1$					

to form a ring, would be analogous to the one triangle-two tetrahedra ring found, e.g., in meyerhofferite, $CaB_3O_3(OH)_5 \cdot H_2O$, (Christ and Clark 1956) and the two triangles-two tetrahedra ring found in borax, $Na_2B_4O_5(OH)_4 \cdot 8H_2O$, (Morimoto, 1956). It has, in fact, been postulated that discrete $[B_3O_3(OH)_4]^{-1}$ polyions exist in aqueous solutions (Ingri, Lagerström, Frydman, and Sillén, 1957), and that monoclinic metaboric acid, HBO_2, contains infinite chains of composition $[B_3O_4(OH)_2]_n^{-n}$ (Zachariasen, 1952).

For gowerite, the space group $P2_1/a$ (or $P2_1/n$) and the unit-cell contents $4[CaO \cdot 3B_2O_3 \cdot 5H_2O]$ are consistent with the presence of insular polyions, $[B_3O_3(OH)_4]^{-1}$, dimers, $[B_6O_7(OH)_6]^{-2}$, or infinite chains, $[B_3O_4(OH)_2]_n^{-n}$. The structural formulas corresponding to these three possibilities would be for gowerite, $Ca[B_3O_3(OH)_4]_2 \cdot H_2O$, $CaB_6O_7(OH)_6 \cdot 2H_2O$, and $Ca[B_3O_4(OH)_2]_2 \cdot 3H_2O$, respectively. The determination of the crystal structure of gowerite is currently in progress by the present authors.

We are grateful to a number of our colleagues in the U. S. Geological Survey for their help. R. C. Erd made available to us the crystals of gowerite, Erd, J. F. McAllister, and Hy Almond permitted us to read their manuscript in advance of publication, Mary E. Mrose prepared the *x*-ray powder patterns of gowerite, and Daniel E. Appleman calculated the *d*-spacings on a digital computer.

REFERENCES

CHRIST, C. L. (1959), Nature of the polyions contained in hydrated borate crystals (abstract): Am. Crystal. Assoc. meeting, Ithaca, N. Y. July 20–24.

CHRIST, C. L. AND CLARK, JOAN R. (1956), The structure of meyerhofferite, $2CaO \cdot 3B_2O \cdot 7H_2O$, a $P\bar{1}$ crystal, determined by the direct method of Hauptman and Karle: *Acta Cryst.*, **9**, 830.

ERD, RICHARD C., MCALLISTER, JAMES F. AND ALMOND, HY (1959), Gowerite, a new hydrous calcium borate, from the Death Valley region, California: *Am. Mineral.*, **44**, 911–919.

INGRI, NILS, LAGERSTRÖM, GÖSTA, FRYDMAN, MINA AND SILLÉN, LARS GUNNAR (1957), Equilibrium studies of polyanions. *II.* Polyborates in $NaClO_4$ medium: *Acta Chem. Scand.*, **11**, 1034.

MORIMOTO, NOBUO (1956), The crystal structure of borax: *Mineral. J.* (*Japan*), **2**, 1.

ZACHARIASEN, W. H. (1952), A new analytical method for solving complex crystal structures: *Acta Cryst.*, **5**, 68.

THE AMERICAN MINERALOGIST, VOL. 45, JANUARY–FEBRUARY, 1960

TODOROKITE AND PYROLUSITE FROM VERMLANDS TABERG, SWEDEN

Pontus Ljunggren, *University of Lund, Lund, Sweden*

During the course of an examination of the soft iron ore of Vermlands Taberg in western Sweden (P. Ljunggren, 1958) manganese mineralization was found to have taken place both in the goethitized iron ore and in the argillized wall-rock. The manganese oxides are found as veins in the soft iron ore, as impregnations in the argillized wall-rock and in secondary calcite veins. A formation of dendrites of manganese oxides is also very common. This manganese mineralization is mainly concentrated to the border zone between the soft iron ore and the argillized skarn and leptite rocks. The width of the manganiferous veins hitherto found, often less than ten centimetres, is too small to allow any profitable mining of manganese ore.

The quite predominating manganese oxide mineral in these veins is pyrolusite. In a secondary calcite vein cutting the soft iron ore another manganese oxide mineral was found and identified as todorokite (T. Yoshimura, 1934; C. Frondel, 1953). An examination of the pyrolusite and the todorokite is given in the present paper.

Todorokite

The todorokite is found as black aggregates in a 5 cm. wide secondary calcite vein in the soft iron ore. The aggregates consist of small needle-shaped crystals (maximum size 0.2×0.01 mm.) arranged spherulitically or dendritically in the calcite vein.

The mineral was found upon *x*-ray examination to be identical with todorokite (Mn, Ba, Ca, Mg) $Mn_3O_7 \cdot H_2O$, as described by C. Frondel in 1953 and T. Yoshimura in 1934. The d-values of todorokite from Todoroki and from Vermlands Taberg are given in Table 1. The DTA curve of todorokite from Vermlands Taberg is given in Fig. 1. It shows endothermic peaks at 105°, 330°, 660°, 730°, 810°, and a small deflection at 965° C. The sample upon which this DTA was performed was extremely pure, and the endothermic reactions recorded are typical of the todorokite of this locality. No other minerals have been identified in the sample by microscopic or *x*-ray methods.

A spectrochemical analysis of the todorokite was carried out in order to discover the content of some of the trace elements which are of most interest for the geochemistry of manganese (cf. P. Ljunggren, 1958b):

$Zn = 0.001\%$ $V < 0.001\%$
$Ni < 0.001\%$ $Ba = 0.01\%$

Table 1. *X*-Ray Powder Spacings for Todorokite from Todoroki (C. Frondel, 1953, p. 766) and from Vermlands Taberg. —Fe Radiation, Mn Filter, Camera Diameter 114.83 mm.

Todoroki d (in Å)	I	Vermlands Taberg d (in Å)	I
9.65	10	9.67	vs
7.2	.5		
4.81	8	4.78	m
4.46	3	4.47	vw
3.20	4	3.22	vw
2.45	3	2.43	vw
2.40	4	2.39	vw
2.216	4	2.21	vw
2.150	1		
1.981	1	1.97	vw
		1.74	vvw
		1.68	vvw
1.419	4	1.42	vw
1.392	1		
1.331	5		

Pb = 0.001% Rb < 0.001%
Bi < 0.001% K = 0.1 %

The spectrographic analysis shows furthermore small amounts of Ca and Mg (less than one per cent), but it is not possible to state whether this is due to a small admixture of Ca-Mg-bearing minerals, whether these elements are included in the todorokite structure or whether they were possibly adsorbed upon the surface of the todorokite aggregates.

Pyrolusite

The pyrolusite is found as more or less earthy aggregates, both in the soft iron ore and in the argillized skarn and leptite. No crystals are seen upon macroscopic examination. An *x*-ray powder analysis gave the following cell dimension:

$$a = 4.40 \text{ Å}$$
$$c = 2.87 \text{ Å}$$
$$c/a = 0.652$$

these values being identical with those given by A. M. Byström in 1949 (p. 171).

A spectrochemical analysis of the pyrolusite of this locality gave the following trace element composition:

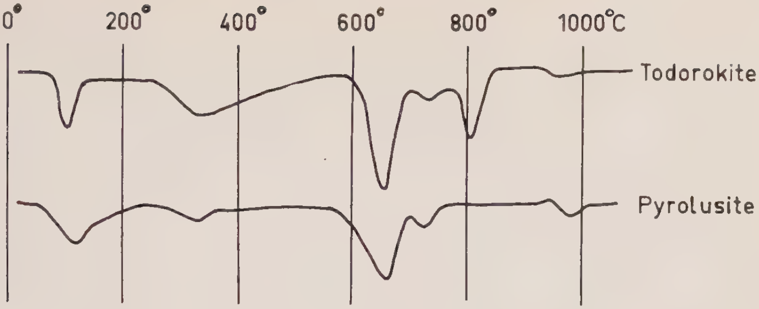

FIG. 1. DTA curves of todorokite and pyrolusite from Vermlands Taberg.

$Zn \leq 0.001\%$

$Ni = 0.01\ \%$

$Pb < 0.001\%$

$Bi < 0.001\%$

$V < 0.001\%$

$Ba < 0.001\%$

$Rb < 0.001\%$

These figures demonstrate that the pyrolusite is unusually pure. The very low value of Ba is especially remarkable as Ba is strongly adsorbed by MnO_2.

A DTA curve of the pyrolusite of Vermlands Taberg is given in Fig. 1. It shows endothermic peaks at 120°, 330°, 665°, 730°, and 980° C., and one exothermic peak at 940° C. The two peaks at 940° and 980° C. are unusually strong when compared with the curves of pyrolusites given by J. L. Kulp and J. N. Perfetti in 1950 (p. 244).

CONCLUSIONS

The similarity between the todorokite and the pyrolusite from Vermlands Taberg is striking. The DTA curves are almost identical as is also the chemical composition. Typical for both the minerals examined is the unusually low content of trace elements, which in itself must give some clue to the formation of these manganiferous veins and impregnations.

The soft iron ore of Vermlands Taberg is known to have arisen through a weathering of magnetite ore in Preglacial time. The magnetite was altered into hematite, which eventually changed into goethite; the goethite was the final stage of the alteration. Contemporaneously, the magnesium-dominant skarn minerals changed into antigorite and the feldspar-bearing rocks into kaolinitic masses. These transformations meant a complete change in mineralogical composition, resulting mainly in a formation of (OH)-bearing minerals. The iron of the iron ore was not removed from the rock system as is evident from the present features of the ore bodies. The manganese of the original iron ore seems to have become somewhat enriched during the transformation into soft iron ore (cf. Table III, P. Ljunggren, 1958a). It is therefore probable that the manganese of the manganiferous veins, now to be found as pyrolusite and todorokite, originated in the wall-rock in connection with the transformation of the latter. A possible source is the skarn minerals which underwent a thorough rebuilding upon their alteration into antigorite.

The remarkably low content of some of the trace elements in the pyrolusite and the todorokite may be explained through the conditions under which these minerals were formed. These veins cut both the soft iron ore and the argillized wall-rock; this indicates that they were formed during a late phase of the alterations. The physical condition of the argillized rocks and of the soft iron ore bodies prevented any further considerable transport of waters which could carry suitable cations to the manganese dioxide. It is a well-known fact that manganese dioxides strongly absorb certain cations, amongst them those given in the above spectrochemical analyses (P. Ljunggren, 1955). The most plausible explanation for the purity of the manganese oxide minerals of Vermlands Taberg is not the presence of very pure waters in the rock system but the very low permeability of the enclosing argillaceous rocks which prevented water containing these trace element cations from reaching the MnO_2 minerals.

REFERENCES

BYSTRÖM, A. M., 1949: The crystal structure of ramsdellite, an orthorhombic modification of MnO_2.—*Acta Chem. Scand.*, **3**, 163–173.

FRONDEL, C., 1953: New manganese oxides: hydrohausmannite and woodruffite.—*Am. Mineral.*, **38**, 761–769.

KULP, J. L. AND PERFETTI, J. N., 1950: Thermal study of some manganese oxide minerals. —*Mineral. Mag.*, **29**, 239–251.

LJUNGGREN, P., 1955: Geochemistry and radioactivity of some Mn and Fe bog ores. —*Geol. Fören. Förh.*, **77**, 33–44.

LJUNGGREN, P., 1958a: The soft iron ores of Vermlands Taberg.—*Geol. Fören. Förh.*, **80**, 59–70.

LJUNGGREN, P. , 1958b: Origin of the manganese ore deposit of Bölet, southern Sweden.—*Kungl. Fysiografiska Sällskapets i Lund Förh.*, **28**, No. 10.

YOSHIMURA, T., 1934: "Todorokite," a new manganese mineral from the Todoroki mine, Hokkaido, Japan.,—*Journ. Fac. Sci. Hokkaido Univ. Sapporo, Ser. 4,* **2**, 289–297.

THE AMERICAN MINERALOGIST, VOL. 45, JANUARY–FEBRUARY, 1960

AN *X*-RAY FLUORESCENCE METHOD FOR THE QUANTITATIVE DETERMINATION OF SMALL AMOUNTS OF MONTMORILLONITE IN KAOLIN CLAYS*

David N. Hinckley and Thomas F. Bates,† *The Pennsylvania State University, University Park, Pa.*

During the course of an investigation of the kaolin deposits of the Coastal Plain of Southeastern United States it became evident that in order to better understand the genesis of the deposits a method was needed of measuring the small amounts of montmorillonite associated with the kaolinite. The method developed utilizes the difference in base exchange capacity of the two minerals. It consists of exchanging the Sr^{++} ion onto the montmorillonite, removing the excess strontium by dialysis, analyzing the exchanged sample for strontium by *x*-ray fluorescence, and computing the percentage of montmorillonite from these results according to a curve derived from known standards. This method makes the following assumptions:

1) The base exchange capacity of the sample is due primarily to montmorillonite, *i.e.* the base exchange capacity of the kaolinite is negligible in comparison to montmorillonite.
2) The base exchange capacity of the montmorillonite in the standards is the same as that of montmorillonite in the sample.

Preparation of Standards

Standards were prepared by mixing varying proportions of Wyoming bentonite with Georgia kaolin. The weighings were made after the clays had been ground to pass 200 mesh, dried at 105° C., and placed for several days in a constant humidity atmosphere produced by $CaCl_2 \cdot 6H_2O$. The clays were intimately mixed by passing the material through a 100 mesh sieve several times and by shaking vigorously in a jar between sievings.

Strontium Ion Exchange

To a one gram sample taken from the standard mixture and placed in a 75-ml. test tube, 50 ml. of 1N $SrCl_2$ solution is added. After stoppering, the tube is vigorously shaken and allowed to sit one hour. The sample is then transferred into $1\frac{1}{8}''$ diameter cellophane dialyzer tubing which has

---

* Contribution No. 59–15, Mineral Industries Experiment Station, The Pennsylvania State University, University Park, Pennsylvania.

† Graduate Assistant and Professor of Mineralogy, Department of Mineralogy and Petrology, The Pennsylvania State University, University Park, Pennsylvania.

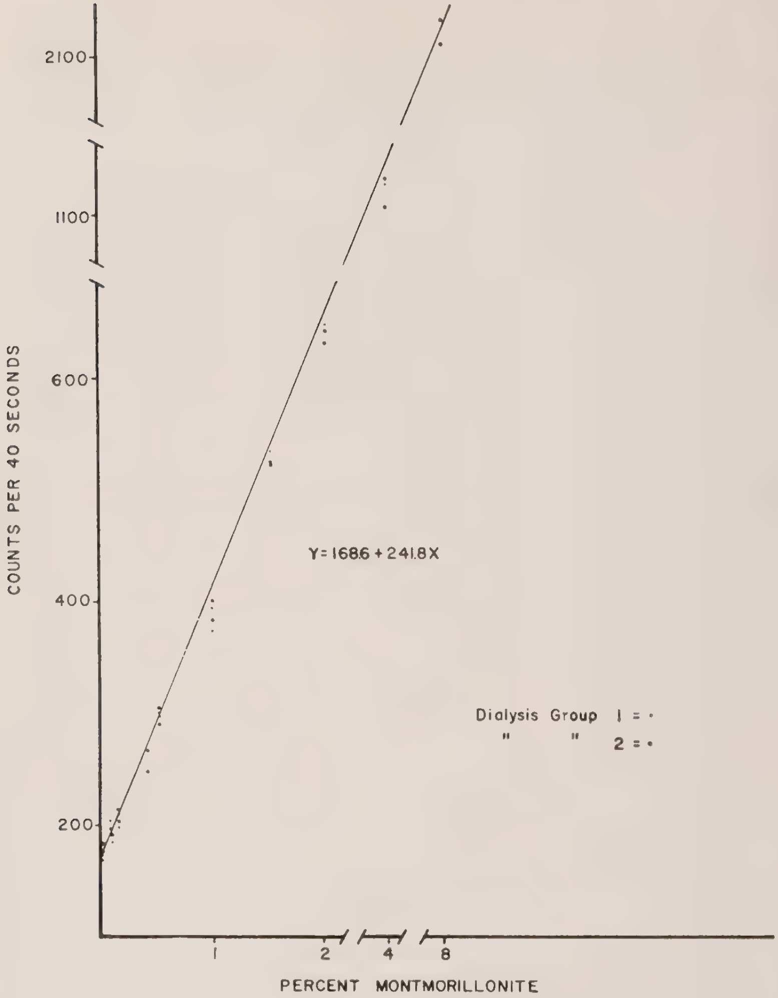

FIG. 1. Per cent montmorillonite versus counts per 40 seconds (x-ray fluorescence analysis of exchange Sr^{++}).

previously been cut into 15-inch lengths and tied at one end. The filled tube is then suspended from both ends in a 1-quart, wide-mouth mason jar which is filled with distilled water and allowed to remain undisturbed for 24 hours at which time the water is changed. While changing the water the sample is agitated by massaging the dialysis bag. This is repeated for 10 consecutive days. On the 11th day the tubing is left suspended in the jar and by use of a fan the amount of liquid in the tube is sufficiently reduced by evaporation to permit washing the sample from the tubing into a small jar for drying and storage. After drying the sample is pulverized and mixed in the jars by use of a rubber policeman and is then ready to be packed in holders for *x*-ray fluorescence analysis.

X-ray Fluorescence Analysis

For this work an XRD-5 General Electric *x*-ray unit with counting apparatus is used with a LiF analyzer crystal and a .005 collimator. With the tube operating at 50 KV and 50 MA, a 40 second background count is taken at about 29°2θ and subtracted from the average of two 40 second sample counts which are taken at a previously determined maximum intensity position for the $Sr^{+2}K\alpha$ wave length (about 25°2θ). A plot of counts versus per cent montmorillonite indicates the relationship to be essentially linear as shown in Fig. 1. For the construction of this regression line ten standards ranging from 0.00% to 8.00% montmorillonite were taken in duplicate and separately dialyzed as previously described. After dialysis two packings were made from each for the *x*-ray analysis.

A statistical analysis of the results shows that the differences in machine and dialysis error not significant at the .90 probability level. A combined regression line, $y=168.6+241.8x$, is constructed from which unknowns can be determined with a precision of approximately ±0.5% in the 0.5–8.0% range.

THE AMERICAN MINERALOGIST, VOL. 45, JANUARY–FEBRUARY, 1960

THE CELL CONSTANTS OF ARTIFICIAL SIDERITE*

W. E. SHARP, *Institute of Geophysics, University of California*
Los Angeles 24, California

The artificial siderite used to measure the cell constants was prepared in the following way. Equal molar quantities of solid $NaHCO_3$ and $FeSO_4 \cdot 7H_2O$ were placed in a 120 ml. capacity stainless steel bomb which was half filled with water. The sealed bomb was then heated to 200° C. After reaching 200° C., CO_2 was pumped into the bomb until a total pressure of 500 bars had been reached. The bomb was maintained at 200° C. and 500 bars for 3 days. This procedure served to stabilize the precipitated $FeCO_3$. The white precipitate was then removed, filtered, and dried in an oven at 100° C. It partly oxidized to a yellow-brown color while drying. The dried material was placed in a "simple squeezer" high pressure apparatus, Kennedy and Griggs (1956), and heated to 600° C. at a pressure of 15 kb. The final product used in the x-ray work consisted of siderite together with a small amount of magnetite.

---

* Contribution No. 165, Institute of Geophysics.

Earlier attempts to prepare siderite were less successful. Mixtures of $FeCl_2 \cdot 4H_2O + Na_2CO_3 \cdot H_2O$ and $FeSO_4 \cdot 4H_2O + Na_2CO_3 \cdot H_2O$ with total $CO_2 + H_2O$ pressures of 50–200 bars in a bomb resulted only in forming magnetite. A small amount of siderite was, however, prepared by precipitating amorphous $FeCO_3$ and $Fe(OH)_2$ from solutions of $FeSO_4$ and Na_2CO_3 at atmospheric pressure. The solutions were kept covered with kerosene to prevent oxidation from the air. The precipitate was allowed to settle and the excess solution decanted off. The remaining water was removed by adding acetone and filtering. The material was dried in a vacuum oven at 110° C. However, most of the material still oxidized. This material was subsequently run as above in the "simple squeezer" at 500° C. and 15 kb. The resulting product was a mixture of hematite and siderite.

Table 1. X-Ray Powder Data for Artificial Siderite

Indices	$d_{obs.}$	$d_{calc.}$	$100\ I/I_0$
01.2	3.591	3.591	25
10.4	2.789	2.791	100
11.0	2.341	2.345	20
11.3	2.131	2.132	27
20.2	1.962	1.964	30
02.4	1.794	1.796	15
01.8	1.735	1.737	35
11.6	1.730	1.730	44
12.2	1.505	1.506	19
21.4	1.425	1.426	16
20.8	1.395	1.396	7
03.0	1.353	1.354	20
12.8	1.199	1.199	17
21.10	1.086	1.086	17
13.4	1.081	1.081	26
22.6	1.066	1.066	17

An x-ray powder diffraction pattern of the siderite-magnetite mixture, finely ground and mixed with vaseline, was obtained at 25° C. in a Norelco high angle recording diffractometer using FeKα radiation ($\lambda = 1.9373$ Å) and a Mn filter, with a scanning speed of $\frac{1}{8}°$ (2θ) per minute. High purity pre-calibrated NaCl was used as an internal standard.

The hexagonal unit-cell belonging to the space group $R\bar{3}c$ was obtained by a least squares treatment. The hexagonal cell constants are:

$$a_0 = 4.690 \pm 0.002 \text{ Å}, \quad c_0 = 15.370 \pm 0.003 \text{ Å}, \quad Z = 6, \quad \text{axial ratio } c/a = 3.277.$$

This compares closely with the values for natural material given in Dana's System of Mineralogy (1951) p. 167.

$$a_0 = 4.71\ kX, \qquad c_0 = 15.43\ kX;$$

$$a_0 = 4.677\ kX, \qquad c_0 = 15.267\ kX.$$

The calculated rhombohedral dimensions are: $a_{rh} = 5.795$Å, $\alpha = 47°45'$. The d-spacings and the corresponding indices are given in Table 1.

The calculated density is 3.941 which compares with the measured density of 3.96 ± .01, Dana's System of Mineralogy (1951) p. 168.

ACKNOWLEDGMENTS

I wish to thank Drs. Carl Pistorius and Julian Goldsmith for their help and encouragement during the preparation of this manuscript.

REFERENCES

PALACHE, C., BERMAN, H., AND FRONDEL, C. (1951), Dana's System of Mineralogy, Vol. II: John Wiley & Sons, Inc., New York.

GRIGGS, D. T., AND KENNEDY, G. C. (1956), A simple apparatus for high pressures and temperatures: *Am. Jour. Sci.*, **254,** 722–735.

SMITH, HERBERT J. (1918), On equilibrium in the system ferrous carbonate, carbon dioxide and water: *J. Am. Chem. Soc.*, **40,** 879–883.

Note added in proof—

The lattice constants of artificial siderite have also recently been determined by D. L. Graf (personal communication) using the same method. His results, found by extrapolation on back reflection measurements are:

$$a_0 = 4.6887 \text{ Å}, \ c_0 = 15.373 \text{ Å}; \ a_{rh} = 5.7954 \text{ Å}, \ \alpha = 47°43.3'$$

THE CANADIAN MINERALOGIST

The Canadian Mineralogist is published by the Mineralogical Association of Canada. It continues the publication known previously as *Contributions to Canadian Mineralogy*, which first appeared as parts of the *Geological Series of The University of Toronto Studies* until 1948. It was then sponsored by the Walker Mineralogical Club, and appeared as parts of *The American Mineralogist* from 1949 to 1955, the last issue being Vol. **5,** No. 7.

The first number of *The Canadian Mineralogist*, Vol. **6,** Part 1, appeared in 1957 under the editorship of Professor L. G. Berry, Queen's University, Kingston, Ontario. The current number for 1959, Vol. **6,** part 3, has now appeared. The Journal publishes papers in the fields of crystallography, geochemistry, mineralogy, petrology and allied sciences in either English or French. It is issued once a year, and is sent to all members of the Mineralogical Association of Canada. The annual fee for ordinary and associate members is $2.00; for corporate members, including libraries, $5.00; for student members, $1.00. Membership in the Association is subject to the approval of the executive committee.

Inquiries regarding membership, and remittances should be sent to Mr. S. Kaiman, Secretary, Mineralogical Association, c/o Mines Branch, 555 Booth Street, Ottawa, Canada.

Discussion at the Copenhagen Meeting

Under New Mineral Names in this issue (on page 257) is a reference to a paper by Dr. R. C. Mackenzie on the classification and nomenclature of the clay minerals. This paper is to serve as the basis for a discussion at Copenhagen in 1960. It is urged that all interested read this paper and send their comments to Dr. Mackenzie, at Macaulay Institute for Soil Research, Craigiebuckler, Aberdeen, Scotland, *with copies to* Dr. M. Fleischer, U. S. Geological Survey, Washington 25, D. C., representing the Nomenclature Committee of the M.S.A., *and to* Dr. Duncan McConnell, Ohio State University, Columbus 10, Ohio, the M.S.A. representative on the International Mineralogical Association Commission on New Minerals and Nomenclature.

NOTICES OF MEETINGS

International Mineralogical Association

The *Second* General Meeting of the *International Mineralogical Association* will be held in the Mineralogical Museum of the University of Copenhagen in Denmark between August 18 and 25, 1960. Besides the business meetings of the delegates and the meetings of the existing commissions, there will be two symposia: 1) Mineral synthesis (including high-pressure work), and 2) Feldspars (in all their aspects). Those planning to attend should write Dr. J. L. Amoros, Museo de Ciencias Naturales, Paseo de la Castellana 84, Madrid, Spain at once; if giving a paper in either symposium, submit a title. Those not registered with the International Geological Congress should send $10 to Dr. Hans Clausen, Mineralogisk Museum, Øster Volgade 7, Copenhagen K, Denmark, *at once* and give dates, kind of room (A best, B, C, or private lodging), one or two beds, etc.

Ninth National Clay Conference

On October 6, 7, and 8, 1960, the Ninth National Clay Conference will be held at Purdue University, Lafayette, Indiana, under the auspices of the Clay Minerals Committee of the National Academy of Sciences-National Research Council.

Two symposia of invited papers will be held on the topics of "Engineering Aspects of Physico-Chemical Properties of Clays" and "Clay-Organic Complexes." In addition to these special symposia there will be general sessions of contributed papers. All those having contributions should contact Dr. J. L. White, Chairman, Ninth National Clay Conference, Agronomy Department, Purdue University, Lafayette, Indiana. The title and an abstract of approximately 250 words should be sent in by June 1.

Further information and a preliminary announcement of the Conference may be obtained by writing to Dr. White.

Frequency Control Symposium

The 14th annual Frequency Control Symposium, sponsored by the U. S. Army Signal Research and Development Laboratory, will be held May 31–June 2 at the Shelburne Hotel, Atlantic City, N. J. The symposium has been held previously at the Berkeley-Carteret Hotel, Asbury Park, N. J.

Approximately 40 technical papers will be presented during the three-day sessions at which an attendance of 800 or more is expected, including representatives of most of the Free World nations.

Technical papers will deal with piezoelectric resonators, fundamental properties and synthesis of quartz, crystal oscillators and filters, Masers, gas cells, atomic beam devices, and applications of atomic frequency standards, including World Wide Clock Synchronization.

Dr. E. A. Gerber, director of the Frequency Control Division, of the Signal Laboratory, is general symposium chairman.

International Mineralogical Association

The time table for the Second General Meeting of this Association at the University of Copenhagen in Denmark in August 1960 is as follows:

Friday Aug. 19 to Sunday Aug. 21		Meetings of the various Commissions
Monday Aug. 22—	Morning:	Council Meeting
	Afternoon:	First Business Meeting of Delegates
Tuesday Aug. 23—	Morning Afternoon	Symposium on Mineral Synthesis (Chairman: Prof. J. R. Goldsmith)
Wednesday Aug. 24—	Morning:	Second Business Meeting
	Afternoon:	Symposium on Feldspars, Pt. 1 (Chairman: Prof. F. Laves)
Thursday Aug. 25—	Morning:	Symposium on Feldspars, Pt. 2
	Early Afternoon:	First meeting of the newly-elected Council
	Afternoon:	1) Continuation of symposia (if any speakers remain) 2) Round table discussion on Nomenclature of Polymorphic Forms and Transitions

BOOK REVIEWS

VECTOR SPACE AND ITS APPLICATION IN CRYSTAL-STRUCTURE INVESTIGATION, by MARTIN J. BUERGER. John Wiley and Sons, Inc., New York, 1959. xiv+347 pp., $6\frac{1}{8}\times 9\frac{1}{4}$ in., 186 figs., 31 tables. Price $12.00.

With the publication of this book the crystallographer has available for the first time a complete one-volume reference and exposition on the Patterson function and the methods for its interpretation in crystal-structure analysis. The author, who has himself made numerous original contributions to the theory and practice of this intriguing field, gives the reader the benefit of his comprehensive knowledge and practical experience in a clear, readable style.

The book contains 15 chapters, the first being a brief statement defining the phase problem in crystal-structure analysis, and the last, a retrospective glance over the relationship of the material covered in the book to the crystal-structure field as a whole. The 13 other chapters provide a carefully developed groundwork of theory, judiciously interspersed with numerous practical examples. Chapters 2, 4, and 5 define the Patterson function and give in detail its characteristics and pitfalls, together with some of the means for avoiding the latter. Chapter 3 is entirely devoted to some interesting early examples of the use of Patterson maps in the solution of crystal structures. The wide scope of A. L. Patterson's original papers is once again demonstrated by the author's numerous references to them throughout the first few chapters. The importance of symmetry and its effects in Patterson projections and in Harker sections, as well as its use in the implication theory originally developed by the author, are covered in Chapters 6 and 7. Vector sets are introduced in Chapters 8 and 9, and their relationship to the Patterson function is clarified. Chapters 10 through 13 are devoted to the theory and practice of image-seeking and superposition functions in two and three dimensions. Numerous illuminating examples are given from original crystal-structure determinations by the author and his students. Finally Chapter 14 deals with the problems caused by the presence of substructures in complex crystals and suggests methods of attack in such cases.

At the end of each chapter there is an extensive bibliography, and the book contains a comprehensive index. Detailed tables together with many illustrations enhance the overall presentation. The general format is designed to assist both the student and the casual reader; typographical errors have been kept to a minimum and only a few minor ones were noted by this reviewer. The cover of the book, with its vector set diagram, is most attractive, and on the endpapers are reproduced the Patterson representations of the 17 plane groups (also given in Chapter 6, Fig. 12B).

Undoubtedly not everyone would agree with the author on all aspects of his presentation. The emphasis and space allotted to some subjects (*e.g.* implication theory) reflect the personal views of the author and are not necessarily to be taken as a guide to the relative importance of the various methods. Subject to this minor reservation, there should be general agreement that the book fills a real need and it should become a working volume in the library of anyone interested in crystal-structure analysis.

JOAN R. CLARK
U. S. Geological Survey
Washington 25, D. C.

PRINCIPLES OF MINERALOGY, by WILLIAM H. DENNEN. The Ronald Press Company, New York, 1959. v+429 pages. Price $7.50.

This new introduction to mineralogy has many original features. According to the author's preface its goal is "first, to provide students in geology and allied fields with a mineralogical background that will aid them in studies where the nature of the solid state is an important consideration; second, to provide a text, nonmathematical in treatment, which is broad enough to provide a base for continuing mineralogical studies and detailed enough to bridge the gap now existing between introductory mineralogical work and advanced studies in crystallography, crystal chemistry, petrology, and geochemistry; and finally, to provide convenient descriptive material covering the more common minerals and mineral groupings for examples and laboratory reference."

The text is divided into seven chapters: 1, Symmetry (69 pages); 2, Fundamentals of Crystal Chemistry (26 p.); 3, Mineralogical Relations (29 p.); 4, Physical Characteristics of Minerals (26 p.); 5, Chemical Testing (24 p.); 6, Mineralogy (40 p.); 7, Mineral Descriptions (196 p.). There is also a 3-page table of atomic parameters in an appendix and subject and mineral indexes. The mineral descriptions cover about 150 species. Over 600 names are included in the mineral index, most of these appearing in the text only under the listing of "related minerals." Determinative tables are not included.

The opening chapters differ markedly from comparable chapters in other mineralogy textbooks. The first chapter, which in another book might have been entitled Crystallography, is clearly an adaptation of the first ten chapters of Buerger's *Elementary Crystallography*. As a consequence no reference is made to goniometry, crystal projection and many other subjects of importance. A distinguishing feature of the second chapter is a discussion of "The Architecture of Atoms," including reference to quantum mechanics, wave mechanics, the Pauli exclusion principle, and other matters not commonly referred to in connection with the treatment of chemical bonding in mineralogical texts.

Except in the sections dealing with chemical testing and mineral description there is little reference to observations, experiments or phenomena. The only historical reference noted appears on page 256, "the first mineral structure to be worked out (by W. H. Bragg) was that of halite." Even here there is no hint as to how the structure was "worked out." Such a treatment, emphasizing constructs and models, must give the beginner a rather distorted view not only of mineralogy but of science generally. In places it is unpleasantly reminiscent of attempts at popularization of some of the more esoteric aspects of physics so common in the mass periodicals in recent years.

It seems that the book has not been mineralogically edited. Incorrect dates are given for some of the standard works cited and the first, instead of the current, editions of Strunz, Tabellen and Hey's Index are referred to. Some mineral formulas, for instance that of colemanite, are not given in the best modern form. Though the diagrams of crystal structures are, on the whole, excellent and the inclusion of the skutterudite and columbite structures as well as others not usually found in mineralogy texts is most welcome, some of the crystal structure drawings are misleading or erroneous. Some structures, for example that of corundum, are shown by only a partial cell giving a faulty impression. The structure diagram of niccolite is misdrawn and mislabelled. A tabulation on page 105 improperly suggests that one of the cell dimensions of stannite must be double the corresponding dimension in chalcopyrite. On page 135 the impression is given that the terms *isotropic* and *anisotropic* are connected only with optical properties. In Fig. 1-42, copied from Buerger's *Elementary Crystallography*, the errors in the original have been retained. In this figure one of the symmetry diagrams is incomplete and four others violate the conventions stated in the text.

The decline in the art of crystal drawing, recently deplored by Professor Ramdohr (*Fortschr. Miner.* **37**: 27–35, 1959, p. 28), is painfully evident in this book. Many of the crystal drawings in the first chapter are poorly executed and some, especially the one at the upper right of Fig. 1-51 and the one in the middle of the upper row of Fig. 1-52, ought not to be acceptable even as the exercises of a beginner.

It is regrettable that the author in his eagerness to improve and modernize, has sought chiefly to discard and change and so has discarded most of the virtues of the older books along with many of their faults. Gains have been realized only at the cost of losses. Whether the former outweigh the latter may be questionable. Still, this book will be of interest to all who are concerned with the teaching of elementary mineralogy.

A. Pabst
Department of Geology
University of California, Berkeley

GEMSTONES OF NORTH AMERICA, by John Sinkankas. xv+675 pages, 175 illustrations (6 in color). D. Van Nostrand Co. Inc., Princeton, N. J., 1959. Price, $15.00.

This book is written for the amateur mineral collector and lapidarist. Detailed descriptions and often maps are given that will direct the collector to little-known localities. Where it was possible for the reviewer to check against his personal knowledge, these were accurate and complete. The geographical and locality index will be a great aid to the tourist who is also a collector. Within the limits of the clientele to which it is directed, it is more accurate, authentic, and complete than most popular books on gemstones.

The professional mineralogist will find the book a great aid in answering questions posed by the layman.

C. B. Slawson
University of Michigan

THE POWDER METHOD IN X-RAY CRYSTALLOGRAPHY, by Leonid V. Azároff and Martin J. Buerger, McGraw-Hill Book Company, Inc., New York, 1958. xv+342 pp., 6×9 in., Price $8.75.

"The powder method in *x*-ray crystallography" is a book that many mineralogists, chemists, metallurgists and ceramists have looked for in the literature of *x*-ray crystallography, published in English, and yet never have found. It represents a unique presentation of the method and its interpretation. It is at once comprehensive (complete), readable, practical and yet not too long nor encyclopedic.

After a brief treatment of elementary *x*-ray diffraction theory, two informative chapters deal with the design, adjustment and use of the powder cameras. A third chapter deals with the procedures for taking powder photographs. These five introductory chapters have a thread of continuity and are not a collection of disjointed facts and techniques.

Chapter 6 gives the fundamental equations relating to the interplanar spacings d_{hkl} to the cell edges and to the reciprocal-cell edges. The reciprocal lattice is discussed in chapter 9.

The identification of all the reflections in a powder photograph is of fundamental importance. C. Runge in 1917 clearly recognized that a solution to this problem could be found using the methods of Number Theory. The real use of Number Theory however was not made until 1948 by Hesse, and further modified in 1949 by Lipson. Stosick (1949) used linear Diophantine equations for indexing the powder photographs. The authors present an excellent treatment of analytical methods for indexing powder photographs including that of Hesse-Lipson and that of Ito. These methods are illustrated with worked out examples.

Students will be very grateful to the authors for the clear presentation of the material in the chapters on the "Reduced Cells and Their Application" and "Homogeneous Axes and the Delaunay Reduction."

The last four chapters deal with (1) methods of identifying substances, (2) sources of errors in measured spacings, (3) the practice of attaining accuracy, and (4) the appearance of the powder photographs, all presented in the lucid style so characteristic of this book.

Four useful tables make up the appendix. A very convenient time-saver is the table for the conversion of d to Q.

In this reviewer's opinion this book is a close approach to an ideal treatment of the subject.

George T. Faust

CLAYS AND CLAY MINERALS, Edited by Ada Swineford, National Academy of Sciences, National Research Council Publ. 566, vii+360 p., Washington, D. C., 1958, Price $4.50 (Proc. 5th Natl. Conf. on Clays and Clay Minerals, Urbana, Illinois, October 8–10, 1956).

This volume contains the papers presented at the 1956 conference held at the University of Illinois. The 27 papers listed below are published in full:

"Analysis of consistencies of kaolin-water systems below the plastic range."—Robert B. Langston and Joseph A. Pask
"Water vapor sorption on lithium kaolinite"—R. Torrence Martin
"Altered siliceous volcanics as a source of refractory clay".—L. B. Sand and L. L. Ames, Jr.
"Filtration theory for oil-well drilling fluids."—D. T. Oakes
"Surface conductance of sodium bentonite in water."—H. van Olphen and M. H. Waxman
"Diagenetic modification of clay mineral types in artificial sea water."—U. Grant Whitehouse and Ronald S. McCarter
"Glauconitic mica in the Morrison formation in Colorado."—W. D. Keller
"Density and structure of endellite."—Fred L. Pundsack
"New data on sepiolite and attapulgite." Fred A. Mumpton and Rustum Roy
"High temperature phases in montmorillonites."—George Kulbicki
"A discussion on the origin of clay minerals in sedimentary rocks."—Charles E. Weaver
"Statistical relationships of minor constituents of some nontronites."—Joseph A. Kornfeld
"Effects of a synthetic resin on differential thermal analysis of loess."—J. B. Sheeler, R. L. Handy, and D. T. Davidson
"Clay mineral distribution in the soil areas of Arkansas."—C. L. Garey
"Muscovite weathering in a soil developed in the Virginia Piedmont."—C. I. Rich
"Clay mineral distribution in the Hiawatha sandy soils of northern Wisconsin."—B. E. Brown and M. L. Jackson
"Clay mineralogy of Pennsylvanian sediments in southern Illinois."—Herbert D. Glass
"Clay minerals at a Pennsylvanian disconformity."—Jane A Dalton, Ada Swineford, and J. M. Jewett
"Clay mineralogy of Recent sediments from the Mississippi Sound area."—I. H. Milne and W. L. Shott
"A kinetic study of the dehydroxylation of kaolinite."—G. W. Brindley and M. Nakahira
"Heterogeneity in montmorillonite."—James L. McAtee, Jr.
"Layer charge and interlamellar expansion in a muscovite."—Joe L. White
"Experimental structure factor curves of montmorillonites."—Edward C. Jonas
"Random interstratification in organophilic bentonites."—James L. McAtee, Jr
"Gravimetric determination of monolayer glycerol complexes of clay minerals."—Earl B. Kinter and Sidney Diamond
"Surface areas of clay minerals as derived from measurements of glycerol retention."—Sidney Diamond and Earl B. Kinter
"Temperature stabilities of montmorillonite- and vermiculite-glycol complexes."—W. F. Bradley, R. A. Rowland, E. J. Weiss, and C. E. Weaver

Mineralogists and petrologists will be pleased to find the itinerary of the field trip in the area near Urbana included in this volume. About one-third of the papers are concerned with physico-chemical studies on clay systems. The rest deal with topics on the mineralogy and petrology of clays and soils.

Mineralogists and petrologists and others interested in clay mineralogy will find this volume as indispensable as its predecessors.

George T. Faust

OUR MINERAL RESOURCES, by Charles M. Riley, John Wiley & Sons, Inc., New York, 1959. x+338 pages, 102 figures. Price $6.95.

This is a clearly written and well illustrated text for elementary economic geology.

The author states in the preface that the book is designed both as a text for an introductory course in economic geology for the training of professional geologists, and as a text for a "cultural" course in earth sciences intended to acquaint non-geology students with the mechanism of ore genesis, occurrence and production. The author admirably fulfills the second purpose, but falls somewhat short of accomplishing the first.

The book is divided into two main sections with six appendices: (I) Metallic Minerals, (II) Nonmetallic Minerals.

Chapter 1, Principles of Ore Deposition, is by far the most outstanding contribution of the text. The author manages in a most able way to condense the literature on this subject without violating the integrity of the substantive matter. However, the later chapters lack development, and thus impairs the effectiveness of this section.

Chapters 2 through 9, respectively, discuss ore deposits of Iron; Aluminum; Copper; Lead and Zinc; Tin and Tungsten; Gold and Silver; Nickel, Chromium and Platinum; and Uranium and Vanadium. Chapter 10, Miscellaneous Metals, including information on Manganese; Mercury; Molybdenum; Cobalt; Titanium; Antimony; Magnesium; Beryllium; Bismuth and Cadmium is too encompassing and too brief to be effective.

The second section includes brief resumes on Ground Water, Coal, Petroleum, Rock Building Materials, Gem and Gemstones and Miscellaneous Nonmetallic Minerals. Again, development of substantive matter is sacrificed for brevity's sake and the section possesses a rather limited discussion of general uses, occurrences, characteristics and localities of nonmetallic minerals.

The six appendices are welcome additions and include a Glossary, List of Chemical Elements, Geologic Time Scale, List of Valuable Nonmetallic Minerals and a short General Reference.

In the reviewer's opinion this book will meet the needs of colleges and small universities which have a pre-geology curriculum and/or survey courses in earth sciences. The text is also recommended as supplementary reading to augment courses in Conservation.

William A. Kneller
Eastern Michigan University
Ypsilanti, Michigan

INTERNATIONAL TABLES FOR X-RAY CRYSTALLOGRAPHY. Vol. II, Mathematical Tables. Editors: J. Kasper and K. Lonsdale. xviii+444 pages, with 39 figures. Published for the International Union of Crystallography by The Kynoch Press, Birmingham, England. Price £5 15s. Members of learned scientific societies may obtain personal copies for £3 10 s.

Volume II contains the following sections:

1. Introduction
2. Basic mathematics
3. Crystal geometry

4. Diffraction geometry
5. Physics of diffraction methods
6. Fourier synthesis and structure factors
7. Special topics
8. Miscellaneous exponential and trigonometric tables
9. Dictionary of crystallographic terms in English, French, German, Russian and Spanish.

INDEX OF CRYSTALLOGRAPHIC SUPPLIES. Second edition, 1959, edited by A. J. Rose, published by Commission on Crystallographic Apparatus of the International Union of Crystallography, 125 pages+xxvi, paper bound, $10\frac{5}{8}$ in.×$8\frac{1}{4}$ in. Price $2.50 per copy shipped by surface mail; bank check or postal money order (C.C.P. Paris 6168–45) should be made payable to Société française de Minéralogie et de Cristallographie (I.U.Cr.), 1, rue Victor-Cousin, Paris 5^e, France.

Contents: I. *List of Equipment and Suppliers:* The material is classified in 11 categories corresponding to its use: supply of crystals, sample preparation; physical, morphological and optical properties; microradiography; *x*-ray spectrography; determination of crystal structure by *x*-ray, electron and neutron diffraction; physical and chemical analyses, and computations. A brief specification is sometimes included. The main office of the suppliers is given and only materials that are commercially available are listed.

II. *Literature References:* reference to publications on the interpretation of experimental data, e.g., charts, tables, technical documents; books on crystallography published since 1903; a list of crystallographical periodicals.

III. *Advertisements.*

IV. *Addresses of Manufacturers and Suppliers:* including branches in other nations (up to 10).

W. Parrish
Philips Laboratories
Irvington-on-Hudson
New York, U.S.A.

NEW MINERAL NAMES

Karrenbergite

Eckart Walger. Inaug. Diss., Univ. Freiburg, 1958, p. 52–54; from an abstract by K. F. Chudoba in *Hintze's Handb. Mineralogie, Erganzangsband* **II**, Lief. 10, 737–738 (1959).

A preliminary description. Analysis gave SiO_2 40.90, Al_2O_3 5.25, Fe_2O_3 14.43, FeO 8.24, MgO 4.37, CaO 1.73, Na_2O 0.81, K_2O 0.20, H_2O 18.42, ign. loss 6.18, sum 100.53 per cent. This is calculated to the montmorillonite-type formula $(Mg_{0.58}Fe''_{0.62}Fe'''_{0.97}Al_{0.19})_{2.36}(Si_{3.64}Al_{0.36})\cdot Ca_{0.16}Na_{0.14}K_{0.02}$, intermediate between nontronite and saponite.

X-ray powder data are 15.23 vs, 4.57 m, 3.05 w, broad, 2.06 w, broad, 1.53 m. Indices of refraction: α'1.510, γ'1.528, X brownish-yellow, Z dark olive-green. Fibrous, greenish-brown, transparent.

The mineral occurs in a geode in hyalo-dacite, on scalenohedral calcite that is partly replaced by chalcedony and is associated with yellow transparent opal and yellow fibrous cristobalite (lussatite). It is covered by fine reddish natrolite. The occurrence is in the Karrenberg, near Reichweiler, Pfalz.

The name is for the locality.

Michael Fleischer

Norsethite

Charles Milton, M. E. Mrose, E. C. T. Chao, and J. J. Fahey, Norsethite, $BaMg(CO_3)_2$, a new mineral from the Green River formation, Wyoming, *Bull. Geol. Soc. Am.*, **70**. 1646 (1959) (abs.)

The mineral occurs as clear to milky white circular plates or flattened rhombohedral crystals 0.2–2 mm. across. Forms observed: $c\{001\}$, $a\{11\bar{2}0\}$, $m\{10\bar{1}0\}$, $r\{10\bar{1}1\}$. Probably space group $R32\text{-}D_3^7$, $a_0$5.02, $c_0$16.75 Å, a_{rh} 6.29, α 47°02′; Z=1 in the rhombohedral cell. The strongest *x*-ray lines are 3.015 (100), 3.860 (35), 2.656 (35), 2.512 (35), 2.104 (35), 1.931 (35), 1.864 (35). Cleavage rhombohedral good, fracture hackly. Analysis made on 0.1 g. gave BaO 52.9, CaO 0.5, MnO 0.1, MgO 13.9, Fe_2O_3 (total Fe) 0.4, CO_2 31.2, SiO_2 0.3, insol. 0.5, total 99.8%. Infusible. Insoluble in water, decomposed by cold dilute HCl.

Luster vitreous to pearly, H. 3½, G. 3.837 (measured), 3.84 (calcd.). Optically uniaxial, negative ω 1.694, ϵ 1.519.

Norsethite occurs in black dolomitic oil shale below the main trona bed in the Westvaco trona mine, Sweetwater County, Wyoming, associated with shortite, labuntsovite, searlesite, loughlinite, pyrite, and quartz. It also occurs in similar association and with northupite in gray shale.

The name is for Keith Norseth, geologist of the Westvaco trona mine.

M. F.

Fenaksite

M. D. Dorfman, D. D. Rogachev, Z. I. Goroshchenko, and A. V. Mokretsova. *Trudy Mineralog. Muzeya Akad. Nauk S.S.S.R.* No. 9, 152–157 (1959) (in Russian).

Analyses of two samples from the same pegmatite (by A. V. M. and Z. I. G., resp.) gave SiO_2 60.14, 60.54; TiO_2 0.06, 0.04; Al_2O_3 1.10, 0.66; Fe_2O_3 1.32, 1.54; FeO 12.45, 12.49; MgO 0.46, 0.70; MnO 2.34, 2.49; CaO 0.64, 0.74; Na_2O 6.77, 7.51; K_2O 11.48, 11.71; H_2O^- 0.76, 0.78; H_2O^+ 2.40, 0.67; F 0.23, 0.47, sum 100.15, $100.34-(0=F_2)=100.06$, 100.14%. Determinations on a third sample gave H_2O^- 1.12, H_2O^+ 0.91%. Spectrographic analysis by N. N. Kolesnikov showed, in addition to the elements listed Ba—trace, Cu, Zr, Sr—faint lines. After subtraction of a small amount of adularia (calculated from Al_2O_3), these analyses correspond to the formula $(K, Na)_4(Fe'', Mn)2(Si_4O_{10})_2$ (OH, F) with K:Na nearly 1:1. Fenaksite is decomposed by acids with the deposition of silica. It fuses easily before the blowpipe to a green glass; in the reducing flame, the powder becomes magnetic. From the composition, it may be referred either to the apophyllite group or to the mica group.

The mineral occurs in grains up to 2–4 cm. in diameter.

It is light rose in color, luster pearly on the two cleavages, which are at an angle of 122° to one another. Hardness 5–5½. G. 2.744 (pycnometer). It is optically biaxial, positive; *ns* (Na) α 1.541, β 1.560, γ 1.567, 2V 84°, Z=*b*, plane of optic axes (001), Z: cleavage I=20°, Y:cleavage II=49°, X:cleavage II=8°.

Laue and rotation photographs show the mineral to be monoclinic, space group *C* 2/*m*, *C*2, or *Cm*, a_0 14.95, b_0 6.98, c_0 9.79 (not stated whether Å or kX), β 112°, Z=2. *X*-ray powder data by N. N. Sludsko are given; the strongest lines are 3.03 (10), 2.46 (7), doublet 3.55, 3.44 (7), 2.88 (6), 2.71 (6), 1.875, 1.835 (6), 1.752 (6).

The name is for the composition.

Discussion.—There must be an error in the optical data; the indices of refraction given indicate an optically negative mineral with 2V 61°. Perhaps β should be 1.550, which would give 2V 74°?

The name is unfortunate because it is so easily confused with phenakite. This may be the Mineral No. 5 of Dorfman (see *Am. Mineral.* **44,** 910 (1959)).

M. F.

Canasite

M. D. Dorfman, D. D. Rogachev, Z. I. Goroshchenko, and E. I. Uspenskaya. Canasite, a new mineral. *Trudy Mineralog. Muzeya Akad. Nauk S.S.S.R.*, No. 9, 158–166 (1959) (In Russian).

Chemical analyses of two samples from the same pegmatite, by E.I.U. and Z.I.G., respectively, gave SiO_2 56.08, 55.71; TiO_2 0.10, 0.06; Al_2O_3 0.55, 0.20; Fe_2O_3 1.41, 0.72; FeO 0.71, 0.36; MgO 0.05, 0.26; MnO 0.38, 0.41; CaO 20.95, 20.39; Na_2O 8.01, 7.08; K_2O 8.47, 10.63; H_2O^- 0.49, 0.60; H_2O^+ 1.11, 1.25, F 2.21, 2.17; Cl 0.22, ; CO_2 0.20, ; P_2O_5 0.04, 0.08; sum. 100.98, 99.92−(0=F_2) 0.96, 0.91=100.02, 99.01%.

A footnote to the first analysis states that "the determination of Na provokes doubts." Spectrographic analysis shows, in addition to the elements listed above, Sr-medium, Ni, Cu-weak, Be insignificant traces. After deducting small amounts of magnetite (calculated from Fe_2O_3) and adularia (calculated from Al_2O_3), these analyses give the formula: $(Na, K)_5 Ca_4 (Si_2O_5)_5(OH, F)_3$. The mineral is decomposed by acids with the separation of silica. Easily fusible to a transparent glass in the blowpipe or alcohol flame.

Canasite occurs in grains up to 3 cm. in diameter. Transparent and translucent, color greenish-yellow, streak colorless. Luster vitreous. The mineral has a perfect cleavage and a very perfect cleavage at an angle of 118° to the first. Brittle, fracture splintery, breaks into long acute-angled or wedge-shaped pieces. When ground, gives a felty mass. G. (pycnometer) 2.707.

The mineral is optically biaxial, negative, *ns* (Na) α 1.534, β 1.538, γ 1.543, 2V 58°. The optic axial plane is (010), Y=*b*, Z: less perfect cleavage=2°. Polysynthetic twinning was observed, with the twinning plane at an angle of 8° to the less perfect cleavage.

Laue, rotation, and DeJong photographs showed canasite to be monoclinic, space group *C*2/*m*, C_2, or *Cm*, a_0 18.87, b_0 7.24, c_0 12.60Å, β 112°. Unindexed *x*-ray powder data are given; the strongest lines are 3.074 (broad)—10, 1.814—9, 2.901—8, 1.638—8, 4.68—7, 4.80—6, 2.354—6.

The mineral occurs with fenaksite (see preceding abstract). Lamprophyllite occurs in fractures in canasite. The name is for the chemical composition.

DISCUSSION. Presumably to be classed as a phyllosilicate. This may be Mineral No. 6 of Dorfman (*see Am. Mineral.* **44**, 910 (1959). The indices of refraction given do not correspond to the figure given for 2V.

M. F.

Metakahlerite

KURT WALENTA. Die sekundären Uranmineralien des Schwarzwaldes. *Jahresheft geol. Landesamt Baden-Württemberg*, **3**, 17–51 (1958).

The mineral was found as sulfur yellow rare scaly aggregates in the Sophia Shaft, Baden Microchemical tests showed Fe, U, As. Composition presumably Fe $(UO_2)_2$ $(AsO_4)_2 \cdot 8H_2O$. Cleavage (001) excellent, (100) good. Luster pearly on (001). Optically uniaxial to biaxial, negative with 2V up to 22°, *ns* ϵ 1.608, ω 1.642, both ±0.002, weakly pleochroic, E nearly colorless, O pale yellow. Not fluorescent. The *x*-ray powder diagram indicates this to be a meta-form; the strongest lines are 3.59 (10), 8.55 (9), 4.29 (6), 5.11 (5), 2.15 (5), 2.11 (5).

M. F.

Meta-uranospinite

KURT WALENTA. Die sekundaren Uranmineralien des Schwarzwaldes. *Jahresheft geol. Landesamt Baden-Württemberg*, **3**, 17–51 (1958).

Name given to the dehydration product of uranospinite from the Clara shaft, Wittichen, Baden, characterized by higher indices of refraction than uranospinite, $\gamma = 1.618$. Weakly pleochroic, X colorless, Z pale yellow. Readily rehydrates to uranospinite. Formula presumably Ca $(UO_2)_2$ $(AsO_4)_2 \cdot 8H_2O$.

M. F.

Unnamed Ca, Sr, U oxides

J. PROTAS. Contribution a l'étude des oxydes d'uranium hydratés. *Bull. soc. franc. mineral. crist.*, **82**, 239–272 (1959).

Pseudo-hexagonal reddish-orange crystals, up to 0.5 mm., were found in geodes and in fissures in gummite on altered pitchblende from the Margnac II Mine. Microchemical tests and spectrographic analysis showed Ca, Sr, and U. Analysis gave UO_3 83.9, H_2O 7.4%. Phosphate, sulfate, carbonate, and silicate were absent. The crystals showed (001) (dominant), (010), (110), (111), and rarely (101). G·5.29±0.05. Orthorhombic with a_0 14.06±0.05, b_0 24.12±0.10, c_0 14.16±0.05Å. Cleavage (001) good. Biaxial, negative, β 1.94, γ 1.96, 2V 38±3°. The *x*-ray powder pattern has strongest lines 3.11 (vs), 3.47 (s-vs), 6.82 (s), 3.53 (s), 3.17 (ms), 1.966 (ms).

When the mineral is heated in water at 100°, it is transformed into material giving a powder pattern identical with that given by pale yellow spherulites associated with the orange mineral. The strongest lines are 7.09 (vs), 3.49 (s), 3.13 (s), 1.951 (ms).

M. F.

Unnamed ("Mineral X")

W. T. EPPRECHT, W. T. SCHALLER, AND A. C. VLISIDIS. Über Wiserit, Sussexit, und ein weiteres Mineral aus den Managanerzen vom Gonzen (bei Sargans). *Schweiz mineralog. petrog. Mitt.*, **39**, 85–104 (1959).

An unknown fibrous mineral associated with wiserite (see page 256) gave *x* ray powder data and fiber diagrams that were indexed on a monoclinic cell with a_0 11.55±0.05,

b_0 3.4±0.3, c_0 8.18±0.05 kX, β 109.5°. The fiber axis is parallel to b. The strongest lines are (in kX) 10.75 s, 5.4 s, 3.68 s, 2.93 s, 1.791 s. Optical data were uncertain because of intergrowth with wiserite; α ranged from 1.690–1.710, γ was about 1.76. Extinction inclined, up to 5°. Spectrographic analyses of mixtures with wiserite showed the same elements as in wiserite, so the mineral is probably a manganese borate.

M. F.

Unnamed

Jean Papageorgakis. Ein neues Bariummineral der Marmore von Candoglia in der unteren Val d'Ossola. *Schweiz. mineralog. petrog. Mitt.* **39**, 333–335. (1959).

The mineral occurs in clefts between barite layers and calcium silicate rock in the Candoglia marble, associated with barite, barium feldspar, quartz, epidote, and calcite. It forms bright gray columns up to 5 cm. long and 1 cm. thick. Luster vitreous to pearly, somewhat greasy on fractures. Brittle, H. =6. G. (pycnometer) 3.13. Cleavage prismatic, parting pinacoidal. Optically uniaxial to biaxial, negative, 2V 0–10°, *ns* ω 1.595, ϵ 1.589.

Analysis by H. Schwander of material picked under the binoculars gave SiO_2 31.5, Al_2O_3 19.5, CaO 12.0, BaO 23.5, Na_2O 0.6, K_2O 0.8, SO_3 9.9, H_2O 2.4, Cl tr., sum 100.2%. This gives $5BaO \cdot 8CaO \cdot 7Al_2O_3 \cdot 19SiO_2 \cdot 4SO_3 \cdot 5H_2O$ (Recalculation gives $Na_{0.7}K_{0.6}Ba_{5.5}Ca_{7.7}Al_{13.7}Si_{18.8}O_{72}(SO_3)_4 \cdot 5H_2O$ M.F.). The SO_3 would correspond to 29.2% barite, but microscopic and *x*-ray study, which showed only faint lines of barite, indicated that no more than 5% barite could be present. The mineral may be related to scapolite, but the indices of refraction are low for the high content of BaO.

M. F.

Dixeyite

Vladi Marmo. Dixeyite—a new natural hydrous aluminium silicate. *Schweiz. mineralog. petrog. Mitt.*, **39**, 125–132 (1959).

The mineral was found in a small outcrop of amphibolite 1 mile north of the village of Belihun, Kangari Hills, central Sierra Leone. The amphibolite is believed to occupy a very narrow zone along the margin of ultrabasic rock at its contact with granodiorite. The rock consists of hornblende, quartz, magnetite, and an unknown isotropic colorless mineral; a chemical analysis, but no mode, of the rock is given. Separation by heavy liquid gave a concentrate "Predominantly containing the unknown isotropic mineral." Analysis of this concentrate by Aulis Heikinnen gave SiO_2 51.72, TiO_2 0.55, Al_2O_3 21.15, Fe_2O_3 2.68, FeO 2.76, MnO 0.15, MgO 2.17, CaO 2.56, Na_2O 0.34, K_2O 0.32, P_2O_5 0.45, CO_2 none, H_2O^+ 10.26, H_2O^- 5.03, sum 100.14%. From this, an unstated amount of hornblende and magnetite is deducted, leaving (in moles) SiO_2 730, Al_2O_3 166, K_2O 3.5, CaO 2, H_2O 570, or approximately $Al_2O_3 \cdot 4\text{–}5\ SiO_2 \cdot 3\text{–}4\ H_2O$. Some quartz was present. Analysis of "a few mg. of reasonably pure material" gave SiO_2 63.14, Al_2O_3 23.65, Fe traces, CaO 0.05%, confirming the above formula. ($Al_2O_3 : SiO_2 = 1 : 4.5$.)

X-ray powder data showed some variation; 2 patterns gave a_0 7.55, 7.7Å; "this suggests that the lattice may not be exactly cubic." Calculations gives 22.55 O atoms per unit cell, which suggests that a_0 should be doubled to 15.2Å. The strongest *x*-ray lines are 3.32, 3.40 (s), 3.09, 3.19 (s), 2.27 (s).

G. approximately 2.51–2.52, *n* 1.5057. The mineral is perfectly isotropic.

The name is for F. Dixey, Director, British Overseas Geological Surveys, first government geologist of Sierra Leone.

Discussion.—An unsatisfactory description.

M. F.

Dneprovskite

M. N. Ionov. Cassiterite and wood tin from the Omchug placers. *Trudy Vses. Magadansk N.-I. Inst.*, **19,** 9–16 (1957); from an abstract by E. M. Bonshtedt-Kupletskaya in *Zapiski Vses. Mineralog. Obshch.*, v. **88,** 311–312 (1959).

The name was proposed in 1944 by P. I. Skornyakov for wood tin of radiating fibrous structure from the Dnepropetrovsk deposits, northeastern U.S.S.R.

Discussion.—As the abstractor states, an unnecessary name.

M. F.

Khovakhsite, Tuvite

N. N. Shishkin and V. A. Mikhailov. Study of the composition of ores of the Khovakh cobalt deposits. *Sborn. mater. tekhn. inform.*, **6,** 5–23 (1956).

Yakhontov, L. K. Initial products of the weathering of safflorite. *Vestnik Mosk. Univ.* **1958,** No. 2, 147–156; from abstracts by E. M. Bonshtedt-Kupletskaya in *Zapiski Vses. Mineral. Obshch.* **88,** 317 (1959).

These are names used in the literature of economic geology for oxidation products of smaltite and safflorite. Khovakhsite is light to dark brown, earthy, luster waxy or resinous, H. 2½–3, G. 2.81. The composition ranges from $Fe_2O_3 \cdot 2(Ca, Co)O \cdot As_2O_5 \cdot 3\text{–}6H_2O$ to $Fe_2O_3 \cdot 4\text{–}8$ (Ca, Co, Ni) O. $2\text{–}4\ As_2O_5 \cdot nH_2O$. Fine lamellar to fibrous, extinction parallel, birefringence low, *n* variable 1.65–1.73. Mostly amorphous to *x*-rays.

Tuvite is a name applied to material constituting a further stage of the oxidation; it is yellow, brittle. The names are for the Khovakh deposits of the Tuva Autonomous Region. U.S.S.R.

Discussion.—As the abstractor states, it is impossible to determine whether these are minerals or mixtures. They should not have been named.

M. F.

Parbigite

Yu. V. Mirtov. Parbigite, a new mineral of the collinsite group. *Vestnik Zap.-Sib. and Novosib. geol. Upr.* **1958,** No. 1, 72–75; from an abstract by E. M. Bonshtedt-Kupletskaya, *Zapiski Vses. Mineral. Obshch.*, **88,** 318–319 (1959).

The mineral was found in drill core from a depth of 236 m. in the Parbig region, Tomsk oblast, in cavities in sandstone, associated with calcite and spherosiderite. It forms radial-fibrous aggregates, rarely pyramidal or prismatic crystals (0.5–1 mm). White, pale yellow, or colorless. Cleavage in one direction very perfect; under the microscope 4 cleavages were noted at angles: $C_1\text{-}C_2 = 88°$, $C_1\text{-}C_3 = 72°$, $C_1\text{-}C_4 = 56°$, $C_3\text{-}C_4 = 49°$. Luster silky to vitreous, H. about 3, G. 3.08. Optically biaxial, negative, *ns* α 1.633, β 1.658, γ 1.670, 2V 70–74°, $C{:}\gamma = 18\text{–}23°$. Easily fusible to a brown slag. Spectrographic analysis showed major Ca, Fe, P, Mg, minor Sr and Ba.

Discussion.—The difference in optical sign is insufficient basis for giving a new name. The mineral is presumably messelite.

M. F.

Pallite

Laurent Capdecomme and René Pulou. Sur la radioactivité des phosphates de la région de Thiès (Sénégal). *Compt. rend. acad. sci. France*, **239,** 298–290 (1954).

Edmond Latrilhe. Contribution a l'étude des phosphates alumineux de la région de Thies (Sénégal). *Haut Comm. Repub. Afrique occidentale franc., Bull. service geol. et prospection minière* No. **25,** 1–84 (1959).

Chemical analyses and *x*-ray data show that the principal minerals present in the aluminum phosphate zone are crandallite and pallite (=ferrian millisite), with minor augelite and rare wavelite and turquoise. Analyses of two samples estimated to contain 95% pallite+5% crandallite gave, resp., P_2O_5 26.28, 27.36; Al_2O_3 25.74, 30.50; sol. Fe_2O_3 11.97, 9.86; CaO 6.94, 6.63; MgO 0.42, 0.53; Na_2O 1.95, 1.86; K_2O none, none; loss on ign. 15.98, 16.22; SiO_2 5.36, 3.57; TiO_2 (insol.) 2.14, 1.63; Fe_2O_3 (insol.) 1.14, 2.19; MnO_2 0.47, 0.00; F 0.46, 0.55; sum 98.85, 100.90%. Uranium is present in amounts up to 140 ppm U in pallite and four times as much in crandallite.

The name is for the village of Pallo.

DISCUSSION.—Unnecessary name for ferrian millisite.

M. F.

Hormites

R. C. MACKENZIE. The classification and nomenclature of clay minerals. *Clay Minerals Bull.*, **4**, No. 21, 52–66 (1959).

The name hormites is suggested by R. H. S. Robertson as a group name for the sepiolite-palygorskite group. The name is from the Greek for chain.

DISCUSSION.—This is another example of the deplorable practice of cluttering the literature with unnecessary names (see *Am. Mineral.* **41**, 536 (1956)). I have urged repeatedly that such suggestions should be circulated privately for comment and should not be put into print until there is near unanimity on their desirability.

See note on page 244 of this issue.

M. F.

NEW DATA

Sterrettite, Kolbeckite

M. E. MROSE AND BLANCA WAPPNER. New data on the hydrated scandium phosphate minerals: sterrettite, "eggonite," and kolbeckite. *Bull. Geol. Soc. Am.*, **70**, 1648–1649 (1959) (abs.).

X-ray fluorescence analysis of sterrettite from Fairfield, Utah, of "eggonite" from Altenberg, Belgium (?), and of kolbeckite from Schmeideberg, Saxony (type localities) showed that scandium is a major constituent. *X*-ray study (unit cells given) showed that the structure is of the metavariscite type and the formulas should be of the type $AXO_4 \cdot 2H_2O$. Sterrettite, supposedly $Al_6(PO_4)_4(OH)_6 \cdot 5H_2O$ (Dana's system, 7th Ed., vol. 2, p. 965) is probably $ScPO_4 \cdot 2H_2O$; the unit cell is nearly the same as for synthetic $ScPO_4 \cdot 2H_2O$. The identity of eggonite with sterrettite is confirmed. Kolbeckite, supposedly a silicate-phosphate of Be, Ca, and Al (Dana's system, 7th Ed., vol. 2, p. 1015–1016) may be $(Sc, Be, Ca)(PO_4, SiO_4) \cdot 2H_2O$.

DISCUSSION.—This doubles the number of minerals known to contain more than 1% Sc_2O_3.

M. F.

Iriginite

G. YU. EPSHTEIN. On the molybdates of uranium—moluranite and iriginite. *Zapiski Vses. Mineral. Obshch.*, **88**, 564–570 (1959) (in Russian).

Data available previously were summarized in *Am. Mineral.*, **43**, 379 (1958). Additional data: Color canary-yellow, luster vitreous. Fracture uneven. Hardness 1–2, higher in aggregates. G. 3.84 (probably too low because of impurities). Indices of refraction, α 1.730 ± 0.003, $\beta \sim 1.82$, $\gamma \sim 1.93$. Extinction parallel. The mineral does not fluoresce. It is soluble in acids on heating. Analysis by M. M. Stukalova gave MoO_3 38.62, UO_3 41.92, CaO 0.46, loss on ignition 9.70, insol. 9.04, sum 99.74%, corresponding to $MoO_3 : UO_3 : H_2O = 1.84 : 1 : 3.70$ or $UO_3 \cdot 2MoO_3 \cdot 4H_2O$. A potentiometric pH determination by N. I. Komarova gave pH 4.4, so the formula is given as $H_2(UO_2)(MoO_4)_2 \cdot 3H_2O$. A D.T.A. curve shows a large and broad endothermic effect at 100–400°, a sharp exothermic effect at 480°.

X-ray powder patterns (more than 50 lines) were obtained by Yu. V. Kazitsyn in 1952 and A. I. Komkov in 1959. The former found strongest lines: 3.222 (10), 1.129 (8), 2.625 (6), 2.142 (6), 1.836 (6), 1.249 (6), 1.206 (6), 1.188 (6), 1.165 (6), 6.4 (5), 1.533 (5). The latter found 6.19 (10), 3.20 (9), 1.628 (9), 2.14 (8), 1.127 (8), 1.529 (7), 2.61 (6), 2.07 (6), 1.688 (6), 3.30 (5), 3.09 (5), 1.962 (5) 1.185 (5).

M. F.

Moluranite

G. Yu. Epshtein. On the molybdates of uranium—moluranite and iriginite. *Zapiski Vses. Mineral. Obshch.*, **88,** 564–570 (1959) (in Russian).

Data available previously were summarized in *Am. Mineral.*, **43,** p. 380 (1958). Additional data: Isotropic, *n* 1.97–1.98. G. about 4. Soluble in acids on heating. Light gray in reflected light, reflecting power about the same as that of pitchblende. Amorphous to *x*-rays. *X*-ray powder data on heated material correspond to those of U_3O_8. Analysis by M. M. Stukalova gave MoO_3 38.50, UO_2 10.30, UO_3 32.35, SiO_2 4.56, loss on ignition 14.03, sum 99.74%, corresponding to $UO_2 \cdot 3UO_3 \cdot 7MoO_3 \cdot 20H_2O$. A D.T.A. curve shows a large and broad endothermic effect (40–400°) and small exothermic effects at 500°, 800°, and 980°.

M. F.

REDEFINITION OF MINERAL

Wiserite

W. T. Epprecht, W. T. Schaller, and A. C. Vlisidis. Über Wiserit, Sussexit, und ein weiteres Mineral aus den Manganerzen von Gonzen (bei Sargans). *Schweiz. mineralog. petrog. Mitt.*, **39,** 85–104 (1959).

The mineral wiserite, described in 1842 as a manganese oxide-carbonate and later discredited as pyrochroite, was shown by Epprecht in 1944 to give a distinctive *x*-ray pattern (see *Am. Mineral.* **32,** 485 (1947)). Restudy shows that the previously published analyses were in error; the mineral is a hydrous borate, not an oxide or carbonate. The CO_2 reported was present as rhodochrosite.

Two samples were purified, and new analyses by A.C.V. gave: B_2O_3 17.58, 16.32; MgO 2.79, 3.00 (spec. detn. by H. J. Rose); FeO tr., tr.; MnO 63.13, 65.23 (total Mn as MnO; a little MnO_2 was present); CaO 3.23, 0.75; H_2O^+ 7.85, 8.00 (total H_2O); H_2O^- 0.35, n.d.; Cl 3.02, 2.95; F none (<0.1), n.d.; CO_2 tr., tr.; Al_2O_3 (+tr. Fe) 1.00, 0.45; insol. 1.20, 3.60; P_2O_5, SO_3 not present; total 100.15, $100.30-(0=Cl_2)$ 0.68, 0.67=99.47, 99.63%; G. 3.42, n.d. These lead to the formula 4 (Mn, Mg, Ca) $O \cdot B_2O_3 \cdot 2H_2O$, with Cl replacing part of the H_2O (Better—$Mn_4B_2O_5(OH, Cl)_4$; M.F.). Spectrographic analysis of a mixture of wiserite and an unknown mineral (Mineral X, see pg. 254) showed also traces of As, Bi, Cu, Ni, Pb, Sb, Sn, Sr, and Zn.

Rotation diagrams show wiserite to be tetragonal with a_0 14.27±0.01, c_0 3.31±0.01 kX, Z=4. *c* is parallel to the fibers. Cleavage is perfect across the fibers. Indexed *x*-ray powder photographs of 4 samples are given. The strongest lines (in kX) are 14.2 vs, 2.53 s, 6.40 ms. 3.36 ms, 2.87 ms, 2.35 ms.

Indices of refraction are somewhat variable: α 1.700–1.717, γ 1.753– about 1.76. Extinction parallel. Z is perpendicular, X parallel to the fiber direction. Uniaxial to slightly biaxial, negative. Weakly pleochroic with X bright—to dark orange-brown, Z colorless to bright orange-brown.

Wiserite occurs in fibers, intimately intergrown with pyrochroite, an unidentified mineral (see page 254), and sussexite (near the end member, optical and *x*-ray data given).

M. F.

SHALE'S

LISTING OF FINE BULK MINERALS FOR SCIENTIFIC STUDY PURPOSES

SOLD BY THE POUND

ACTINOLITE (Calif.) Green radiating masses	$ .30 per pound
APATITE (Mexico) Yellow crystals and sections	4.50 per pound
KYANITE (Brazil) Blue crystal blades up to 3″	1.50 per pound
CORUNDUM var **SAPPHIRE** (Africa) Mostly blue masses & Xl sections	1.25 per pound
CORUNDUM var **RUBY** (Madagascar) Pink to red Crystal sections	5.75 per pound
BARITE (Calif.) Brown crystals and masses	.50 per pound
MARTITE (Calif.) Black crystal sections and masses	.45 per pound
JET (Utah) Black limb sections and pieces	1.95 per pound
ARAGONITE (Nevada) White stalatitic sections and masses	.45 per pound
KERNITE (Boron, Calif.) White crystal sections and masses	.40 per pound
QUARTZ (Brazil) Crystals and sections w/ inclusion of Phantoms	2.50 per pound
GRIFFITHITE (Calif.) Brown masses	2.50 per pound
BORNITE (Arizona) Pure masses, colorful	1.25 per pound
COLEMANITE (Calif.) Grayish crystals and sections	1.75 per pound
FLUORITE (New Mexico) Green masses	.45 per pound
CHROME ZOISITE with hornblende & Ruby inclusions (Africa)	.95 per pound
PEACOCK COPPER & IRON ORE (Arizona) Irridescent masses	.95 per pound
OPTICAL CALCITE (Mexico) second grade transparent cleavages	2.25 per pound
GEM GRAVELS (Burma) Small gravels containing Spinel, Corundums, etc.	6.00 per pound
TOPAZ (Brazil) Crystal sections and pieces	3.50 per pound
OOLITE (Calif.) Black masses	.35 per pound
TURITELLA AGATE (Wyoming) Brown masses	.45 per pound
IDOCRASE (Calif.) Green masses	.40 per pound
HOWLITE (Calif) White masses some with black web	.45 per pound
JADEITE (Burma) Cut massive pieces showing color, some cores	3.75 per pound
PYRITE (Utah) Crystal sections and masses	.60 per pound
TURQUOISE (Nevada) Mine run vein Turquoise in rock	1.75 per pound
BRAZILIANITE (Brazil) Yellow opaque massive pieces	4.50 per pound
GERMANITE with some Tennantite (Africa) Black massive	20.00 per pound
SPODUMENE (Brazil) Crystals up to 2″. White partly gem	7.50 per pound
HANKSITE (Calif.) Crystals up to 2″	1.50 per pound

OUTSTANDING MINERAL SPECIMENS FROM OUR LARGE STOCK

CARNOTITE with some Pitchblende (Emory Co., Utah) One of the largest and richest pieces found. 7x10—weight 15 pounds—$175.00

URANINITE replacing **WOOD** (Emory Co., Utah) Very rich—2x3—weight 23 ounces—$25.00

TOURMALINE (Himalaya Mine, Mesa Grande, Calif.) New find of fine Specimens. Fine double terminated crystals mostly pink. Approximately 2″ long ½″ thick—$15.00 and $17.50 each. Single terminated approximately 1″ to 1½″ very fine pink—$5.00; $7.50 and $10.00 each

PYRITE CRYSTALS (Island of Elba) Beautiful bright crystals. Approximately 2″ to 3″—$5.00; $7.50 and $10.00 each

CHRYSOBERYLS (Brazil) Fine mostly complete greenish Crystals. Approximately ½″—$2.00 and $3.00—½″—¾″—$4.00 and $5.00 each

BRAZILIANITE (Brazil) Specimens showing one or more crystal faces. ¾″ over 1″—$5.00; $7.50 and $10.00 each

PARTIES INTERESTED IN RECEIVING FREE LISTINGS OF NEW ARRIVALS IN FINE MINERAL SPECIMENS FROM WORLD LOCALITIES PLEASE CONTACT.

SHALE'S

9226 W. Pico Blvd.
Los Angeles 35, Calif.

Phone—CR-6-8222

LARGE EXHIBITION SPECIMENS

Allanite. Ontario. Black massive with some feldspar 5½ x 7½″, $12.50

Azurite. Arizona. Polished stalactite section showing concentric banding. Beautiful deep blue color. Polished both sides. 2¾ x 4½″, $50.00

Austinite. Utah. White drusy with adamite on rock 5 x 6″, $15.00

Berthierite. Br. Columbia. Xline with andorite, stibnite, etc. 4 x 5″, $25.00.

Copper. Michigan. Choice, partly xled, partly wire copper, 7 x 8″, $35.00

Corvusite. Utah. Blue black massive. 3 x 6″, $17.50

Cyrtolite. Ontario. Choice group of brown crystals 6 x 8″, $35.00

Fergusonite. Ontario. Unusually large brown crystals and crystal sections in pegmatite 3 x 4″, $7.50, $10.00; 4 x 5″, $15.00

Gadolinite. Norway. Massive with some feldspar 3 x 4″, $15.00

Galena. Kansas. A choice group of cubic crystals with xled sphalerite on chert 12 x 11 x 6″, $50.00

Hemimorphite (Calamine). Penna. Light brown xled on xline hemimorphite 7 x 8″, $17.50; 8 x 13″, $25.00

Lead. Sweden. A nearly pure mass 2 x 3¼″, $35.00. A vein of native lead in rock 3 x 4½″, $15.00

Niocalite. Quebec. Light yellow xline in calcite 3 x 4″, $4.00; 4 x 6″, $10.00

Picromerite. Germany. Exceptionally well crystallized, some with halite, anhydrite 2 x 3″ to 3 x 4″, $5.00, $7.50, $10.00, $15.00, $17.50

Pyrite. Elba. Magnificent bright pyritohedral crystal groups 3 x 4½″, $17.50; 4½ x 5½″, $25.00; 4 x 4½″, $35.00

Scheelite. Nova Scotia. A very showy scheelite-quartz vein 5 x 10 x 5″, $35.00

Uraninite (Pitchblende). Hottah Lake, N.W.T. A rich mass with hematite and secondary uranium minerals, polished, 4½ x 5½″, $200.00

Grenville marble cut by pegmatite. A splendid textbook example with a 12 x 16″ polished surface. Opposite surface shows a large vug filled with secondary calcite deposited from solution. Part of the calcite has been removed by natural erosion to reveal large feldspar crystals. Photo on request. 12 x 16 x 6″, $37.50

All prices are list at Rochester, New York

Ward's Mineral Specimen Catalog F M 12 is now available. If you haven't received a copy, please ask for it.

WARD'S *NATURAL SCIENCE ESTABLISHMENT, INC.*
P.O. BOX 1712
ROCHESTER 3, N.Y.

GEORGE BANTA COMPANY, INC., MENASHA, WISCONSIN, U.S.A.